THE EFFECT OF DAMPING ON THE SEISMIC RESPONSE OF EQUIPMENT IN BUILDINGS

by

© ALLISON B. SCHRIVER, B.Sc.E., M.Sc.E.

A Thesis

Submitted to the School of Graduate Studies

in Partial Fulfilment of the Requirements

for the Degree

Doctor of Philosophy

McMaster University

December 1986

THE EFFECT OF DAMPING ON THE RESPONSE OF EQUIRMENT ...

DOCTOR OF PHILOSOPHY (1986)

(CIVIL ENGINEERING)

McMASTER UNIVERSITY

Hamilton, Ontario

TITLE: The Effect of Damping on the Seismic Response of Equipment in Buildings

AUTHOR: Allison B. Schriver, B.Sc.E. (University of New Brunswick)

M.Sc.E. (University of New Brunswick)

SUPERVISOR: Dr. A. C. Heidebrecht

NUMBER OF PAGES: x, 210

ABSTRACT

This thesis studies the effects that nonproportional damping has on the vibrational characterisitics of two and three level systems. In addition, error levels in response prediction are estimated for two simplified time history procedures and a response spectrum technique.

It is shown that nonproportional damping creates significant changes in the damped frequency, damping ratio and mode shape of each mode of vibration of the system relative to those found for a similar system exhibiting proportional damping.

The study of the prediction of the maximum system response to seismic base motions demonstrates that there exist three regions where different dynamic analysis procedures should be used. A physically uncoupled analysis should be used for very small mass ratios and a standard modal analysis should be used for large mass ratios. A complex modal analysis should be used if the mass ratio is of an intermediate value. Diagrams are supplied which allow one to readily determine which of the three methods is the most appropriate for a design.

ACKNOWLEDGEMENTS

The author wishes to express his sincere appreciation and thanks to his supervisor, Dr. A. C. Heidebrecht, for his guidance, advice and many useful suggestions during the preparation of this thesis.

Sincere thanks are also extended to the other members of this author's supervisory committee: Dr. Drysdale, Prof. Siddall and Dr. Tso. Their comments and suggestions have been a great help.

Acknowledgements are also due to the Department of Civil Engineering and the School of Graduate Studies of McMaster University and the Natural Sciences and Engineering Research Council of Canada for their financial assistance, which made this thesis possible.

TABLE OF CONTENTS

LIST OF FIGURES

LIST OF TABLES

CHAPTER 1

GENERAL INTRODUCTION

An overall view of major engineering structures, such as nuclear power plants, would reveal complicated structural systems containing many components of varying size and importance. As with any engineered structure, it is necessary that the response of the system to different sets of loading conditions be determined. The system can then be designed or redesigned according to the calculated response.

Before the response of the system can be determined, however, an appropriate simplified model of the system must be obtained. In the case of complex structural systems, it is very difficult to include all of the components in one model. On the other hand, a model could be used which looked at the overall system as a set of subsystems corresponding to the variously sized components.

In many cases, such as nuclear power plants, the overall structure can easily be described as containing the main structural support elements, the main large power production oriented components and the smaller auxiliary components. This tri-level view of the system can then be used to model the system with three levels of subsystems. In

general, however, any given structural system might be modelled as one, three or even five levels of subsystems, depending on the complexity of the actual system. For the purposes of this research, the structural models are considered to be composed of up to three levels of subsystems, as might be envisioned in a nuclear power plant.

The three levels of subsystems are referred to as the tertiary, secondary, and primary subsystems. These different levels are differentiated mainly by mass. It might be said that the levels denote small, medium and large subsystems. The primary subsystem refers to the main structural components of the system which support most or all of the equipment, piping and other components. The secondary subsystem(s) normally consists of the large components and equipment and any large diameter piping. The tertiary subsystem(s) then consists of the small components, equipment and piping. The ratio of the masses can range from 0.10 down to 0.0004 for tertiary to secondary and from 0.003 down to 0.0001 for secondary to primary.

The primary subsystem is subjected to any ground motion that might impact the location of the structure being considered. As a result, the response of the primary subsystem, at all the points of attachment, serves as the input excitation to the secondary and/or tertiary subsystems. Similarly, the response of the secondary subsystems serve as the input excitation for any attached

tertiary subsystems. At the same time, it must be remembered that the resulting response of a higher level subsystem will feed back down into the lower levels and modify, to some degree, those responses.

Any major structural system must be designed to resist a design level of seismic activity. However, in order to carry out the design, the engineer must first be able to determine the response of the system to the expected ground motion.

The expected ground motion can be represented as a response spectrum, an actual recorded ground time history or an artificial or simulated time history. The artificial time history would be based on a predetermined "design" response spectrum. The actual response of the system can be described by maximum acceleration, velocity and displacement, maximum equipment distortion, or maximum base shear and overturning moment.

For purposes of this research, the structural system is assumed to remain elastic. This allows the problem to be addressed from a modal analysis point of view and is consistent with the fact that nuclear power plants, a major set of structures to which this research can be applied, are designed to respond elastically.

Depending on the complexity of the system being analyzed, the seismic response can be obtained using physically uncoupled, modal or coupled analysis and time

history or response spectrum techniques. Unfortunately, as the system being modelled becomes more and more complicated, the analysis methods become more complicated. This complication often arises due to numerical problems created by the presence of extremely large and small elements in the same mass and/or stiffness matrix. The problem can also be complicated if the different subsystems have damping characteristics which yield a coupled system exhibiting nonproportional damping. Nonproportional damping implies that the standard method of obtaining uncoupled differential equations will not work since the transformation which is used will not uncouple the damping matrix. As a result, engineers begin to look for methods which simplify the analysis and/or model while maintaining an acceptable level of accuracy.

Presently, there are methods(2,13,14,17,21,22,26) of handling the three level system which yield conservative results but do not provide a good insight into the actual response of tertiary subsystems. In many cases these methods yield very conservative results. As a result, the accurate determination of the seismic response of tertiary subsystems and the corresponding errors involved in the standard methods of analysis are a valid research objective. An improved knowledge of the level of error involved in the standard methods would be a definite help in improving the seismic design of these complex systems.

Before the error can be evaluated, a method must be found which can supply the "exact" result. Once determined, it is beneficial if this method is used to demonstrate the effect that damping has on the predicted response of tertiary and secondary subsystems subjected to seismic activity. This improved understanding can lead to improved analysis and more appropriate design.

Key to the accurate analysis of one of these complex systems is the accurate determination of the damping that exists in each of the subsystems. This is a key since damping is one of the controlling factors associated with the maximum seismic response of a structural system. In the same way, an improved knowledge of the error associated with simplified methods of handling nonproportional damping is another key factor in the analysis and design of three level systems.

1.2 Literature Review

A review of the literature on the seismic analysis of structures reveals that very little work has been done on the topic of tertiary subsystem response analysis.

In the past, especially for tertiary subsystems, it was common to consider the different subsystems to be uncoupled. In other words, it was assumed that the response of a particular subsystem was not affected by the response of any higher level subsystem. As a result, the primary

subsystem would be analyzed for a given ground motion and the resulting response would be used as the input to the secondary subsystems. Similarly, the secondary subsystem response would be used as the input to the tertiary subsystems. This technique has been used in the past to develop amplification methods of determining maximum secondary level responses(8 and 24).

In reality, however, all subsystems within a structure are coupled together and their response is dependent on the response of all the other subsystems, to a greater or lesser extent.

The initial work which recognized this fact involved the mapping out of areas where this interaction effect was insignificant. Each of the studies set out decoupling criteria(3,4,5,12) based on the mass and frequency ratios of the uncoupled systems. If the criteria was met, then an uncoupled analysis could be carried out and the interaction effects ignored.

Later, studies were made which attempted to account for this interaction between subsystems, but mostly for two level structural systems.

Two of these studies were done in parallel in the late 1970's by Ruzicka and Robinson(21) at the University of Illinois and by Sackman and Kelly(22) at the University of California at Berkeley. Both studies developed simple expressions for the coupled vibrational characteristics of a

system, based on the uncoupled characteristics of the subsystems. The expressions were also based on the fact that the secondary subsysten mass and stiffness elements were small relative to those corresponding to the primary subsystem and that the frequencies of the uncoupled subsystems were tuned to each other. Next, expressions were developed for the response of the coupled system based on standard modal analysis and, in the case of the Illinois study, Fourier transforms and, in the case of the Berkeley study, LaPlace transforms.

The case of nonproportional damping was solved in the Illinois study by using frequency domain analysis. The Berkeley study assigned uncoupled damping ratios to the corresponding coupled modes, except for the tuned modes. The two closely spaced modes were assigned the arithmetic average of the damping ratios of the two uncoupled modes. Finally, Ruzicka and Robinson developed estimates of the maximum response assuming the Fourier transform of the ground motion was approximately linear. Similarly, Sackman and Kelly developed estimates of the maximum response but assumed that the ground motion was of a short duration (ie. product of duration and beat frequency much less than unity).

Another study by Kiureghian, etal(17) developed expressions for coupled dynamic characteristics based on the uncoupled characteristics and a perturbation technique. The

secondary system response was then estimated using random vibration theory and expressions were developed for the cross correlation between the modal responses. The case of nonproportional damping was handled in the same way used by Sackman and Kelly.

Perhaps the most extensive study of systems containing two levels of subsystems was carried out by Villaverde and Newmark(20) at the University of Illinois. They developed expressions for dynamic characteristics and response of a system made up of a multi-degree of freedom primary subsystem and a multi-degree of freedom secondary subsystem which could be attached to the primary subsystem at one or two points. The vibrational characteristics were estimated from the uncoupled characteristics and the maximum response was obtained using a modified response spectrum technique. Unlike the previous studies, this study dealt with the case of nonproportional damping using complex modal analysis.

Several other similar studies(2,10,11,18,19) were also carried out in an attempt to account for the interaction between primary and secondary levels of a system exhibiting classical or proportional damping.

The author has found three studies that deal directly with third or tertiary level subsystems. The first study was done by A. C. Heidebrecht(13) at McMaster University. To maintain simplicity, a three degree of

freedom coupled system was examined and coupled damping ratios were proportioned from the uncoupled damping ratios, based on strain energy. The actual response of the system was determined using modal analysis and integration of the transformed uncoupled equations of motion. The response was calculated for four actual earthquake motions and one spectrum compatible artificial earthquake ground motion.

The study found very large amplifications when two or three of the uncoupled frequencies were tuned. The study went on to suggest criteria for the uncoupling of the system and maximum amplifications to be used if the system must be considered to be coupled. Finally, it was suggested that the results were conservative but a suggestion could not be made as to possible reductions without further study and analysis.

The second study was carried out by T. Aziz(2) at Atomic Energy of Canada Limited. It was assumed that the three uncoupled subsystems were tuned to each other and the coupled damping ratios were taken as three per cent in each mode. The report suggests expressions for coupled modal properties, as well as maximum values of amplification that could be used. These would then be incorporated in a response spectrum type analysis.

The most recent report was made by Hernried and Sackman(14). They developed expressions for the dynamic response of tertiary subsystems using a perturbation

technique and LaPlace transforms. The maximum response is given either as a simple expression, in terms of the response spectrum, or is given in terms of a convolution of Greene's function with the base motion. The report does not, however, suggest areas where these results must be used instead of the simpler standard modal analysis or physically uncoupled analysis.

Finally, papers and reports have been presented which describe methods of analyzing structural systems which exhibit nonproportional damping. An early paper by Clough and Mojtahedi(6) concluded that it was best to use the undamped mode shapes to transform the equations of motion and integrate directly the coupled equations. The mass and stiffness matrices are diagonalized but the equations are coupled by the damping matrix which, in general, is not diagonalized by the same transformation.

More recently, results have been presented which, like Villaverde and Newmark, use complex modal analysis to transform and diagonalize a modified equation of motion. A report was released in 1983 by Igusa and Kiureghian(15) and in the past year two papers were presented by Singh and Ashtainy(23) and Veletsos and Ventura(25).

With research continuing on the simpler two level systems, much less time has been devoted to three level systems. As a result, a tertiary subsystem must be analyzed, normally, as an uncoupled subsystem of the overall system.

One way to account for the interaction between the three levels of subsystems is to carry out a completely coupled analysis. Alternatively, one can carry out a double application of the previously described methods for two level systems, use the approximate maximum amplifications that have been given for three level systems or use the expression given by Hernried and Sackman.

A major source of inaccuracy has not been handled in a detailed fashion. This source lies in the handling of nonproportionally damped systems. It will be shown later that this covers the vast majority of damping cases. In many of the reports covered, the typical solution is to use the uncoupled damping ratios for the widely spaced modes and use an average (arithmetic or geometric) damping ratio to define the damping in both of the closely spaced modes.

Further study should be carried out in this area. One needs to know how the nonproportional damping affects the dynamic characteristics of the systems. Estimates need to be made as to what level of error is introduced if a simplified (uncoupled or modal analysis) procedure is used to calculate the seismic response of the system.

1.3 Scope and Objectives

The main objective of this research is to investigate the basic time history seismic response calculation methodologies that are available and determine the level of error introduced when the simplified procedures are used, rather than the general one. In addition, this research presents some of the effects that nonproportional damping have on the dynamic characteristics of two and three level structural systems.

Perhaps the most important factor governing the seismic response, especially maximum response, of a structural system is the level of damping that is present within the structure. At the same time, damping within a complex structure is one of the hardest structural characteristics to evaluate and model satisfactorially. Hence, the effect of damping, especially nonproportional damping, on the predicted seismic response of two and three level systems is the area of study.

The overall objective of this thesis can be broken down into three specific objectives:

1) The compilation of the usual methods of time history analysis used in seismic analysis.

2) The evaluation of the error introduced by simpler methods of analysis.

3) The development of an improved understanding of how nonproportional damping affects the dynamic characteristics

and response of the system.

It is hoped that this research will give the engineer an improved view of how damping affects system characteristics and responses. In addition, the engineer will be able to look at the results of this study and select the method of analysis which will provide the best balance between simplicity of application and accuracy of results for the damped linear system that he or she is dealing with.

1.4 Approach to the Problem

The approach to this research problem is three staged in nature. The first stage involves an investigation to determine the time history procedures which have been or could be used in the calculation of the maximum seismic response of a structural system. Two response spectrum techniques(20,27) are also used although they are non-time history procedures.

A total of four time history procedures are identified. Two of the procedures give "exact" results, in the sense of being able to handle any symmetric damping matrix, and two of the procedures involve some sort of simplification in order to be used.

The second stage involves the comparison and evaluation of the different procedures as they are applied to the same two and three level systems. The two "exact" procedures give identical results and, as a result, the

computationally faster procedure is retained and the other eliminated.

The comparison is conducted over a range of parameter values and the errors introduced by the simplified procedures are evaluated.

Finally, dynamic characteristics are compared for systems exhibiting proportional and nonproportional damping. This comparison gives an indication of how damping affects these characteristics.

It should be noted that a series of experiments were carried out in an attempt to, at least partially, verify the results that were being generated by the "exact" procedure. Details are provided in Appendix V.

The general thrust of the research is to give the engineer a better understanding as to how nonproportional damping affects system characteristics and predicted maximum seismic response when different analysis procedures are used.

1.5 Thesis Organization

This thesis can be broken up in four sections. The first section is the introduction. This reviews previous work done in this or related fields, sets out the objectives and limitations of this study and describes the approach that is used to solve the problem.

The second section deals with the subject of time

history analysis and presents four time history methods of solving the problem. In addition, a description of time histories used, modal combination techniques suggested and experimental verification carried out in the study are given.

The third section involves the actual computations that were made for each system selected and for each procedure that was to be evaluated. The computations were done for both two and three level systems for various values of selected system parameters.

The final section is a chapter of conclusions and recommendations related to the results that were obtained in the third section. This will also include suggestion as to how an engineer might apply these results in a design and/or analysis situation.

CHAPTER 2

TIME HISTORY RESPONSE CALCULATIONS

2.1 Introduction

The seismic analysis of a given structural system depends on the handling of three independent components. An adequate and/or representative model of the expected system input excitation, an appropriate mathematical model of the structural system and a valid technique for the analysis of the dynamic response of the system are all necessary prerequisites for an acceptable degree of confidence in the final result, the seismic response of the system.

This chapter will address the selection of a set of historic earthquake ground motions, which will act as the input excitation, and the selection of a set of methods of determining the dynamic response of a system. The development of mathematical models for the system will be covered in later chapters.

2.2 Earthquake Ground Motions

The analysis done for this research was carried out using twelve historic earthquake time histories. These earthquake time histories have been recommended in a thesis by J. C. Wilson(28).

In that thesis an attempt was made to select a limited number of historic earthquakes time histories. These would be broadly representative of possible seismic activity which might affect nuclear power plant sites and yet provide a statistically valid set of input motions.

The twelve time histories were selected based on several criteria: soil conditions, Richter magnitude, peak acceleration, duration of the ground motion and distance from the epicentre. The selection was made such that two sets (a set implies two horizontal orthogonal time histories at a specific location and time) were from rock sites, stiff soil sites and deep cohesionless soil sites. In addition, each event had to have a Richter magnitude of at least 6 (preferably between 6.5 and 7), at least one of the two horizontal components of each set had to have a peak acceleration greater than 10% of the acceleration due to gravity, "far" and "near" events were to be represented and all the records had to have a duration of at least 30 seconds.

Six sets were selected from the available earthquake data for the western United States and the actual baseline

corrected strong motion acceleragrams were obtained from the data published by the California Institute of Technology(1). A listing of the twelve records is provided in Table 2.1 and plots of the actual time histories are provided in Appendix I.

2.3 Physically Uncoupled System Analysis

The dynamic response of a system represents the time dependent motion the system undergoes due to some applied loading. For a lumped mass model where only horizontal displacements are considered significant, the number of lumped masses indicates the number of degrees of freedom of the system. This is the minimum number of coordinates needed to define the positions of the components of the system. The main difference between seismic analysis and other forms of dynamic analysis is that the ground or base acceleration induces an inertial forcing function on the system, rather than a set of directly applied loads.

Normally, the structural system is simplified, for modelling purposes, to a system of lumped masses. For example, the three storey frame shown in Figure 2.1(a) can be considered to have three significant degrees of freedom (ie. the lateral deflection at the level of each floor). As a result, the floor mass plus half of the column masses above and below the floor are lumped at the floor level. This results in a lumped mass model shown in Figure 2.1(b).

The simplest form of time history analysis that can be carried out on such a lumped mass system involves the assumption that each subsystem is completely uncoupled from the other subsystems. In this way, once the base input motion to the subsystem is known, the response of the subsystem can be calculated. As was noted earlier, this involves the assumption that the response of attached higher level subsystems has no effect on the response of the subsystem being evaluated.

Consider the coupled lumped mass model shown in Figure 2.2(a). The coupled two degree of freedom system is composed of two single degree of freedom subsystems having masses of M_p and M_s. For a completely uncoupled analysis, the system is simplified to look like the system shown in Figure 2.2(b). An equation of dynamic equilibrium can now be written for both of the uncoupled systems.

$$M_p\ddot{X}_p+C_p\dot{X}_p+K_pX_p = -M_p\ddot{U}_g(t) \qquad (2.01)$$

$$M_s\ddot{X}_s+C_s\dot{X}_s+K_sX_s = -M_s(\ddot{X}_p(t)+\ddot{U}_g(t)) \qquad (2.02)$$

Equation 2.01 can be numerically integrated and the response X_p of the primary subsystem determined. Once X_p is known equation 2.02 can be solved numerically for X_s. This same procedure could be repeated as many times as necessary, depending on the number of subsystems within the system.

It should be noted that the subsystems need not be single but could also be multi-degree of freedom systems.

This is one method that can be used to determine the

seismic response of a secondary or tertiary level subsystem. It must be remembered, however, that there is a basic assumption underlying this method. Ignoring upper level interaction may produce significant errors in the calculated seismic response.

2.4 Standard Modal Analysis

A more general method of handling the problem of solving for the seismic response of a structural system is presented in this section.

Consider the system illustrated in Figure 2.2(a). A free body can be taken of each lumped mass in the system and an equation of dynamic equilibrium written for each. These coupled equations are called the equations of motion of the system.

If it is assumed that the base of the lumped mass system is subjected to an earthquake acceleration, then the equations of motion can be written in a matrix equation of the form(7)

$$[M]\{\ddot{X}_t\}+[C]\{\dot{X}\}+[K]\{X\} = \{0\} \qquad (2.03)$$

where

$$\{\ddot{X}_t\} = \{\ddot{X}\}+\{1\}\ddot{U}_g(t). \qquad (2.04)$$

The values within the three square brackets represent the symmetric mass, damping and stiffness matrices, $\{X\}$ represents the vector of relative structural displacements and the single and double dots represent single and double differentiation with respect to time. Equation 2.03 can be

reexpressed, using equation 2.04 as the standard equation of motion for earthquake response:

$$[M]\{\ddot{X}\}+[C]\{\dot{X}\}+[K]\{X\} = -[M]\{1\}\ddot{U}_g(t) = P(t) \quad (2.05)$$

It can be shown that the coupled equations of 2.05 can be transformed into N uncoupled equations of the form(7)

$$\ddot{Y}_i+2\zeta_i\omega_i\dot{Y}_i+\omega_i^2 Y_i = P_i^*/M_i^* \quad (2.06)$$

Here Y, ζ, ω, P^* and M^* represent the modal displacement, damping ratio, circular frequency, forcing function and mass of the transformed system. The actual transformation is $\{X\}=[\Phi]\{Y\}$, where $[\Phi]$ represents the matrix of eigenvectors corresponding to the undamped form of the system described in equation 2.05.

A major assumption is made in moving from equation 2.05 to 2.06. It is assumed that the transformation that uncouples the mass and stiffness matrices also uncouples the damping matrix. It can be shown(9) that this assumption will hold if

$$[\underline{K}][\underline{C}] = [\underline{C}][\underline{K}] \quad (2.07)$$

where:

$$[\underline{K}] = [M]^{-1/2}[K][M]^{-1/2} \quad (2.08)$$

$$[\underline{C}] = [M]^{-1/2}[C][M]^{-1/2} \quad (2.09)$$

If the damping matrix can be diagonalized, then the system is said to exhibit proportional damping.

Equation 2.06 can be solved for the response of each mode independent of the other modes and these modal responses can be added together to yield the total response.

The seismic response of the system can be calculated

using numerical integration. The integration is carried out using the linear acceleration technique. If the acceleration varies linearly over a time increment, then the velocity and displacement must vary as a quadratic and cubic respectively. Expressions can be developed for the value of the acceleration, velocity and displacement at the end of the time increment, in terms of the initial values at the start of the time increment. One such set of expressions for the response at time t_{n+1}, given conditions at time t_n, is(13)

$$\ddot{Z}_{n+1} = \frac{-[G^2\ddot{Z}_n+(2\zeta G+G^2)\dot{Z}_n+(\zeta G+G^2/3)Z_n+\ddot{U}_{n+1}]}{[1+\zeta G+G^2/6]} \quad (2.10)$$

$$\dot{Z}_{n+1} = \dot{Z}_n+(\ddot{Z}_{n+1}+\ddot{Z}_n)/2 \quad (2.11)$$

$$Z_{n+1} = Z_n+\dot{Z}_n+\ddot{Z}_n/3+\ddot{Z}_{n+1}/6 \quad (2.12)$$

where $$\ddot{Z} = \ddot{Y}/g \quad (2.13)$$

$$\dot{Z} = \dot{Y}/\Delta t/g \quad (2.14)$$

$$Z = Y/\Delta t^2/g \quad (2.15)$$

The constant G is the product of the modal circular frequency and the time step of integration (Δt). These can be combined with equation 2.04 to yield the modal and total responses.

2.5 Direct Integration of the Coupled Equations of Motion

In the previous section, the standard method of modal analysis for seismic excitation was presented. If, however, the system being considered does not exhibit proportional damping, then the method cannot be applied without some level of error being introduced. Another option is to integrate the coupled equations of motion directly.

Clough and Penzien(7) present a method for this step by step integration, based on the linear acceleration assumption. The method can be expressed by the following equations which determine the response at the end of the time step, given the initial values.

The change in displacement can be determined from the matrix equation:

$$[K']\{\Delta X(t)\} = \{\Delta P(t)\} \tag{2.16}$$

where:

$$[K'] = [K]+(6/\Delta t^2)[M]+(3/\Delta t)[C] \tag{2.17}$$

$$\{\Delta P(t)\} = \{P(t+\Delta t)\}-\{P(t)\} +[M]\{(6/\Delta t)\{X(t)\}+3\{X(t)\}\} +[C]\{3\{X(t)\}+(\Delta t/2)\{X(t)\}\} \tag{2.18}$$

The change in velocity can now be found as

$$\{\Delta X(t)\}=(3/\Delta t)\{\Delta X(t)\}-3\{X(t)\}-(\Delta t/2)\{X(t)\} \tag{2.19}$$

Finally:

$$\{X(t+\Delta t)\} = \{X(t)\}+\{\Delta X(t)\} \tag{2.20}$$

$$\{X(t+\Delta t)\} = \{X(t)\}+\{\Delta X(t)\} \tag{2.21}$$

$$\{X(t+\Delta t)\} = [M]^{-1}[\{P(t+\Delta t)\}-[C]\{X(t+\Delta t)\} -[K]\{X(t+\Delta t)\}] \tag{2.22}$$

The variables such as Δt and ΔX indicate an increment in

time (Δt) or a change in a variable (ΔX) over the time increment Δt.

Now the seismic response of a system can be calculated whether or not it possesses proportional damping.

The two main drawbacks of this method, however, are quite substantial. The first is that the computational effort is greatly increased since matrix calculations are carried out at each time step, as opposed to scalar or vector calculations in modal analysis. The second drawback is that the modal characteristics and response are lost. These can be of great interest when attempting to interpret the results and the effect that certain parameters have on the system characteristics and response.

2.6 Complex Modal Analysis

This section presents a second method for the handling of the seismic analysis of a system that exhibits nonproportional damping. In this method, the equation of motion is rewritten into a form which can be diagonalized, so long as the mass, damping and stiffness matrices are symmetrical.

Consider the following equations:

$$[M]\{\ddot{X}\}+[C]\{\dot{X}\}+[K]\{X\} = -[M]\{1\}\ddot{U}_g(t) \qquad (2.23)$$

$$[M]\{\dot{X}\}-[M]\{\dot{X}\} = \{0\} \qquad (2.24)$$

The first equation is simply the standard equation of motion and the second is added so that these two NxN matrix

equations can be combined to form one 2Nx2N matrix equation containing only two symmetric matrices.

$$\begin{bmatrix}[0] & [M] \\ [M] & [C]\end{bmatrix}\begin{Bmatrix}\{\ddot{X}\} \\ \{\dot{X}\}\end{Bmatrix} + \begin{bmatrix}-[M] & [0] \\ [0] & [K]\end{bmatrix}\begin{Bmatrix}\{\dot{X}\} \\ \{X\}\end{Bmatrix} = \begin{Bmatrix}\{0\} \\ -[M]\{1\}\ddot{U}_g\end{Bmatrix} \quad (2.25)$$

Now let

$$[A] = \begin{bmatrix}[0] & [M] \\ [M] & [C]\end{bmatrix} \quad (2.26)$$

$$[B] = \begin{bmatrix}-[M] & [0] \\ [0] & [K]\end{bmatrix} \quad (2.27)$$

$$\{Y\} = \begin{Bmatrix}\{\dot{X}\} \\ \{X\}\end{Bmatrix} \quad (2.28)$$

$$\{Q(t)\} = \begin{Bmatrix}\{0\} \\ -[M]\{1\}\tilde{U}_g(t)\end{Bmatrix} \quad (2.29)$$

Equation 2.25 becomes

$$[A]\{\dot{Y}\}+[B]\{Y\} = \{Q(t)\} \quad (2.30)$$

Assuming that $\{Y\} = \{\phi\}e^{\lambda t}$, (2.31)

for the homogeneous form of equation 2.30 produces an eigen problem of the form:

$$[\lambda[A]+[B]]\{\phi\}e^{\lambda t} = \{0\} \quad (2.32)$$

or

$$[\lambda[A]+[B]]\{\phi\} = \{0\} \quad (2.33)$$

since $e^{\lambda t}$ can not be zero for any finite time.

This eigenvalue/vector problem can be solved for the set of 2N eigenvalues and corresponding eigenvectors.

It can be shown(26) that the eigenvectors are orthogonal with respect to the A and B matrices. In addition, $b_i/a_i = -\lambda_i$ (2.34)

where: $a_i = \{\phi_i\}^T[A]\{\phi_i\}$ (2.35)

and $$b_i = \{\phi_i\}^T[B]\{\phi_i\}. \tag{2.36}$$

If it is assumed that $\{Y\}=[\Psi]\{Z\}$, where $[\Psi]$ represents the matrix of eigenvectors and $\{Z\}$ represents a vector of amplitudes, then equation 2.30 becomes

$$[A][\Psi]\{\dot{Z}\}+[B][\Psi]\{Z\} = \{Q(t)\} \tag{2.37}$$

$$[\Psi]^T[A][\Psi]\{\dot{Z}\}+[\Psi]^T[B][\Psi]\{Z\} = [\Psi]^T\{Q(t)\} \tag{2.38}$$

Since it was shown that the eigenvectors are orthogonal to each other with respect to the A and B matrices, equation 2.38 can be expressed as a series of uncoupled equations of the form:

$$a_i\dot{Z}_i+b_iZ_i = q_i \tag{2.39}$$

It should be noted that if the damping matrix allows for vibrational motion, then the 2N uncoupled equations will actually be made up of N pairs of complex conjugate equations. As a result, the calculated responses of a pair of complex conjugate equations will also be complex conjugates and yield a purely real response when added together.

In order to determine the modal response for each of the 2N uncoupled modal equations numerically, an assumption is made with respect to the time variation of the system response or the forcing function. For purposes of the computer analysis used in this research, it is assumed that the first derivative of the response would vary linearly over a small time increment Δt. As a result, at the time increment n+1,

$$(\dot{Z}_i)_{n+1} = (\dot{Z}_i)_{n+1} \tag{2.40}$$

$$(Z_i)_{n+1} = (Z_i)_n + ((\dot{Z}_i)_n + (\dot{Z}_i)_{n+1}) * \Delta t/2 \tag{2.41}$$

Consider one of the 2N uncoupled equations at the end of the time increment n+1.

$$a_i(\dot{Z}_i)_{n+1} + b_i(Z_i)_{n+1} = (q_i)_{n+1} \tag{2.42}$$

Substituting equations 2.40 and 2.41 into 2.42 yields

$$(\dot{Z}_i)_{n+1} = \frac{(q_i)_{n+1} - b_i\{(Z_i) + (\Delta t/2)(\dot{Z}_i)_n\}}{[a_i + b_i(\Delta t/2)]} \tag{2.43}$$

$$(Z_i)_{n+1} = (Z_i)_n + (\Delta t/2)[(\dot{Z}_i)_n + (\dot{Z}_i)_{n+1}] \tag{2.44}$$

Given the conditions at the beginning of the time increment, these two equations can be used to evaluate the response at the end of the time increment. The computer can use these to easily work through a given time history and calculate the system response at each time step.

2.7 Modal Combination Techniques

Different methods of time history analysis have been covered in the previous sections of this chapter. These varied in the amount of computational effort required to calculate the maximum seismic response of the system. All of the methods, however, since they involve a step by step numerical integration over time, often require more effort than an engineer may find justifiable.

Response spectrum techniques are alternatives to the time history analysis procedures. Using these in conjunction with a modal combination technique can allow an engineer to

circumvent time domain calculations, provided the resulting errors are acceptable.

A response spectrum is a plot of the maximum response of a series of single degree of freedom systems for a specific excitation. These plots are made as a function of the frequency and damping ratio of the individual single degree of freedom system. Since a mode of vibration of a structural system can be treated as a single degree of freedom, the maximum response of the mode can be calculated as the product of the modal amplitude (obtained from the response spectrum for the corresponding damping ratio), the mode shape and the modal participation factor.

The problem arises that the modal maxima may be known but there is no information as to how they relate to each other as a function of time. It is not known whether they occur simultaneously or whether they are spread out over the time of the system response. This information is lost when the response spectrum is generated. It is left for the modal combination technique to try and approximate the effect.

The first technique that one might employ is the SRSS (square root of the sum of the squares) technique. This method estimates the maximum seismic response as the square root of the sum of the squares of the modal maxima. If the modal maxima at level k, within the system, are represented as X_{k1}, X_{k1}, ..., X_{kn}, then the maximum response at level k

(X_k) may be approximated as

$$X_k = [X_{k1}^2+X_{k2}^2+\ldots+X_{kn}^2]^{1/2} \tag{2.45}$$

This method gives its best estimates of maximum response when the modal frequencies are well spaced.

If the system exhibits closely spaced modes it is preferable to have an alternate technique. One such technique is the rule proposed by Rosenblueth(17). The rule says that the maximum response can be approximated as

$$X_k = [\Sigma X_{kr}^2+\underset{i\neq j}{\Sigma\Sigma} X_{ki}a_{ij}X_{kj}]^{1/2} \tag{2.46}$$

where: $$a_{ij} = 1/[1+R^2] \tag{2.47}$$

$$R = [\omega_i-\omega_j]/[\zeta_i'\omega_i+\zeta_j'\omega_j] \tag{2.48}$$

$$\zeta_i' = \zeta_i+2/\omega_i s^* \tag{2.49}$$

The parameter s^* represents the duration of a segment of white noise. Equation 2.46 represents the maximum response of the system to the white noise. The use of this expression, then, assumes that an earthquake time history can be approximated by a segment of white noise. It was found convenient, for earthquakes of the southern California type, to take the value of s^* to be approximated by 12.5(17), rather than try to approximate it for every time history.

Another similar technique is called the complete quadratic solution(27). Here

$$X_k = [[\Sigma\Sigma X_{ki}a_{ij}X_{kj}]^{1/2} \tag{2.50}$$

where

$$a_{ij} = \frac{8[\zeta_i\zeta_j]^{1/2}[\zeta_i+r\zeta_j]r^{3/2}}{(1-r^2)^2+4\zeta_i\zeta_j r(1+r^2)+4(\zeta_i^2+\zeta_j^2)r^2} \tag{2.51}$$

$$r = \omega_i/\omega_j \tag{2.52}$$

Since the modal maxima are calculated as a matter of course in any modal time history program, these modal combination techniques can be used to give an estimate of the actual maximum response. An evaluation can then be made to see if any of the methods provide satisfactory results and, if so, over what ranges of parameters.

TABLE 2.1 EARTHQUAKE RECORDS (part 1) (Ref. 28)

	RECORD	COMP	DATE	MAG	SOIL TYPE
1	3838 Lankershim Blvd L.A. (bsmt)	N-S	02/09/71	6.4	Rock
2	3838 Lankershim Blvd L.A. (bsmt)	E-W	02/09/71	6.4	Rock
3	Caltech Seismological Laboratory	E-W	02/09/71	6.4	Rock
4	Caltech Seismological Laboratory	N-S	02/09/71	6.4	Rock
5	El Centro	N-S	05/18/40	6.7	Stiff Soil
6	El Centro	E-W	05/18/40	6.7	Stiff Soil
7	Hollywood Storage P.E. Lot. L.A.	N-S	02/09/71	6.4	Stiff Soil
8	Hollywood Storage P.E. Lot. L.A.	E-W	02/09/71	6.4	Stiff Soil
9	Eureka Federal Bldg (bsmt)	N79E	12/21/54	6.5	Deep Cohesionless
10	Eureka Federal Bldg (bsmt)	N11W	12/21/54	6.5	Deep Cohesionless
11	8244 Orion Blvd. L.A.	N-S	02/09/71	6.4	Deep Cohesionless
12	8244 Orion Blvd. L.A.	E-W	02/09/71	6.4	Deep Cohesionless

TABLE 2.1 EARTHQUAKE RECORDS (part 2) (Ref. 28)

	RECORD	MAX. ACCEL (g)	APPROX. SOURCE DISTANCE (km)	EARTHQUAKE EVENT	BOOK REF. NO.
1	3838 Lankershim Blvd L.A. (bsmt)	.167	24	San Fernando	L166
2	3838 Lankershim Blvd L.A. (bsmt)	.150	24	San Fernando	L166
3	Caltech Seismological Laboratory	.192	37	San Fernando	G106
4	Caltech Seismological Laboratory	.089	37	San Fernando	G106
5	El Centro	.348	08	Imperial Valley	A001
6	El Centro	.214	08	Imperial Valley	A001
7	Hollywood Storage P.E. Lot. L.A.	.211	35	San Fernando	D058
8	Hollywood Storage P.E. Lot. L.A.	.170	35	San Fernando	D058
9	Eureka Federal Bldg (bsmt)	.258	25	Eureka	A008
10	Eureka Federal Bldg (bsmt)	.168	25	Eureka	A008
11	8244 Orion Blvd. L.A.	.255	20	San Fernando	C048
12	8244 Orion Blvd. L.A.	.134	20	San Fernando	C048

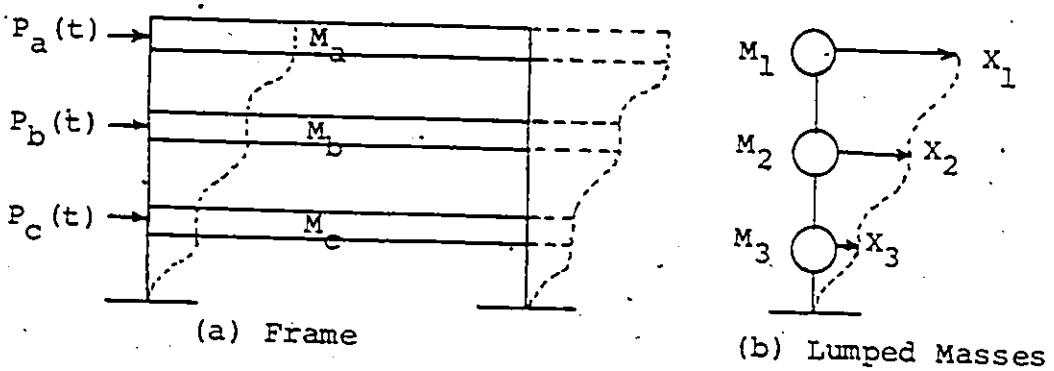

Figure 2.1 Frame Reduced to Lumped Masses

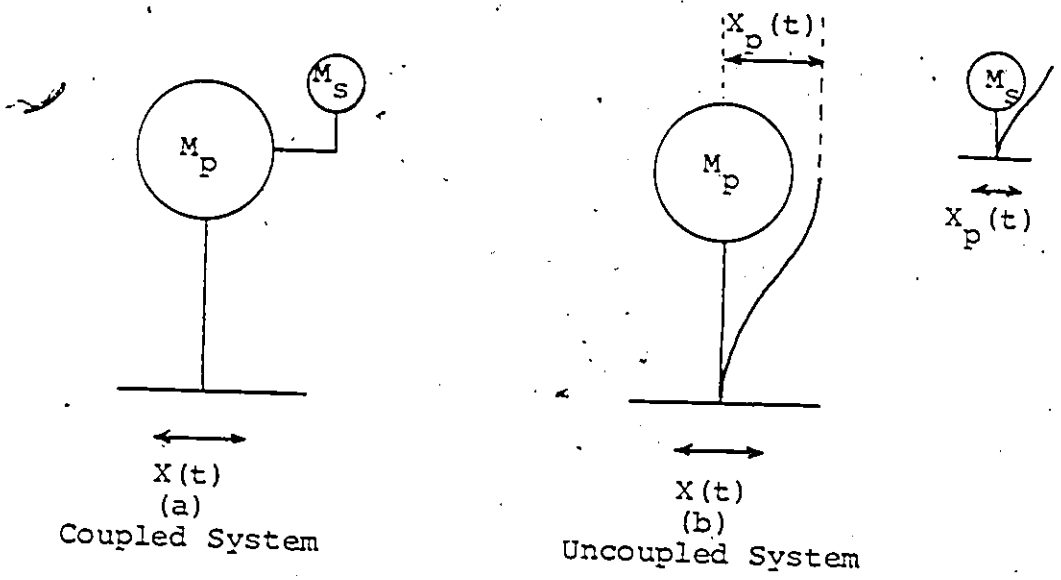

Figure 2.2 A Coupled Versus an Uncoupled System

CHAPTER 3

EFFECT OF NONPROPORTIONAL DAMPING ON SYSTEM CHARACTERISTICS

3.1 System Parameters

The analytical and experimental basis of the methods to be used in the following chapters are set out in the previous sections of this work. The attention of the remainder of this study is directed to the investigation of the free and forced vibrations of these systems.

The effect of nonproportional damping on the free vibration characteristics of the system is considered in this chapter. The cases involving proportional damping are a particular subset of the general nonproportional damping case.

Three types of parameters must be defined if the system is to be completely described. These parameters pertain to the mass, natural frequency and damping of the subsystems that comprise the overall coupled system.

The first set of parameters is the system mass ratios (μ). These are defined as

$$\mu_{ij} = M_i/M_j. \tag{3.01}$$

The next set is the system frequency ratios

$$\theta_{ij} = \omega_i^2/\omega_j^2. \tag{3.02}$$

The final set is related to the subsystem damping ratios:

$$\alpha_i = (\zeta_i/\zeta_p)(\omega_p/\omega_i). \qquad (3.03)$$

The subscripts i and j refer to the subsystems in question: primary, secondary or tertiary (ie. i = p,s or t).

Each of these parameters must be defined for each subsystem above the primary subsystem. The system is completely described once these parameters plus the primary natural frequency and damping ratio have been defined.

With the system defined, the next step is to determine the vibrational characteristics of the coupled system.

3.2 Interpretation of Characteristics of Nonproportionally Damped Systems

The system characteristics can be obtained by setting up the complex eigenvalue/vector problem for the system. The set up and evaluation are described in Chapter 2. The system characteristics are based on these eigenvalues and eigenvectors.

The remainder of this section is concerned with developing a physical interpretation for these complex valued eigenvalues and eigenvectors.

In setting up the eigenproblem, it is assumed that the time dependent response of the system can be represented as

$$\{Y\} = Ae^{\lambda t}\{\phi\}. \qquad (3.04)$$

A is an arbitrary constant, λ is the complex eigenvalue and $\{\phi\}$ the complex eigenvector. Since λ is complex, it can be expanded such that

$$\lambda = a+bi. \tag{3.05}$$

As a result,

$$\{y\} = e^{at}e^{ibt}\{\phi\}. \tag{3.06}$$

It can be seen now that the free vibration response is made up of an exponential time decay function, controlled by the constant "a", and an oscillating term controlled by the constant "b".

Recalling the expression for the damped free vibration response of a single degree of freedom system, it can be seen that the $-\zeta\omega$ in the single degree of freedom analysis case corresponds to "a" in the complex case. Similarly, since

$$e^{ibt} = \cos(bt)+i\sin(bt), \tag{3.07}$$

it can be seen that "b" corresponds to the damped natural frequency of the mode.

The complex eigenvector $\{\phi\}$ contains both displacement and velocity components. The two components (displacement and velocity) within the complex eigenvector are related by the factor "λ". These displacement and velocity components of $\{\phi\}$ may be represented, respectively, by $\{r\}$ and $\{s\}$ such that

$$\{\phi\} = \begin{Bmatrix}\{r\}\\ \{s\}\end{Bmatrix}. \tag{3.08}$$

Equation 3.04 may now be expressed as

$$\{Y\} = Ae^{\lambda t}\begin{Bmatrix}\{r\}\\ \{s\}\end{Bmatrix}. \tag{3.09}$$

The lower half of this equation corresponds to displacement

$$\{Y\}_l = Ae^{\lambda t}\{s\}. \tag{3.10}$$

The upper half corresponds to velocity (eq'n 2.28) which may also be obtained by differentiating the expression for the displacement.

$$\{Y\}_u = Ae^{\lambda t}\{r\} \tag{3.11}$$

$$\{Y\}_u = \frac{d(\{Y\}l)}{dt} = A\lambda e^{\lambda t}\{s\}. \tag{3.12}$$

Therefore

$$\{r\} = \lambda\{s\}. \tag{3.13}$$

The eigenvector may now be reexpressed as

$$\{\phi\} = \begin{Bmatrix}\lambda\ \{s\}\\ .\{s\}\end{Bmatrix}. \tag{3.14}$$

This implies that the eigenvector $\{\phi\}$ represents N unknowns, not 2N.

Once the transformation procedure (equations 2.37 to 2.39) has been carried out and the matrix equation has been uncoupled, an equivalent complex participation factor can be calculated.

$$D_i = P_i^*/A_i^* \tag{3.15}$$

where:

$$P_i^* = -\lambda_i\{s\}_i^T[M]\{1\} \tag{3.16}$$

$$A_i^* = \{\phi\}_i^T[A]\{\phi\}_i \tag{3.17}$$

This can then be used to multiply the original eigenvector and yield a unit participation eigenvector.

It will be shown in section 4.1 that the complex

nature of the eigenvector leads to a time dependent free vibration mode shape and amplitude for nonproportionally damped systems. This is in contrast to the proportional system where only the amplitude is time dependent.

3.3 Comparison of Proportionally Versus Nonproportionally Damped System Characteristics

For purposes of these comparisons, limitations are placed on the values of the uncoupled subsystem parameters. These limitations allow for a reasonable set of possible combinations and yet cover the critical cases. This lends itself to an easier interpretation of the results.

Consider a two level system. The full description of this type of system requires the definition of three uncoupled subsystem parameters as well as the primary damping ratio and frequency. The three parameters are the mass ratio (μ), frequency ratio (θ) and α. The symbols, defined in equations 3.01 to 3.03, for the parameters are simplified for a two level system by dropping the subscripts since they are not needed to differentiate between similar parameters.

Each of these three parameters can be assigned an infinite range of values. In order to maintain a manageable set of combinations, the values of each parameter must be restricted. It is felt that values of the frequency ratio away from unity are not as critical as unity and, therefore,

the frequency ratio is limited to unity. For most structures the secondary damping ratio is less than the primary. With this in mind, α is limited to the range from 0 (most nonproportional) to 1.0 (proportional damping). The smallest mass ratio to be expected is about 0.0001 and so the mass ratio values of 0.01, 0.001 and 0.0001 are used.

When considering a three level system three more parameters are required to completely describe the coupled system. The original three parameters, for a two level system, are still used but are now identified by subscripts. The additional parameters pertain to the tertiary subsystem. They are the tertiary mass ratio (μ_{ts}), frequency ratio (θ_{ts}) and α_t. The same limits are placed on these three parameters as are set above for the secondary subsystem.

The example plots that are used to illustrate the observations and explanations are predominantly based on the two degree of freedom system. This choice is made because an explicit solution exists for the solution to the complex eigen problem for a two degree of freedom system.

With the explicit two degree of freedom solution, the two sets of complex conjugate solutions are obtained in a systematic fashion and allow for a systematic separation of modes.

The three degree of freedom system does not have an explicit solution and, as a result, the solution must be obtained from computer eigensolvers. A computer program

solves in an iterative and a random fashion. This does not allow for a consistent sorting of the modes of vibration if it is based solely on modal frequency.

Consider the results presented in Tables 3.1 and 3.2 for the coupled frequency. In moving from α=1.0 to α=0.0 the relative frequencies of the two modes switch. For α=1.0 mode A has the lower frequency but for α=0.0 mode B has the lower frequency. For these cases of very closely spaced modes, the two modes can be sorted logically if the explicit solution is used. If, however, one is just given two frequencies from an iterative computer solution, then one cannot always make consistent sorting decisions based solely on the modal frequencies.

For a three degree of freedom system with very closely spaced modes, the three modes cannot be separated in a consistent manner based on coupled frequencies of the system. This limits the study of the effects that varying dampings have on the different modes of a coupled system since the modes cannot be separated in a manner that will allow consistent comparisons between systems having different damping characteristics.

For this study, numerical evaluations are carried out using both two and three level systems. Figure 3.1 to 3.4 present the effect that a change in α has on the system characteristics. Each figure represents a particular system characteristic for two systems with different mass ratios.

The four figures are for coupled damping ratios, frequencies, secondary level displacement - eigenvector magnitude and eigenvector phase angle. Each figure includes two mass ratios (μ=0.01, 0.0001).

Tables 3.1 and 3.2 give a numerical description of frequency and damping variations with α. These are supplied since the frequencies are closely spaced and Figure 3.2 does not give a clear indication of how they vary with α. Figures 3.5 and 3.6 give a graphical representation of complex eigenvector elements for a proportionally and nonproportionally damped three degree of freedom system.

The following observations are consistent between the two types of systems.

Referring to Figure 3.1(b), it can be seen that the system exhibits three distinct regions. In the leftmost region the damping ratio of the first mode is very close to the secondary damping ratio while the second mode damping ratio remains relatively constant and very close to the primary damping ratio. The centre region differs from the first in that in this region both modal damping ratios vary in the same manner. Both modal damping ratios (near proportional damping) can be approximated by the average of the uncoupled damping ratios. The right region is a reverse of the left. The first mode has a relatively constant damping ratio approximating that of the primary subsystem and the second mode exhibits a damping ratio very similar to

the secondary damping ratio.

It should be noted that the same plot for the system with the larger mass ratio (Fig. 3.1(a)) demonstrates only one region and it behaves much like the central region of 3.1(b). This central region expands or contracts about $\alpha=1.0$ (proportional damping) depending on the value of the mass ratio and the primary damping ratio. The region is reduced by either decreasing the mass ratio or increasing the primary damping ratio.

The plots of coupled frequency (Figures 3.2(a) and 3.2(b)) are inconclusive. As a result, a tabular presentation is also given in Tables 3.1 and 3.2. Several observations can be made from these tables. First, a larger mass ratio leads to a larger frequency spacing. Second, the case of proportional damping ($\alpha=1.0$) is the case of the largest frequency spacing, if only α is varied. Finally, in moving from a proportional to a nonproportional case, the relative frequencies of the two modes can switch. In other words, for $\mu=0.0001$, mode A has the lower frequency for $\alpha=0.6$ but mode B has the lower frequency for $\alpha=0.8$.

Tables 3.1 and 3.2 also contain information about the damping characteristics of the systems. Table 3.1 contains the value of the real portion of the complex eigenvalue (a). This term controls the decay of the vibration of the system but in its present form does not provide much qualitative information. Table 3.2, on the

other hand, presents an equivalent damping ratio which can be compared directly with the uncoupled quantities. The results presented also support the observation that the coupled damping ratios can be approximated by the average of the uncoupled damping ratios near proportional damping. Also, away from proportional damping, the damping ratios can be approximated by the uncoupled damping ratios.

Figures 3.3 and 3.4 present results for the secondary level displacement eigenvector. Figure 3.3 presents the eigenvector magnitude and 3.4 presents the corresponding phase angle (relative to the positive real axis).

These terms, magnitude and phase angle, can be demonstrated using Figure 3.5. Figure 3.5 is a graphical representation of a set of eigenvectors for a three level system. Each set of three vectors represents the displacement portion of the eigenvector. The eigenvector magnitude represents the actual length of the vector. The phase angle is the angle the vector makes with the horizontal axis.

Figures 3.3 and 3.4 show that changes in secondary damping ratio produce only small changes in the magnitude and phase angle of a secondary level eigenvector element for a system with a large mass ratio. On the other hand, similar changes in the damping ratio for a system with a small mass ratio can lead to changes in eigenvector magnitudes on the

order of 300 or 400 per cent. The phase angle can vary from 0 to 90 to 180 degrees.

These eigenvectors are required if one is to successfully uncouple the complex equations of motion. It should also be noted that only three of the actual six eigenvectors are presented in Figures 3.5 and 3.6. This is because the other three are simply complex conjugates of the first three.

Figure 3.5 presents the three eigenvectors for the three modes of the two selected systems. The proportional case has all of its elements exactly in and out of phase. The nonproportional case shows the tertiary and secondary levels to be 60, 120 and 120 degrees out of phase with each other in each of the three modes.

Figure 3.6 presents the three modal elements for the tertiary level for nonproportional and proportional cases. It can be seen that the proportionally damped case has its elements exactly out of phase with each other. The nonproportional case has elements which are not in or out of phase. It can also be seen that the two systems have elements of different magnitudes in spite of the fact that only the damping has changed.

For each system, especially μ=0.0001, it can be seen that the case of proportional damping requires a less complicated method of description. Figure 3.1 to 3.4 also demonstrate that an increase in the system mass ratio can

also simplify the results since the high mass ratio system contains only one distinct region while the lower contains three.

TABLE 3.1

COUPLED FREQUENCIES AND DAMPING TERMS

$\mu = 0.0010$

ζ_s	α_s	F_A	a_A	F_B	a_B
.00	.0	3.000	-.1062	2.997	-.8363
.01	.2	2.999	-.3345	2.998	-.7967
.02	.4	2.983	-.6380	3.013	-.6819
.03	.6	2.953	-.7335	3.034	-.7750
.04	.8	2.952	-.8233	3.042	-.8739
.05	1.	2.949	-.9131	3.044	-.9728

$\mu = 0.0001$

ζ_s	α_s	F_A	a_A	F_B	a_B
.00	.0	3.000	-.0095	2.996	-.9330
.01	.2	3.000	-.2005	2.996	-.9305
.02	.4	2.999	-.3931	2.996	-.9264
.03	.6	2.998	-.5906	2.997	-.9174
.04	.8	2.994	-.8282	3.000	-.8684
.05	1.	2.981	-.9331	3.011	-.9520

System: $\theta = 1.000$

$\zeta_p = 0.050$

$F_p = 3.000$ Hz.

TABLE 3.2

COUPLED FREQUENCIES AND DAMPING RATIOS

$\mu = 0.0010$

ζ_s	α_s	F_A	ζ_A	F_B	ζ_B
.00	.0	3.000	.0056	2.997	.0444
.01	.2	2.999	.0177	2.998	.0423
.02	.4	2.983	.0340	3.013	.0360
.03	.6	2.953	.0394	3.034	.0406
.04	.8	2.952	.0443	3.042	.0457
.05	1.	2.949	.0508	3.044	.0492

$\mu = 0.0001$

ζ_s	α_s	F_A	ζ_A	F_B	ζ_B
.00	.0	3.000	.0005	2.996	.0495
.01	.2	3.000	.0106	2.996	.0494
.02	.4	2.999	.0209	2.996	.0491
.03	.6	2.998	.0313	2.997	.0487
.04	.8	2.994	.0440	3.000	.0460
.05	1.	2.981	.0498	3.011	.0503

System: $\theta = 1.000$

$\zeta_p = 0.050$

$F_p = 3.000$ Hz.

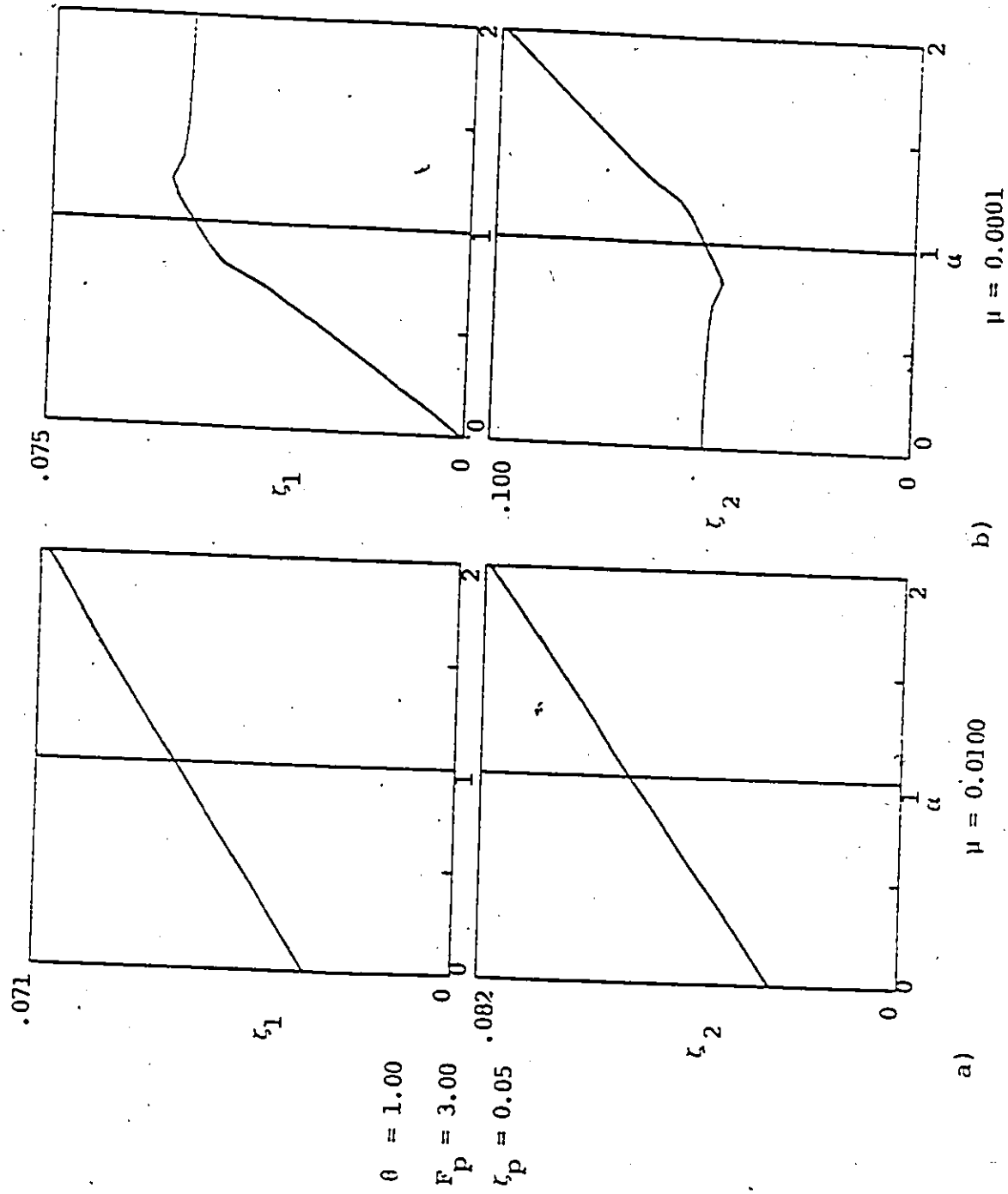

Figure 3.1 Coupled Damping Ratio

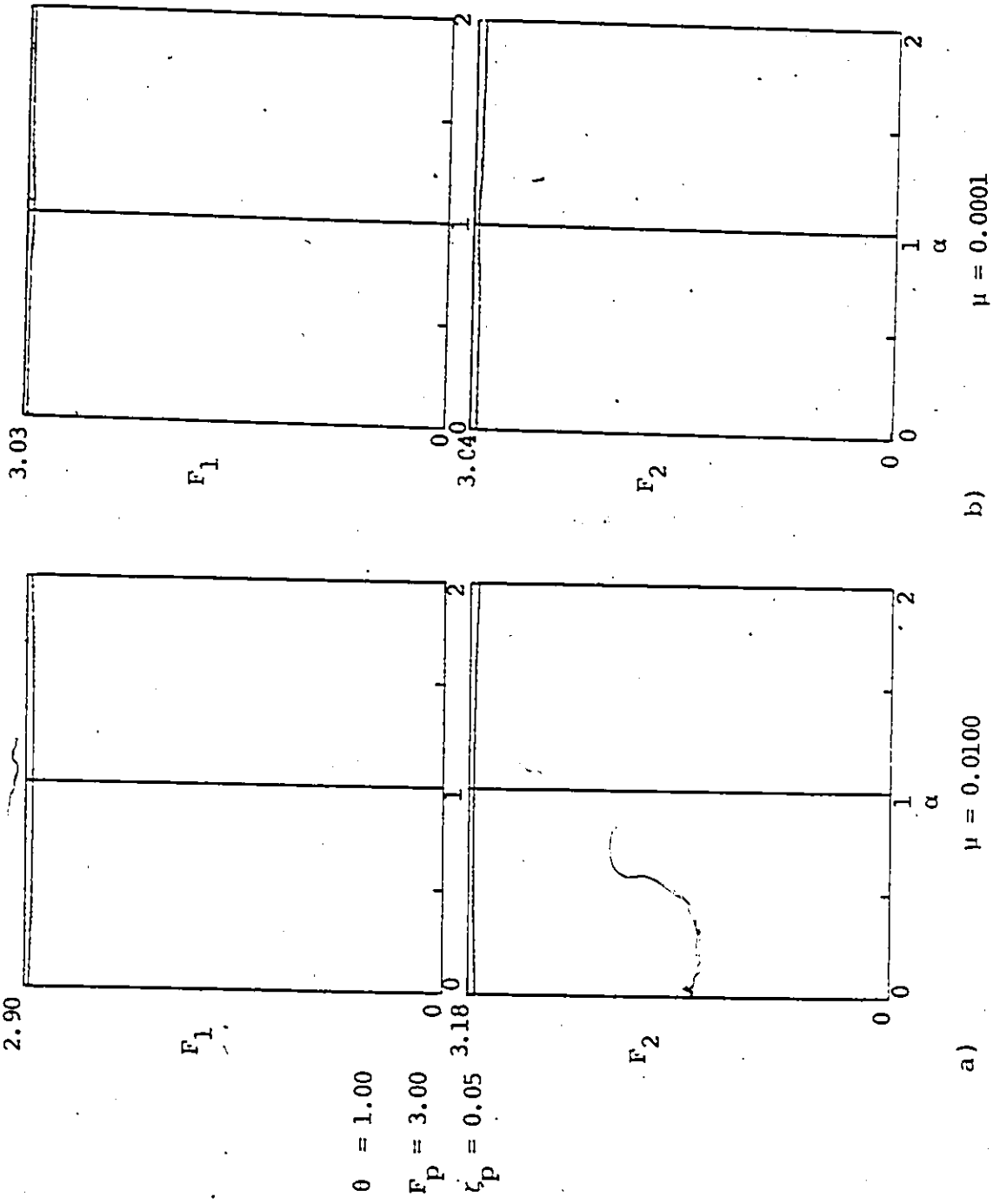

Figure 3.2 Coupled Damped Frequencies

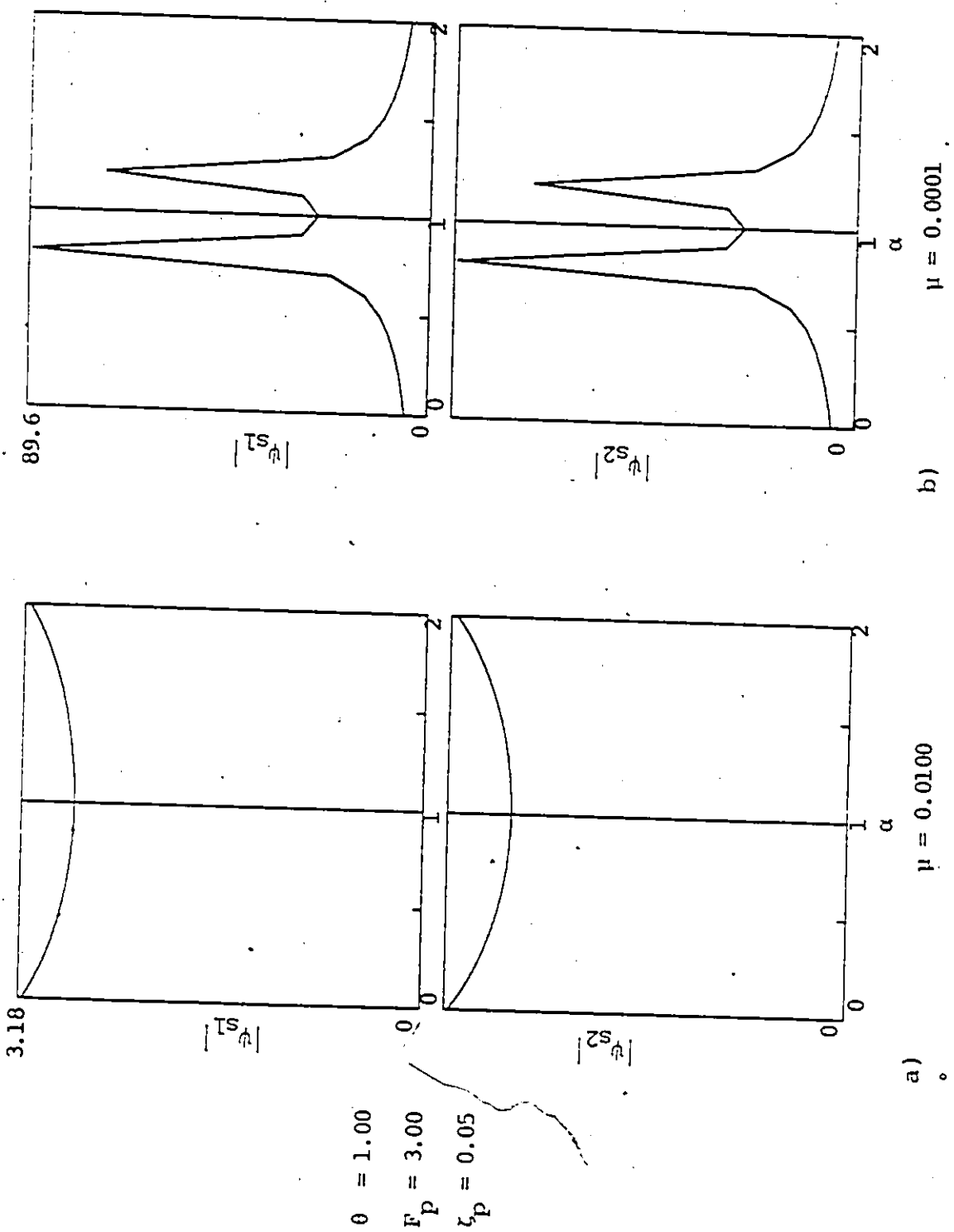

Figure 3.3 Secondary Level Eigenvector Magnitude

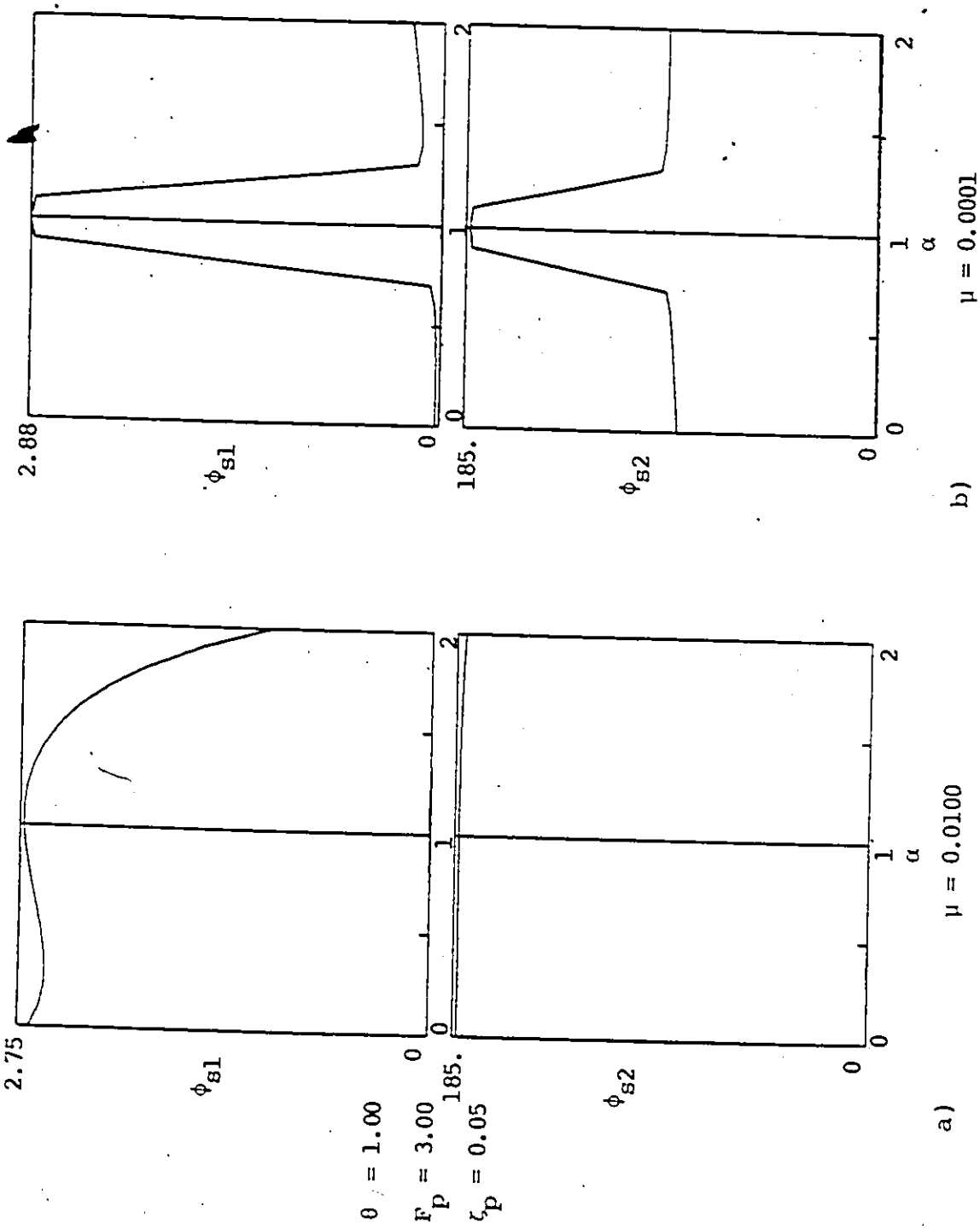

Figure 3.4 Secondary Level Eigenvector Phase Angle

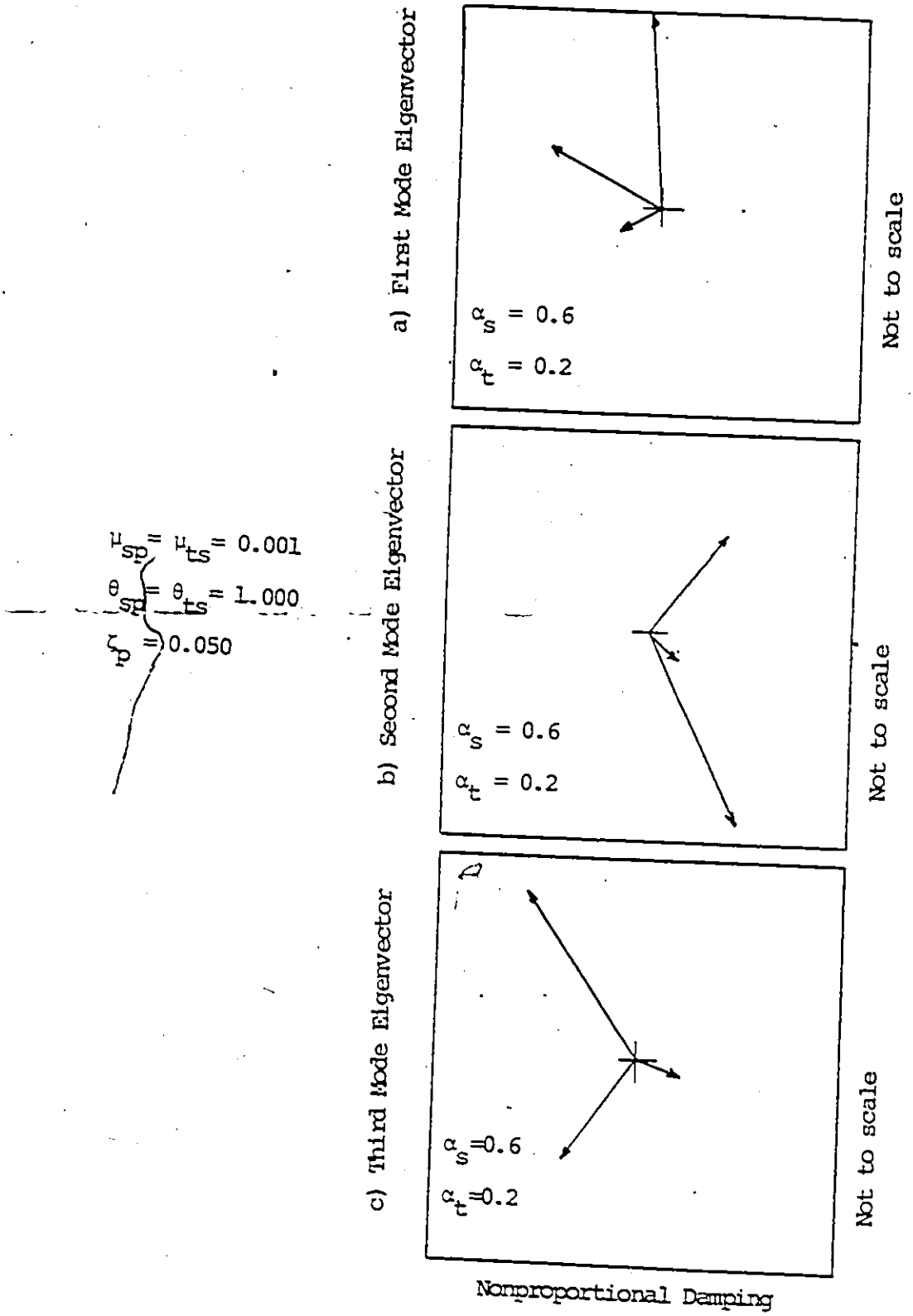

Figure 3.5(a) Three Level System Eigenvectors

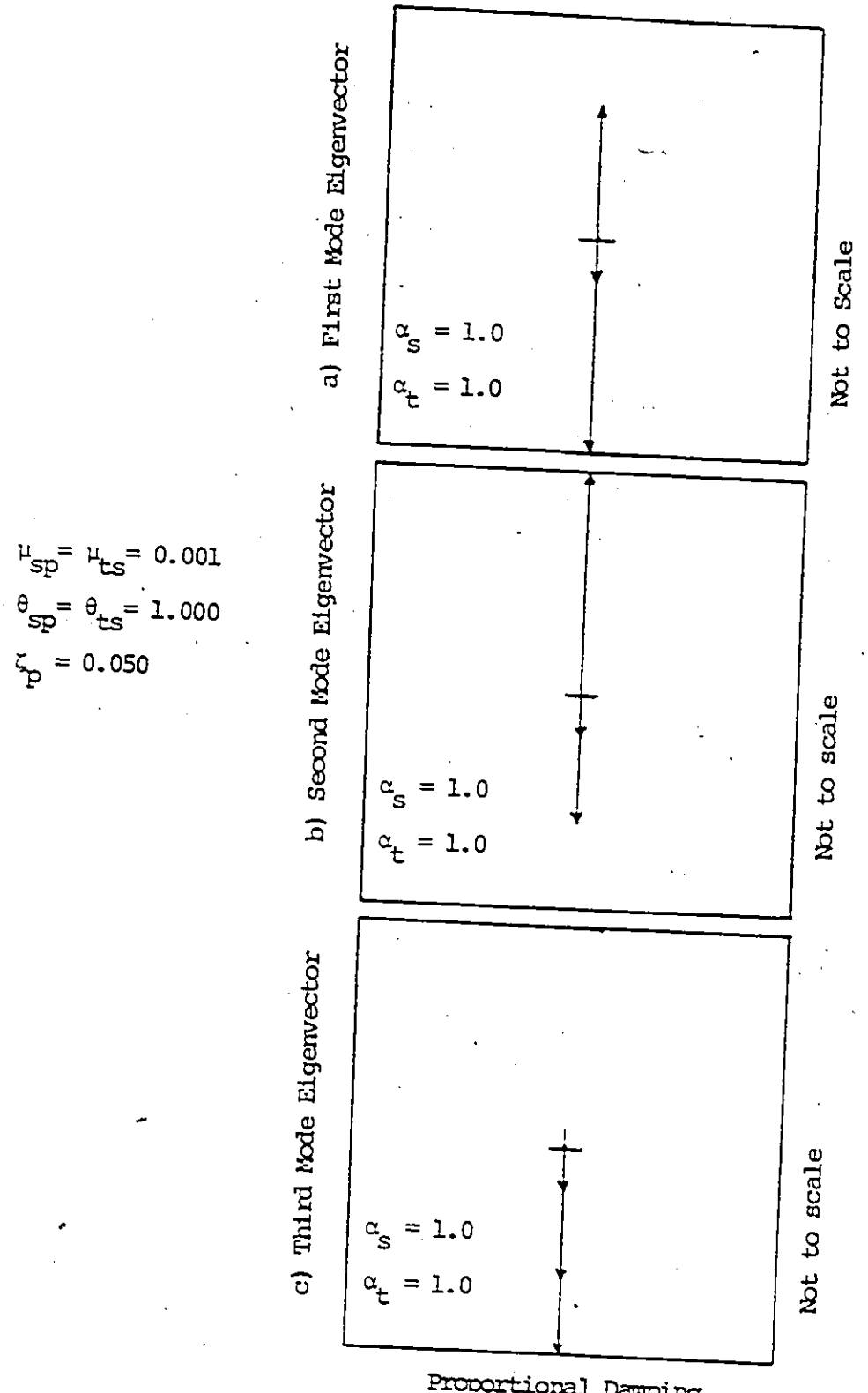

$\mu_{sp} = \mu_{ts} = 0.001$

$\theta_{sp} = \theta_{ts} = 1.000$

$\zeta_p = 0.050$

Figure 3.5(b) Three Level System Eigenvectors

$\mu_{sp} = \mu_{ts} = 0.001$

$\theta_{sp} = \theta_{ts} = 1.000$

$\zeta_p = 0.050$

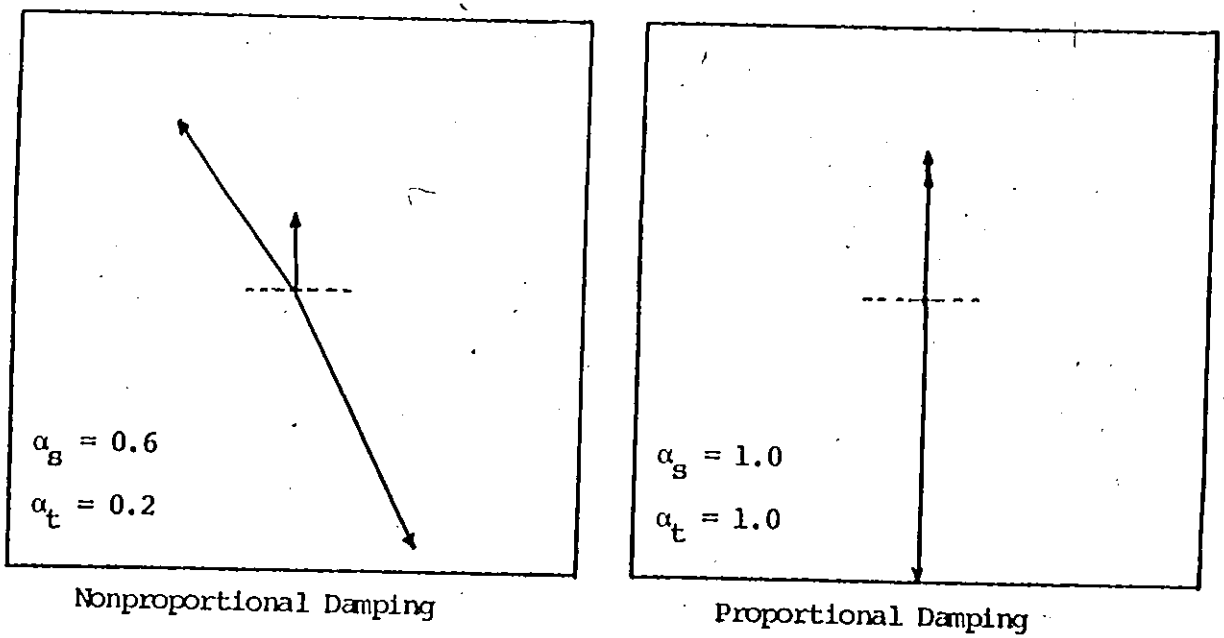

Figure 3.6 Tertiary Level Eigenvector Elements

CHAPTER 4

DAMPED MODAL RESPONSE

4.1 Free Vibration

In section 4.2 a physical interpretation is put on the real and imaginary parts of the complex eigenvalue. The complex eigenvector, however, is a little more difficult to interpret. This section improves on the description of a complex eigenvector. It should be pointed out that in the complex analysis, the eigenvectors are complex, even for the case of proportional damping.

In an attempt to improve the understanding of what these eigenvectors mean, an expression is set out that can be used to examine the mode shape as it varies over time in free vibration.

In the solution of the homogeneous form of the equation of motion (free vibration), it is assumed that the system responds as

$$\{Y\} = e^{\lambda t}\{\phi\} \tag{4.01}$$

The response of one mode may be obtained by combining the solutions for the complex conjugate pair of eigenvalues and eigenvectors, normalized to a unit complex participation factor, corresponding to the mode in question.

$$\{Y\} = e^{\lambda jt}\{\phi\}_j + e^{\lambda j^* t}\{\phi\}_{j^*} \quad (4.02)$$

where the "*" denotes the complex conjugate.

The subscript k = 1,N indicates the mode for which the response is being determined. The subscripts j and j* represent the pair of complex conjugate eigenvalue/vectors which correspond to k.

$$\{Y\}_k = e^{(a+ib)t}\{\phi\}_j + e^{(a-ib)t}\{\phi\}_{j^*} \quad (4.03)$$

$$\{Y\}_k = e^{at}e^{ibt}\{\phi\}_j + e^{at}e^{-ibt}\{\phi\}_{j^*} \quad (4.04)$$

Remembering that

$$e^{ibt} = \cos(bt)+i\sin(bt) \quad (4.05)$$

the above equation can be reduced to:

$$\{Y\}_k = 2e^{at}[\{\phi_R\}_j\cos(bt)-\{\phi_R\}_j\sin(bt)] \quad (4.06)$$

For a particular level "l" within the system, 4.06 may be reexpressed as

$$Y_{kl} = A^* e^{at}\cos(bt+\theta) \quad (4.07)$$

where

$$A^* = 2[(\phi_R)_{jl}^2+(\phi_I)_{jl}^2]^{1/2} \quad (4.08)$$

$$\theta = TAN^{-1}[-(\phi_R)_{jl}/(\phi_I)_{jl}] \quad (4.09)$$

These equations, 4.07 to 4.09, can be related to the graphic representation of an eigenvector given in Figure 4.5. The amplitude A^* represents twice the magnitude of the eigenvector. The factor of two arises from the fact that two complex conjugates are combined to determine the response. The actual response can be represented on Figure 4.5 as twice the projection of the eigenvector on the real (horizontal) axis. The time variation of the mode shape is

obtained by rotating the eigenvector at a rate equal to the damped frequency and taking twice the projection of each eigenvector element on the real axis. It is found, for proportional damping, that the shape of each mode remains constant and only its magnitude is changed, as is expected. The constant shape is caused by the fact that all the eigenvector elements have the same ratio of real and imaginary components.

In the case of nonproportional damping, however, both the magnitude and the actual shape of the mode vary over the complete cycle. It can be seen from the final expression for the response in mode k that any particular level l within the system mode shape will vary sinusoidally. However, each element of the eigenvector corresponding to each level of the system has a different proportion of real and imaginary components. Due to these differing proportions, a phase angle exists in the response between any two levels represented by the eigenvector. As a result of this phase angle, the levels, in general, do not become maximum or minimum at the same time within a mode, as is the case for proportional damping. This leads to a mode shape that varies with respect to time.

Figure 4.1 to 4.3 illustrate mode shapes of systems as they vary over one cycle. The only quantity that differs between the systems is α. A value of 1.0 represents a proportionally damped system while 0.6 and 0.25 represent

increasingly more nonproportionally damped systems.

It can be seen from Figure 4.1 that the shape of the mode does not vary over the cycle. Figure 4.3, on the other hand, illustrates a system where the mode shape is continually changing over the cycle.

It should be noted that, for the sake of convenience, the amplitude decay over the cycle has not been included in the plots. These only represent the shape over one cycle.

A distinction should be made, at this point, between eigenvectors and mode shapes. An eigenvector is a set of numbers that can be used, along with all others corresponding to a particular system, to transform the coupled matrix equation of motion for the system into a set of uncoupled scalar equations. The mode shape, on the other hand, is a description of the shape that the system deforms into when it responds in free vibration.

The eigenproblem is based on the assumption of free vibration and a damped system. The assumed response is described by equation 4.01. The eigenvector is a set of complex numbers which can be used to uncouple the modified matrix equation that is used in complex modal analysis. The actual response of a mode is obtained by combining the results for a set of complex conjugate eigenvalues and vectors. When combined, these yield a real valued free vibration response which defines the shape of the mode of

vibration (mode shape).

4.2 Modal Response to a Sinusoidal Base Motion

In addition to the free vibration response of a nonproportionally damped mode of vibration, an expression can also be developed for maximum modal response due to a resonant sinusoidal base motion.

For a unit participation eigenvector, the typical transformed equation of motion is of the form of

$$\dot{Z}_j - \lambda_j Z_j = A\sin(\Omega t) \tag{4.10}$$

where A is the amplitude and Ω is the frequency of the sinusoidal base motion.

The solution of the differential equation is made up of the complementary and particular solutions. Since the complementary solution involves the homogeneous equation (free vibration) it may be ignored if one is concerned with the damped steady state response. $\sin(\Omega t)$ may be expressed as

$$\sin(\Omega t) = -(i/2)(e^{i\Omega t} - e^{-i\Omega t}) \tag{4.11}$$

Substituting equation 4.11 into 4.10,

$$\dot{Z}_j - \lambda_j Z_j = -A(i/2)(e^{i\Omega t} - e^{-i\Omega t}) \tag{4.12}$$

Assuming that the particular solution will be of the form

$$Z_j^P = G_1 e^{i\Omega t} + G_2 e^{-i\Omega t} \tag{4.13}$$

and substituting into equation 4.09, then

$$G_1 = -A(\Omega - i\lambda_j)/2/(\Omega^2 + \lambda_j^2) \tag{4.14}$$

$$G_2 = -A(\Omega + i\lambda_j)/2/(\Omega^2 + \lambda_j^2) \tag{4.15}$$

With these values of G_1 and G_2

$$z_j^p = -A(\Omega\cos(\Omega t)+\lambda_j\sin(\Omega t))/(\Omega^2+\lambda_j^2) \quad (4.16)$$

This expression now gives the amplitude of the modal response with respect to time.

The modal response can now be obtained as

$$\{Y_j\}_p = \{\phi\}_j z_j^p \quad (4.17)$$

$$= -\{\phi\}_j A(\Omega\cos(\Omega t)+\lambda_j\sin(\Omega t))/(\Omega^2+\lambda_j^2) \quad (4.18)$$

When $-\zeta\omega+i\omega_D$ is substituted for λ_j and the imaginary quantities are removed from the denominator, the result is

$$\{Y_j\}_p = -A\{\phi\}_j[U+iV]/(u^2+v^2) \quad (4.19)$$

where $u = \Omega^2-\omega_D^2+\zeta^2\omega^2$ (4.20)

$$v = 2\zeta\omega\omega_D \quad (4.21)$$

$$U = u(\Omega\cos(\Omega t)-\zeta\omega\sin(\Omega t))-v\omega_D\sin(\Omega t) \quad (4.22)$$

$$V = u\omega_D\sin(\Omega t)+v(\Omega\cos(\Omega t)-\zeta\omega\sin(\Omega t)) \quad (4.23)$$

A single mode equivalent response can be obtained by adding the response of the two complex conjugate modes. The total response is simply twice the real part of either modal response. It must be remembered that $\{\phi\}_j$ is a complex quantity.

$$\{Y_j\}_{ptot} = -2A[R\sin(\Omega t)-S\cos(\Omega t)]/(u^2+v^2) \quad (4.24)$$

where $R = (u\zeta\omega+v\omega_D)\{\phi_R\}_j+(u\omega_D-v\zeta\omega)\{\phi_I\}_j$ (4.25)

$$S = \Omega(u\{\phi_R\}-v\{\phi_I\}_j) \quad (4.26)$$

Equation 4.19 can be used to determine the maximum steady state response of the system to a sinusoidal base motion. For small damping ratios (ie. less than 0.05) $\omega=\omega_D$. Let $\omega=\Omega$. The maximum response at level 1 is now given as

$$(Y_1)_{max} = A(r\sin(h) + s\cos(h))/(2\omega\zeta) \quad (4.27)$$

where $r = 2(\phi_R)_{jl}\zeta(\phi_I)_{jl}$ (4.28)

$s = 2(\phi_I)_{jl}\zeta(\phi_R)_{jl}$ (4.29)

$h = TAN^{-1}(r/s)$. (4.30)

4.3 Phase Relationship Between Forced Modal Responses

A brief study was carried out to determine how the modal responses related to each other as the system underwent a resonant sinusoidal base motion. Figure 4.4 and 4.5 represent the typical secondary level results that are obtained for a two degree of freedom system with the given uncoupled characteristics.

Figure 4.4 describes the modal and total response of a system exhibiting substantial nonproportional damping. In this case, it can be seen that the two modes are exactly out of phase with each other at the secondary level. As a result, The total response is the difference between the modal responses. This allows the maximum response to be estimated as the difference between modal maxima. This leads to a total response which is lower than either of the modal responses.

Figure 4.5, on the other hand, describes the response of a similar system exhibiting proportional damping. In this case, the modal responses are not exactly out of phase. This leads to the total response being about ninety degrees out of phase with the modal responses . As a result, the maximum response is not the difference in the

modal maxima but rather is a sum of non maximum modal responses that occur during the short time when the modal responses are in phase.

This difference in modal response combination is tied to the spacing of the modal frequencies. For the nonproportionally damped case, Figure 4.4, the modal frequencies are very close together. Since both modes have essentially the same frequency, the modal amplitudes will have the same variation over time with the exception that the amplitudes will differ depending on the modal damping ratios. The actual response is the product of the modal amplitude and the eigenvector. The phase relationship between the two modes, then, is dependent on the phase relationship between eigenvectors since the amplitudes are in phase. For this system the eigenvectors are 180 degrees out of phase and so are the modal responses.

For the proportionally damped case, the frequencies are spaced more widely. In this case the modal amplitudes do not respond exactly the same. This can lead to a lag between the two modal amplitudes. This slight lag allows for the two modes to add up over some period of time since the modal responses are not always out of phase. This is demonstrated in Figure 4.5.

These observations imply that the maximum of the total response of a system exhibiting significant nonproportional damping may be estimated as the signed sum

of the maximum modal responses.

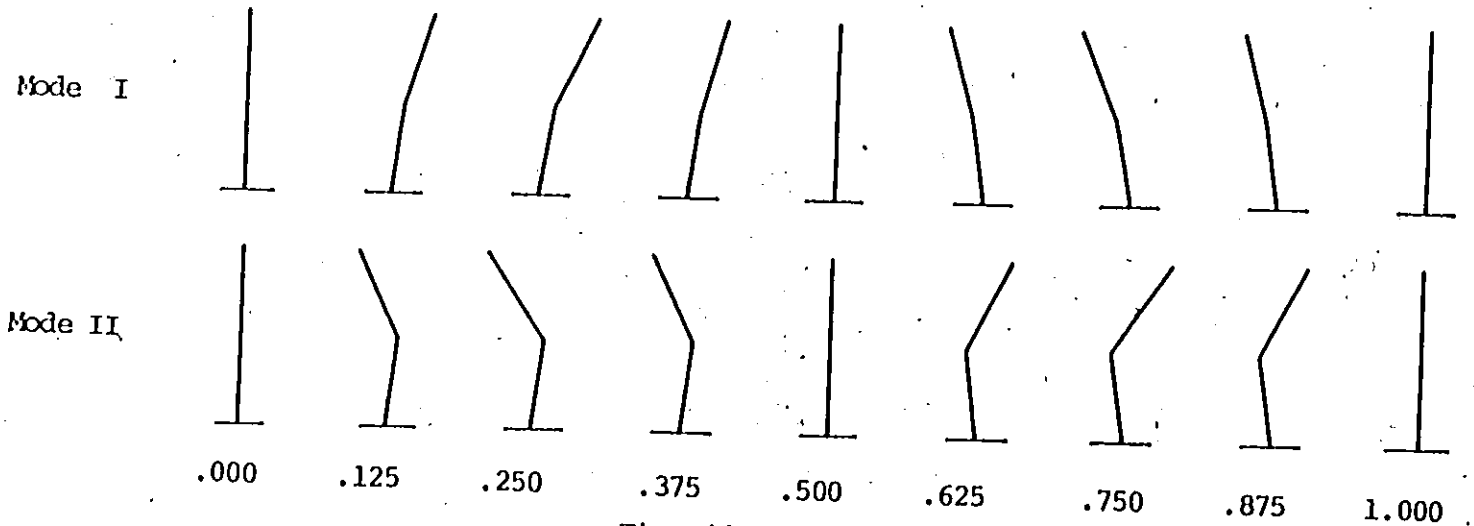

$\mu = 0.001$

$\theta = 1.000$

$F_p = 3.000$

$\zeta_p = 0.050$

$\alpha = 1.000$

Figure 4.1 Free Vibration Modal Response

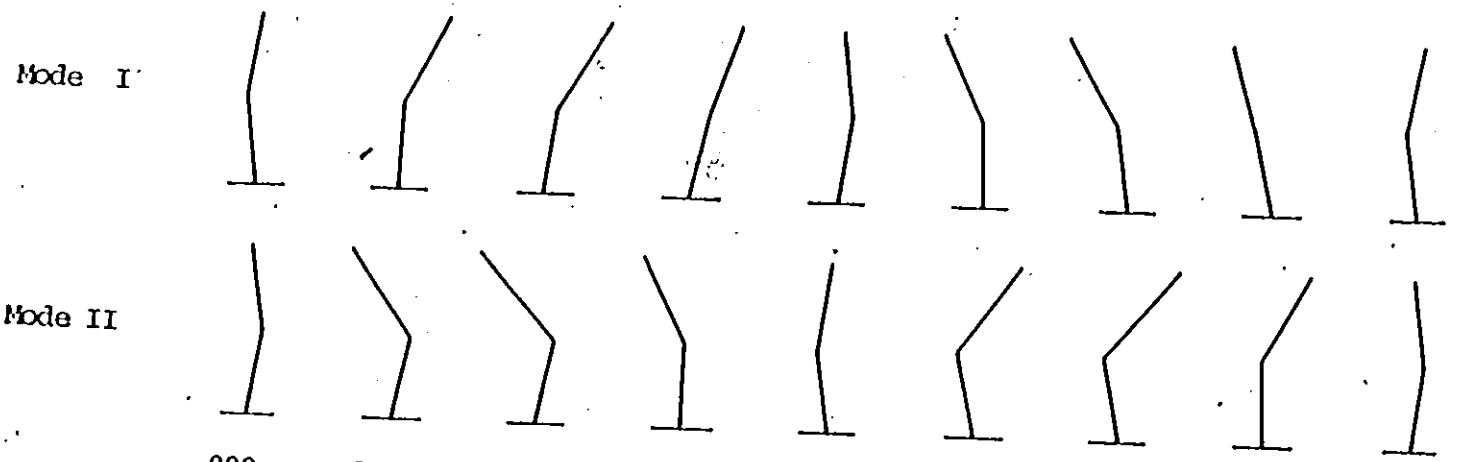

μ = 0.001

θ = 1.000

F_p = 3.000

ζ_p = 0.050

α = 0.600

Figure 4.2 Free Vibration Modal Response

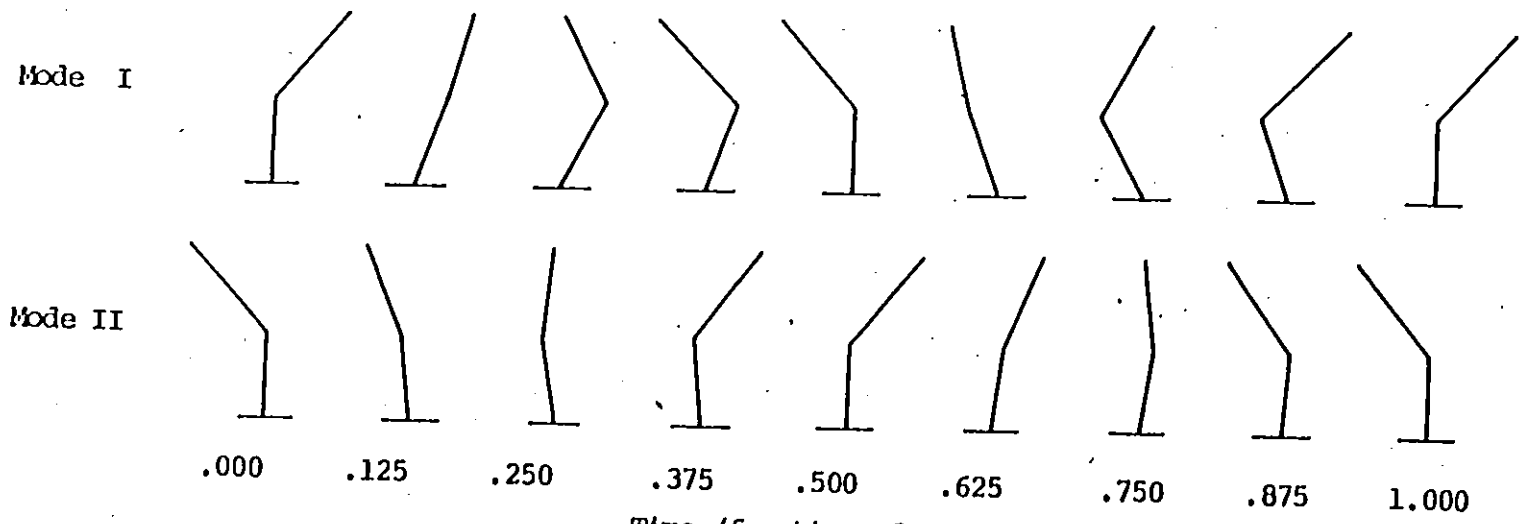

$\mu = 0.001$

$\theta = 1.000$

$F_p = 3.000$

$\zeta_p = 0.050$

$\alpha = 0.250$

Figure 4.3 Free Vibration Modal Response

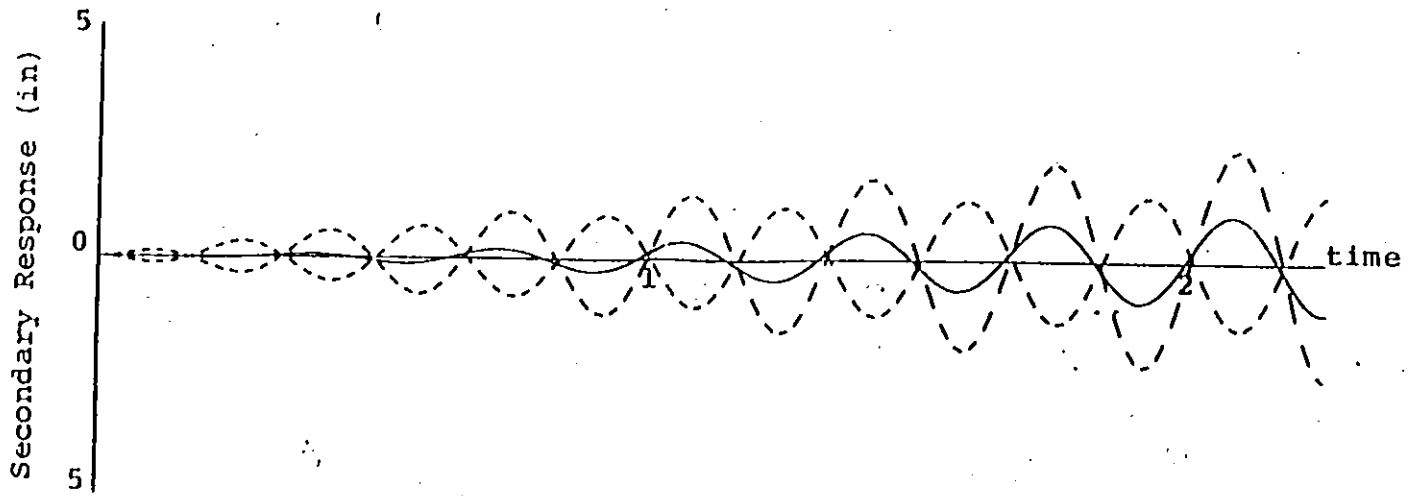

——— Total Response

- - - Modal Response

$\mu = 0.001$

$\theta = 1.000$

$F_p = 3.000$

$\zeta_p = 0.050$

$\alpha = 0.100$

Figure 4.4 Response to 3 Hz Sinusoidal Base Motion

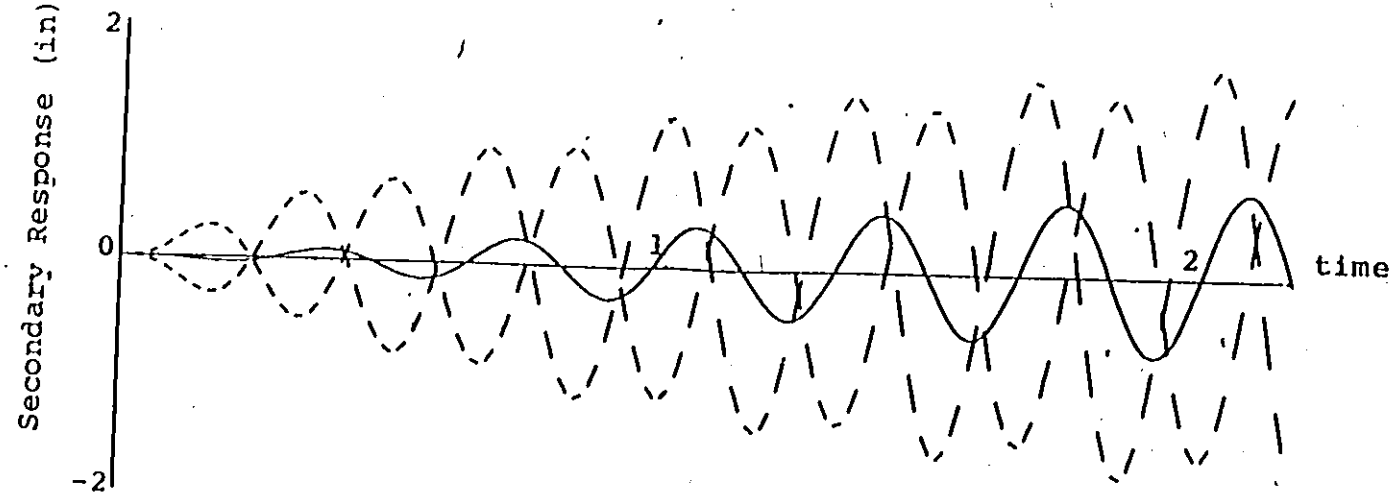

——— Total Response

- - - Modal Response

μ = 0.001

θ = 1.000

F_p = 3.000

ζ_p = 0.050

α = 1.000

Figure 4.5 Response to 3 Hz Sinusoidal Base Motion

CHAPTER 5

TWO DEGREE OF FREEDOM SYSTEM COUPLED CHARACTERISTICS

5.1 System Definition

This chapter is devoted to a study of two level systems. The analysis uses the simplest of two level systems, a two degree of freedom system.

Each level of the system has a mass associated with it. Remembering the standard or complex matrix equation of motion that can be derived for this system, it can be seen that each equation within it can be divided by M_p and thereby eliminate the primary mass from the calculations. What remains, rather, is the ratio of the secondary to primary masses. This quantity is called "μ". Also, the system response is dependent on this quantity rather than the absolute primary and secondary masses. This independence of absolute mass arises from the fact that the inertial forces due to a seismic base motion are proportional to mass and each forcing function on the right hand side of the equation is divided by M_p as well.

Associated with each subsystem mass is an uncoupled circular frequency (ω). Instead of using the frequencies of the subsystems, the quantities of primary frequency and

frequency ratio (θ) are used. This parameter (θ) represents the square of the ratio of secondary to primary frequencies.

The final quantity that is associated with each single degree of freedom system is the damping coefficient (C). This quantity is related to the damping ratio as

$$\zeta_i = C_i/(2M_i\omega_i) \tag{5.00}$$

The damping ratio (ζ_i) can now be used to define the final parameter. It is defined in Chapter 3 as

$$\alpha = (\zeta_s\omega_p)/(\zeta_p\omega_s) \tag{3.03}$$

The importance of this parameter (α) is that a value of unity denotes a system that is proportionally damped. Finally, the motion of each subsystem, with respect to the base, is represented by X_p and X_s.

For purposes of this study, μ is set equal to 0.01, 0.001 and 0.0001, ω_p is set to 18.85 sec^{-1} (3Hz), θ is set to 1.00 and α is varied from 0.0 to 1.0.

5.2 Closed Form Solution for Eigen Problem

(Zero Secondary Damping)

Chapter 2 presents the complex modal analysis procedure for the solution of the seismic response of a system exhibiting nonproportional damping. One of the difficulties of the method is the determination of the 2N complex eigenvalues and corresponding eigenvectors. In all but the simplest cases, this solution must be obtained from "black box" eigen solvers on a computer. As a result, it is

more difficult to follow the effect that the variation of different parameters has on the resulting coupled characteristics of the system. In addition, a closed form solution can serve as a form of verification for other methods of calculating eigenvalues and vectors that may be used.

A single degree of freedom system has a well defined solution, for any damping situation, available in any textbook on structural dynamics. A two degree of freedom system is obviously the next simplest system. Standard procedures can yield closed form solutions for the eigen problem, provided the system is undamped or exhibits proportional damping. This method yields a quadratic, in terms of the eigenvalue, characteristic equation dependent on the system mass and frequency ratios. This quadratic has a closed form solution and leads to a closed form solution for the eigenvectors, as well. The damping ratios are obtained from the assumption of proportional damping.

Unfortunately, the general case of two degree of freedom systems involves systems exhibiting nonproportional damping. The characteristic equation in this case is a quartic in terms of the eigenvalue. This equation is dependent on the mass, frequency and damping ratios.

There is, in general, no closed form solution for a quartic equation. There is, however, an explicit(noniterative) solution for a quartic. This is

described in Appendix V along with the solution for the eigenvectors. Appendix V supplies an explicit method but not a closed form solution to determine the complex eigenvalues and vectors for a two degree of freedom system.

There is, however, at least one nonproportionally damped system for which a closed form solution can be obtained. This is the case of an undamped secondary system. Later in this thesis it is shown that this case of an undamped secondary system is often the "worst case" as far as induced errors in predicted response are concerned.

Consider the case of a primary system having primary and secondary subsystem frequencies of ω, a mass ratio of μ, a primary damping ratio of ζ and a secondary damping ratio of zero ($\alpha=0$). The characteristic equation for this simplified system reduces to

$$\lambda^4 + a\lambda^3 + b\lambda^2 + c\lambda + d = 0 \qquad (5.01)$$

where $a = 2\zeta\omega$

$b = \omega^2(2+\mu)$

$c = 2\omega^3\zeta$

$d = \omega^4$

This leads to the resolvent equation

$$y^3 + py^2 + qy + r = 0 \qquad (5.02)$$

where $p = -\omega^2(2+\mu)$

$q = 4\zeta^2\omega^4 - 4\omega^4$

$r = -(8\zeta^2\omega^6 - 4\omega^6(2+\mu))$

The quantity $(y-2\omega^2)$ can be factored out of equation 5.02.

Therefore, $2\omega^2$ is one of the roots of the resolvent equation. This root can be used to determine the quantity R which is integral to the solution, as shown in Appendix IV.

$$R = (a^2/4 - b + y)^{1/2} \tag{5.03}$$

This can be reduced to

$$R = \omega(\zeta^2-\mu)^{1/2} \tag{5.04}$$

Depending on the sign of the expressions within the square root

$$R = \omega(|\zeta^2-\mu|)^{1/2}, \quad \zeta^2-\mu>0 \tag{5.05}$$

$$R = \pm i\omega(|\omega^2-\mu|)^{1/2}, \quad \omega2-\mu<0 \tag{5.06}$$

$$R = 0, \quad \omega^2-\mu=0 \tag{5.07}$$

The expressions for the roots of the characteristic equation can be developed, using the value of R, as:

$\zeta^2-\mu>0$:
$$2\lambda_{1,2} = -\zeta\omega+(|\zeta^2-\mu|)^{1/2}\omega+(3a^2-R^2 \quad -2b+[4ab-8c-a^3]/R)^{1/2} \tag{5.08}$$

$$2\lambda_{3,4} = -\zeta\omega-(|\zeta^2-\mu|)^{1/2}\omega+(3a^2-R^2 \quad -2b-[4ab-8c-a^3]/R)^{1/2} \tag{5.09}$$

$\zeta^2-\mu=0$:
$$2\lambda_{1,2,3,4} = -\zeta\omega\pm i\omega(4+2\mu-3\zeta^2)^{1/2} \tag{5.10}$$

$\zeta^2-\mu<0$:
$$2\lambda_{1,2,3,4} = -\zeta\omega\pm i\{\omega(|\zeta^2-\mu|)^{1/2}+(|-3a^2+R^2 \quad +2b\pm(4ab-8c-a^3)/R|)^{1/2}\} \tag{5.11}$$

Once the eigenvalues are evaluated the corresponding eigenvectors may be calculated using the expressions given in Appendix V.

It can be seen from equation 5.10 that if $\zeta^2-\mu=0$ (ie. $\mu=\zeta^2$) then the coupled system will possess two modes of vibration which have identical damped frequencies and damping ratios.

When the mass ratio is greater than the square of the damping ratio both sets of eigenvalues exhibit the same real component. As a result, both modes exhibit the same level of damping but differing frequencies. When the mass ratio is less the two modes exhibit differing damping levels and frequencies. These results are in agreement with those plotted in Figure 5.1. This helps verify the computer program results which are produced based on the general explicit solution.

It has been shown, for this simple case, that a closed form solution can be obtained for the complex eigenvalues. A general comparison, however, will require the use of the explicit, but not closed form, solution outlined in Appendix V.

5.3 Complex Coupled Characteristics

With the uncoupled subsystem parameters defined, the next step is to plot the resulting coupled system characteristics (frequencies, damping ratios and eigenvectors) that are predicted by the complex analysis. The plots are made against the independent variable α. For purposes of this study α reduces to the ratio of secondary to primary damping ratios. The range of parameters is given in section 5.1. The primary damping is set to either 3 or 5 per cent.

A set of sample plots are given in Figures 5.1 to

5.4. Referring to Figure 5.1(b), it can be seen that the system exhibits three distinct regions. In the leftmost region the damping ratio of the first mode is very close to the secondary damping ratio while the second mode damping ratio remains relatively constant and close to the primary damping ratio. The central region differs from the first in that in this region both modal damping ratios (near proportional damping) can be approximated by the average of the uncoupled damping ratios. The remaining region is the reverse of the left one with the first mode having a relatively constant damping ratio approximating that of the primary damping ratio. The second mode demonstrates a damping ratio close to that of the secondary subsystem.

The same plot for the higher mass ratio (Fig. 5.1(a)) demonstrates only one zone and that behaves very much like the central region for the lower mass ratio system. The closed form solution results indicate that the two damping ratios should be equal to each other at $\alpha=0.0$ since $(\mu=.01)>(\zeta^2=.0025)$. In order for the damping ratios to be equal the central region must extend to $\alpha=0.0$ since the two outer regions exhibit distinct damping ratios.

Figure 5.2 shows that the damped frequencies are not affected very much by a variation in secondary damping.

The trend demonstrated by the damping ratios is also evident with the magnitudes of the eigenvector. The main difference is that the magnitudes of the eigenvector show a

curvilinear relationship with respect to α while the damping ratios show a more linear relationship.

5.4 Complex Eigenvector Phase Angle

Part of the problem in the interpretation of the complex coupled system results is the complex eigenvector. For the two degree of freedom systems being studied, it is found that most of the eigenvectors exhibit relative phase angles between the secondary and primary levels (within the eigenvector) of 0, 90 or 180 degrees plus or minus a few degrees.

These three relative phase angles between the levels of the system can be interpreted in terms of the mode shape variation. Recalling in Chapter 3 that the physical mode shape is represented by the projection of the rotating eigenvector on the real axis, one can place a physical interpretation on the relative phase angles of 0, 90 and 180 degrees. Essentially a 0 relative phase angle implies that the eigenvector elements and thus the free vibration reponse for the two levels are in phase. On the other hand, a relative phase angle of 180 degrees indicates that the levels are exactly out of phase. In both cases the levels achieve maximum displacements, during free vibration, at the same time. As a result, the maximum secondary level distortion is equal to the difference between the maximum secondary and primary displacements.

The case of the relative phase angle of 90 degrees is slightly different. For free vibration, when one level reaches a maximum (vector lying along the real axis), the other level reaches zero response (vector lying along imaginary axis) and vice versa. The maximum distortion of the secondary level can be determined, however, since both of the levels respond sinusoidally with a phase angle of 90 degrees between them. The frequencies are also the same.

$$X_s = A\sin(\omega t) \tag{5.13}$$

$$X_p = B\cos(\omega t) \tag{5.14}$$

$$[X_s - X_p]_{max} = A\sin D + B\cos D \tag{5.15}$$

where: $D = TAN^{-1}(-B/A)$

5.5 Numerical Evaluation of Transition Points

In the previous section it was shown that much of the phase angle relationship within and between modes could be reduced to 0, 90 or 180 degrees, approximately. This section deals with another observation that can be made from the plots of coupled system characteristics. This characteristic is similar in all the different plots that are common to a coupled system. Especially for more nonproportionally damped systems, each plot can be divided into three regions.

These regions are delineated by points of transition of the curve within each of the plots. This is illustrated in Figures 5.1 to 5.4. Comparison of Figure 5.1(a) to 5.1(b)

shows that this delineation becomes less visible as the mass ratio is increased. Similarly, this lessening occurs with a decrease in the primary damping ratio.

A rough evaluation of this phenomenon was carried out and the results are given in this section. These points, in most cases, are fairly well defined for each coupled system. A series of coupled damping ratio plots were set up and used to determine the points of transition in terms of the system parameter α, for selected values of primary damping ratio and mass ratio. A table was developed which gave the transition point above α=1.0 for each damping and mass ratio. The table is given as Table 5.1.

It was also observed that the two points of transition were equally spaced about α=1.0. The evaluation is based on calculations using the upper point since it exists at α's farther above 1.0 than below 1.0 (ie. minimum point = 0.0).

Rough plots showed that the transition point varied in proportion to the square root of the mass ratio and in inverse proportion to the primary damping ratio. Based on this observation, it is possible to determine a proportionality constant for each combination of damping and mass ratio. The average constant is 0.88. In other words,

$$\alpha_{trans} = 1 \pm .88(\mu^{1/2})/\zeta_p \qquad (5.16)$$

Again referring to Figure 5.1(b), it can be seen that, within the region between these two points, the

damping ratios predicted by complex modal analysis tend to be averages of the uncoupled damping ratios. Similarly, outside these points, the complex modal analysis procedure predicts values which tend to be close to the individual uncoupled damping ratios.

Unfortunately, for some of the other plots, like eigenvector magnitude (Figure 5.3), these points do not delineate the limits for constant or linear relationships but rather points of maximum magnitude of the eigenvector. Between these two points the eigenvector magnitude drops from a peak down to a minimum (at proportional damping) and then back up to another peak at the other transition point.

TABLE 5.1

COMPUTED TRANSITION POINT POSITION (α_{trans})

ζ_p	Mass Ratio				
	0.01	0.003	0.001	0.0003	0.0001
0.01	----	----	----	----	1.90
0.02	----	----	----	1.80	1.50
0.03	----	----	1.90	1.50	1.30
0.04	----	----	1.70	1.40	1.25
0.05	----	1.90	1.60	1.30	1.20
0.06	----	1.90	1.50	1.25	1.15
0.07	----	1.70	1.40	1.20	1.13
0.08	----	1.60	1.35	1.18	1.10
0.09	2.00	1.50	1.30	1.15	1.08
0.10	1.90	1.45	1.28	1.13	1.07

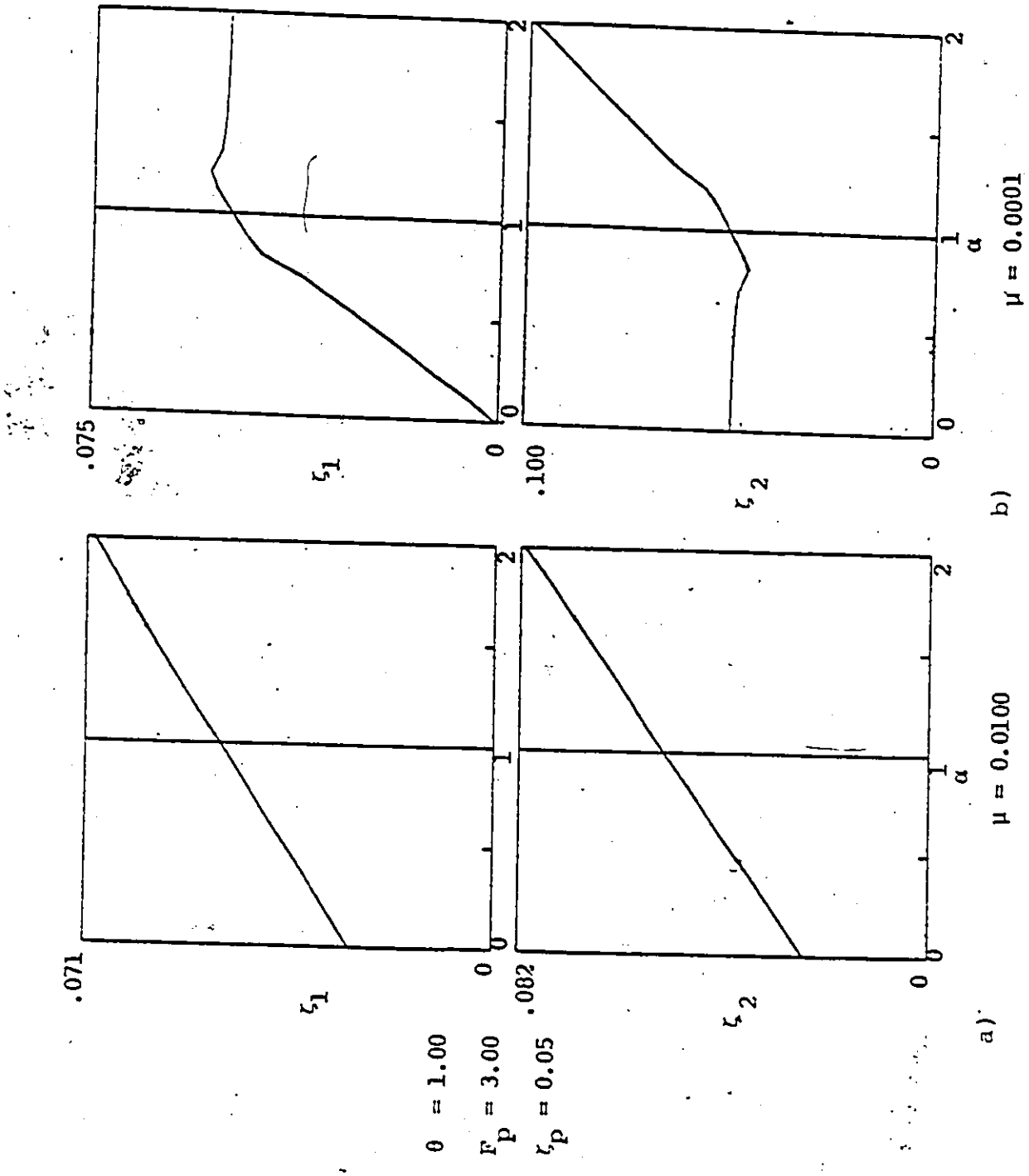

Figure 5.1 Coupled Damping Ratio

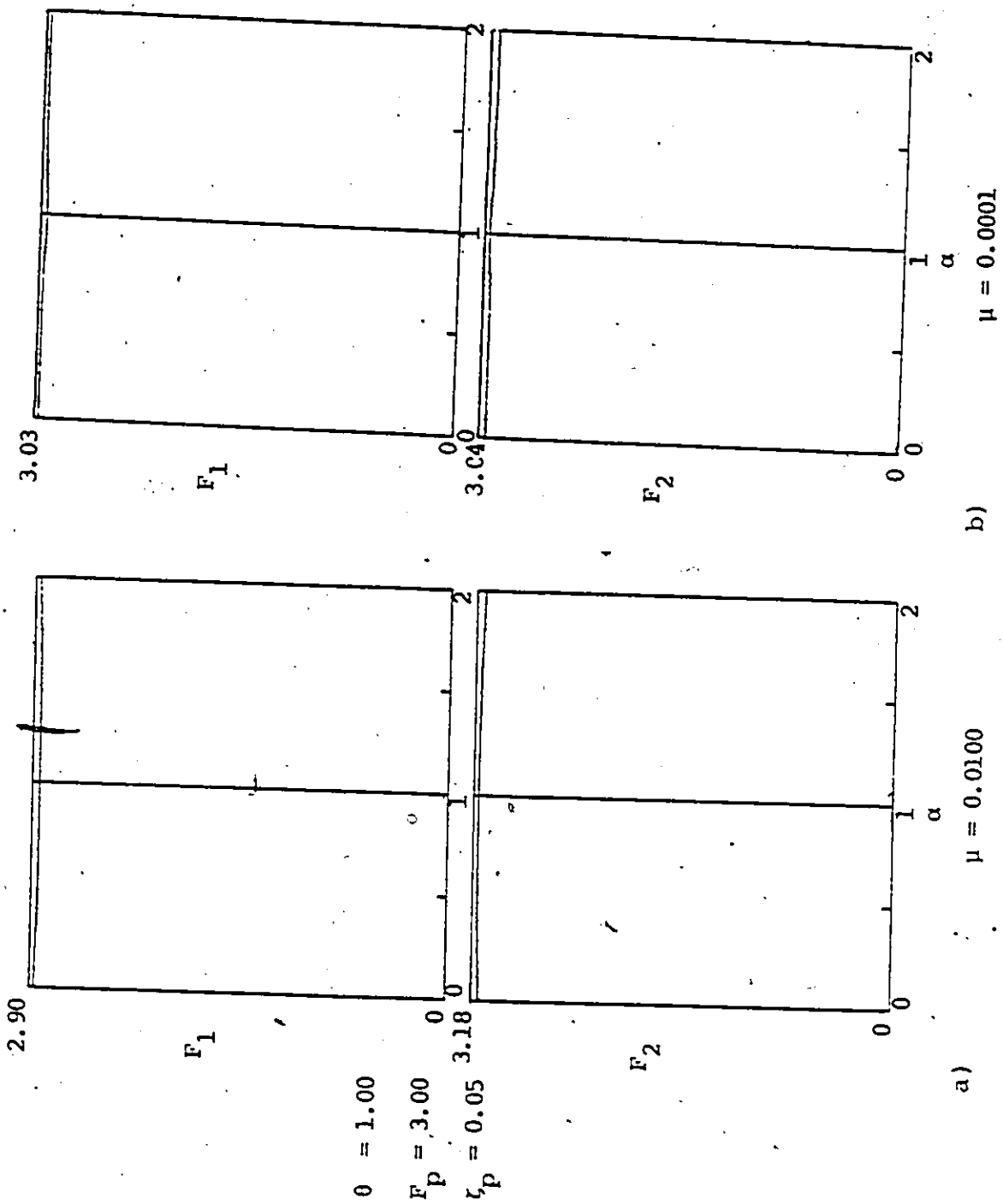

Figure 5.2 Coupled Damped Frequencies

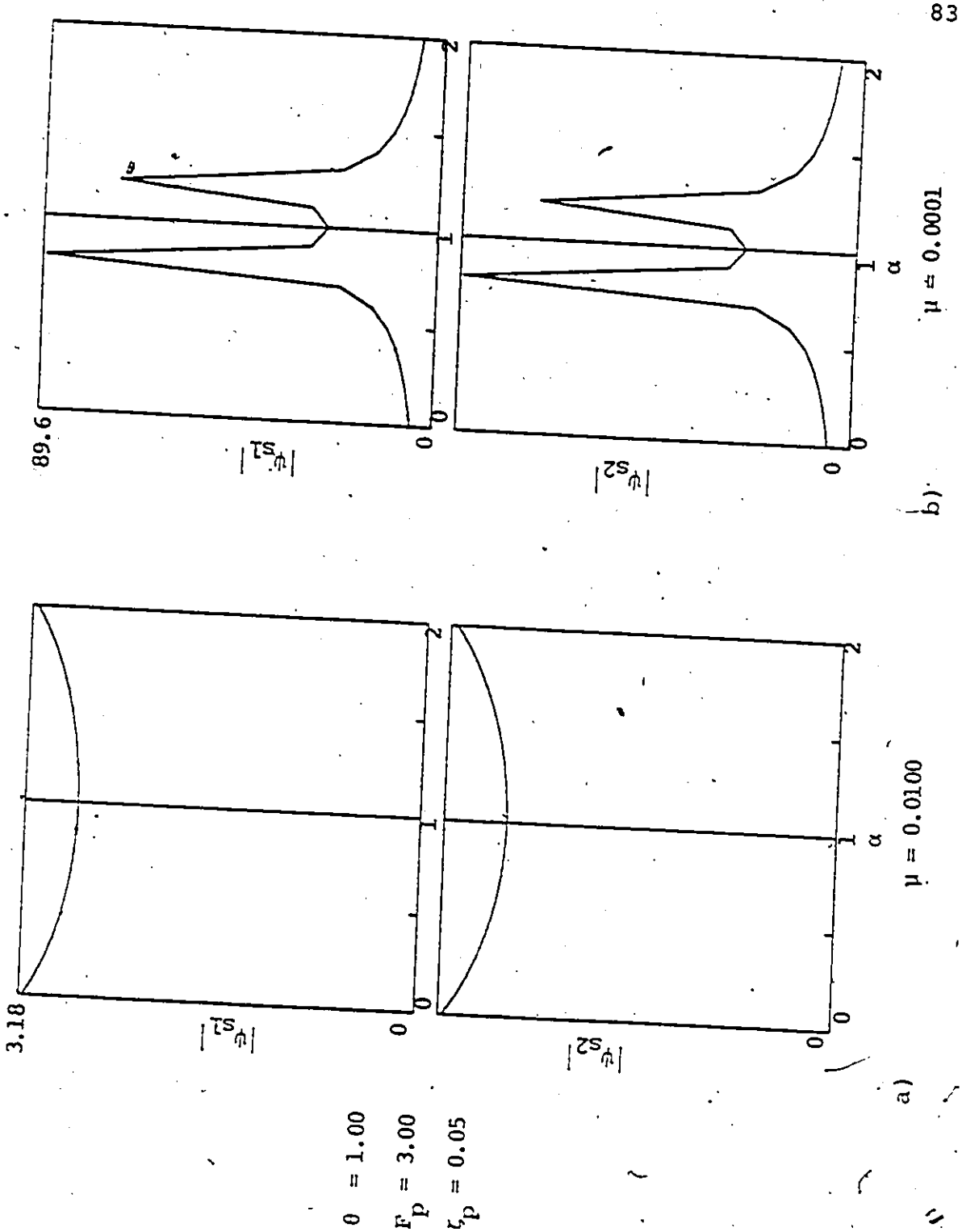

Figure 5.3 Secondary Level Eigenvector Magnitude

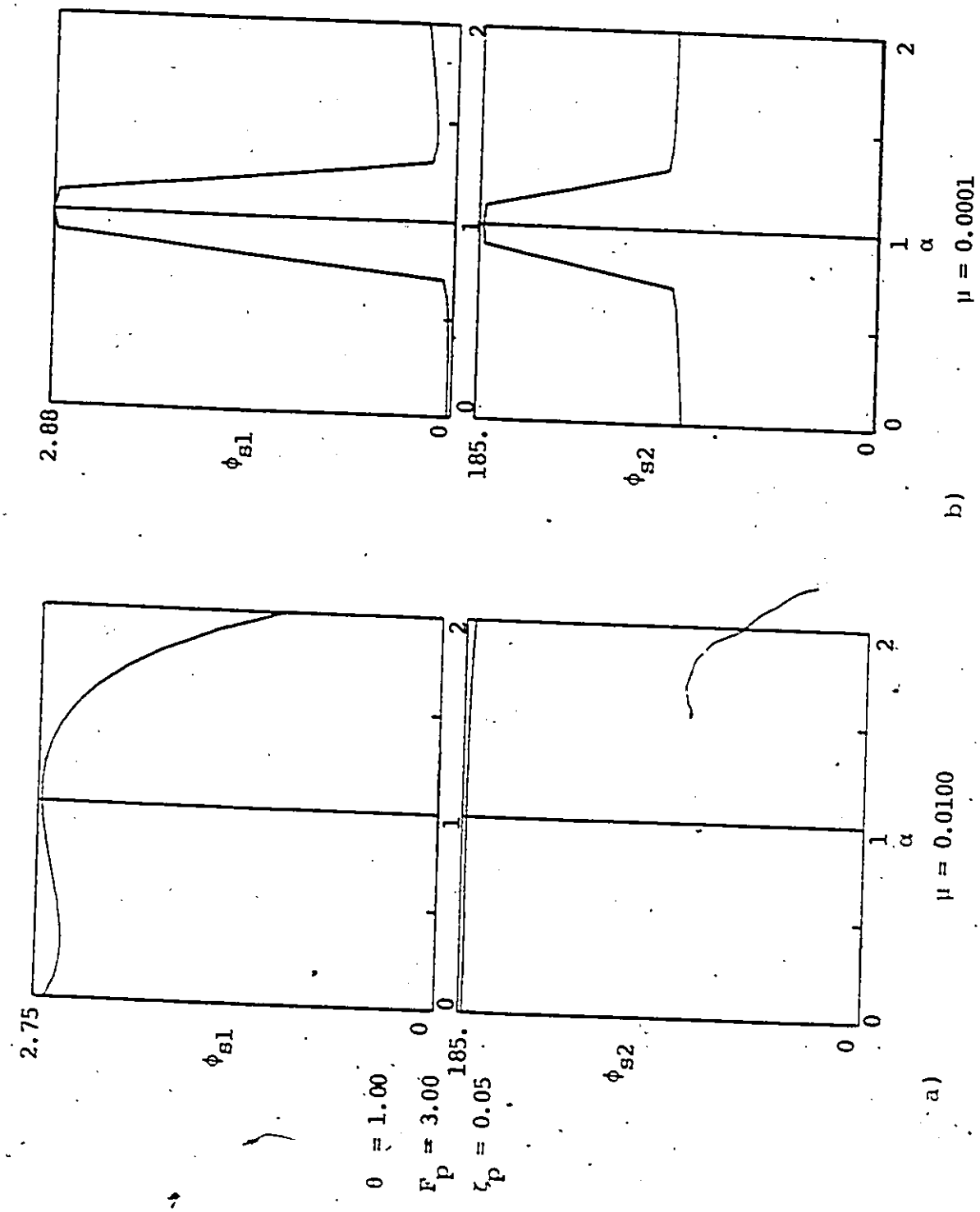

Figure 5.4 Secondary Level Eigenvector Phase Angle

CHAPTER 6

TWO DEGREE OF FREEDOM SYSTEM RESPONSE ESTIMATES

6.1 Statistical Basis of Plots

This section considers the calculation of the response of a system experiencing forced vibration. The calculations are of a time history nature and are described in Chapter 2. The three methods are standard modal analysis, uncoupled analysis and the best estimate or complex modal analysis.

The secondary level response of the various systems is calculated for the twelve time histories described in Chapter 2 using all three methodologies.

Two quantities are calculated from these responses: amplifications and errors. These are then averaged over the time histories and these averages are plotted against ζ.

Amplifications are characteristics of the structural system and are defined as the ratios of peak relative displacement(at a particular level) to peak ground displacement. Errors, on the other hand, are dependent on the method of analysis used. The complex modal analysis procedure is taken to provide the correct response and is used as the basis of the error calculations. The error for a

particular procedure is taken as the percent difference in estimates of maximum secondary level displacement between the simplified and complex procedures.

Each of the plots in this section give a simple representation of the overall results for twelve specific time histories. Figure 6.1 presents a sample of the variation in the amplification and error over the different time histories. These are supplied in the form of histograms.

Essentially each histogram provides a relative measure of the number of occurrences of an event falling into specific ranges. This gives some general indication of how the response varies over a number of selected time histories.

These histograms illustrate the fact that the results are well grouped within a central range of mean plus or minus one standard deviation. However, some results fall well outside this central range.

The average value gives an indication of where this central range occurs and the standard deviation indicates how much scatter can be expected in the results.

It is obvious that not all of the histograms indicate an exact normal distribution but, overall, it does appear to be a reasonable approximation for the majority of cases.

6.2 System Amplifications

The results of this section are concerned with the actual reponse of the system to a specified base motion. Amplifications are not absolute responses but, rather, ones that are scaled according to the level of the base motion. The amplifications are defined as the ratio of maximum relative displacements to maximum ground displacement.

This eliminates the effects of scaling. The same amplification, for a specific ground motion, will be obtained irrespective of whether the motion is scaled up or down, prior to the response calculation.

Since the actual system response is being evaluated, the amplifications are based on the "best estimate" of the system response, defined by the complex modal analysis.

Figures 6.2 and 6.3 represent plots of the average secondary level amplification. Figure 6.2 presents three different curves for three different mass ratios and a primary damping ratio of 5%. It can be seen that as the mass ratio decreases the increase in amplification is reduced. This indicates that an upper limit exists for the system amplification, even as the mass ratio approaches zero.

Both Figures 6.2 and 6.3 show that amplification and, therefore, response of the system decrease as the secondary damping ratio is increased, as is to be expected. Similarly, Figure 6.3 illustrates the decrease in amplification and, therefore, response as the primary

damping ratio increases. In both cases, the decrease in damping leads to a decrease in energy dissipation in the system. Since less energy is dissipated the system attains higher levels of kinetic and potential energy. This increase in energy leads to increases in response and amplification.

6.3 Error Evaluation

The errors that are considered now differ in a fundamental way from the amplifications that were evaluated in the previous section. Errors are characteristics of methods of analysis, for a specified system, while amplifications are a characteristic of the system and are determined using the "best estimate" method. The errors are determined with respect to this "best estimate".

The error used here is a relative error, with respect to complex modal analysis, and is expressed in a per centage form. As with amplifications, this form eliminates the effects of scaling of ground motions and the resulting responses.

Errors are determined for each of the twelve time histories. These are averaged and a standard deviation is calculated. Sample histograms are supplied in Figure 6.1(b) and demonstrate the distribution of error in the estimates of maximum response over the twelve time histories. The distributions are not exactly normal but have been reduced to an average and standard deviation.

Figure 6.4 is a plot of the range of average error in maximum response for the two simplified procedures with respect to mass ratio only. The solid lines indicate the average value and the dashed lines indicate the average plus one standard deviation. This plot is an envelope of all the curves for specified damping characteristics of the system. The primary damping ratio is varied from 0.03 to 0.07 and α ranges from 0 to 1.

The range of α from 0 to 1 is used for these plots since most systems have the secondary damping less than that of the primary. As a result, α would lie between 0 and 1.

It can be seen from this figure that the standard method always underestimates the actual response while the uncoupled method always overestimates the response. In addition, this figure demonstrates that the standard procedure produces smaller errors as the mass ratio increases. The uncoupled procedure, on the other hand, produces smaller errors as the mass ratio decreases.

The last two observations, then, imply that the effect of nonproportional damping decreases with an increase in mass ratio and the effect of interaction decreases with a decrease in the mass ratio. These implications arise since the standard procedure ignores the effects of nonproportional damping (assumes proportional damping) and the uncoupled procedure ignores the effects of interaction.

More detailed plots are also supplied. Figure 6.5 to

6.9 represent the results which Figure 6.4 envelops. Each plot is for a specific value of mass ratio and primary damping ratio. The independent variable in each plot is α, the ratio of secondary to primary damping ratio. These plots demonstrate that the induced error for both simplified procedures diminish as the system approaches proportional damping (α=1).

In the case of the standard procedure, the procedure is based on the assumption of proportional damping and should be expected to yield zero error in a situation where the assumption is fulfilled exactly. In the case of the uncoupled procedure, the increase in damping leads to a reduction in response. This reduced response leads to reduced interaction. This more closely resembles the assumption of zero interaction which is the basis of the procedure.

Comparing Figures 6.5, 6.6 and 6.7 (only ζ_p varies), it can be seen that an increase in the primary damping ratio leads to a decrease in the average error for the uncoupled analysis. Again, the increase in damping reduces the overall response and reduces the effect of interaction. In addition, the increase in primary damping ratio leads to an increase in the error associated with the standard analysis. This implies that nonproportional damping has an increased effect as the overall damping level increases and α does not equal unity.

6.4 Example Cases

Section .6.3 presented a set of figures which illustrate the variation of average error with respect to selected parameters. This section demonstrates how these can be put to use in a preliminary evaluation of the analysis requirements for a design.

If an engineer has established a set of allowable errors for his design, then he can plot these limits on Figure 6.4 and determine the mass ratios at which these intersect the uncoupled and standard curves. For any mass ratio below the uncoupled intersection point an uncoupled analysis can be used and should be within the error limits. Similarly, for any mass ratio above the standard intersection point a standard modal analysis can be used. It should be noted that these two decisions are made without needing to know the damping characteristics of the system. Obviously, however, they will need to be known when the actual response calculations, whichever they are, are made.

If the mass ratio of the design lies between these two points then the engineer should either use the complex modal analysis procedure or, using the primary and secondary damping ratios, go to Figures 6.5 to 6.9 and get a more refined estimate of the expected error. These plots are similar to Figure 6.4 with the exception that they are plotted with respect to α for specific values of mass ratio and primary damping ratio. As before, error limits can be

plotted on the appropriate figure and a decision made as to which of the three methods can or should be used.

If, at this level, neither standard or uncoupled methods seem adequate, then a complex modal analysis should be carried out.

Consider the following numerical examples.

If only an allowable average error of $\pm 15\%$ is specified, certain conclusions can be drawn if the limits of $\pm 15\%$ are plotted on Figure 6.10 (reproduction of 6.4). From this it can be seen that an uncoupled analysis can be carried out for any system having a mass ratio less than .00033. In the same way, a standard modal analysis procedure can be used for any system having a mass ratio greater than .003. If the mass ratio lies between .00033 and .003 then complex modal analysis will be required unless information is available about the damping in the system and the actual mass ratio. This added information would allow for a more refined check.

If it is determined that the mass ratio is 0.001 and the primary damping ratio is 0.05 then Figure 6.6 indicates that a complex modal analysis is only required for α below 0.1 or for a ζ_p less than .005. Figure 6.5 indicates that a standard analysis may be used over all α if $\zeta_p=0.03$. Similarly, an uncoupled analysis may be used over all α if $\zeta_p=0.07$ (Figure 6.7).

If the only piece of information available is that the system mass ratio is .003, plot this value on Figure 6.10. In this case, the engineer can expect average errors of up to +70% using an uncoupled procedure and up to -18% using standard modal analysis.

Finally, consider a system with a mass ratio of .0004, a primary damping ratio of 5% and α of 0.4. Using Figures 6.6 and 6.8 one can set up the following table of expected average errors:

mass ratio	0.0001	0.0010
standard	-7%	-7%
uncoupled	-1%	+4%

The error for a mass ratio of .0004 must now be interpolated from this table. It would probably be best to interpolate based on the log or square root of the mass ratio. This interpolation would then supply the expected error if either of the simplified procedures is used. This can then be used to determine, based on the allowable average error, if one of the simplified methods can be used or if complex modal analysis should be used.

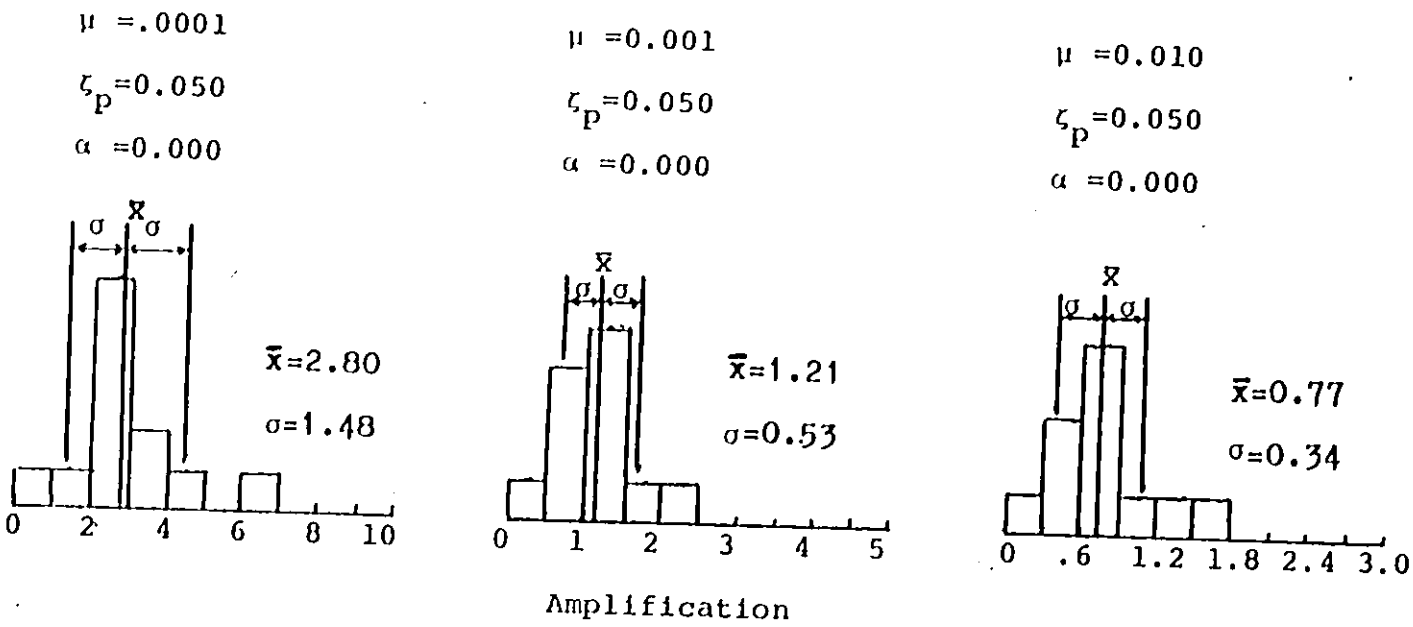

Figure 6.1(a) Distribution of Secondary Level Amplification

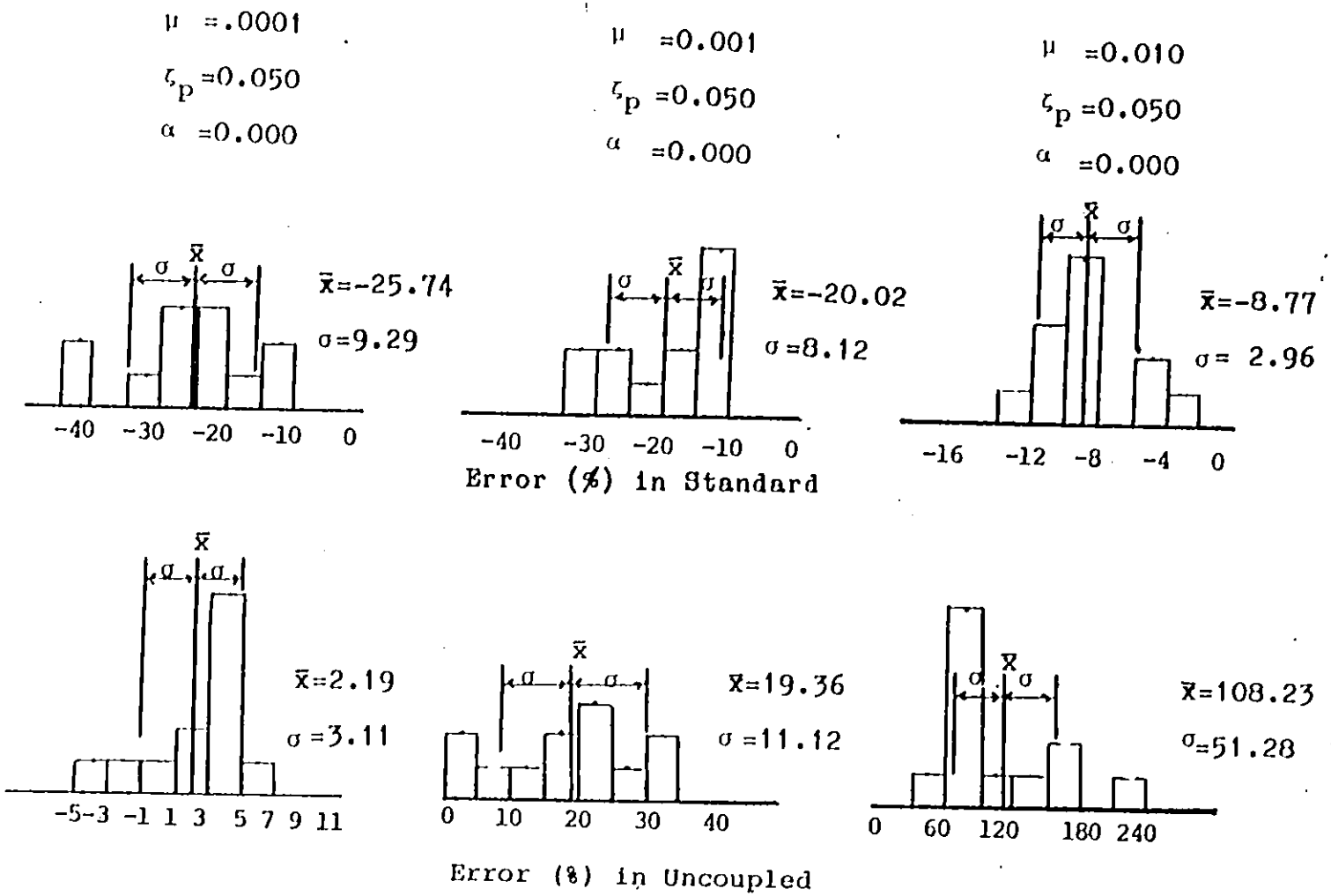

Figure 6.1(b) Distribution of Error in Secondary Level Maximum Response

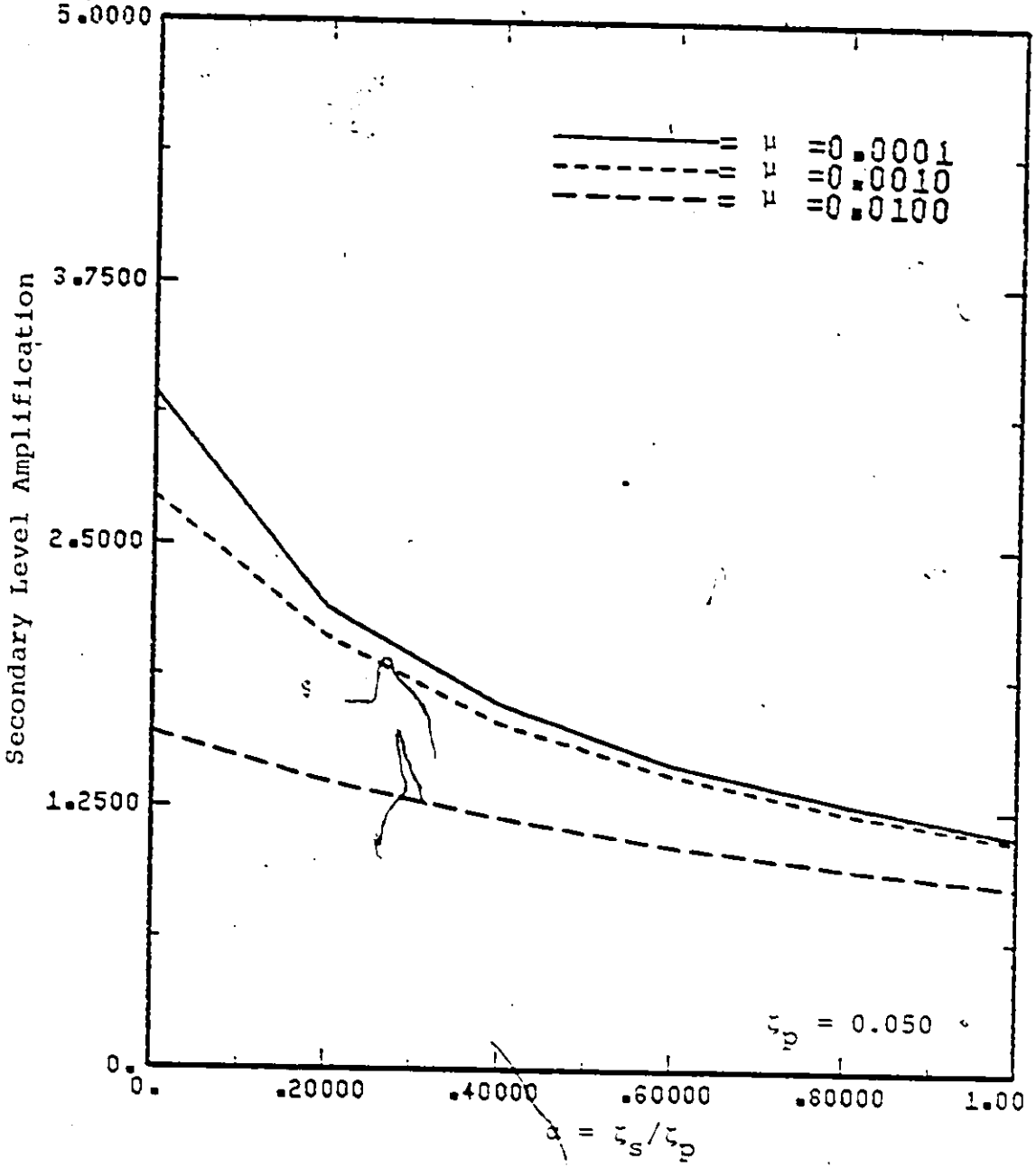

Figure 6.2 Maximum Secondary Level Amplification Averaged Over 12 Time Histories

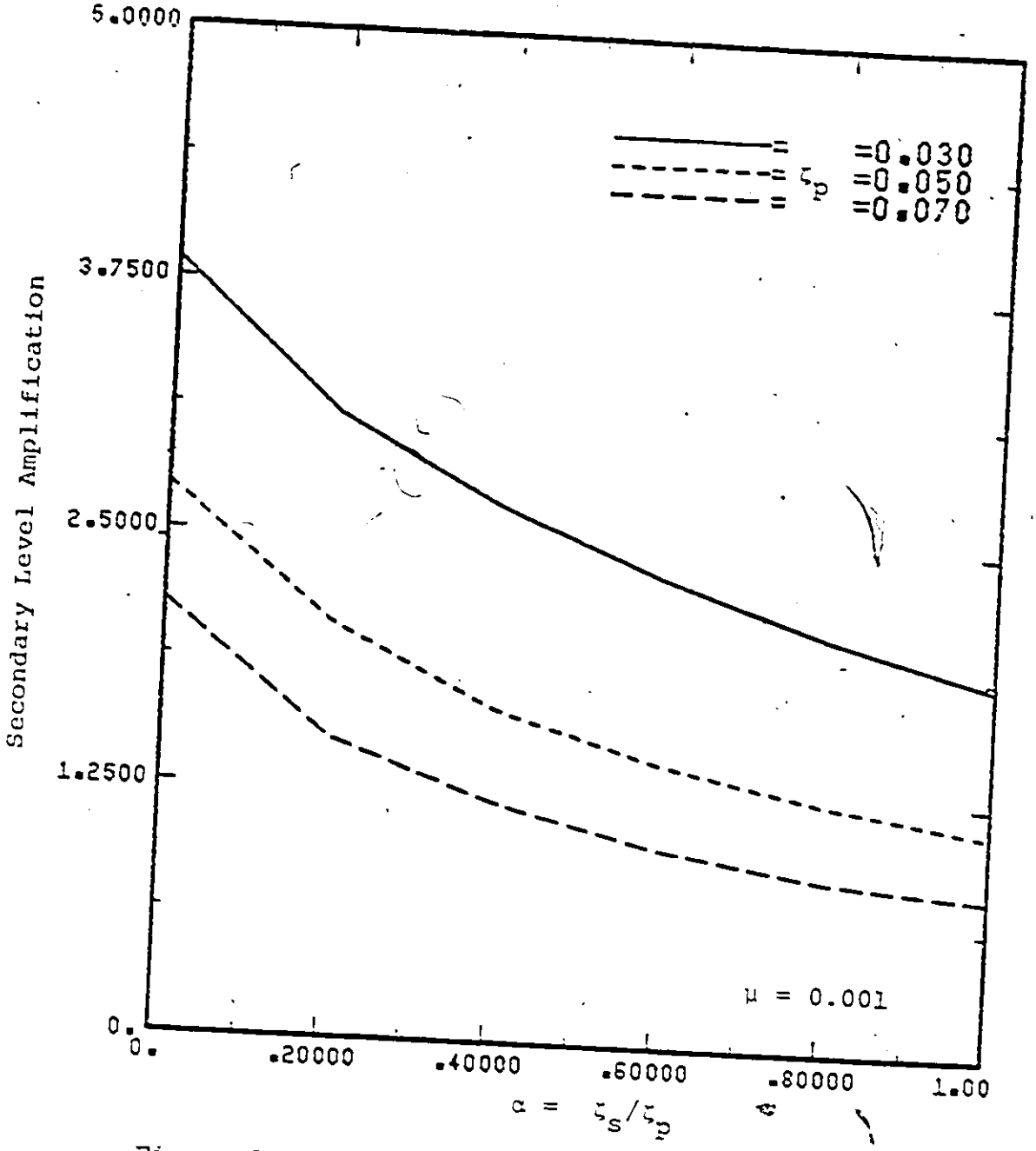

Figure 6.3 Maximum Secondary Level Amplification Averaged Over 12 Time Histories

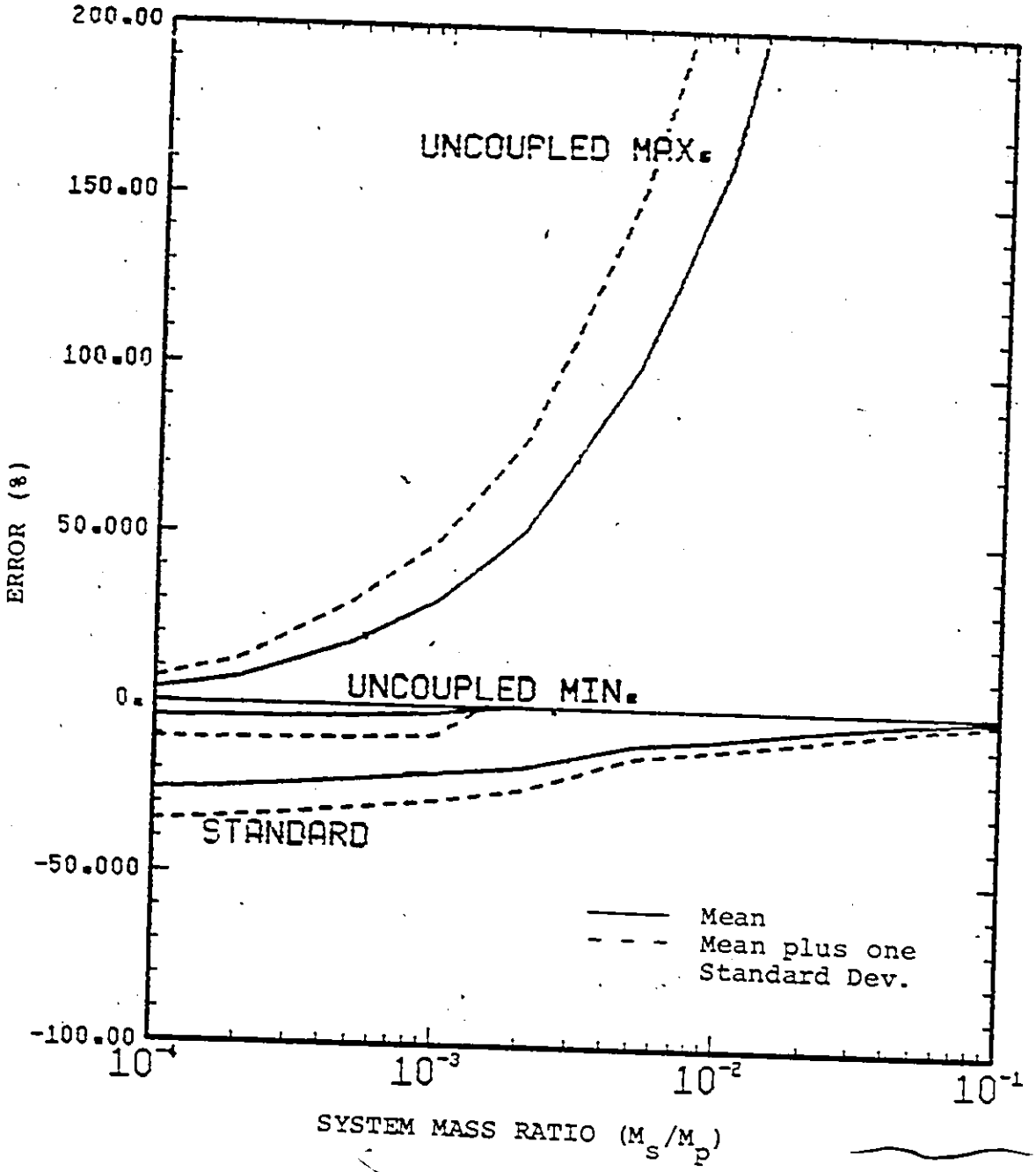

Figure 6.4 Error Envelope for Maximum Secondary Response Estimate Averaged Over 12 Time Histories (range over all ζ)

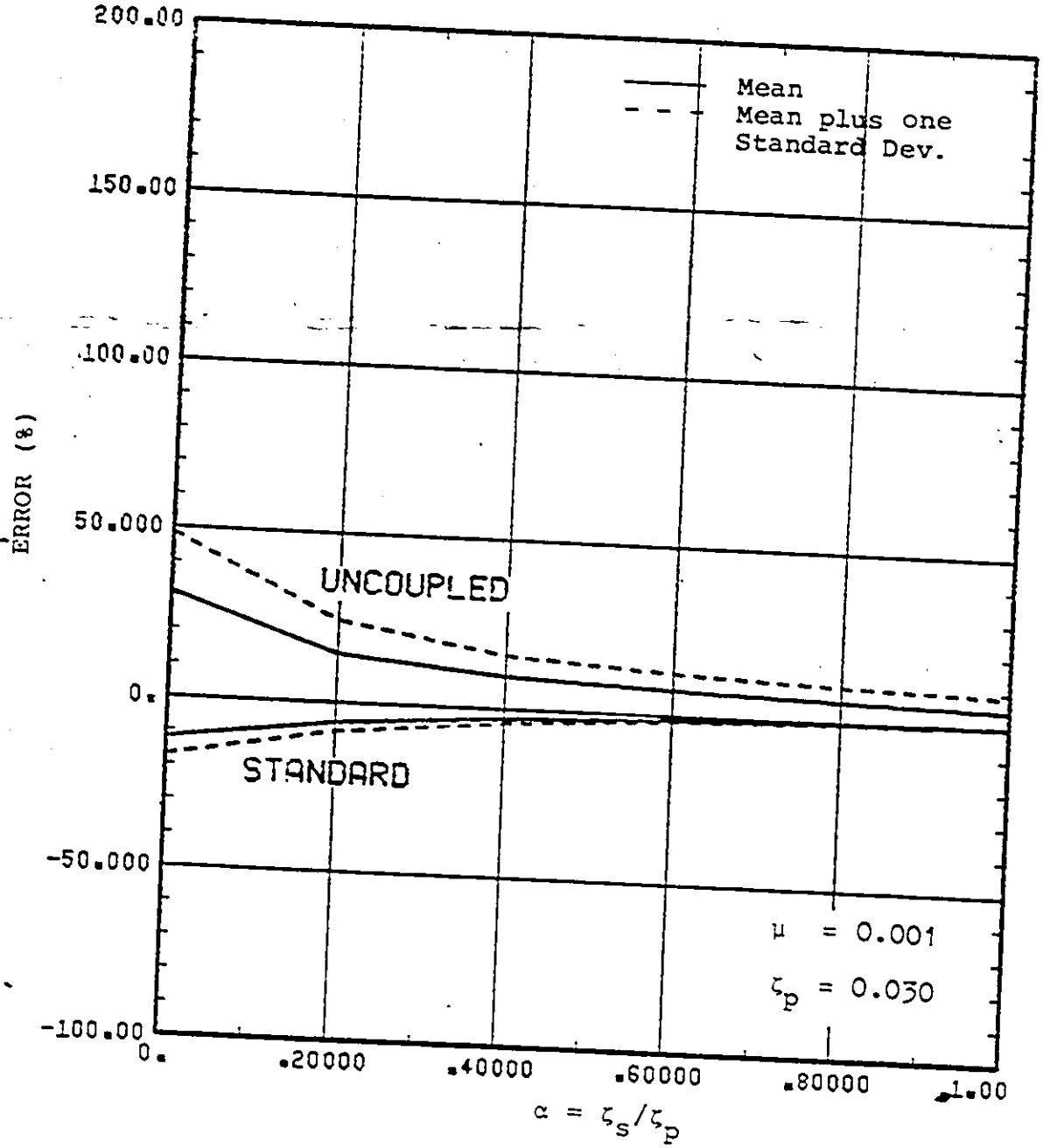

Figure 6.5 Error in Maximum Secondary Response Estimate Averaged over 12 Time Histories

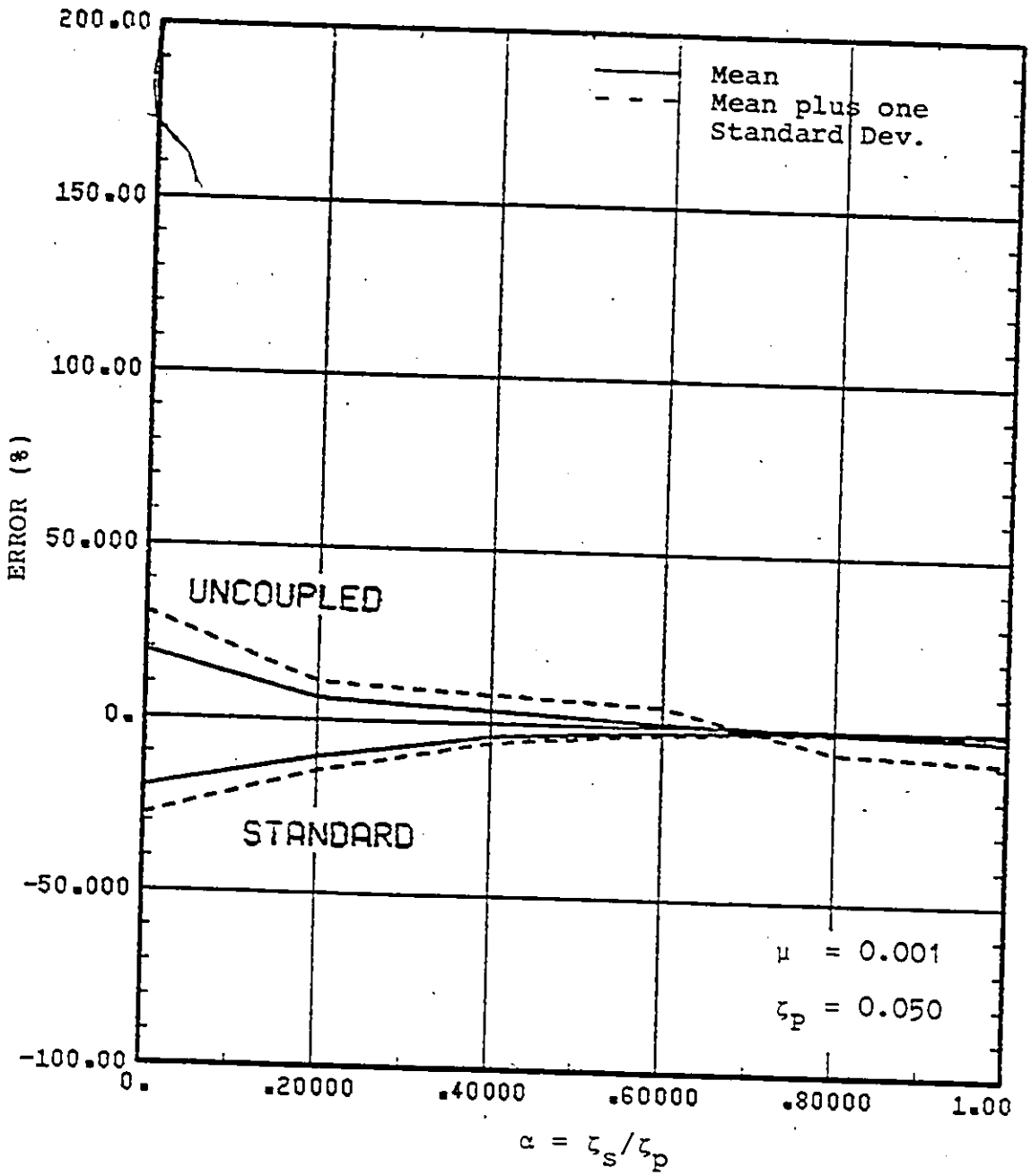

Figure 6.6 Error in Maximum Secondary Response Estimate Averaged over 12 Time Histories

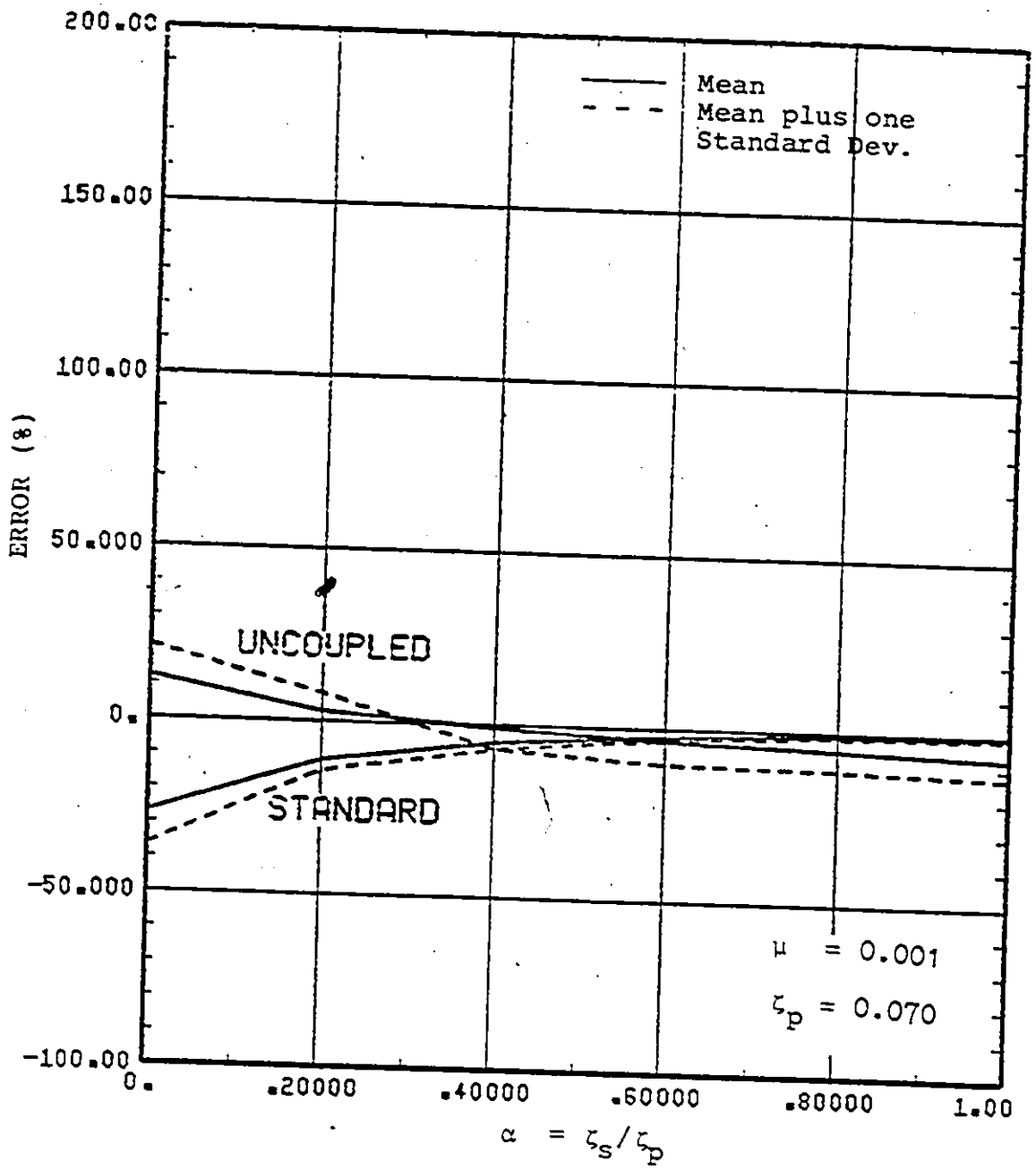

Figure 6.7 Error in MaximumSecondary Response Estimate Averaged over 12 Time Histories

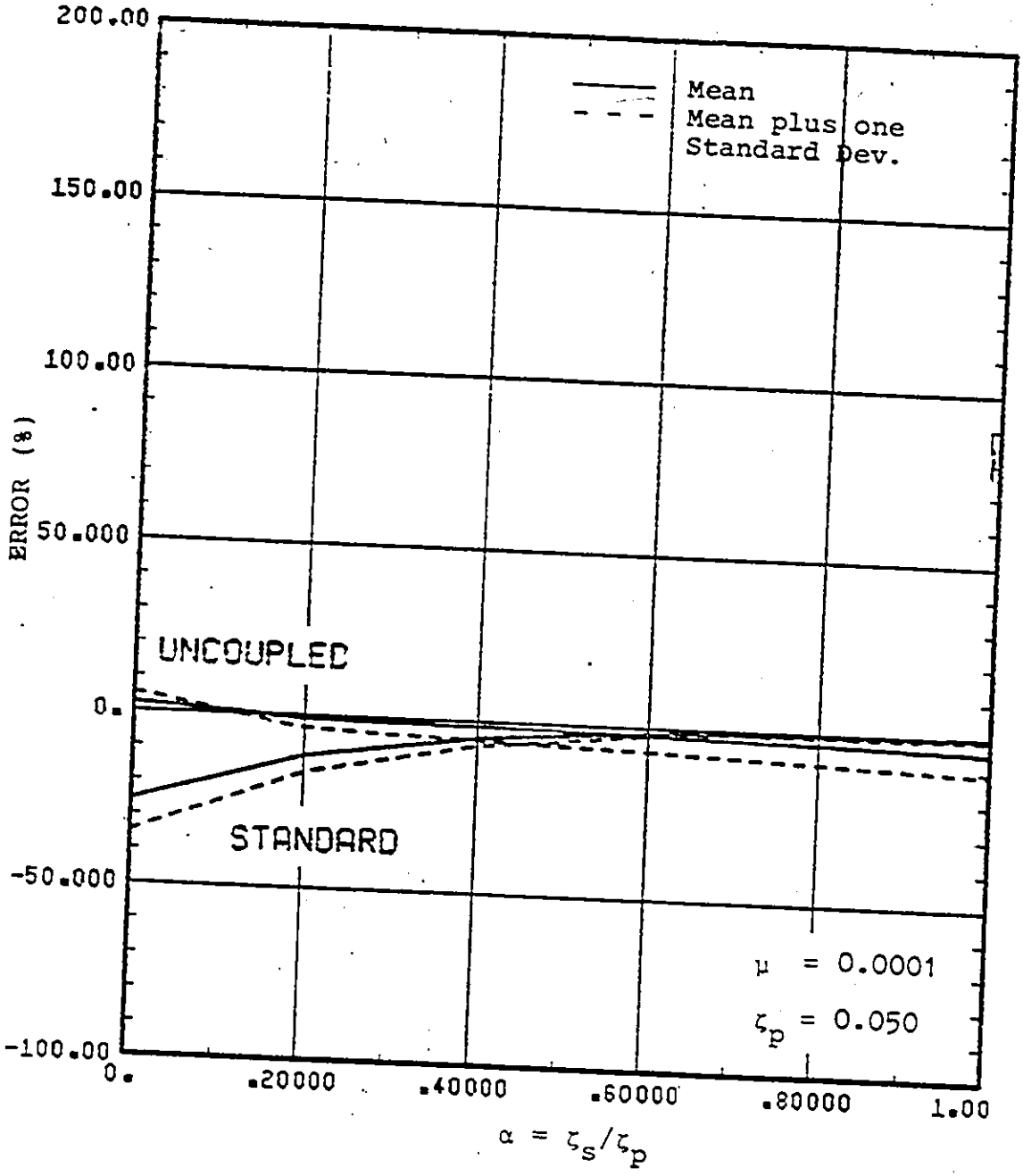

Figure 6.8 Error in Maximum Secondary Response Estimate Averaged over 12 Time Histories

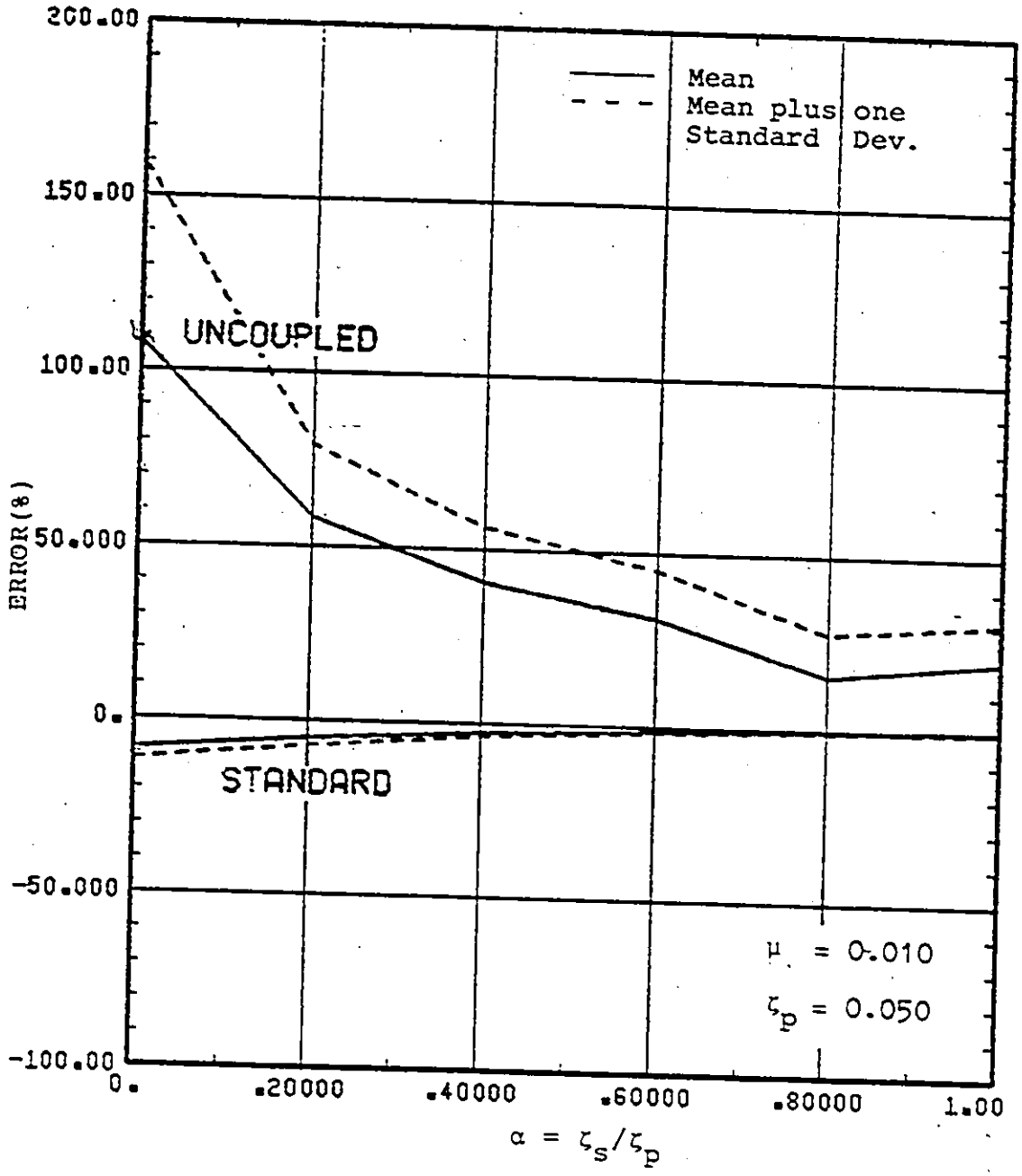

Figure 6.9 Error in Maximum Secondary Response Estimate Averaged over 12 Time Histories

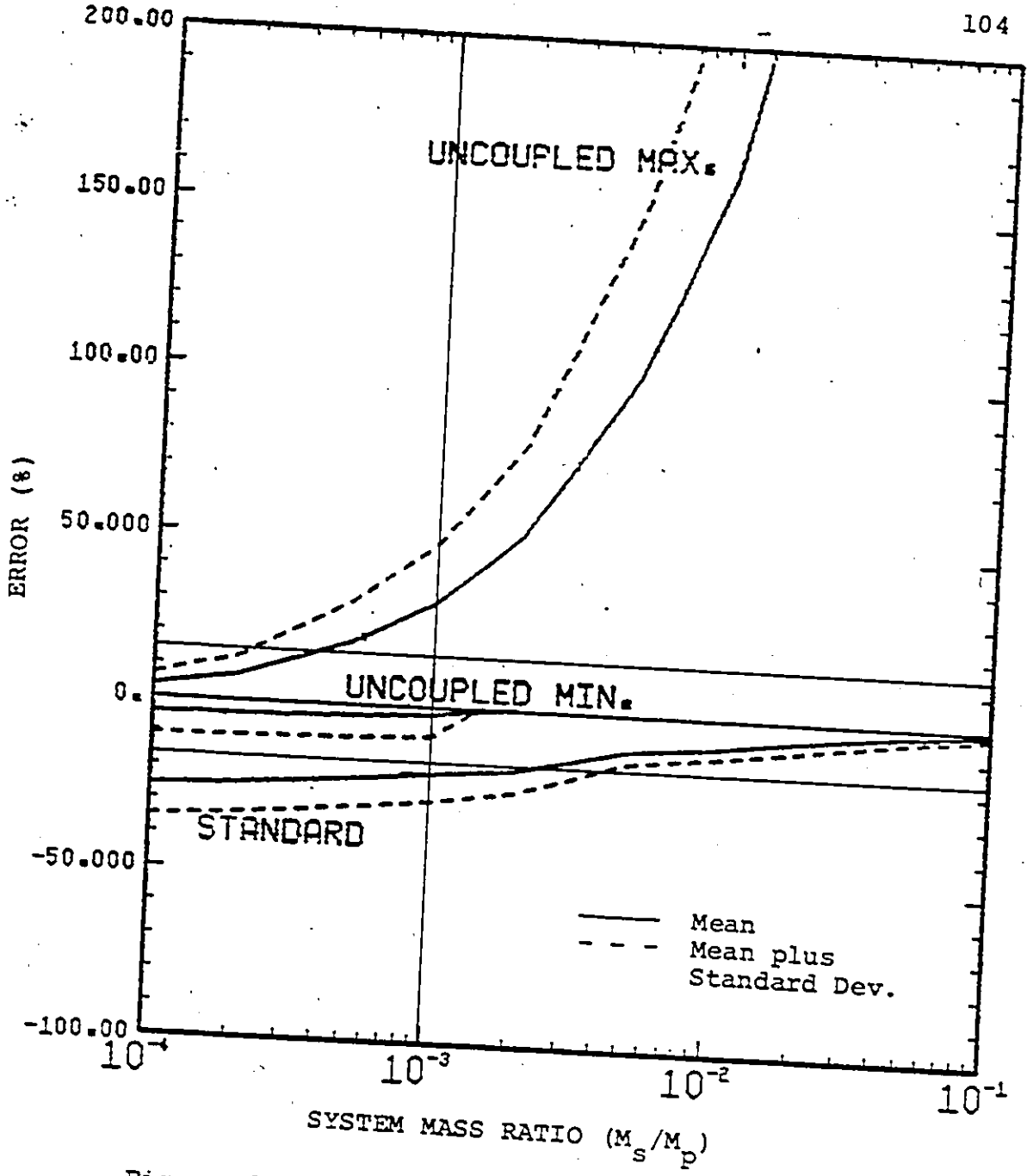

Figure 6.10 Error Envelope for Maximum Secondary Response Estimate Averaged Over 12 Time Histories (range over all ζ)

CHAPTER 7

THREE DEGREE OF FREEDOM SYSTEM

7.1 Coupled System Characteristics

This chapter is very similar to chapters 5 and 6 except that it deals with three level systems. Extra parameters have to be defined, due to the increased complexity of this type of system, and the results are more complicated to present and understand.

This chapter concerns itself with the simplest of three level systems, a three degree of freedom lumped mass model. The first two levels (primary and secondary) are the same as described in chapter 5 and the third level is called the tertiary level. These three degrees of freedom could represent three modes of the three uncoupled subsystems.

Since there are three levels it is necessary to use two mass ratios to define the mass relationship within the system. They are referred to as μ_{sp} and μ_{ts} and represent the ratios of secondary to primary and tertiary to secondary masses.

Each level has an associated uncoupled frequency. Similar to the two degree of freedom system case, the primary uncoupled frequency and two frequency ratios are

used to describe how the uncoupled frequencies are related. Both ratios are defined with respect to the primary frequency as

$$\theta_{sp} = \omega_s^2/\omega_p^2 \tag{7.01}$$

$$\theta_{ts} = \omega_t^2/\omega_p^2 \tag{7.02}$$

The system damping characteristics are based on the three uncoupled damping ratios. α_s is the same as α in chapter 5. Similarly, α_t is defined as

$$\alpha_t = (\zeta_t\omega_p)/(\zeta_p\omega_t) \tag{7.03}$$

In this case, a proportionally damped system requires both α_s and α_t being equal to 1.

For purposes of this study, the mass ratios are set equal to each other. They are assigned values of 0.01, 0.001 or 0.0001 which cover the required range of mass ratios. The primary frequency is set to 3 Hz, θ_{sp} and θ_{ts} are set to unity and α_s and α_t range from 0 to 1.

Following a similar pattern to that used in the study of two level systems, plots are developed for the coupled system characteristics: frequencies, damping ratios and eigenvectors, that arise from the selected uncoupled subsystem parameters. The plots are with respect to α_t for fixed values of the other parameters since α_t is the damping quantity that has the most significant effect on tertiary level response.

The primary damping ratio is fixed to 3 or 5 per cent. A sample set of plots, for two systems, is given in

Figures 7.1 to 7.4.

The four figures are for mass ratios of 0.001 and a primary damping of 5%. Part (a) of each figure is for α_s=0.6 and part (b) is for α_s=1. The case of proportional damping is given in part (b) of each figure at α_t=1.

Chapter 3 describes the difficulty of separating modes in a systematic manner when the results are obtained from a computer subroutine which solves a general eigenproblem. In fact, while varying α's, it is virtually impossible to saperate the three modes properly based on modal frequency alone. This inability to sort out the three modes consistently makes it very difficult to study how a variation in α_t affects the coupled characteristics of one particular mode of the system.

The present plots are obtained by initially ordering the modes for the case of proportional damping. The remainder of the plot is determined based on, first, frequency and, second, on not allowing discontinuities in the damping ratio plot.

Several observations can be made from the plots that are presented in this section. Figure 7.1 contains an interesting phenomenon. For α_t ranging from 0 to 0.3, in 7.1(a) and from 0 to 0.6, in 7.1(b),two modes exhibit a decreasing damping ratio for an increasing α_t. The third mode picks up both the decreases in the two modal damping ratios and the increase corresponding to the increase in α_t.

Above these ranges all three modes exhibit increasing damping ratios for an increase in α_t.

It can be seen in Figure 7.2 that an α_t value of 1.0 yields the largest spacing in coupled frequencies. In the case of 7.2(b), this also represents proportional damping.

The magnitude of the eigenvector (and, therefore, the mode shape) is dependent on the damping characteristics of the system. This is demonstrated in Figure 7.3. The maximum value of the eigenvector magnitude occurs at an α_t value of 0.3 and 0.6 in Figures 7.3(a) and 7.3(b), respectively.

7.2 System Amplifications

This section and the next deal with quantities which are based on the calculated dynamic response of the system. The quantity dealt with in this section is the system amplification. The amplification used in this chapter is defined as the tertiary level maximum relative displacement divided by the maximum base displacement.

First, a note about the mass ratio dependence of the tertiary level response of the system. It was shown by T. Aziz(2), for proportional damping, that the tertiary level response is dependent on the quantity "$\mu_{sp} + \mu_{ts}$", provided that these mass ratios are small. Since this conclusion was based on proportional damping, calculations were made in the course of this work for nonproportionally damped systems.

The calculations were made using the ORIONEW earthquake time history (Table 2.1, time history no. 12) for a system exhibiting a primary damping ratio of 0.05 and α_s=0.6. Three sets of mass ratios were selected such that, $\mu_{sp}+\mu_{ts}$ added up to 0.02, 0.002 and 0.0002. Each set contained four different combinations which included $\mu_{sp}=\mu_{ts}$. This allowed for a numerical check to see if this held for the more general damping case. The results are presented in Figures 7.5 to 7.7.

It can be seen that, for $\mu_{sp}+\mu_{ts}$=0.002(Fig. 7.6) or 0.0002(Fig. 7.7), this statement holds very well. For a value of 0.02, however, it begins to break down for low α_t. This limitation is not very serious since it will be shown that, for this level of mass ratio, the standard modal analysis simplification gives acceptably accurate results. It should be noted that the physically uncoupled analysis is already independent of the system mass ratios and masses.

As a result of these observations, the plots are given for the cases of equal mass ratios, only. When using the plots for a specific system, use mass ratios of $(\mu_{sp}+\mu_{ts})/2$.

The variation in the calculated amplifications, over the 12 time histories, is illustrated in Figure 7.8. These histograms are for three example systems and demonstrate the range of results for each system. As in chapter 6, the average value and standard deviation are plotted on each

histogram. If the results were normally distributed 68% of the results would lie in the area defined by the distance one standard deviation on either side of the average value.

Figures 7.9 to 7.11 give average values of tertiary level amplification. The plots are given in terms of three mass ratios, three α_s and three primary damping ratios.

Figure 7.9 presents three curves for three different sets of mass ratios. It can be seen that as the mass ratio decreases the amplification increases. The rate of increase reduces as the mass ratio decreases. This indicates that a system amplification upper limit exists as the mass ratio approaches zero.

All three figures show the pattern of the amplification being reduced as α_t is increased. Near a zero value of α_t, it can be seen that a change in α_t has a larger effect on the system with a small mass ratio than on a system with a larger mass ratio.

Figure 7.10 demonstrates that the amplification is reduced for an increase in α_s and Figure 7.11 demonstrates that the amplification is reduced for an increase in primary damping ratio.

The observations about α_s, α_t and ζ_p all relate to the level of damping that exists in the system. In each case an increase in the selected parameter implies an increase in the damping level of the total system. This increased damping leads to increased energy dissipation. This

increased energy dissipation leads to reduced response which implies a reduced amplification.

7.3 Error Evaluation

This section of the chapter is devoted to an evaluation of the errors developed when approximations are used to determine the maximum seismic response of the tertiary level of the system. The variation and range of the results for the different time histories is illustrated in Figure 7.12. These histograms are for 3 sample systems.

Figures 7.13 to 7.22 present plots of expected average error in terms of the mass ratios and α_s. Figure 7.13 gives the range of average errors, dependent on mass ratio only. These curves envelope the various curves for all the different combinations of primary damping ratio, α_t and α_s.

Figure 7.13 defines the range of errors that can be expected if a simplified procedure is used to estimate the maximum tertiary level response. The max. and min. refer to the upper and lower limits of the range of average error for the specified procedure. Since both of the limits for the uncoupled procedure are greater than zero, the lower limit is omitted.

Consider a mass ratio of 0.001. From the figure it can be seen that the average error in maximum response prediction (solid line) can range from -40% to 100% for the

standard procedure, depending on the damping characteristics. An uncoupled procedure would generate an error of up to 100%.

Figure 7.13 demonstrates that an increase in mass ratio leads to a decrease in the range of the expected errors for the standard procedure. A larger mass ratio reduces the effect of nonproportional damping since the standard procedure is based on the assumption of proportional damping. Figure 7.13 illustrates the fact that a small mass ratio reduces the range of expected error for an uncoupled procedure. Since the uncoupled analysis ignores interaction, it can be concluded that a smaller mass ratio reduces interaction.

Figure 7.14 to 7.22 are similar to 7.13 except that they are based on more specific conditions (damping) and are plotted against α_t. Figure 7.13 actually envelops these curves.

All 8 of these figures demonstrate that the error in the uncoupled estimate decreases with an increase in α_t. Comparing Figure 7.14, 7.15 and 7.16 shows that the uncoupled error also reduces with increases in α_s. Similarly, 7.15, 7.18 and 7.20 can be used to show that an increase in primary damping decreases expected errors for the uncoupled procedure. All these reductions in error imply a reduction in interaction between the subsystems.

The effects of changes in damping are not so

apparent for the standard procedure. Comparing Figures 7.15, 7.18 and 7.20 implies that a larger primary damping ratio gives a larger expected error, except in specific cases.

The effect of a change in α_s or α_t is even less apparent. Figures 7.14 to 7.16 do not give a consistent set of observations. Depending on the combination of α_s and α_t, the expected error can be plus, minus or zero. Figure 7.16 does show an expected error of zero for the case of proportional damping ($\alpha_s=\alpha_t=1.0$).

A final set of three figures (7.23 to 7.25) show the response calculated by four methods. The difference here is that a non-time history procedure has been included. This is the response spectrum technique incorporating the Rosenblueth method (described in Chapter 2) of combining modal maxima.

These show that an increase in mass ratio leads to a reduced error for the standard procedure and a decreased mass ratio leads to a reduced error for the uncoupled procedure. The main point to be made from these curves is that when the standard modal analysis procedure gives a good estimate of the complex modal analysis procedure, the Rosenblueth procedure demonstrates similar error than the standard modal analysis procedure. As a result, the engineer may consider using the simpler response spectrum technique and expect a similar error in the maximum response estimates.

A point can be made from Figure 7.25. In this plot it can be seen that the standard modal analysis predicted response is not monotonically decreasing with an increase in α_t. This occurs because of the method of proportioning the uncoupled damping ratios to the coupled damping ratios. Due to its large tertiary mode shape (arising from the very small mass ratio), the second mode of the coupled system is more dependent on the tertiary subsystem damping than the other two modes. As a result, the mode 2 response estimate decreases faster, with an increase in α_t, than the other two modes. This leads to a switch from modes 1 and 3 cancelling the response of mode 2 (decreasing total response) to mode 2 cancelling the responses of modes 1 and 3 (increasing response).

A similar situation can arise for the case of a mass ratio of 0.0001 and an increase in the α_s value. The estimated tertiary response (by standard modal analysis) can go up with an increase in secondary damping. In this case, for this small value of mass ratio, the secondary level mode shape for mode 2 is almost zero. This means that for standard modal analysis the second mode damping ratio is almost independent of the secondary damping ratio. Therefore, if the secondary damping ratio goes up then only the first and third modal damping ratios go up. Now the second mode response stays the same, roughly, and the first

and third drop with an increase in α_s. This leads to less cancellation of the dominant second mode response by the other two modes and an apparent increase in total response.

7.4 Example Cases

Section 7.3 presented a set of figures which illustrates the variation of average error with respect to selected parameters. This section demonstrates how these can be put to use in a preliminary evaluation of the analysis requirements for a design.

If an engineer has established a set of allowable average errors for his design then he can plot these limits on Figure 7.13 and determine the mass ratios at which these intersect the uncoupled and standard curves. For any mass ratios below the uncoupled intersection point an uncoupled analysis can be used and will be within the error limits. Similarly, for any mass ratios above the standard intersection point a standard modal analysis can be used. It should be noted that these two decisions can be made even in the absence of knowledge about the damping characterisitcs of the system.

If the mass ratios of the design lie between these two points then the engineer must either use complex modal analysis or, using the uncoupled damping characteristics, go to Figure 7.14 to 7.22 and get a more refined estimate of the expected error. As before, error limits can be plotted

on the appropriate figure and a decision made as to which of the three methods can or should be used.

If, at this level, neither standard or uncoupled methods seem adequate, then a complex modal analysis should be carried out.

Consider the following numerical examples.

An allowable average error of $\pm 20\%$ has been specified. THe first step is to plot the limits of $\pm 20\%$ on Figure 7.26 (reproduction of 7.13). From this it can be seen that an uncoupled analysis can be carried out for any system having a mass ratio less than 0.0002. In the same way, a standard modal analysis can be used for any system having a mass ratio greater than 0.005. If the mass ratio lies between 0.0002 and 0.005 then a complex modal analysis should be carried out unless additional information about damping can be specified. In that case a further evaluation can be made before being required to use complex modal analysis.

In the next situation mass ratios of 0.001 are all that is specified. Again, plot this value on Figure 7.26. In this case the engineer can expect average errors of up to +100% using an uncoupled procedure and from -40 to +100% using a standard modal analysis.

Finally, consider a system with mass ratios of 0.001, a primary damping ratio of 0.05, α_s of 0.6 and α_t of 0.2. Using Figure 7.15 one can see that an uncoupled

analysis will have a average error of +20%. Similarly, a standard modal analysis can be expected to have an average error of -12%.

If the system characteristics do not fall exactly into one of the figures then the error may be interpolated. Best results would be obtained if the interpolation is done based on the log or square root of the mass ratio and linearly for α_s. This interpolation would then supply the expected error if either of the simplified procedures is used. This can then be used to determine, based on the allowable error, whether one of the simpifications can be used or not.

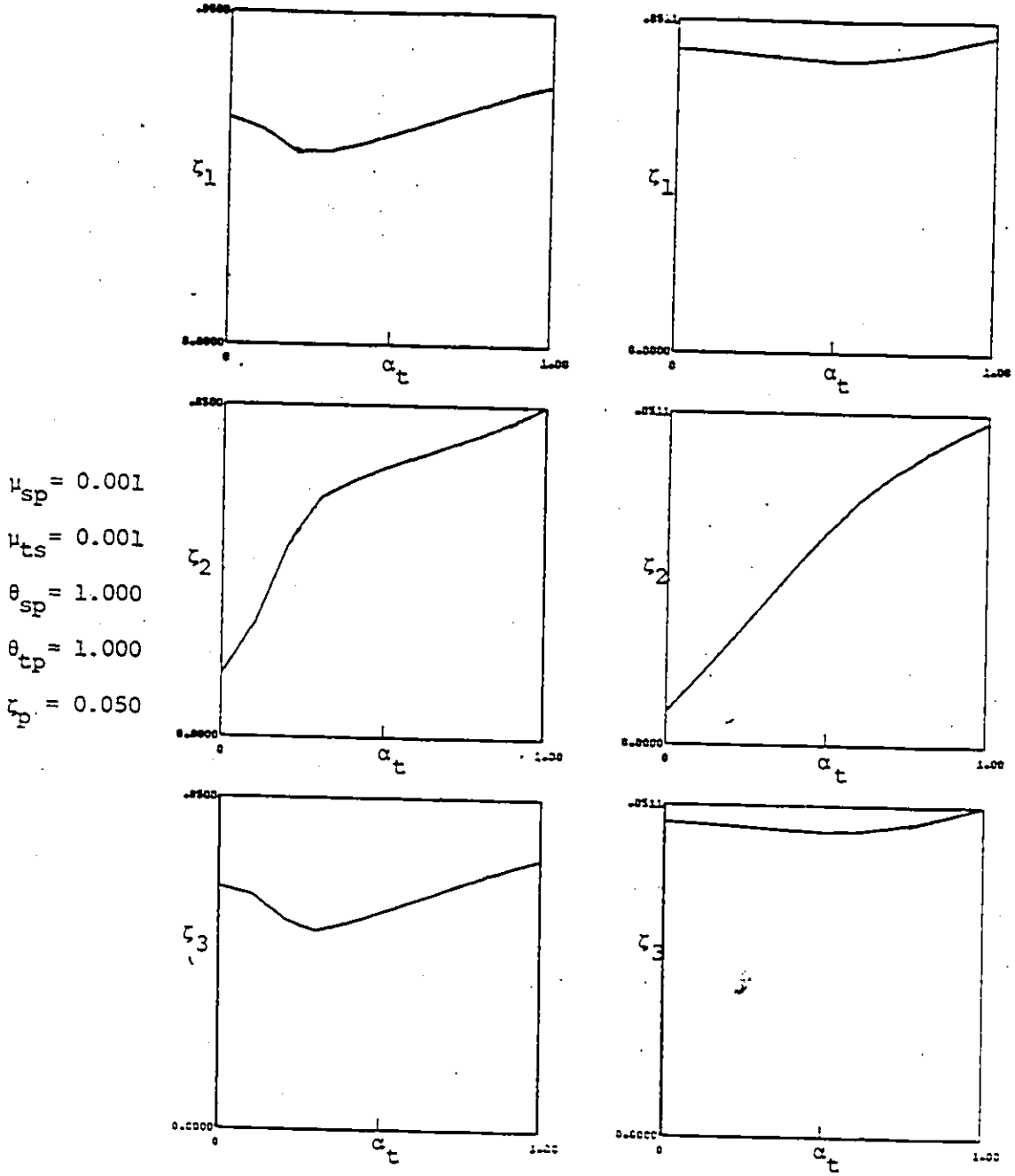

μ_{sp} = 0.001

μ_{ts} = 0.001

θ_{sp} = 1.000

θ_{tp} = 1.000

ζ_p = 0.050

a) α_s = 0.600 b) α_s = 1.000

Figure 7.1 Coupled Damping Ratio

μ_{sp} = 0.001

μ_{ts} = 0.001

θ_{sp} = 1.000

θ_{tp} = 1.000

ζ_p = 0.050

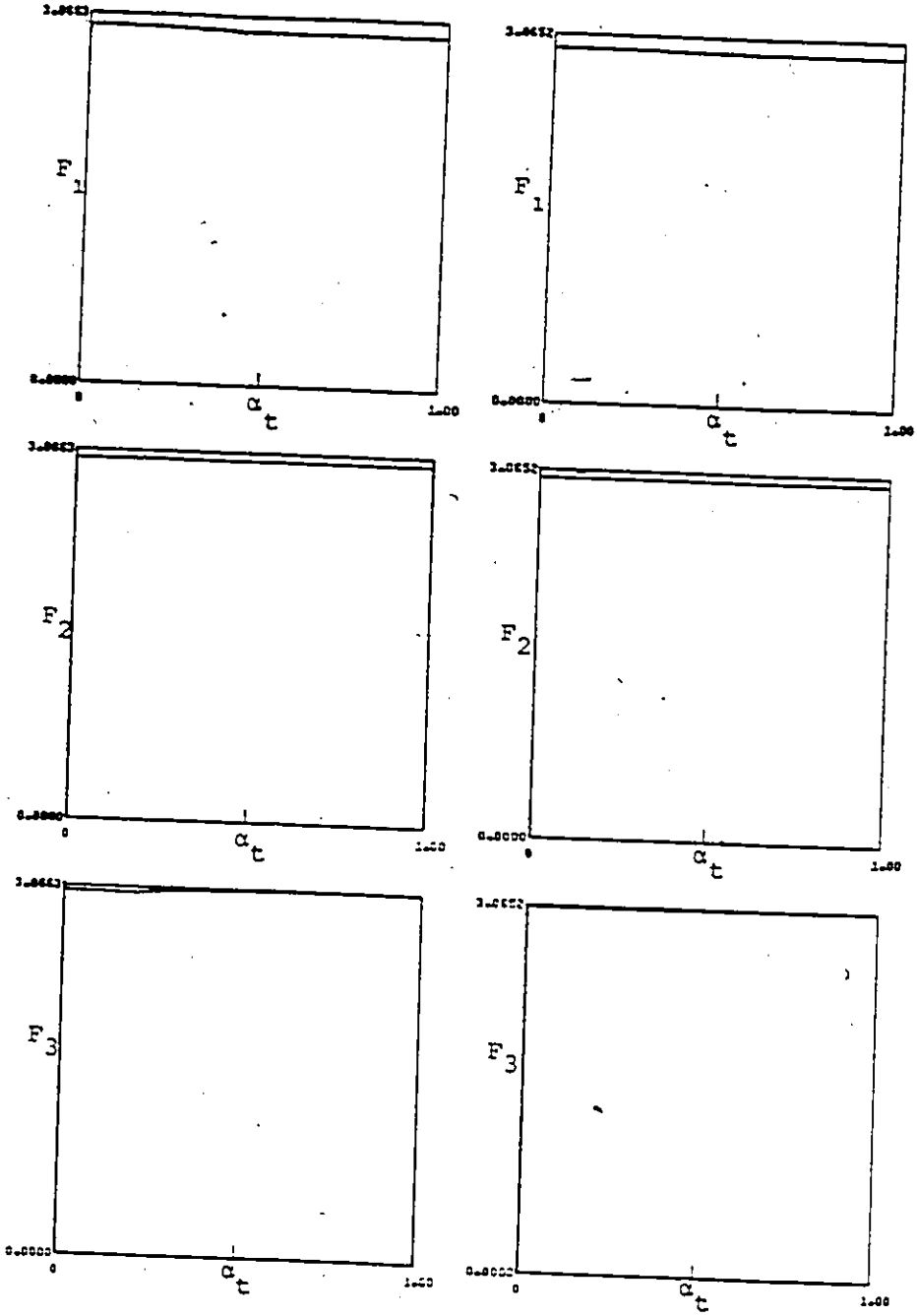

a) α_s = 0.600 b) α_s = 1.000

Figure 7.2 Coupled Damped Frequency

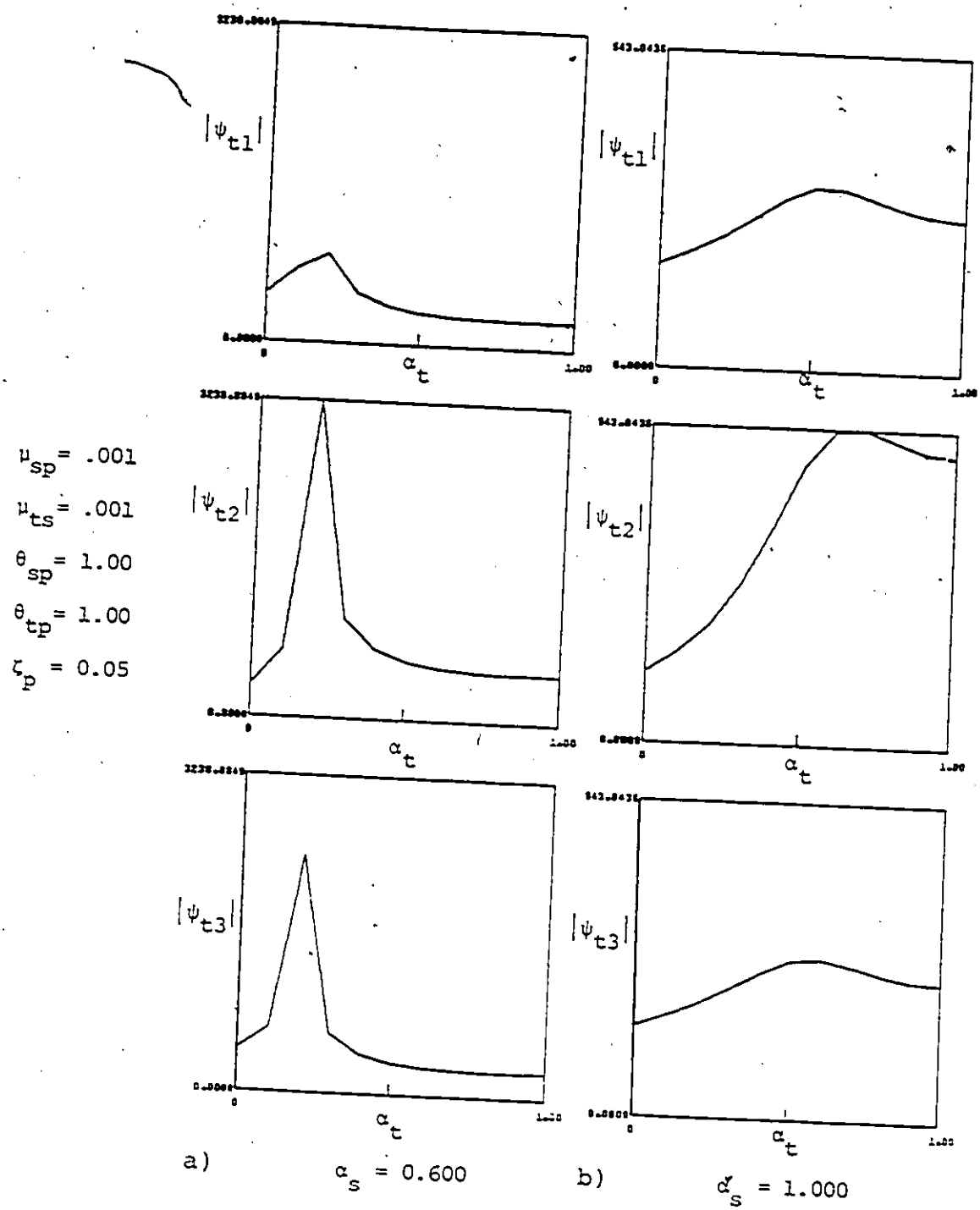

μ_{sp} = .001

μ_{ts} = .001

θ_{sp} = 1.00

θ_{tp} = 1.00

ζ_p = 0.05

a) α_s = 0.600 b) α_s = 1.000

Figure 7.3 Tertiary Level Eigenvector Magnitude

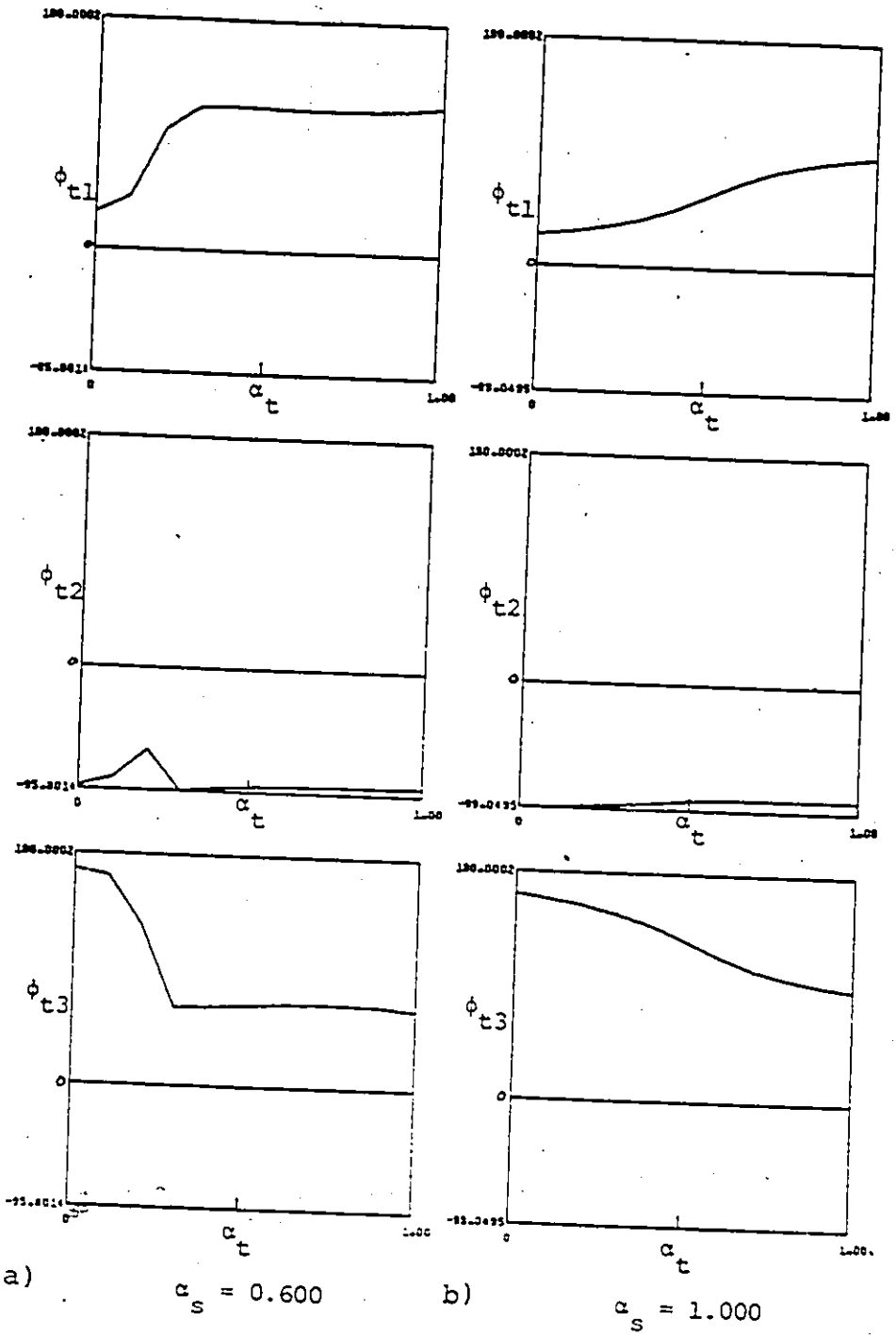

μ_{sp} = 0.001

μ_{ts} = 0.001

θ_{sp} = 1.000

θ_{tp} = 1.000

ζ_p = 0.050

Figure 7.4 Tertiary Level Eigenvector Phase Angle

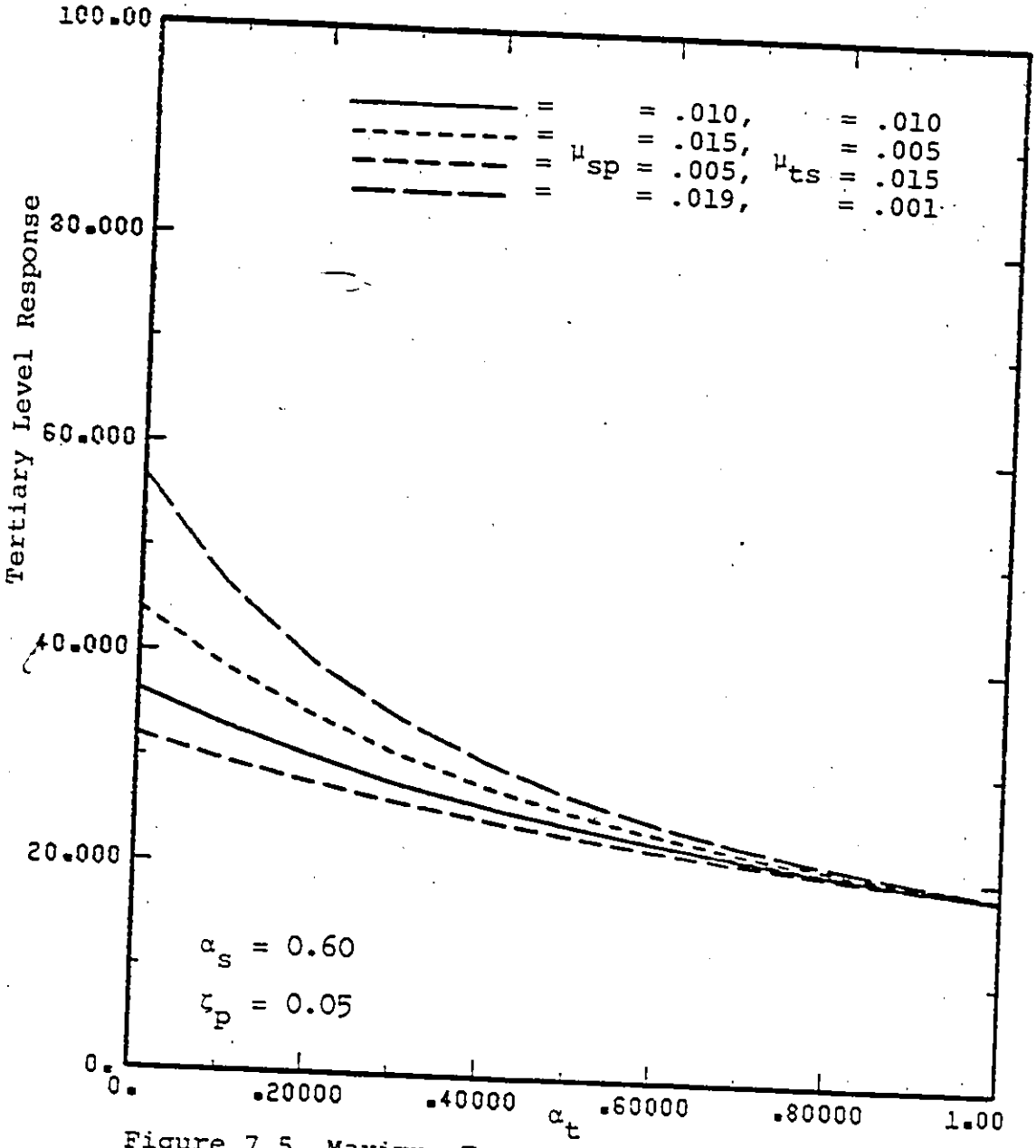

Figure 7.5 Maximum Tertiary Level Response to ORIONEW Earthquake Time History

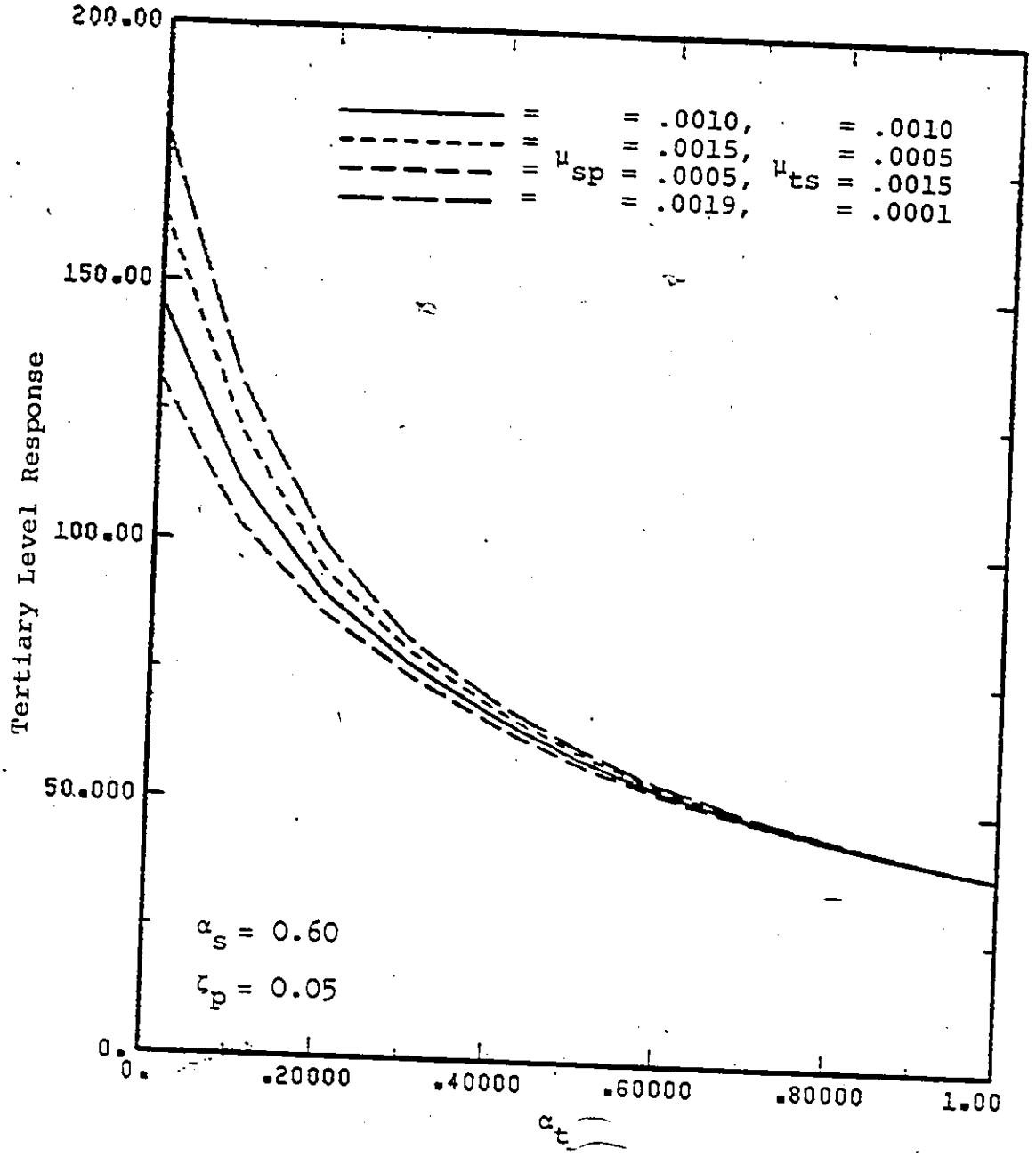

Figure 7.6 Maximum Tertiary Level Response to ORIONEW Earthquake Time History

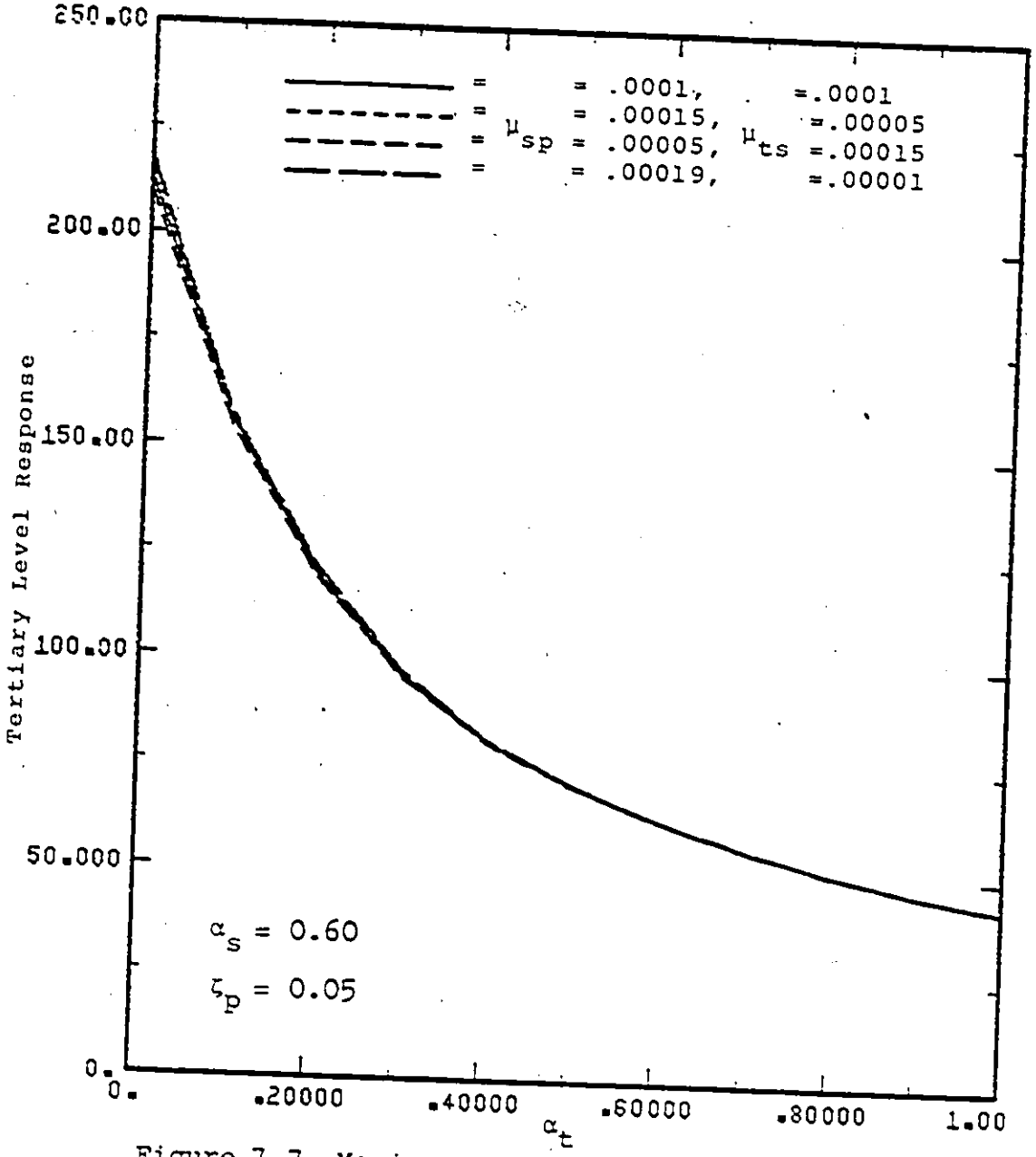

Figure 7.7 Maximum Tertiary Level Response to ORIONEW Earthquake Time History

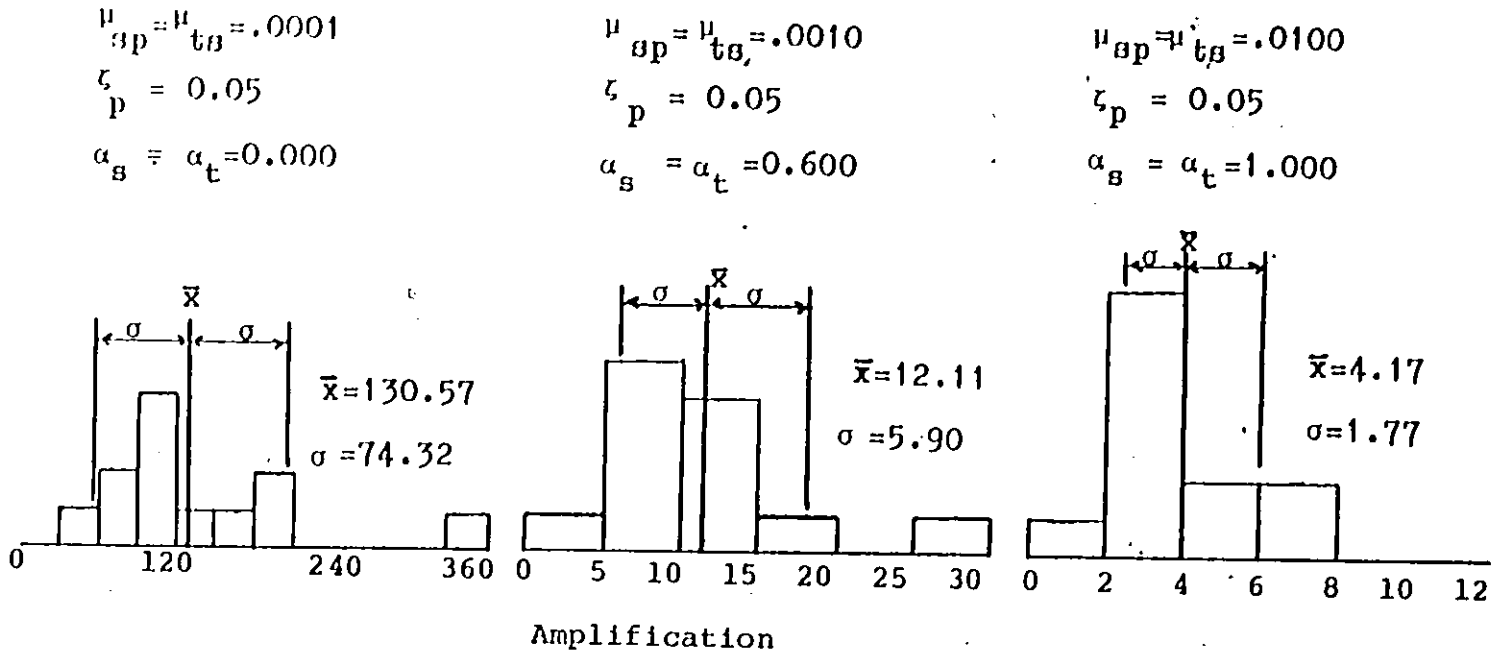

Figure 7.8 Distribution of Tertiary Level Amplification Over Twelve Time Histories

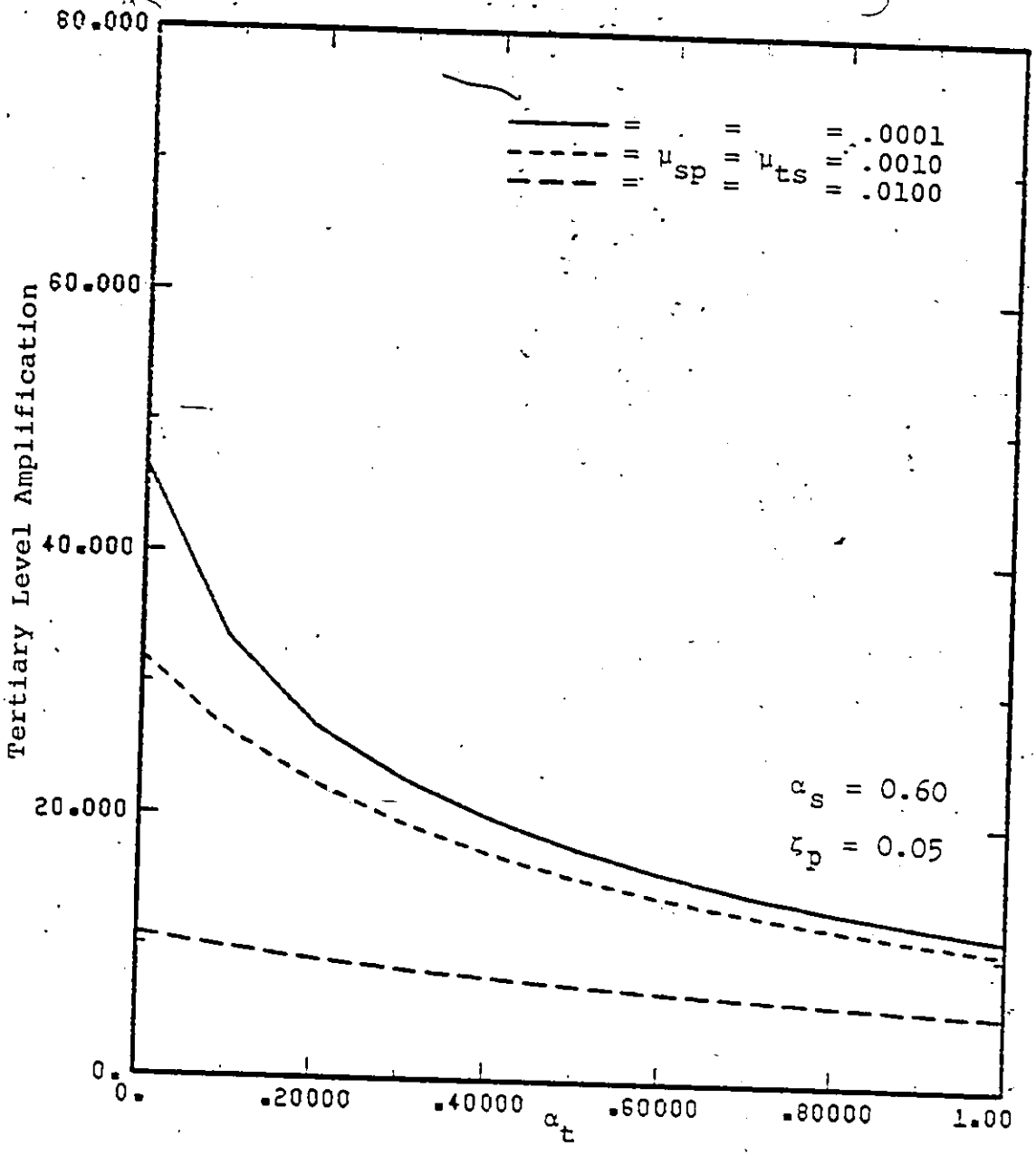

Figure 7.9 Maximum Tertiary Level Amplification Averaged over 12 Time Histories

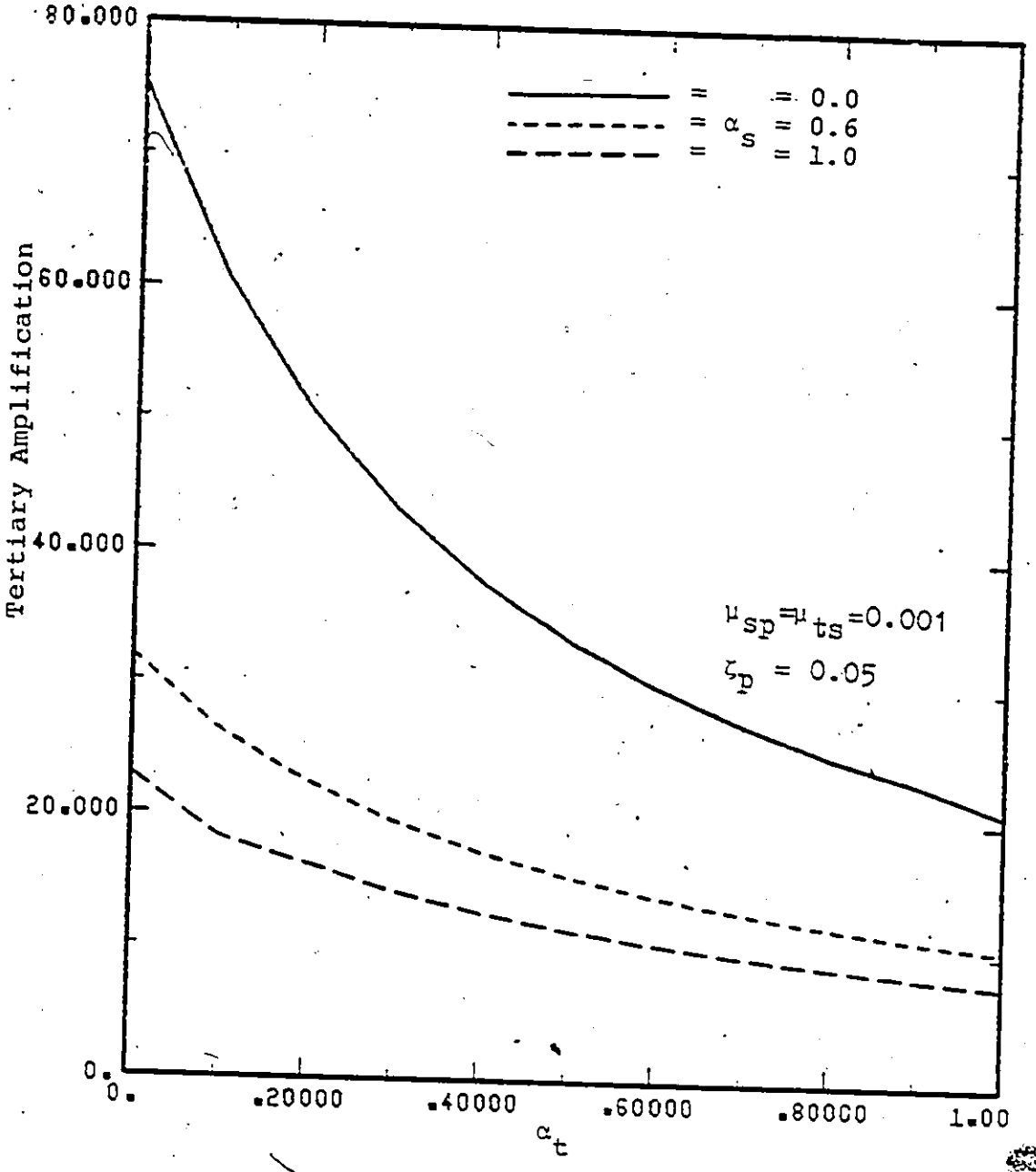

Figure 7.10 Maximum Tertiary Level Amplification Averaged over 12 Time Histories

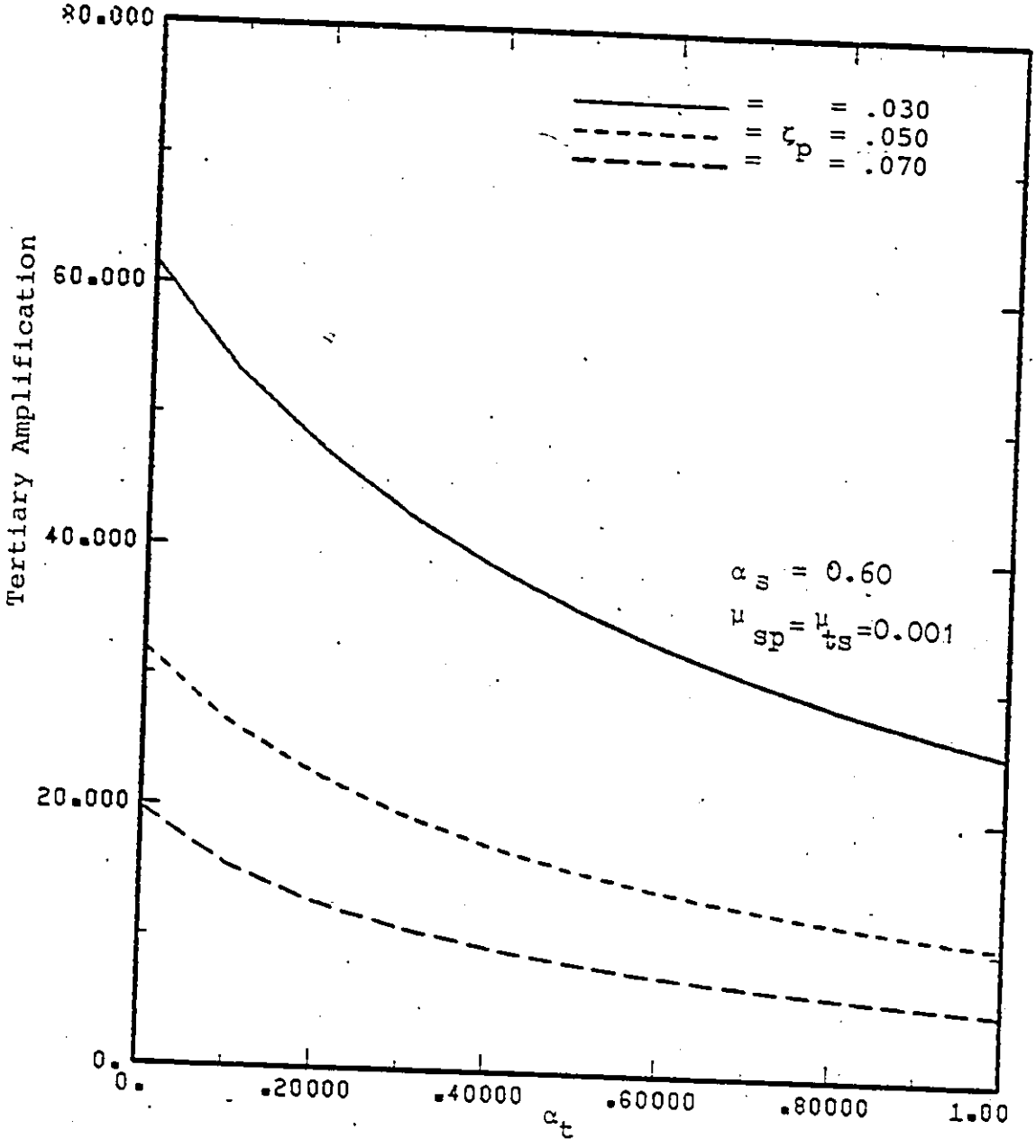

Figure 7.11 Maximum Tertiary Level Amplification Averaged over 12 Time Histories

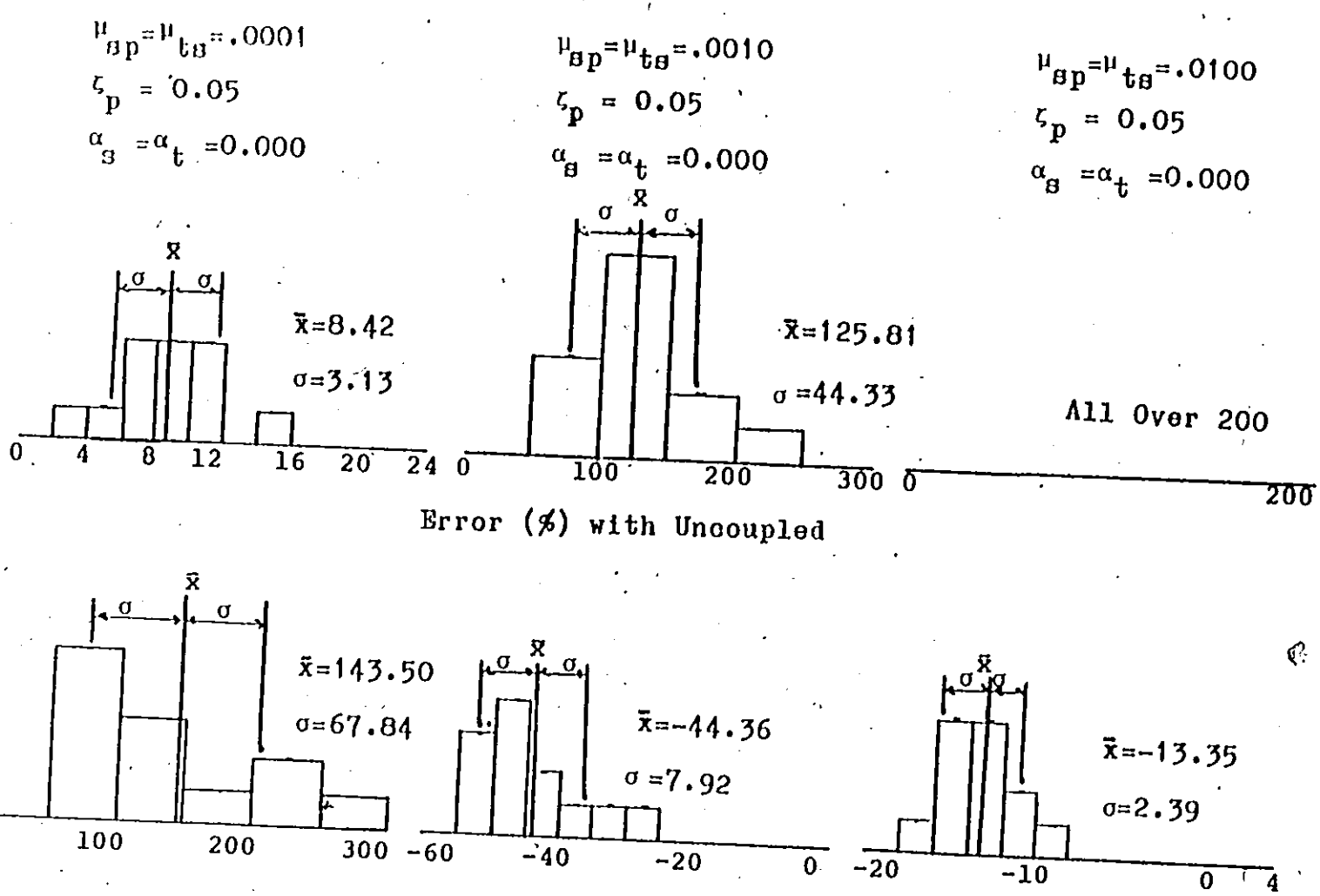

Figure 7.12 Distribution of Error in the Estimates of Tertiary Level Maximum Response

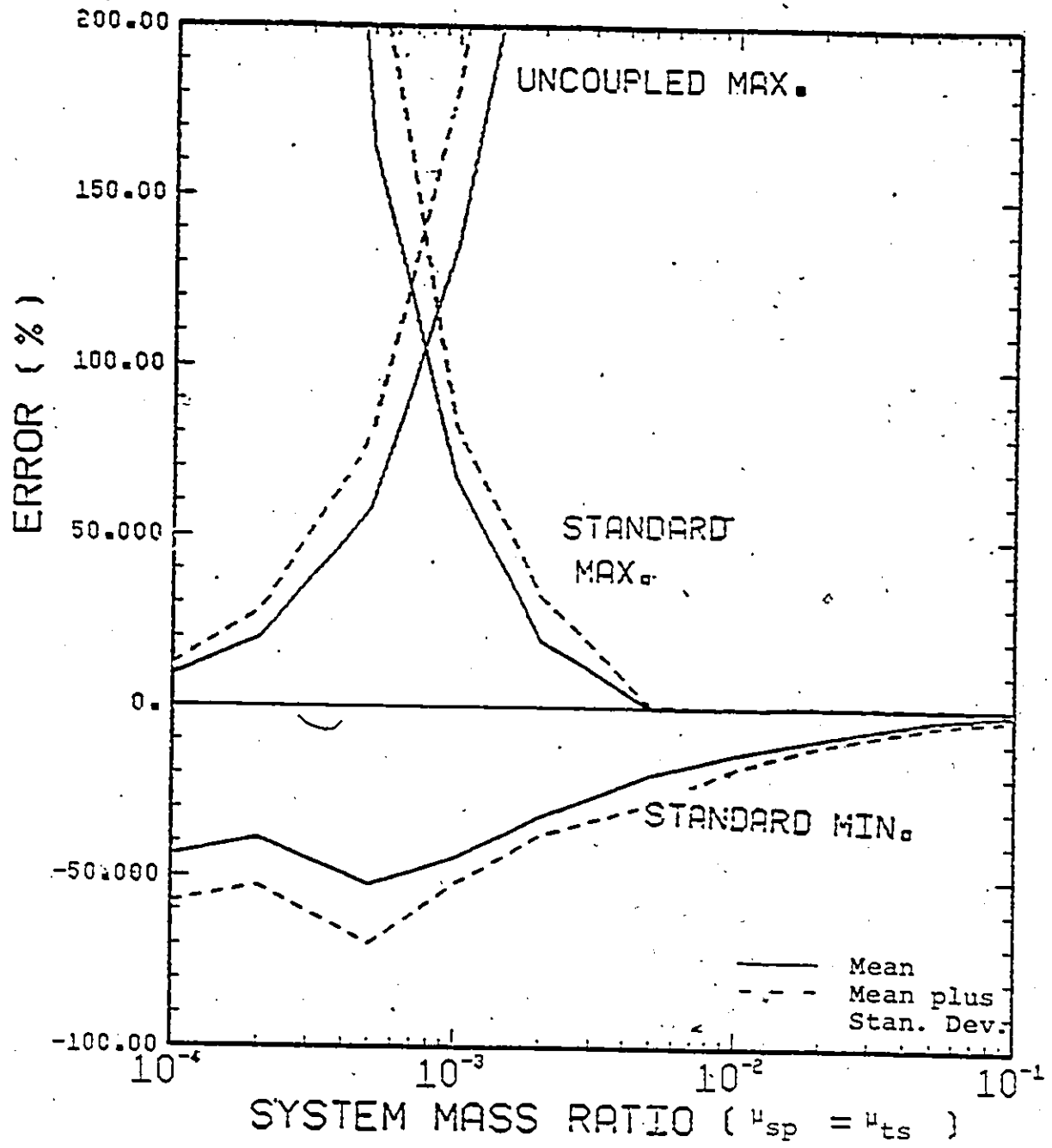

Figure 7.13 Error Envelope for Maximum Tertiary Response Estimate Averaged Over 12 Time Histories (range over various values of α_s and α_t)

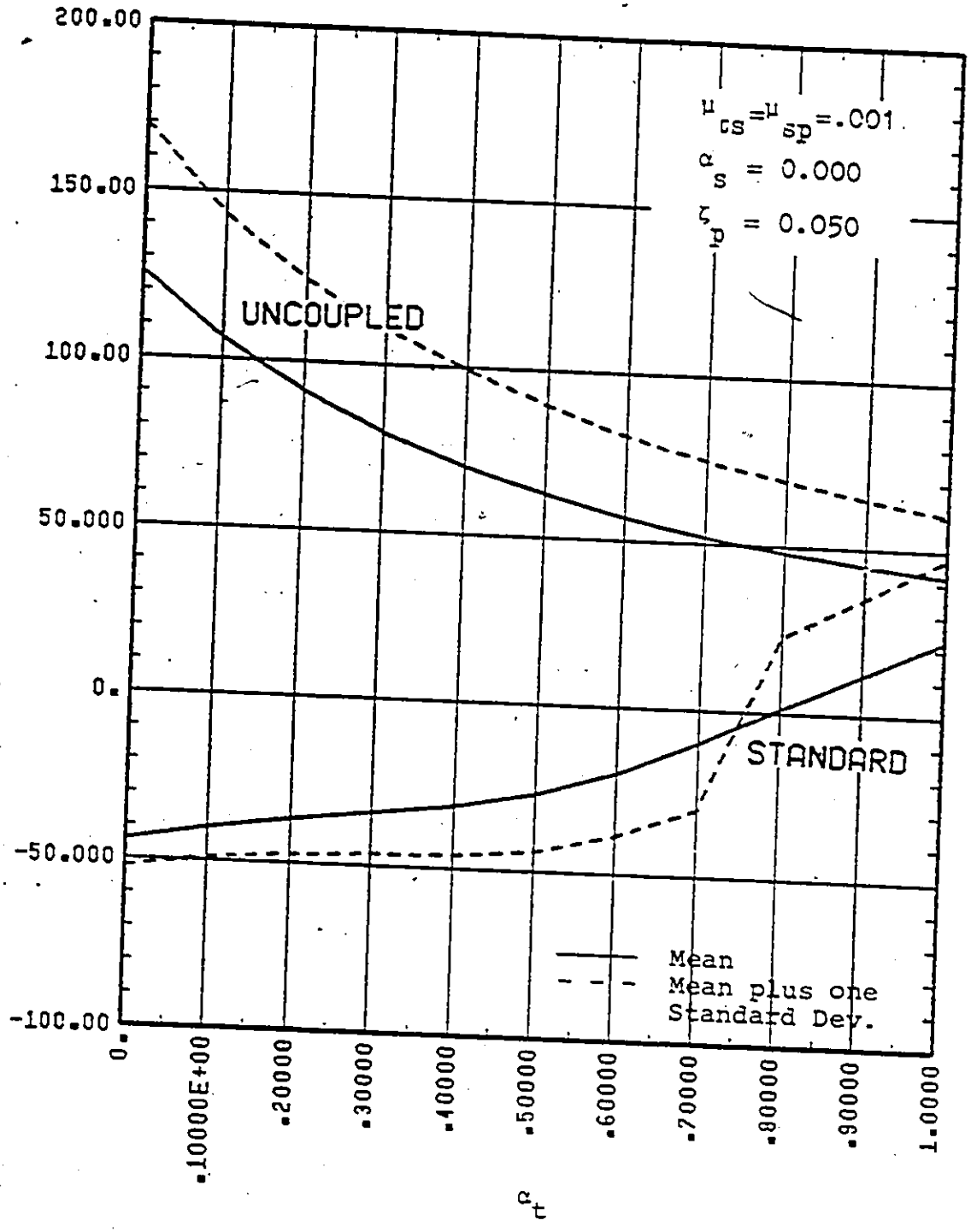

Figure 7.14 Error in Maximum Tertiary Response Estimate Averaged over Twelve Time Histories

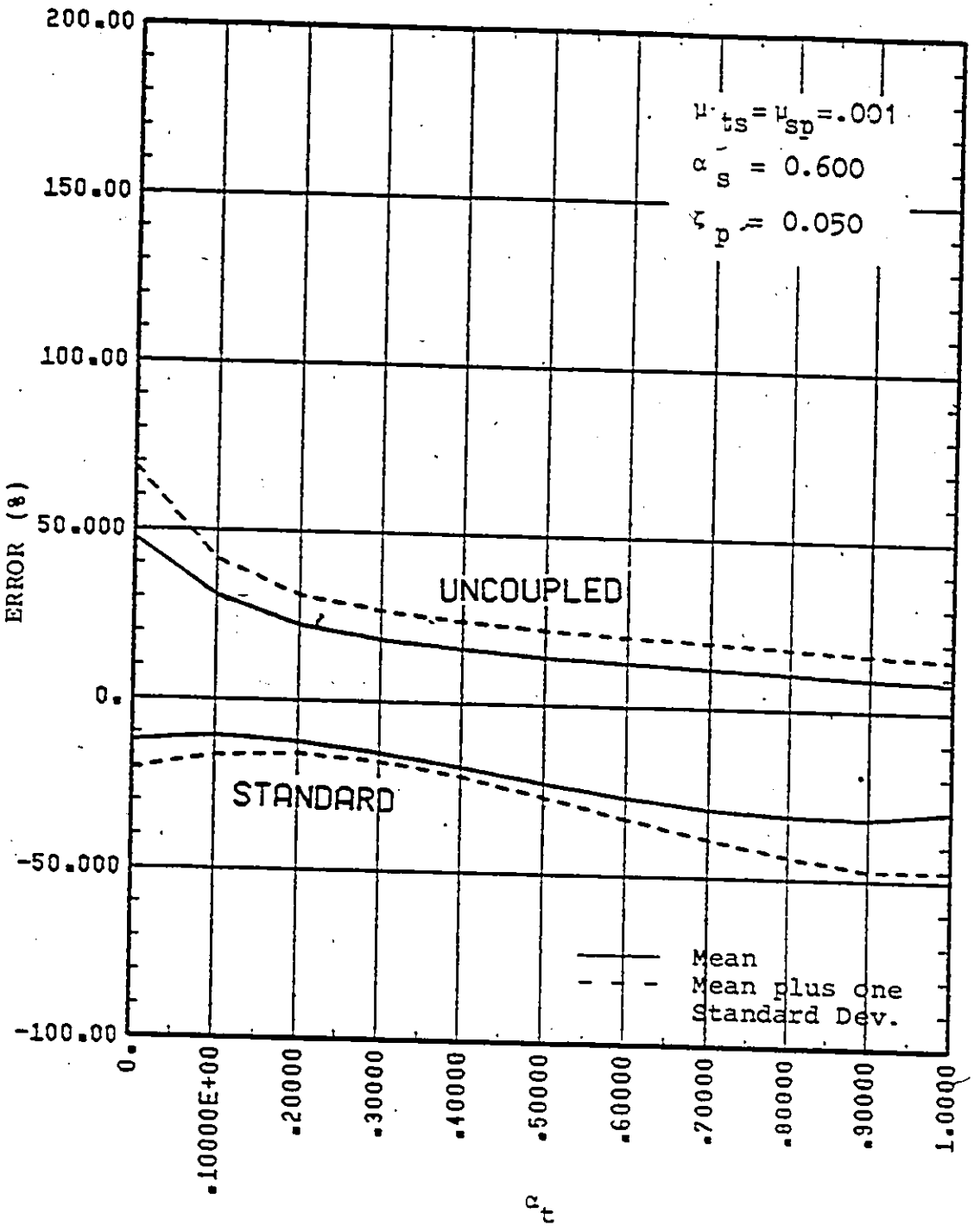

Figure 7.15 Error in Maximum Tertiary Response Estimate Averaged over Twelve Time Histories

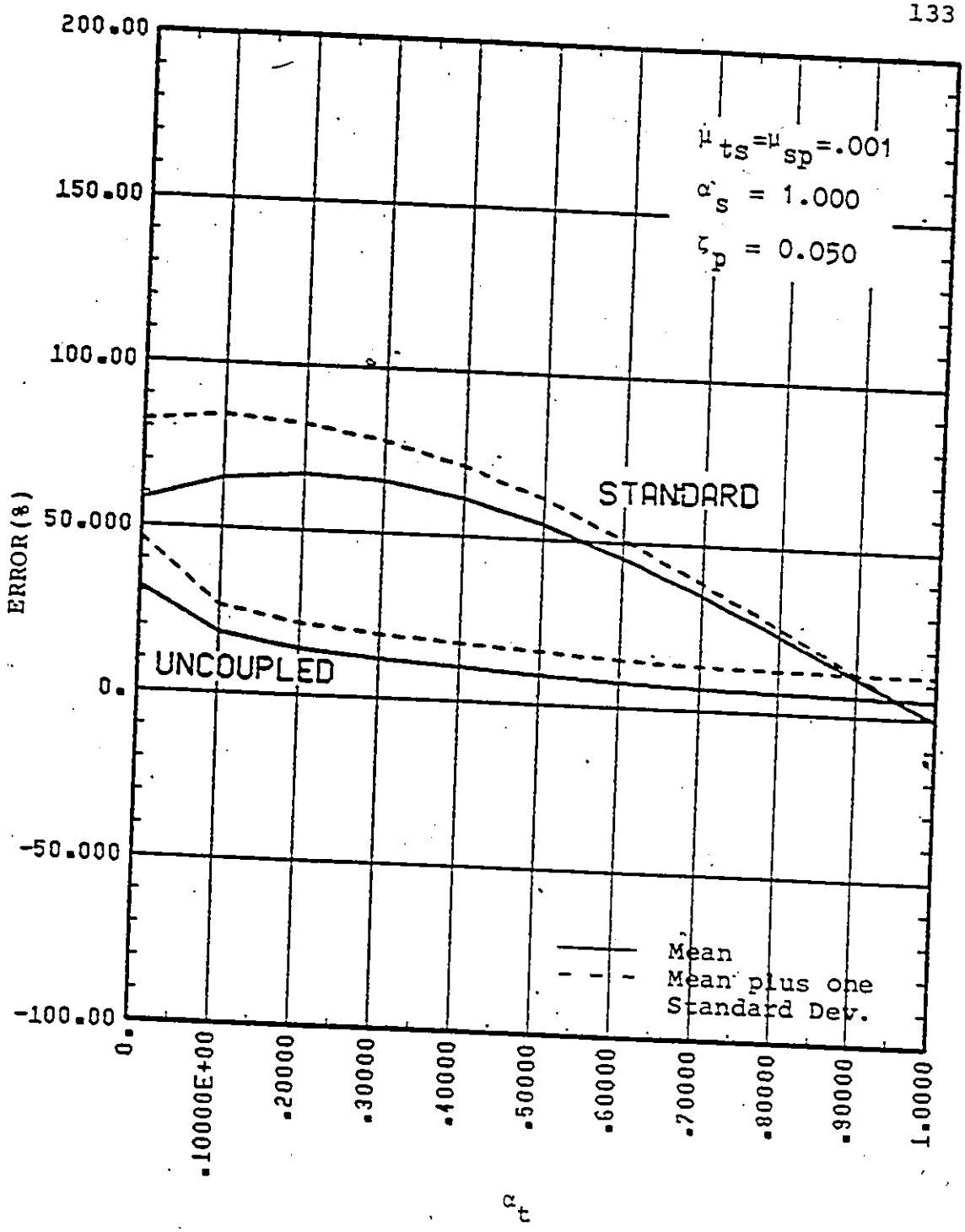

Figure 7.16 Error in Maximum Tertiary Response Estimate Averaged over Twelve Time Histories

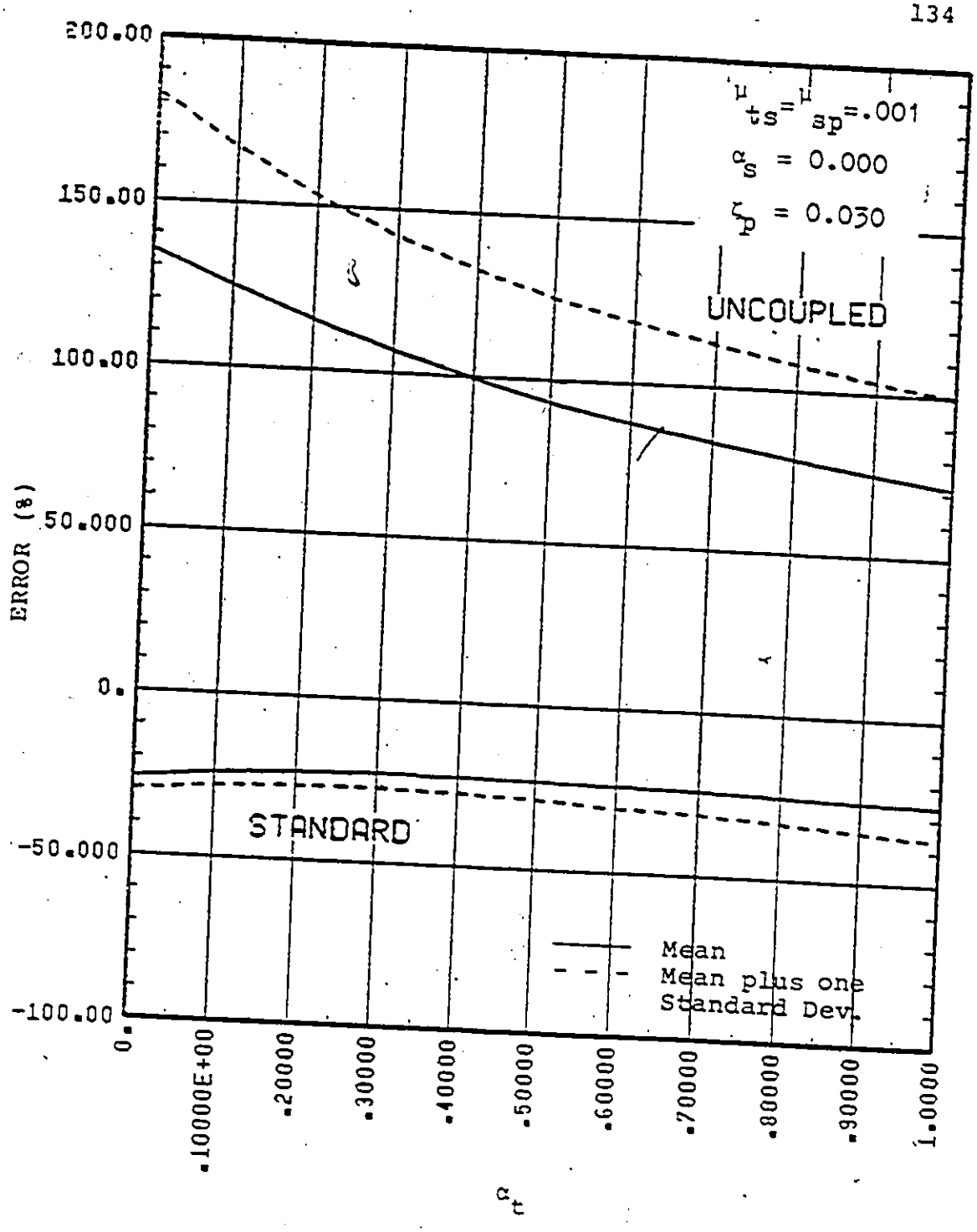

Figure 7.17 Error in Maximum Tertiary Response Estimate Averaged over Twelve Time Histories

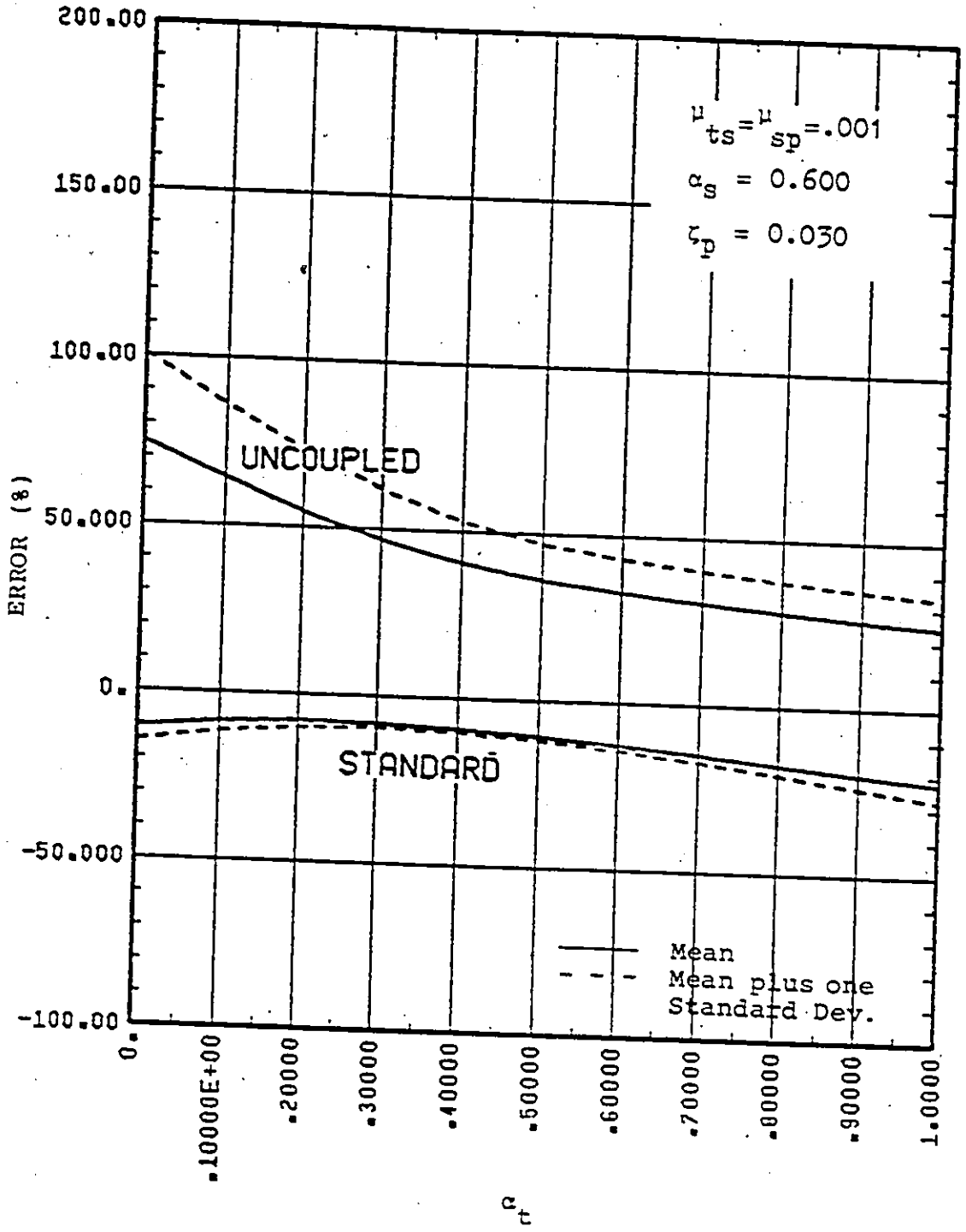

Figure 7.18 Error in Maximum Tertiary Response Estimate Averaged over Twelve Time Histories

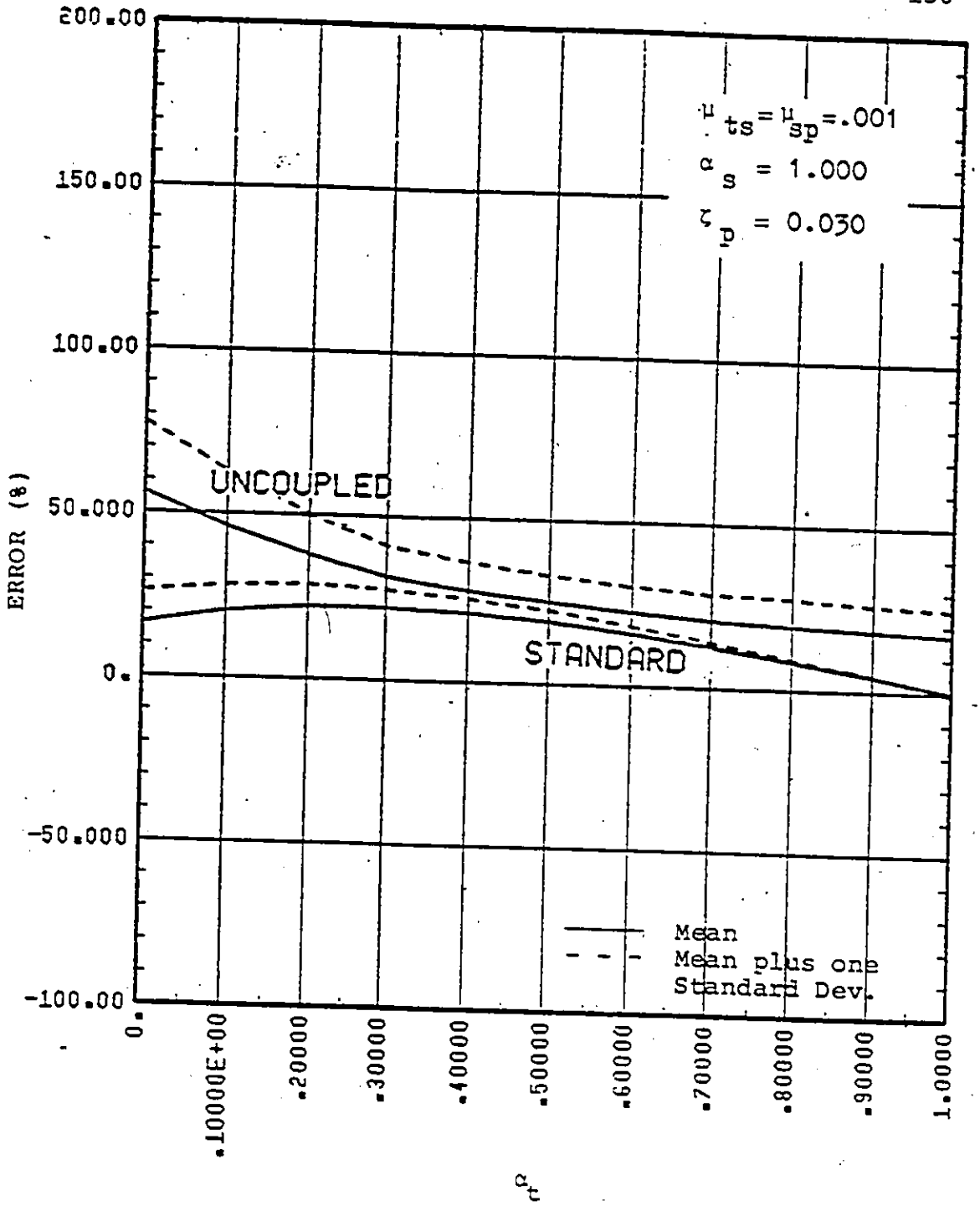

Figure 7.19 Error in Maximum Tertiary Response Estimate Averaged over Twelve Time Histories

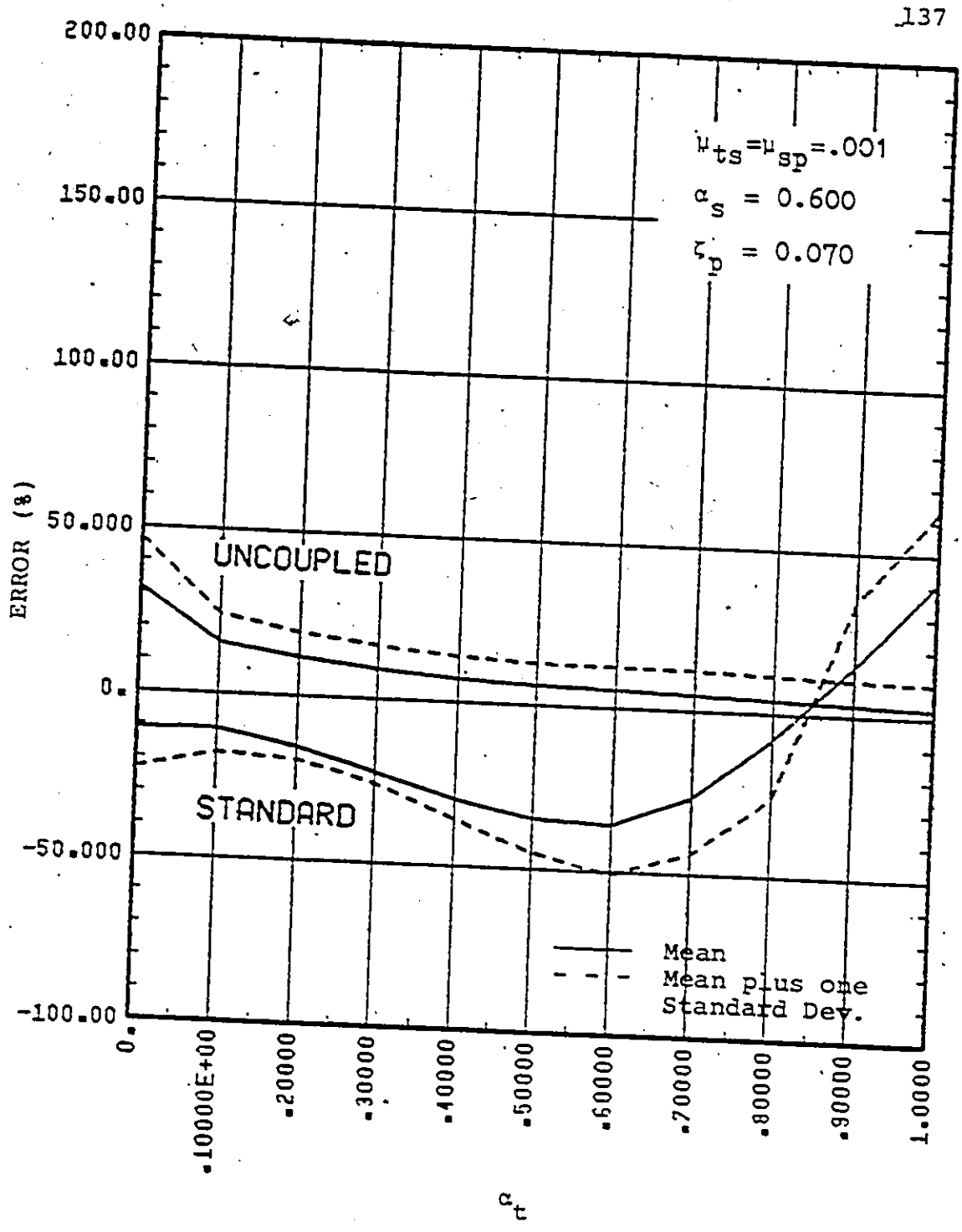

Figure 7.20 Error in Maximum Tertiary Response Estimate Averaged over Twelve Time Histories

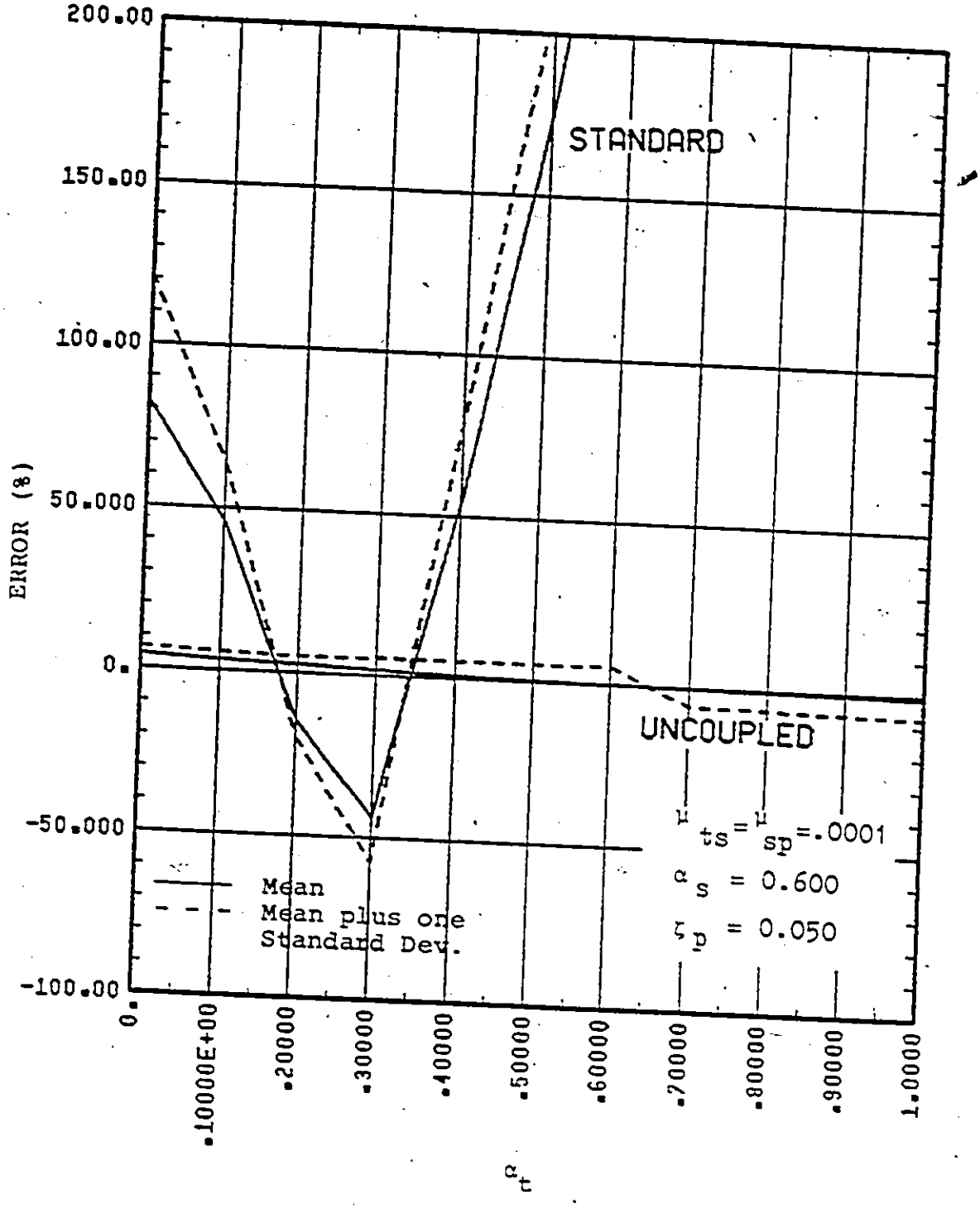

Figure 7.21 Error in Maximum Tertiary Response Estimate Averaged over Twelve Time Histories

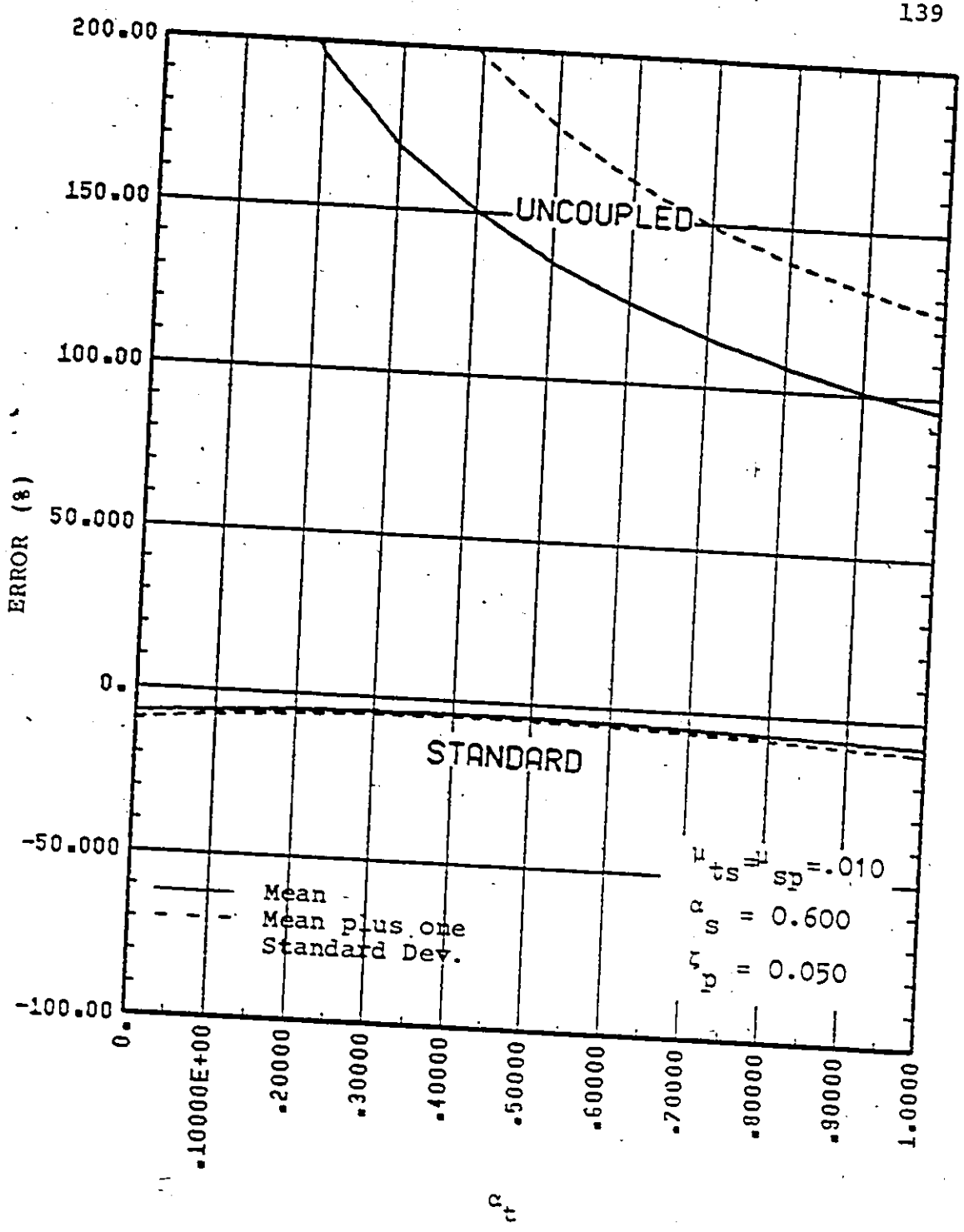

Figure 7.22 Error in Maximum Tertiary Response Estimate Averaged over Twelve Time Histories

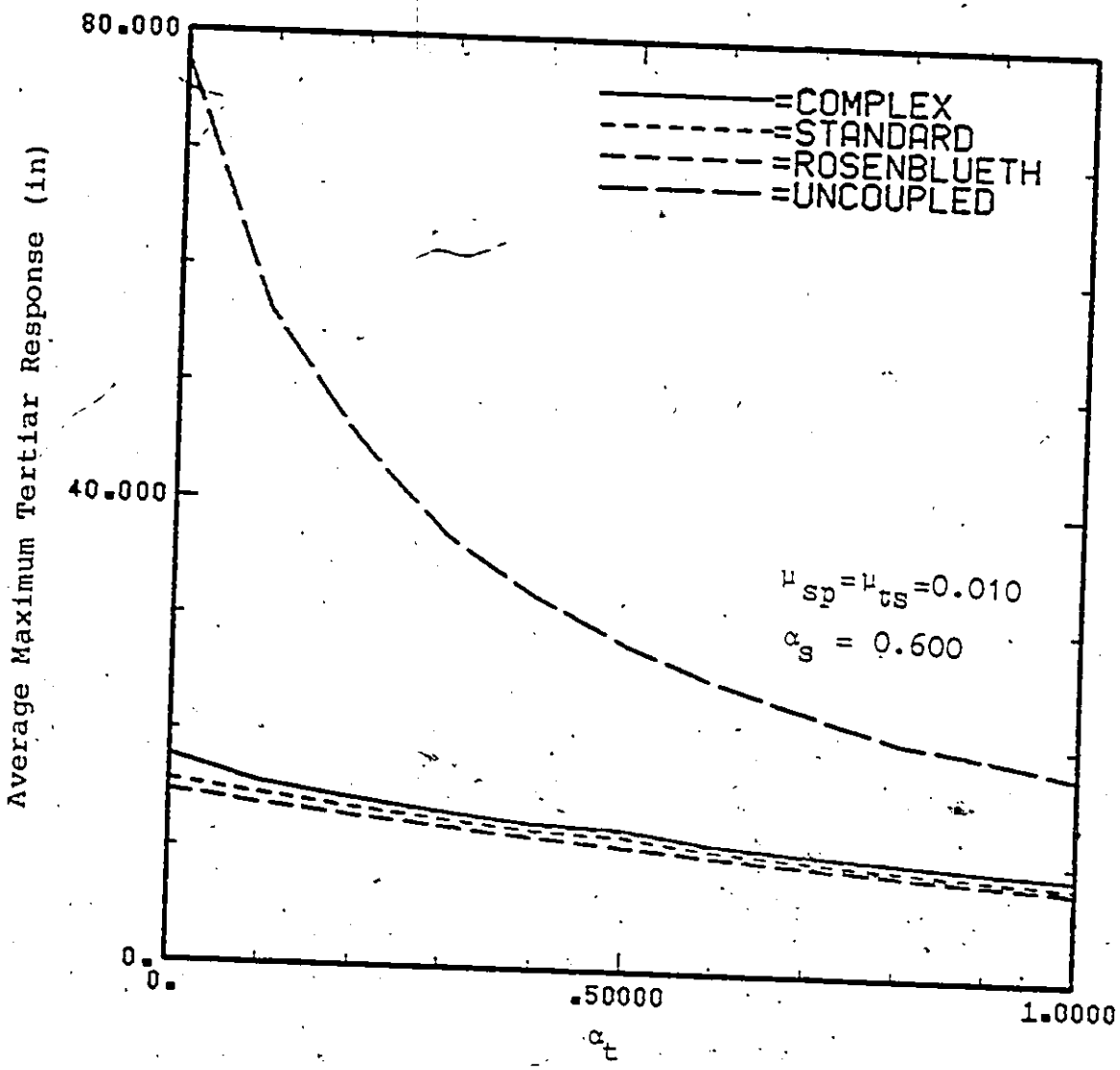

Figure 7.23 Comparison of Maximum Tertiary Response Estimate from Four Different Analytical Procedures

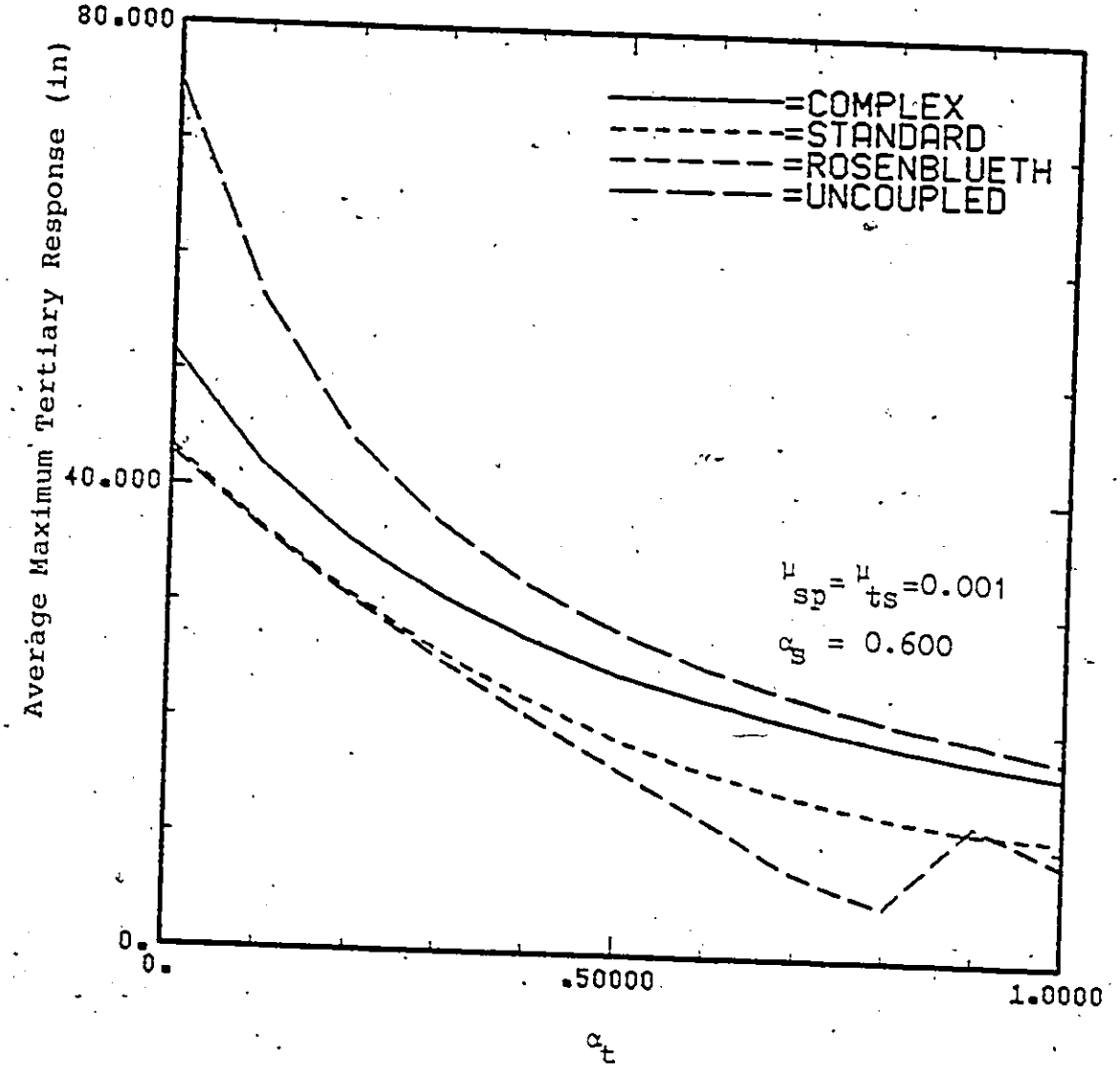

Figure 7.24 Comparison of Maximum Tertiary Response Estimate from Four Different Analytical Procedures

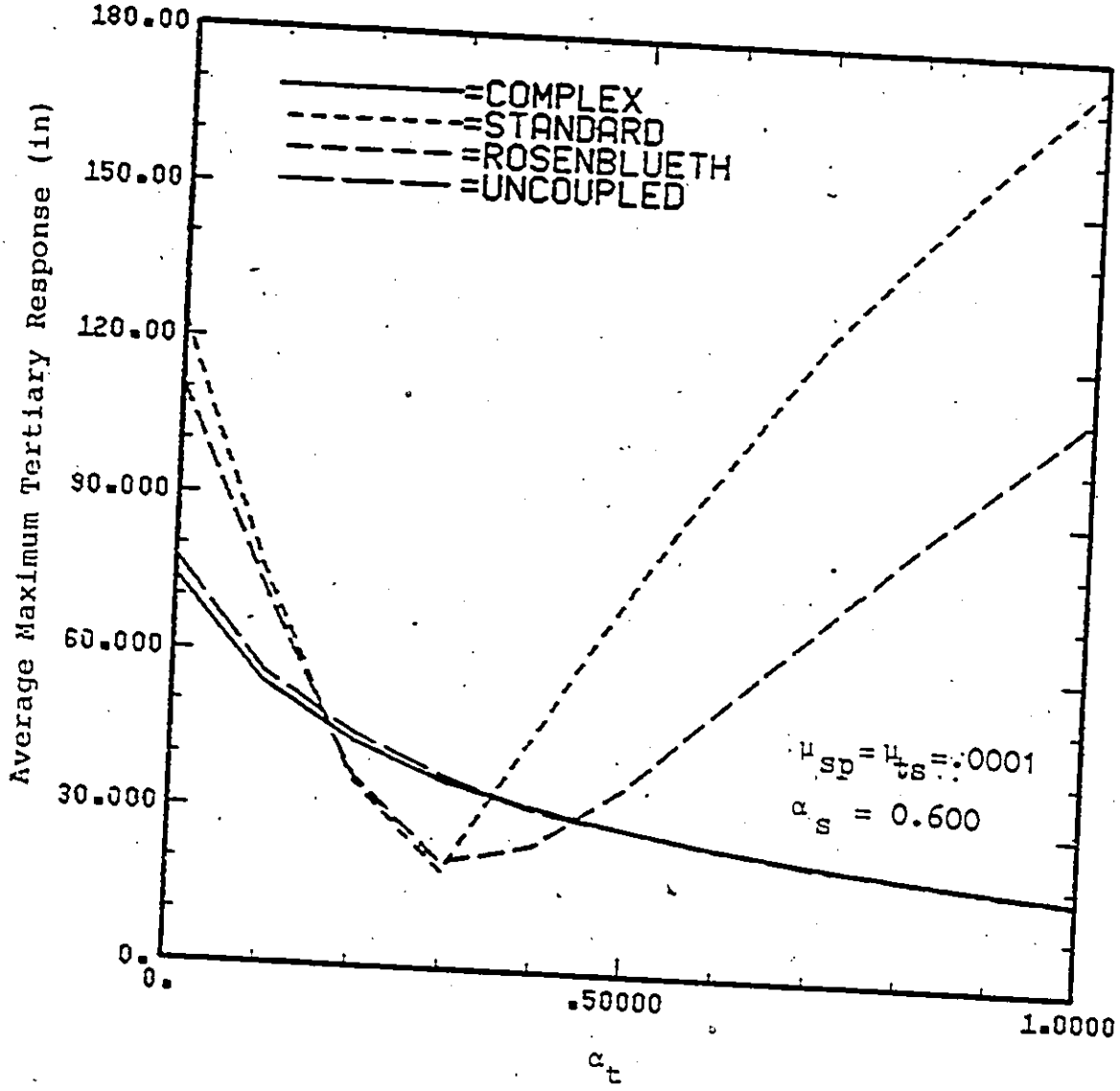

Figure 7.2 5 Comparison of Maximum Tertiary Response Estimate from Four Different Analytical Procedures

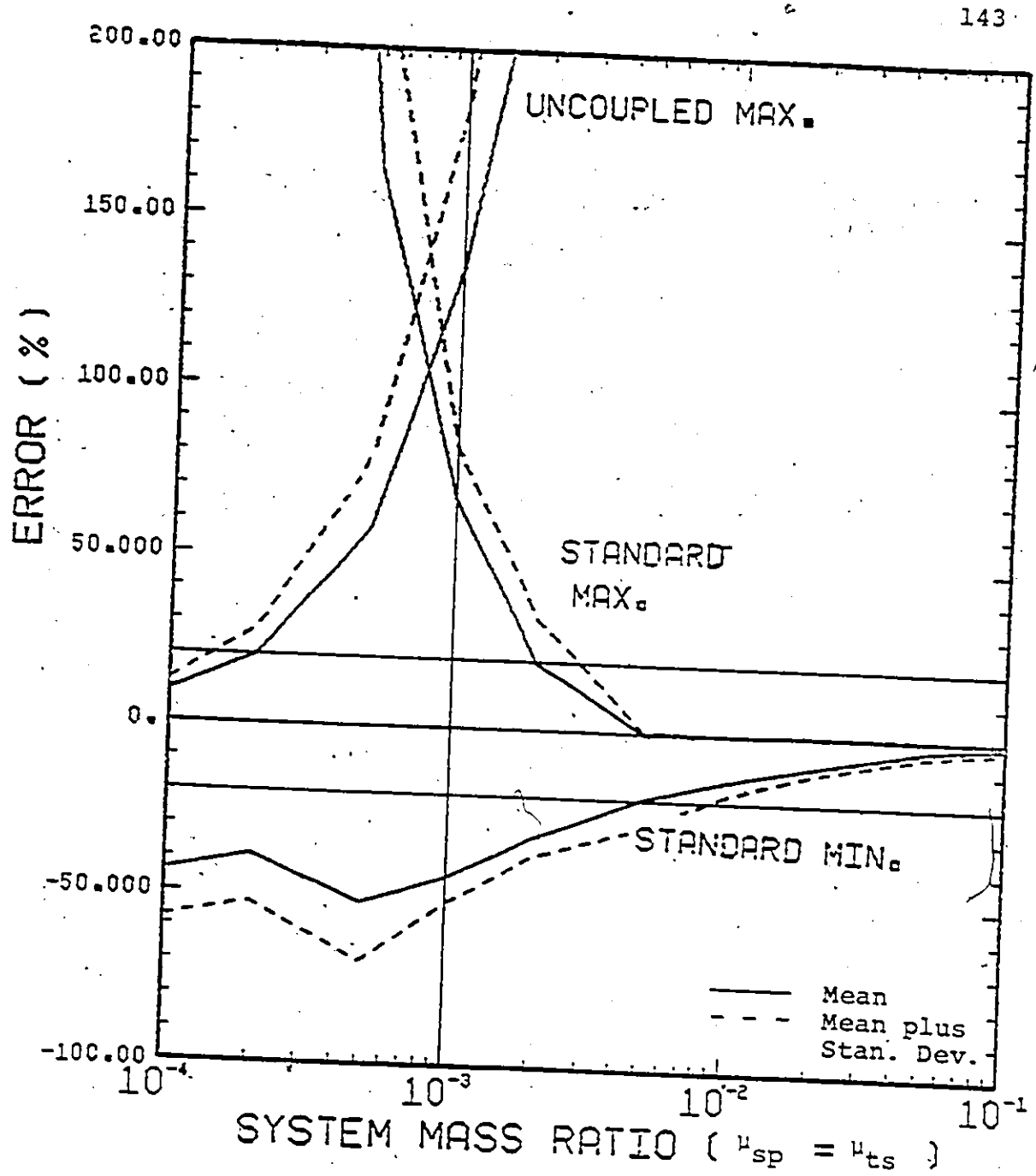

Figure 7.26 Error Envelope for Maximum Tertiary Response Estimate Averaged Over 12 Time Histories (range over various values of α_s and α_t)

CHAPTER 8

CONCLUSIONS AND RECOMMENDATIONS

8.1 Conclusions

This report has studied the ability of simplified procedures to adequately predict the best estimate response of two and three level systems exhibiting nonproportional damping. An investigation has also been made to try and attach a physical interpretation to the various components of the complex eigenvalues and complex eigenvectors that are required to handle the case of nonproportional damping.

The effect of nonproportional damping on the predicted seismic response of two and three level systems becomes more significant as the mass ratios decrease, as the primary damping ratio increases and as the α values move away from unity.

It has been shown that two and three level systems, depending on the acceptable level of error, can exhibit three regions where the three different response calculation procedures may be used. Obviously, complex modal analysis may be used over the entire range of mass ratios and damping ratios. There also exist regions where a physically

uncoupled analysis will introduce an acceptable level of error. These regions are characterized by small mass ratios and high damping ratios. Similarly, standard modal analysis will introduce acceptable levels of error over regions that exhibit large mass ratios, smaller damping ratios and α's that are close to unity.

Curves presented in Chapters 6 and 7 provide an estimate of the reliability of the simpler procedures for different mass ratios and unknown damping characteristics.

In the event that information is available about damping then the refined curves of error estimate can be used to give a better estimate of expected errors.

The ability of the standard modal analysis to properly calculate the seismic response of systems exhibiting nonproportional damping is dependent on two related factors. As was pointed out in Chapter 2, the procedure is based on the assumption that the undamped modes of vibration will uncouple the damping matrix or that the off-diagonal terms, after the transformation, will be insignificant. Since a system with closely spaced modes exhibits larger effects of nonproportional damping, the off-diagonal terms, in this case, become more and more significant and the basic assumption is violated.

Related to this phenomenon is the effect that nonproportional damping has on the actual coupled vibrational characteristics of the system. Nonproportional

damping affects frequencies, damping ratios, eigenvectors and mode shapes. The standard method assumes that the undamped mode shapes can be used at all times.

As the degree of nonproportionality in the damping of the system increases, the damped frequency spacing decreases. In addition, the coupled damping ratios take on values closer to the uncoupled values and the eigenvectors and mode shapes vary more (typically, increasing substantially for uncoupled damping ratios away from proportionality). The closer modal frequencies tend to lead to more modal response interaction which can lead to a total response which is less than that predicted by a standard modal analysis.

The modification to the damping ratios and mode shapes also affects the predicted modal response and, consequently, affects the predicted total response.

In the case of the physically uncoupled analysis procedure, the assumption is made that the interaction of higher levels on lower levels is insignificant. As was expected, this assumption is violated as the mass ratios increase and the damping ratios decrease. This leads to increased errors in the predicted response of these systems.

In regions where standard modal analysis gives adequate accuracy in predicting the required maximum response, the Rosenblueth technique, as applied to a response spectrum procedure, provides a similar level of

induced error. At the same time this technique does not require the more lengthy and costly time history analysis.

8.2 Recommendations

It is recommended that the engineer first make use of the figures supplied in this report before making a decision on which method of analysis to use during the structural design process.

For structures in which standard modal analysis has been found to be acceptable, the Rosenblueth response spectrum technique may be used. This technique usually gives slightly higher errors except for the very small mass ratios where it often outperforms the standard modal analysis. If an uncoupled analysis has been found to be adequate then the engineer may investigate the use of a response spectrum technique of analysis. Response spectrum techniques for multi-level systems have been presented by several authors including Kapur and Shao(16).

As has been pointed out in the conclusions, provided the mass ratios and damping ratios can be specified, a method has been presented that can give the engineer an estimate of the error that can be expected if a simplified procedure is used. The problem lies in the need to be able to specify the structural and excitation characteristics fairly accurately. In many situations the structural characteristics are not well known and no one really knows

what earthquake time history will impact the area of the structure. As a result, it is the recommendation of this author that, especially in dealing with three level systems, research should be concentrated in the attempt to improve the estimation of structural parameters from structural drawings and existing buildings. In addition, there is still room for large improvements in our ability to predict the type of ground motion that might impact a site.

REFERENCES

1. ,"Strong Motion Earthquake Accelerograms - Digitized and Plotted Data", Vol. II, Earthquake Engineering Research Laboratory Report EERL 72-51, California Institute of Technology, Pasadena, California, February 1973.

2. Aziz, T. S., "Coupling Effects for Secondary Systems in Nuclear Power Plants", Proceedings of the Eighth World Conference on Earthquake Engineering, Berkeley, California, 1984.

3. Aziz, T. S. and Duff, C. G., "Decoupling Criteria for Seismic Analysis of Nuclear Power Plant Systems", ASME/CSME Pressure Vessels and Piping Conference with Nuclear and Materials Division, Montreal, June 1978.

4. Biggs, J. M. and Roesset, J. M., "Seismic Analysis of Equipment Mounted on a Massive Structure", Seismic Design of Nuclear Power Plants, 1969, pp 319-343.

5. Chen, C., "The Uncoupling Criteria for Subsystem Seismic Analysis", Fifth International Conference on Structural Mechanics in Reactor Technology, Paper K8/1, 1979.

6. Clough, R. W. and Mojtahedi, S. "Earthquake Response Analysis Considering Non-Proportional Damping", Earthquake Engineering and Structural Dynamics, Vol. 4, 1976, pp 489-496.

7. Clough, R. W. and Penzien, J., Dynamics of Structures, McGraw-Hill Inc., Toronto, 1975.

8. Duff, C. G., "Simplified Method for Development of Earthquake Ground and Floor Response Spectra for Nuclear Power Plant Design", Second Canadian Conference on Earthquake Engineering, McMaster University, Hamilton, Ontario, 1975.

9. Gantmacher, F. R., Matrix Theory, Vol. I, Chelsea Publishing, Bronx, New York, 1960, pg 224.

10. Gelman, A. P., "Determining Interaction Effects in the Seismic Analysis of Components", Second National Congress on Pressure Vessels and Piping, San Francisco, June 1975.

11. Hadjian, A. H. "Earthquake Forces on Equipment in Nuclear Power Plants", ASCE, Vol. 97, No. PO3, 1971, pp 649-665.

12. Hadjian, A. H. "On the Decoupling of Secondary Systems for Seismic Analysis", Sixth World Conference on Earthquake Engineering, 1976, pp 3286-3291.

13. Heidebrecht, A. C., "Analysis of Third Level Seismic Response Characteristics", McMaster University, private communication with C. G. Duff.

14. Hernried, A. G. and Sackman, J. L., "Tertiary Systems", Earthquake Engineering and Structural Dynamics, Vol. 13, 1985, pp 467-479.

15. Igusa, T. and Kiureghian, A. "Dynamic Analysis of Multiply Tuned and Arbitrarily Supported Secondary Systems", Report No. UCB/EERC-83/07, University of California, Berkeley, California, 1983.

16. Kapur, K. K. and Shao, L. C., "Generation of Seismic Floor Response Spectra for Equipment Design", Structural Design of Nuclear Power Plant Facilities, Specialty Conference, Preparatory Paper, Chicago, Illinois, December 17-18, 1973.

17. Kiureghian, A. D. etal, "Dynamic Response of Light Equipment in Structures", Report No. UCB/EERC - 81/05, University of California, Berkeley, California, April 1981.

18. Nakhato, T. and Newmark, N. M., "Approximate Dynamic Response of Light Secondary Systems", Report No. PB-220 906, University of Illinois, Urbana, Illinois, 1973.

19. Nelson, F. C. "The Role of Closely Spaced Modes in the Seismic Response of Equipment in Structures", U.S. National Conference on Earthquake Engineering, Ann Arbour, Michigan, 1975, pp 538-543.

20. Newmark, N. M. and Rosenblueth, E., Fundamentals of Earthquake Engineering, Prentice-Hall, Englewood Cliffs, New Jersey, 1971, pg 310.

21. Ruzicka, G. C. and Robinson, A. R., "Dynamic Response of Tuned Secondary Systems", Structural Research Series No. 485, University of Illinois, Urbana, Illinois, November 1980.

22. Sackman, J. L. and Kelly, J. M., "Rational Design Methods for Light Equipment in Structures Subjected to Ground Motion", Report No. UCB/EERC - 78/19, University of California, Berkeley, California, September 1978.

23. Singh, M. P. and Ashtainy, M. G., "Modal Time History Analysis of Non-Classically Damped Structures for Seismic Motions", Earthquake Engineering and Structural Dynamics, Vol. 14, 1986, pp 133-146.

24. Vanmarcke, E. H., "A Simple Procedure for Predicting Amplified Response Spectra and Equipment Response", Sixth World Conference on Earthquake Engineering, 1976, pp 3323-3327.

25. Veletsos, A. S. and Ventura, C. E., "Modal Analysis of Non-Classically Damped Linear Systems", Earthquake Engineering and Structural Dynamics, Vol.14, 1986, pp 217-243.

26. Villaverde, R. and Newmark, N. M., "Seismic Response of Light Attachments to Buildings", Structural Research Series No. 469, University of Illinois, Urbana, Illinois, February 1980.

27. Wilson, E. L. etal, "A Replacement for the SRSS Method in Seismic Analysis", Earthquake Engineering and Structural Dynamics, Vol. 9, pp 187-194, 1981.

28. Wilson, J. C., "Characteristics of Seismic Floor Motion", M.Eng. Thesis, McMaster University, Hamilton, Ontario, June 1980.

APPENDIX I

PLOTS OF EARTHQUAKE TIME HISTORIES

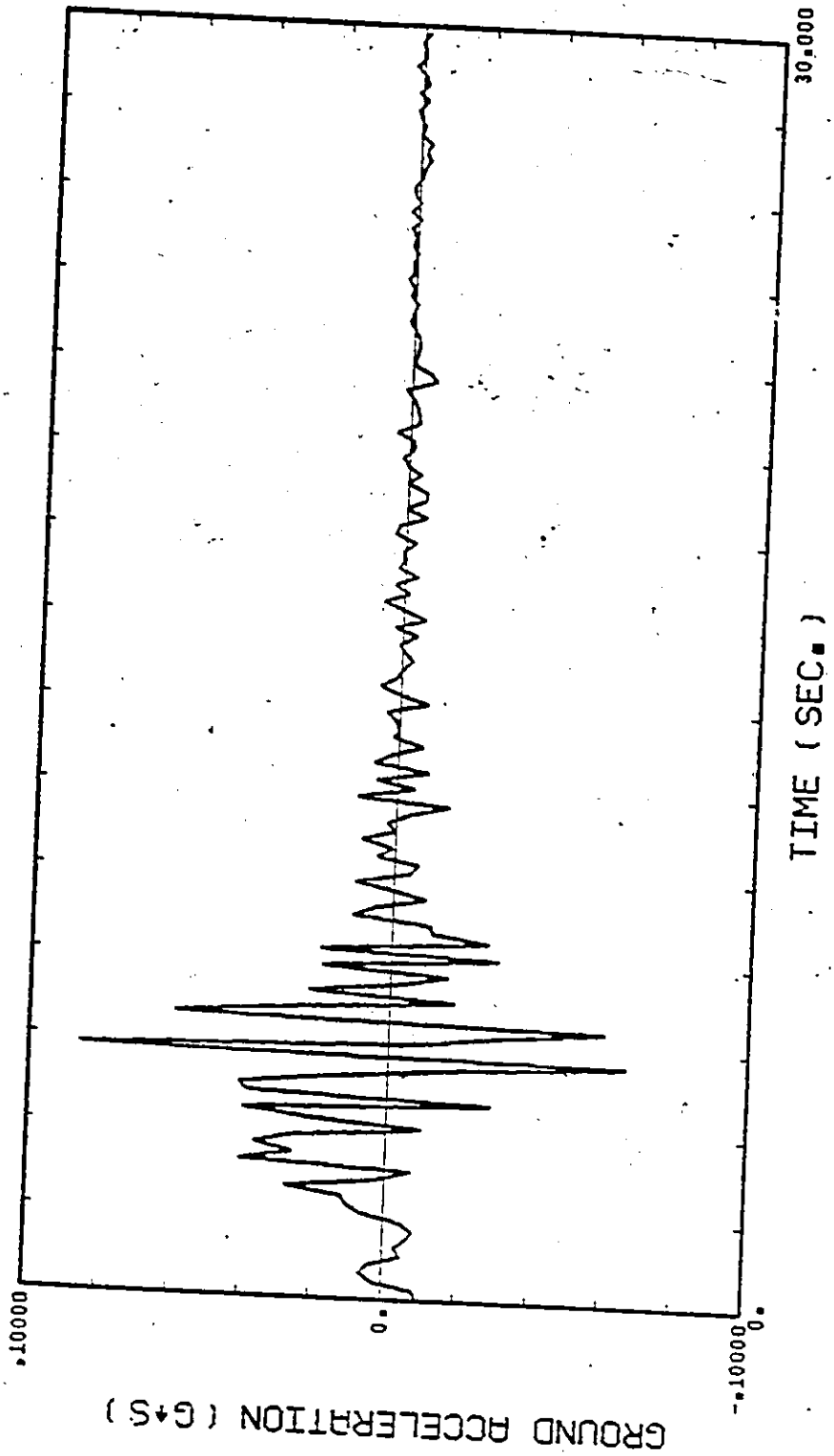

CALEW EARTHQUAKE TIME HISTORY

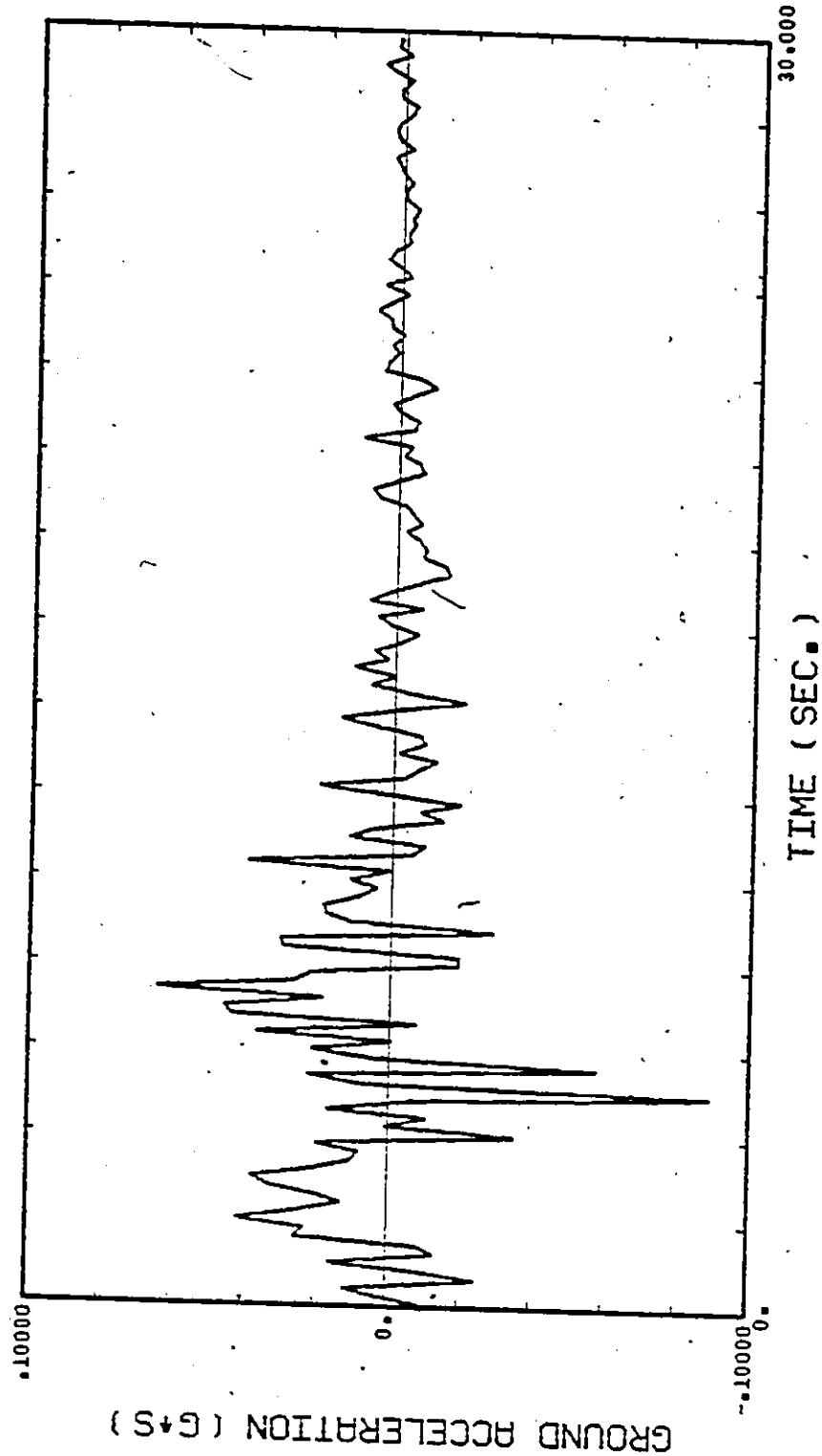

CALNS EARTHQUAKE TIME HISTORY

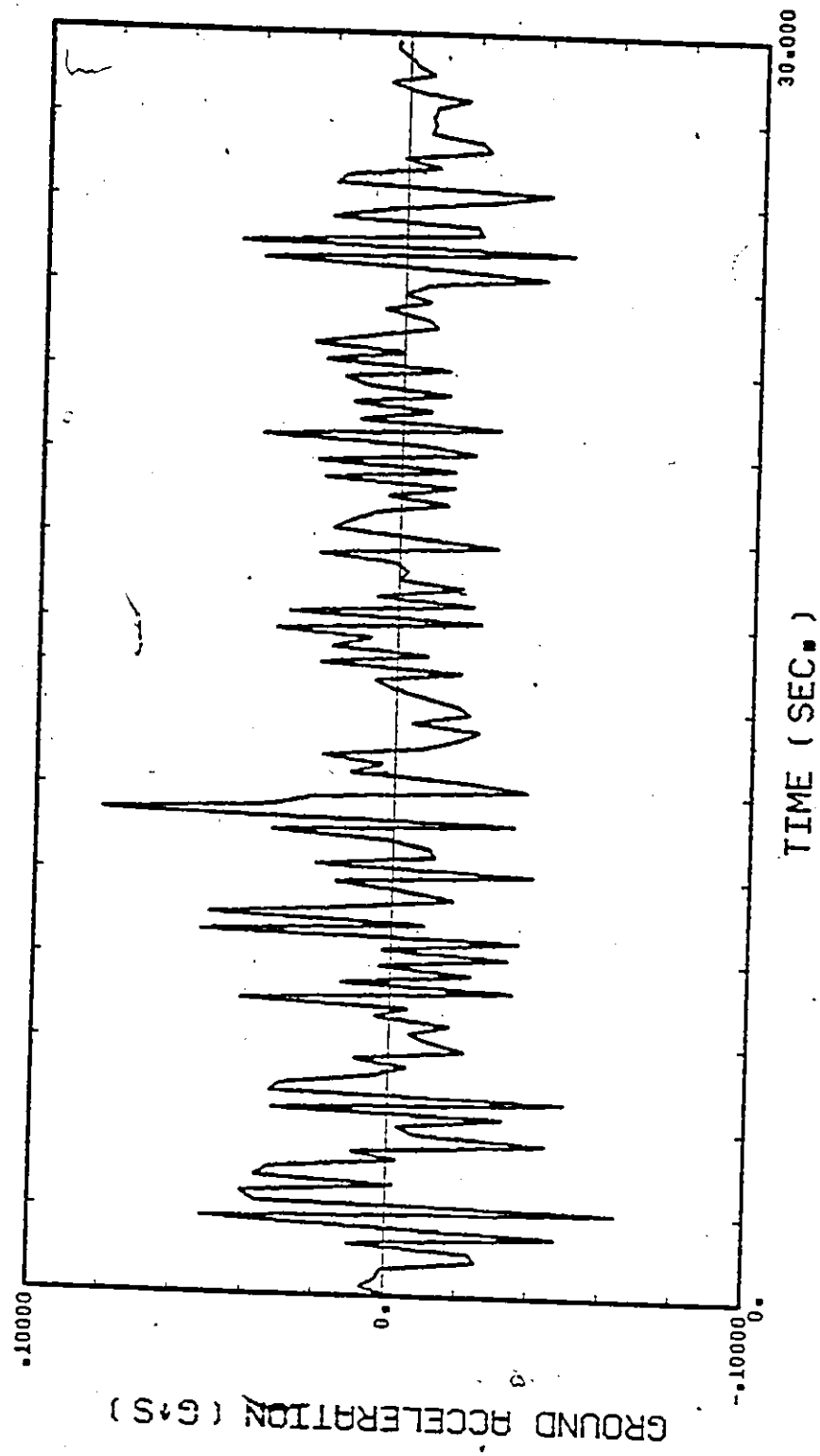

ELCENEW EARTHQUAKE TIME HISTORY

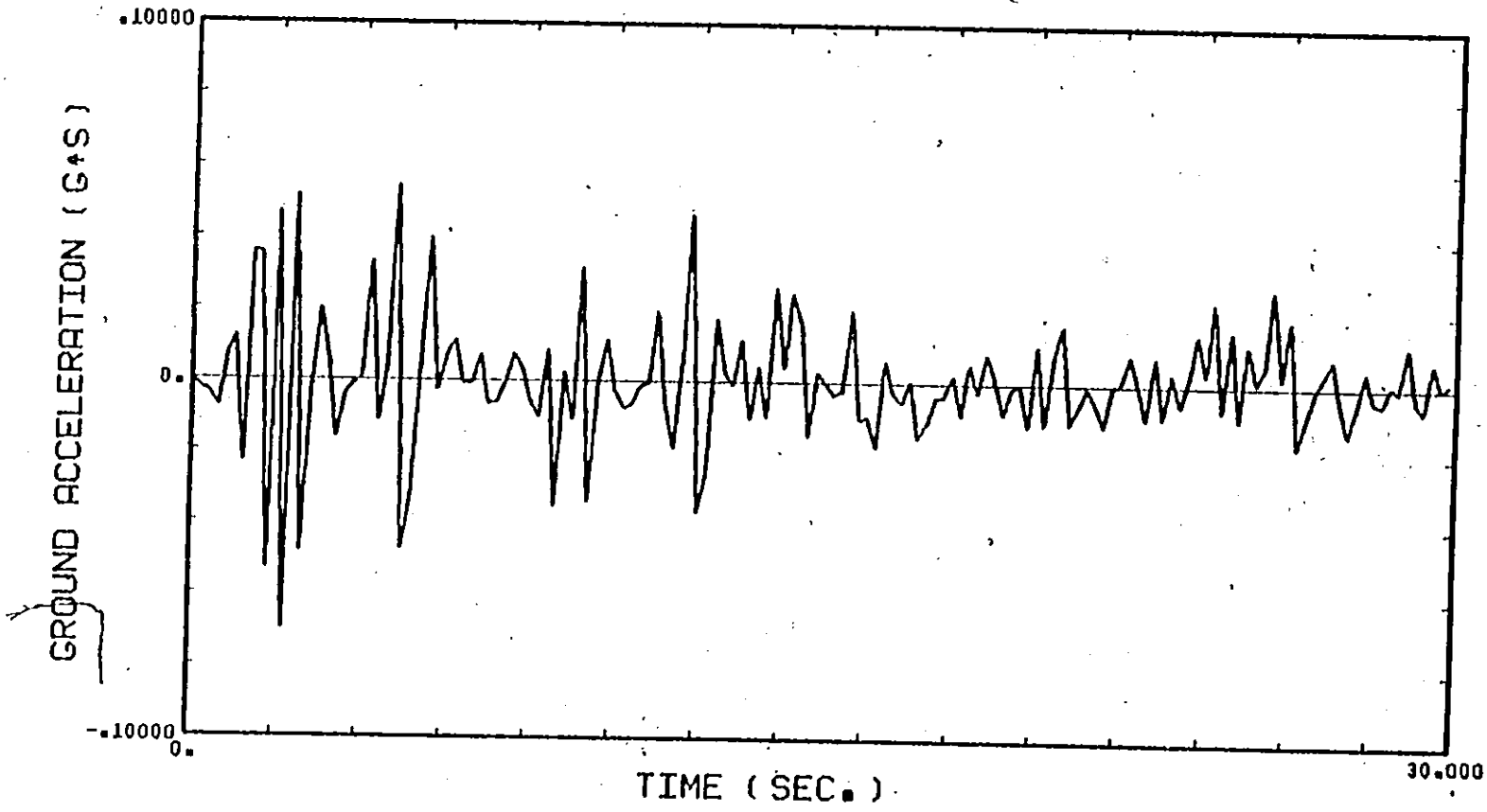

ELCENNS EARTHQUAKE TIME HISTORY

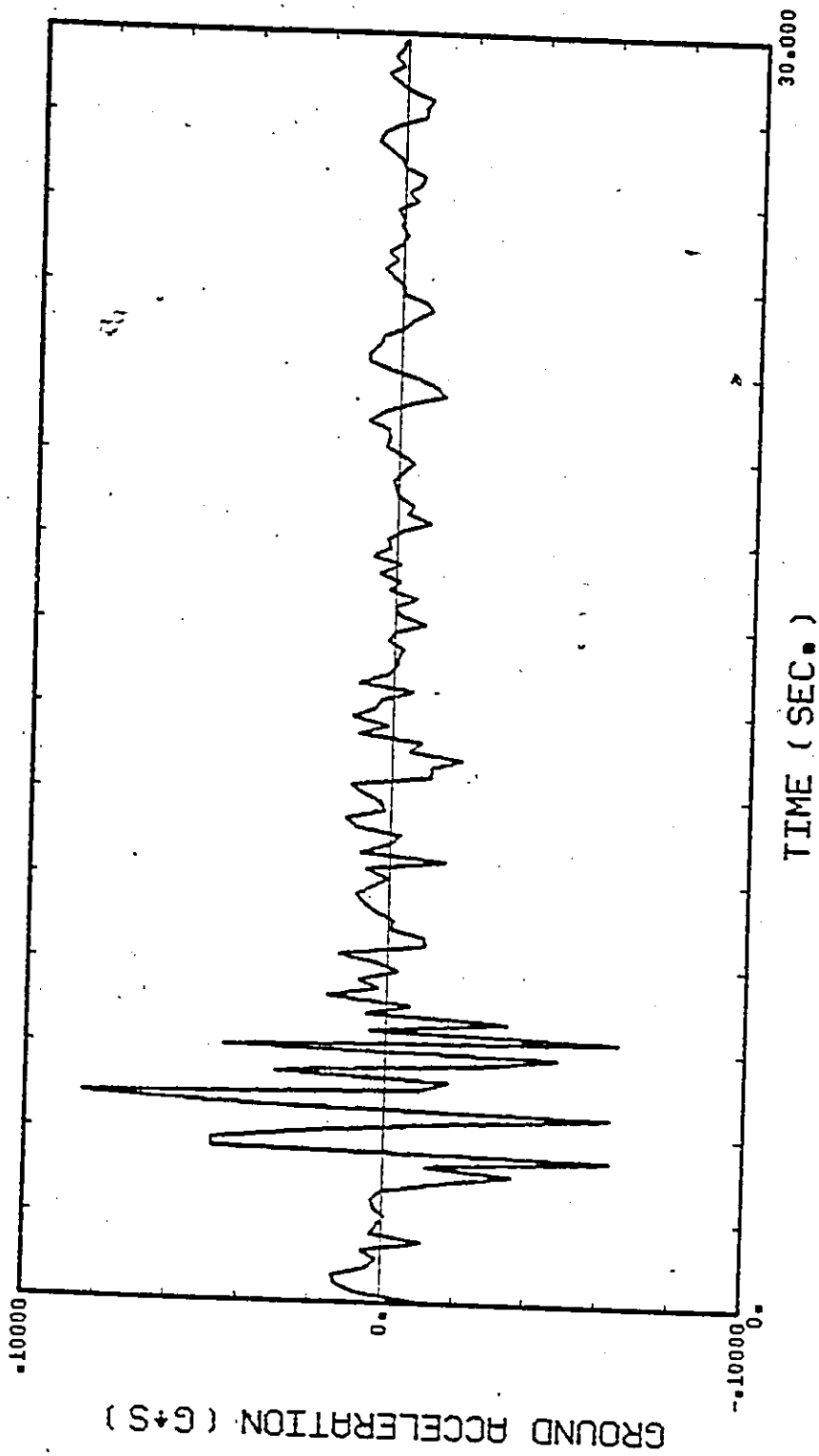

EUREK11 EARTHQUAKE TIME HISTORY

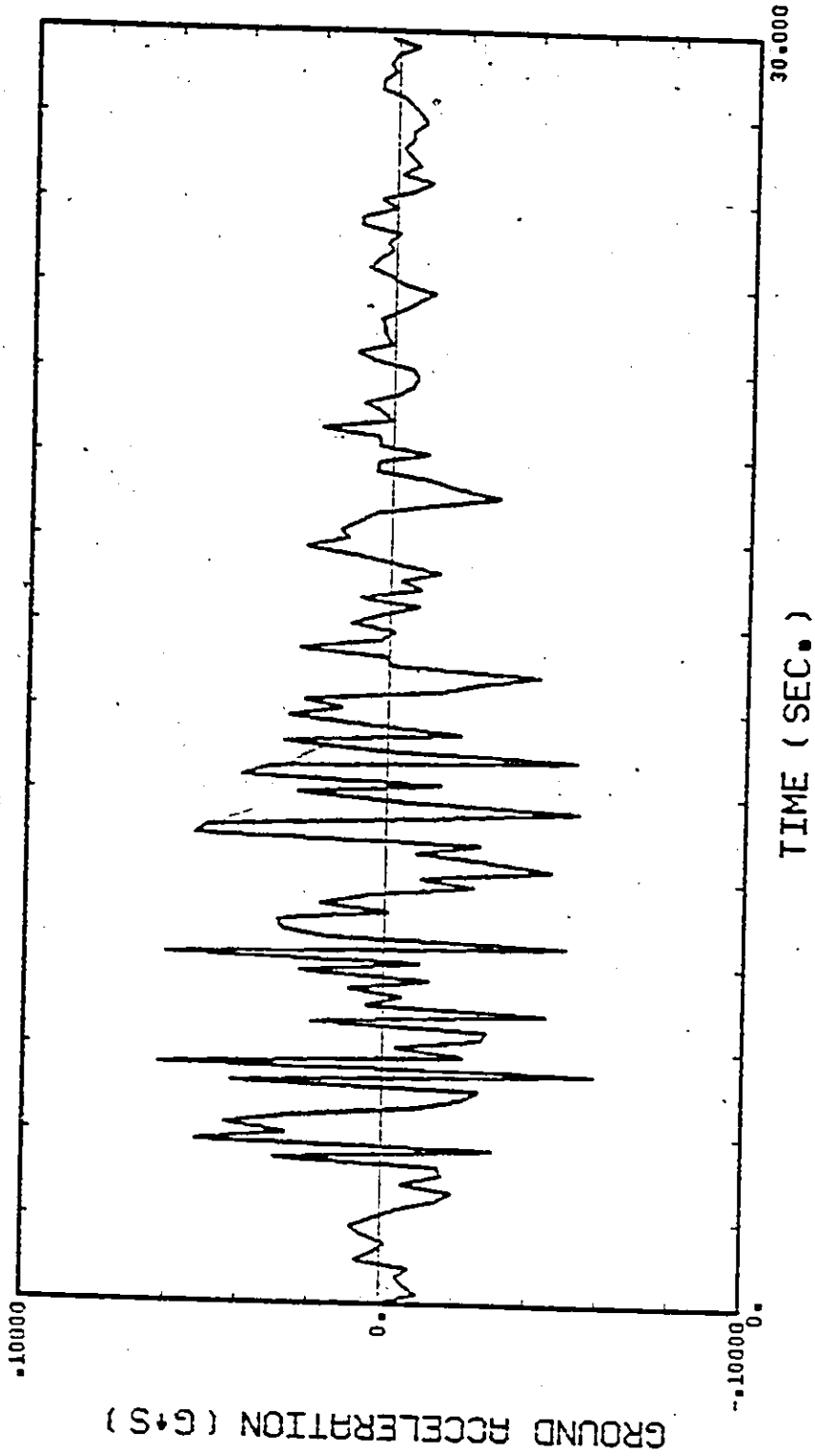

ORIONNS EARTHQUAKE TIME HISTORY

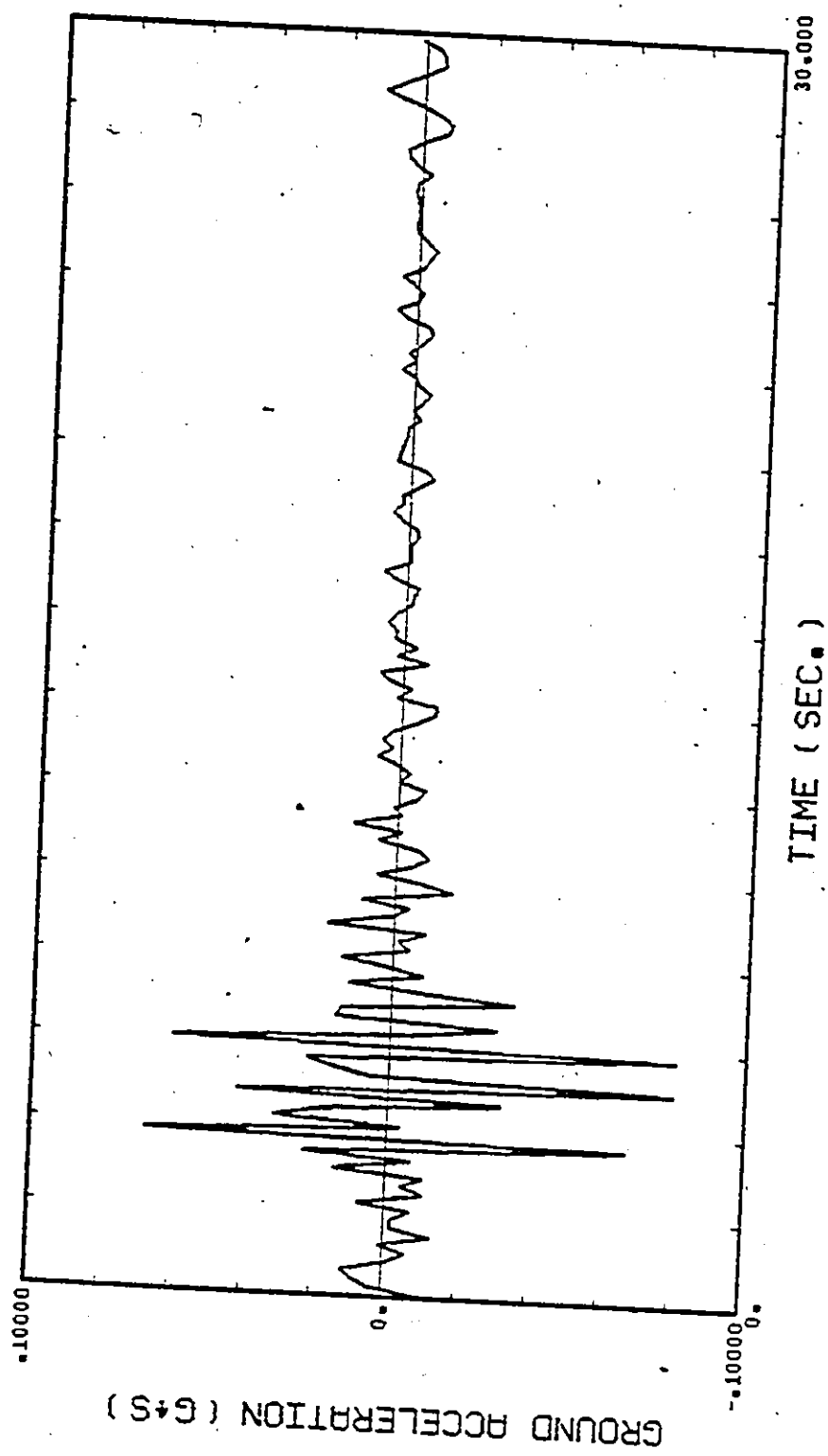

EUREK79 EARTHQUAKE TIME HISTORY

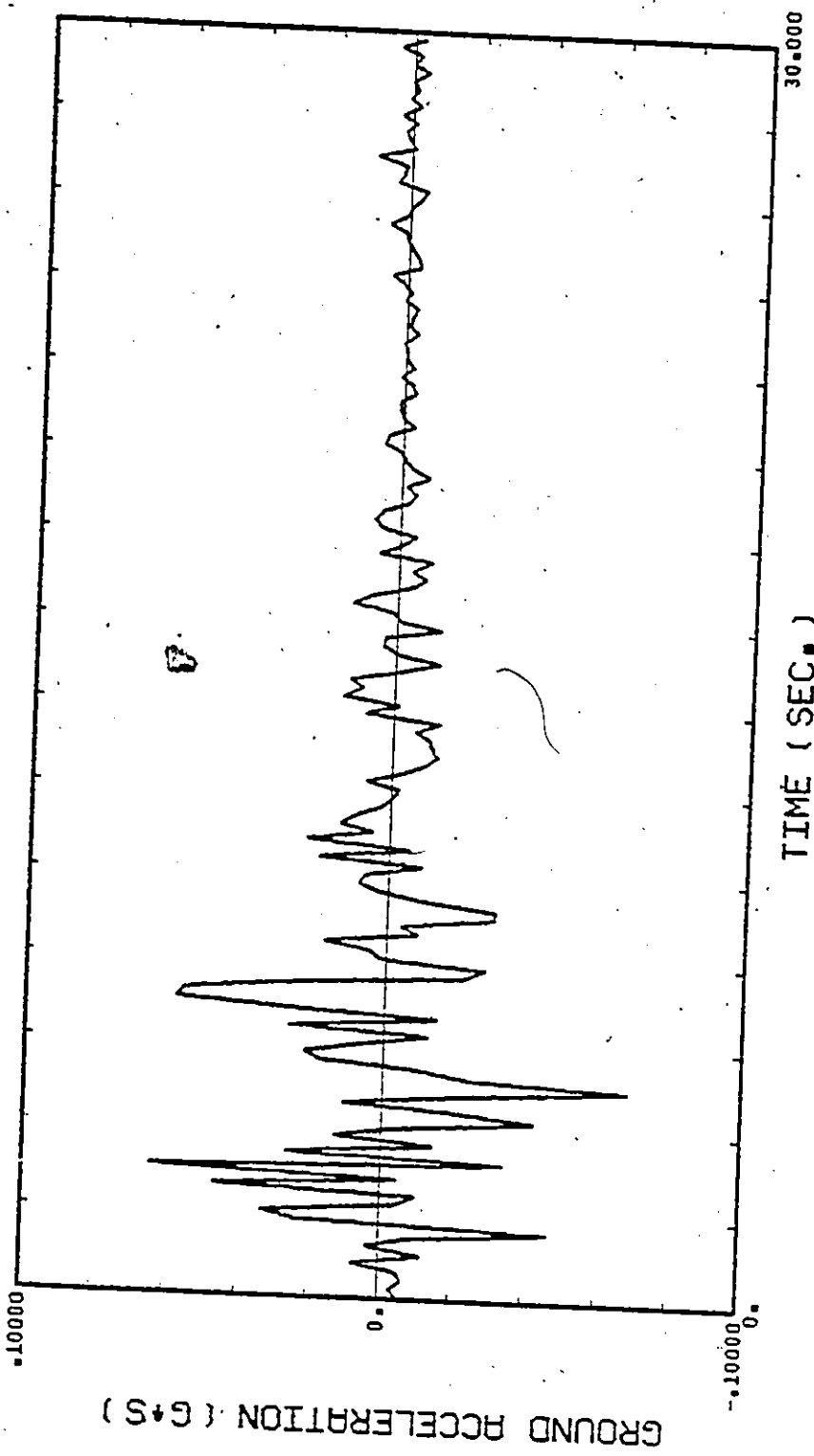

HOLLYEW EARTHQUAKE TIME HISTORY

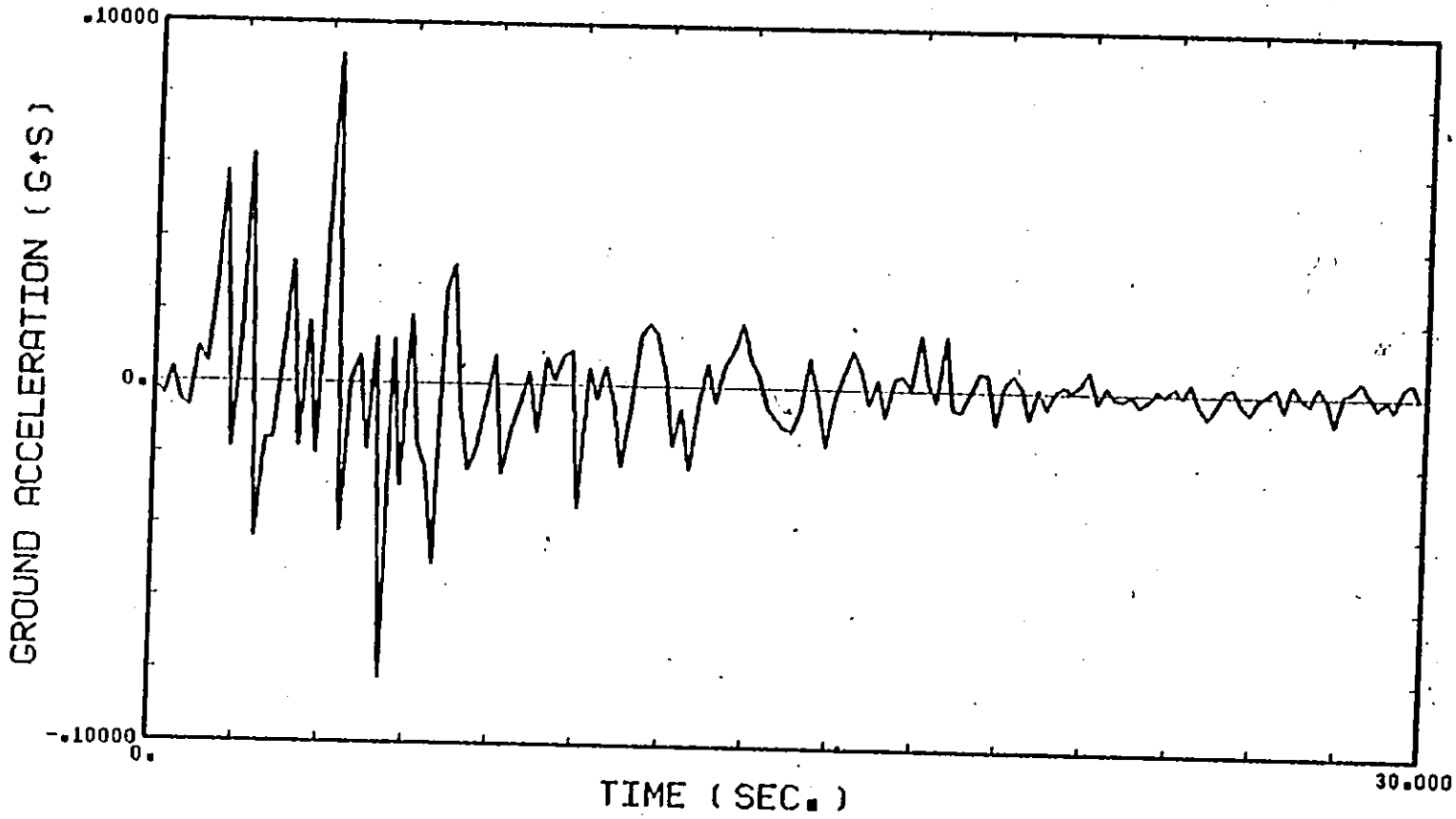

HOLLYNS EARTHQUAKE TIME HISTORY

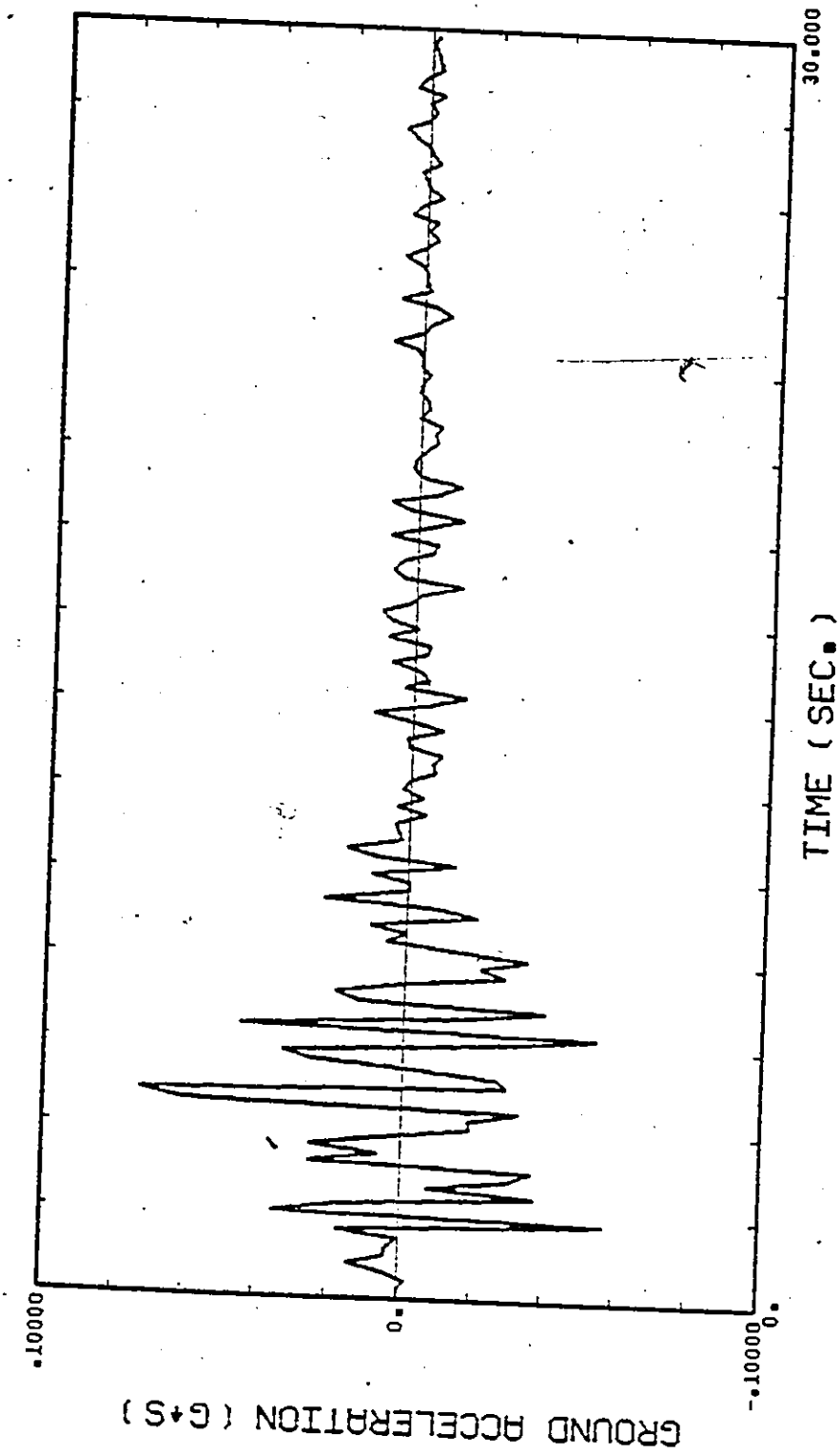

LANKEW EARTHQUAKE TIME HISTORY

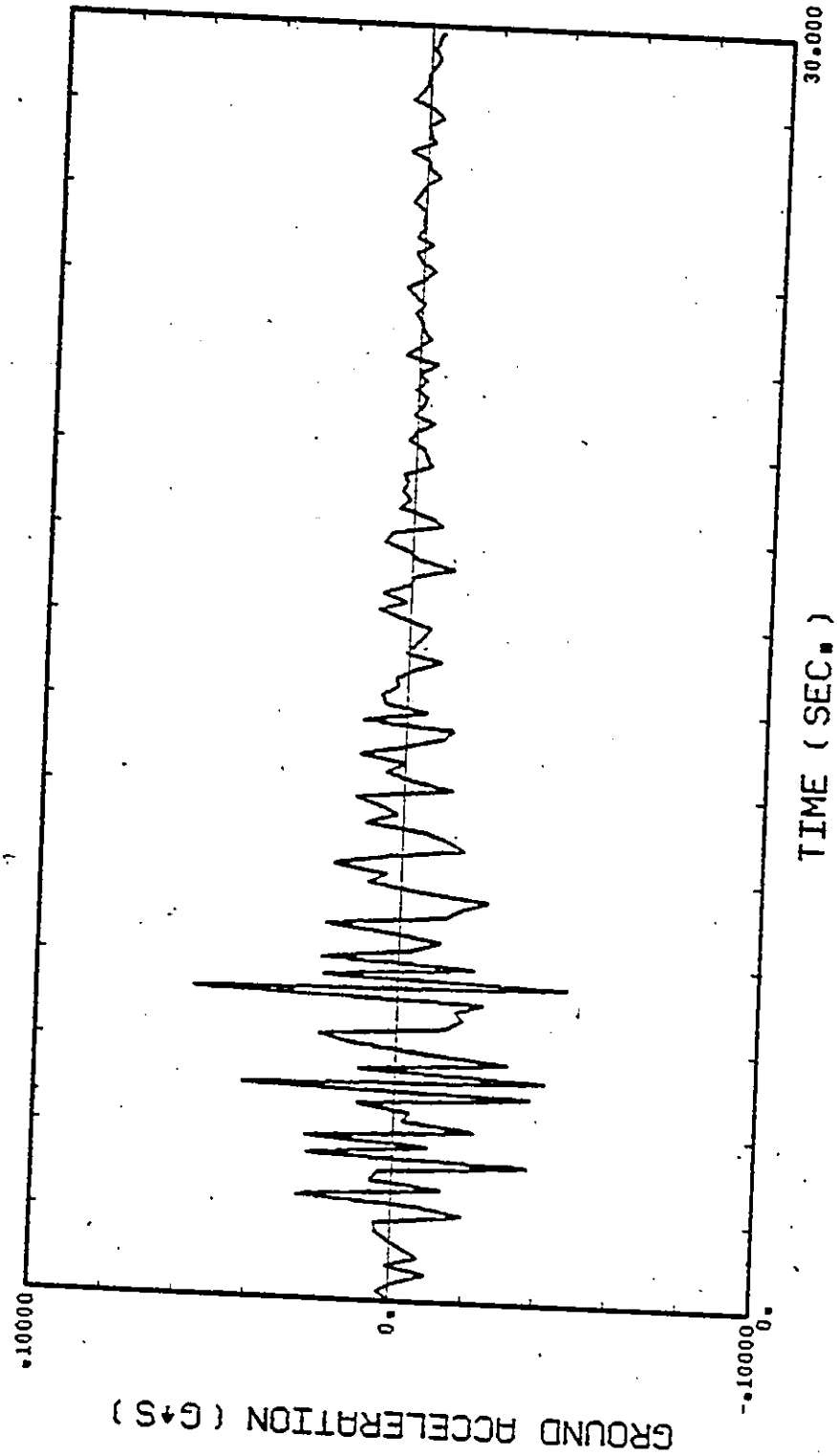

LANKNS EARTHQUAKE TIME HISTORY

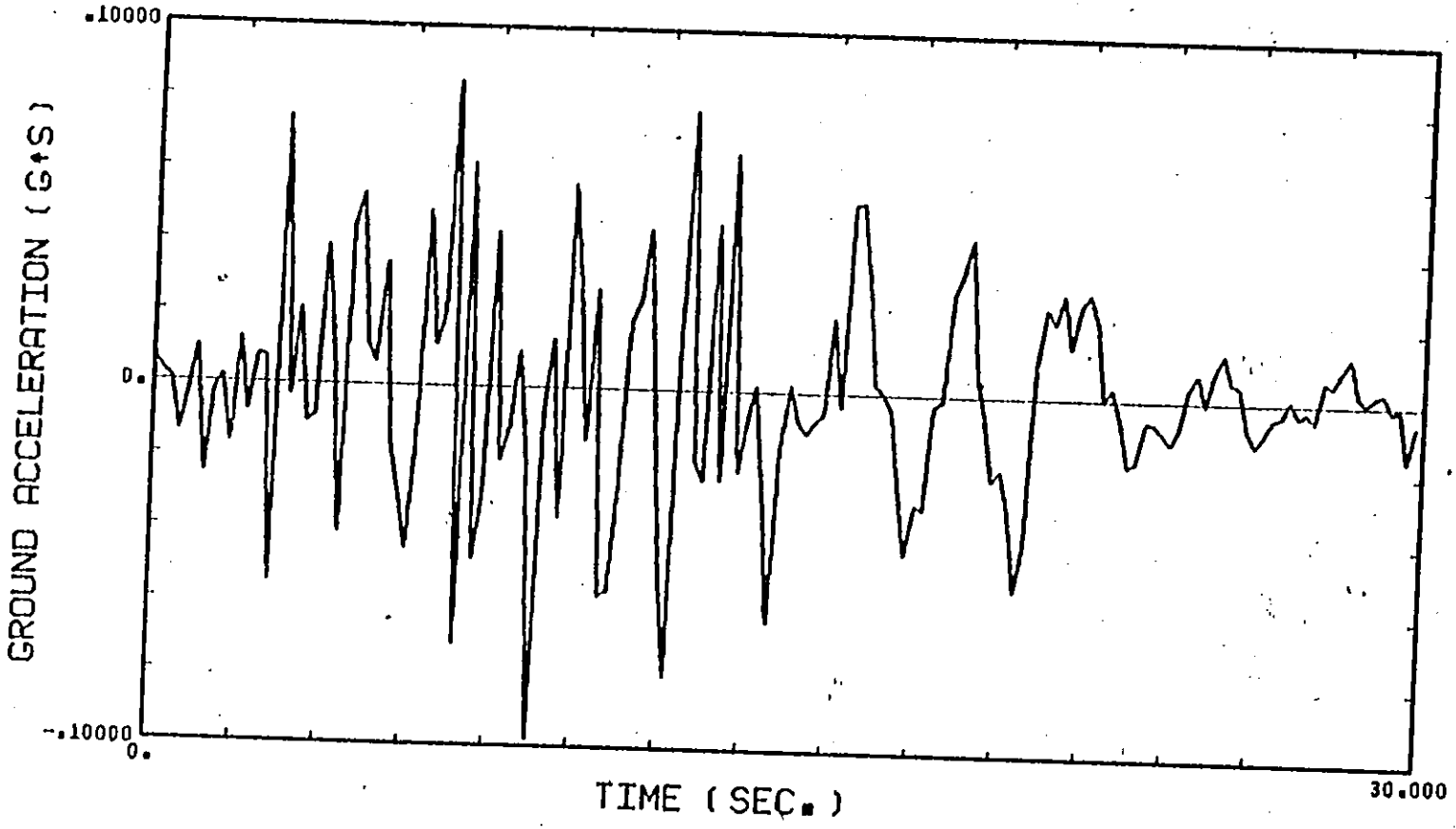

ORIONEW EARTHQUAKE TIME HISTORY

APPENDIX II

NOTATIONS

NOTATIONS

a_i - diagonal term of transformed [A]

[A] - 2Nx2N matrix with [0], [M] and [C]

b_i - diagonal term of transformed [B]

[B] - 2Nx2N matrix with [0], [M] and [K]

[C] - damping matrix

C_p, C_s, C_t - uncoupled damping constants

F_i - natural frequency (Hz)

g - acceleration due to gravity

G - product of modal circular frequency and integration time step

G_1, G_2 - complex constants used in resonant forced vibration

i - square root of minus one

I - subscript denoting the imaginary portion of a complex number

[K] - stiffness matrix

K_p, K_s, K_t - uncoupled stiffnesses

[M] - mass matrix

M_p, M_s, M_t - subsystem masses

N - number of degrees of freedom

p - subscript for primary level

P(t), Q(t) - forcing functions

$q_i(t)$ - complex modal forcing function

R - subscript denoting the real portion of a complex number

r, R, s, S - complex quantities (sec. 5.2)

s - subscript for secondary level

s^* - duration of ground motion

t - subscript for tertiary level

- time

$U_g(t)$ - ground displacement

u, v, $U(t)$, $V(t)$ - complex quantities or functions (sec 5.2)

$\{X\}$ - vector of nodal displacements, with respect to base

X_p - primary level relative displacement

X_s - secondary level relative displacement

$\{Y\}$ - vector made up of $\{X\}$ and $\{\dot{X}\}$

Z_i - complex modal amplitude

$[0]$ - zero matrix

α, α_{sp}, α_{ts} - quantities relating subsystem frequencies and damping ratios

Δt - integration time step

$[\phi]$ - matrix of standard eigenvectors

λ_i - complex eigenvalue

μ, μ_{sp}, μ_{ts} - mass ratios

$\{\phi\}$ - complex eigenvector

$[\Psi]$ - matrix of complex eigenvectors

θ - phase angle

θ, θ_{sp}, θ_{ts} - squares of frequency ratios

ω_i - circular frequency (sec^{-1})

Ω - forcing frequency

APPENDIX III

COMPUTER PROGRAM LISTING

```
      PROGRAM STATS(INPUT,OUTPUT,TAPE5=INPUT,TAPE6=OUTPUT,
     1             GROUND,TAPE7=GROUND)
      INTEGER INDIC(6),HEADER(40),TI(30),IT,IORD(3),I9(3),I8(3)
      INTEGER NAME(12),NN1(20)
      REAL DELI(6),DEL2(6),EVR1(6),EVI1(6),VECR1(6,6),VECI1(6,6)
      REAL UMAX(12,3),RMAX(12,3),MAXRESP(2,30,3),D(3),V(3),ACCEL(3),
     1     AVRGERR(3),SQERR(3),ERR(12,3),DN(12,3)
      REAL M(3,3),C(3,3),K(3,3),A(6,6),B(6,6),MSP,MTS,FSP,FP,MP,
     1     FTS,ORP,ALS(10),ALT(30),F(3),P(3,3),ZETA(3),AD(6,6),
     2     HK(6),EVI(6),EVR(6),VECR(6,6),VECI(6,6),ASAVE(6,6),
     3     A1(6,6)
      REAL DURA,INCR,GA(1500),GA1(12,1500),NMAX(12,3)
      COMPLEX GAM,SCRAP,MAT(6,6),EVAL(6),EVEC(6,6),SCRAP1(6),
     1  AS(6),BS(6),SCRAP2(6),CMPLX,CABS,AIMAG,
     2  Q(6),QS(6),Z(6,2),ZZ(6,2)
      COMMON NALT,ALT,XLEN,YLEN,TI
      COMMON /QUAKE/ DURA,INCR,GA1,N3
      N=3
      N1=N+1
      N2=2*N
      NN=N2-1
      PI=4.0*ATAN(1.0)
      TI(25)=10HCPX  V STAN
      TI(26)=10HCPX  V ROSE
      TI(27)=10HCPX  V UNCP
      NAME(1)=10H      CALEH
      NAME(2)=10H      CALNS
      NAME(3)=10H    ELCENEH
      NAME(4)=10H    ELCENNS
      NAME(5)=10H    EUREK11
      NAME(6)=10H    EUREK79
      NAME(7)=10H    HOLLYEH
      NAME(8)=10H    HOLLYNS
      NAME(9)=10H      LANKEH
      NAME(10)=10H     LANKNS
      NAME(11)=10H    ORIONEH
      NAME(12)=10H    ORIONNS
C
CC  READ IN GROUND ACCLERATION TIME HISTORY.
C
      WRITE(6,401)
      DO 900 I=1,12
      READ(7,454)HEADER
      WRITE(6,455)HEADER
      READ(7,451)DURA,INCR
      N3=DURA/INCR
      READ(7,453)(GA1(I,J),J=1,N3)
      IF(DURA.GT.12.0)DURA=12.0
```

```
      NJ=DURA/INC+
  900 CONTINUE
  451 FORMAT(10F8.0)
  452 FORMAT(*0*,I5,*GROUND MOTION DURATION OF*,F8.3,* DIGITIZED AT*,
     1       F8.4,* SECONDS*)
  453 FORMAT(6F12.0)
  454 FORMAT(20A4)
  455 FORMAT(* *,20A4)
      READ(5,399)MP
      READ(5,399)FP
      READ(5,399)MSP
      READ(5,399)MTS


      READ(5,399)FSP
      READ(5,399)FTS
      READ(5,399)DRP
      READ(5,400)NALS
      NALS=1
      READ(5,399)(ALS(I),I=1,NALS)
      READ(5,400)NALT
      READ(5,399)(ALT(I),I=1,NALT)
      DO 999 I6=1,NALS
      DO 3 I=1,3
       IORD(I)=I
    3 CONTINUE
      WRITE(6,402)MSP,MTS
      WRITE(6,403)FSP,FTS
      WRITE(6,404)DRP,ALS(I6)
      DO 998 I7=1,NALT
      DO 2 I=1,3
         DO 1 J=1,3
            M(I,J)=0.0
            C(I,J)=0.0
            K(I,J)=0.0
    1    CONTINUE
    2 CONTINUE
      M(1,1)=MP
      M(2,2)=M(1,1)*MSP
      M(3,3)=M(2,2)*MTS
      K(1,1)=M(1,1)*4*PI*PI*FP*FP
      K(3,3)=K(1,1)*FTS*FSP*MTS*MSP
      K(2,3)=-K(3,3)
      K(3,2)=K(2,3)
      K(1,2)=-K(1,1)*FSP*FSP
      K(2,1)=K(1,2)
      K(2,2)=K(3,3)-K(1,2)
```

```
      C(3,3)=2.0*M(3,3)*SQRT(K(3,3)/M(3,3))
     1        *ALT(I7)*DRP*SQRT(FTS*FSP)
      C(2,3)=-C(3,3)
      C(3,2)=C(2,3)
      C(1,2)=-2.0*M(2,2)*SQRT(-K(1,2)/M(2,2))
     1        *ALS(I6)*DRP*SQRT(FSP)
      C(2,1)=C(1,2)
      C(2,2)=C(3,3)-C(1,2)
      C(1,1)=2.0*M(1,1)*SQRT(K(1,1)/M(1,1))*DRP
      C(1,1)=C(1,1)-C(1,2)
      K(1,1)=K(1,1)-K(1,2)
C
CC
      CALL NEWMOD(M,C,K,F,P,ZETA,NMAX,RMAX)
C
CC
      CALL UNCOUP(MP,DRP,FP,MSP,ALS(I6),FSP,MTS,ALT(I7),FTS,UMAX)
C
CC
CC    CONSTRUCT A AND B MATRICES
CC
      DO 6 I=1,N2
         DO 5 J=1,N2
            ASAVE(I,J)=0.0
            A(I,J)=0.0
            B(I,J)=0.0
    5    CONTINUE
    6 CONTINUE
      DO 8 I=1,N
         ASAVE(I,I+N)=M(I,I)
         ASAVE(I+N,I)=M(I,I)
         A(I,I+N)=M(I,I)
         B(I,I)=-M(I,I)
         A(I+N,I)=M(I,I)
         DO 7 J=1,N
            ASAVE(I+N,J+N)=C(I,J)
            A(I+N,J+N)=C(I,J)
            B(I+N,J+N)=K(I,J)
    7    CONTINUE
    8 CONTINUE
C
CC    CREATE MATRIX AB=-(A INVERSE)*(B)
CC
      CALL LINV1F(A,N2,E,A1,0,WK,IER)
C
      DO 11 I=1,N2
         DO 10 J=1,N2
            A(I,J)=ASAVE(I,J)
```

```
      EVI1(I)=EVI(I)
      DO 206 J=1,6
       VECR1(J,I)=VECR(J,I)
       VECI1(J,I)=VECI(J,I)


206 CONTINUE
207 CONTINUE
    IF(I7.NE.1)GOTO208
    CALL ORDER(I8,EVR)
208 CONTINUE
    J1=0
    DO 210 I=2,4,2
     II=I+2
     DO 209 J=II,6
      EV1=ABS(EVI(I))
      EV2=ABS(EVI(J))
      IF((EV2-EV1)*2.0/(EV2+EV1).GT.0.001)GOTO209
      J1=1
      J2=2
209  CONTINUE
210 CONTINUE
    IF(J1.NE.0)GOTO211
    IF(J2.LE.0)GOTO216
211 CONTINUE
    J2=J2-1
    CALL ORDER(I9,EVR)
    DO 214 I=1,3
     DO 214 J=1,3
      IF(I8(I).EQ.I9(J))IORD(I)=J
214 CONTINUE
    GOTO217
216 CONTINUE
    CALL ORDER(I8,EVR)
217 CONTINUE
    DO 220 I=1,3
     DO 219 II=1,2
      III=2*I+II-2
      IIII=2*IORD(I)+II-2
      EVR(III)=EVR1(IIII)
      EVI(III)=EVI1(IIII)
      DO 218 J=1,6
       VECR(J,III)=VECR1(J,IIII)
       VECI(J,III)=VECI1(J,IIII)
218  CONTINUE
219 CONTINUE
220 CONTINUE
```

```
            AB(I,J)=0.0
            DO 9 II=1,N2
               AB(I,J)=AB(I,J)+A1(I,II)*B(II,J)
  9         CONTINUE
            AB(I,J)=-AB(I,J)
 10      CONTINUE
 11   CONTINUE
C
C    DETERMINE THE EIGENVALUES/VECTORS(COMPLEX) OF AB.
C
      CALL EIGENP(N2,6,AB,48.0,EVR,EVI,VECR,VECI,INDIC)
C
      DO 204 I=1,NN
         II=I+1
         DO 203 J=II,N2
            JJJ=J
            EV1=ABS(EVI(I))
            EV2=ABS(EVI(JJJ))
            IF(EV1.LE.EV2)GOTO201
200         CONTINUE
            SAVE1=EVR(I)
            SAVE2=EVI(I)
            EVR(I)=EVR(JJJ)
            EVI(I)=EVI(JJJ)
            EVR(JJJ)=SAVE1
            EVI(JJJ)=SAVE2
            DO 202 JJ=1,N2
               SAVE1=VECR(JJ,I)
               SAVE2=VECI(JJ,I)
               VECR(JJ,I)=VECR(JJ,JJJ)
               VECI(JJ,I)=VECI(JJ,JJJ)
               VECR(JJ,JJJ)=SAVE1
               VECI(JJ,JJJ)=SAVE2
202         CONTINUE
201         CONTINUE
            IF(J.NE.N2)GOTO203
            IF(I.NE.NN)GOTO205
            IF(EVI(I+1).GE.0.0)GOTO203
            JJJ=I+1
            GOTO200
205         IF(I/2*2.NE.I)GOTO203
            IF(EVI(I).GE.0.0)GOTO203
            JJJ=I-1
            GOTO200
203      CONTINUE
204   CONTINUE
      DO 207 I=1,6
       EVR1(I)=EVR(I)
```

```
C
      DO 15 I=1,N2
         EVAL(I)=CMPLX(EVR(I),EVI(I))
         DO 14 J=1,N2
            EVEC(I,J)=CMPLX(VECR(I,J),VECI(I,J))
   14    CONTINUE
   15 CONTINUE
      DO 106 I=1,N2
         DO 101 J=1,N
            DO 100 JJ=1,N
               MAT(J,JJ)=2.0*EVAL(I)*M(J,JJ)+C(J,JJ)
  100       CONTINUE
  101    CONTINUE
         GAM=0.
         SCRAP=0.
         DO 103 J=1,N
            SCRAP1(J)=0.
            DO 102 II=1,N
               SCRAP1(J)=SCRAP1(J)+MAT(J,II)*EVEC(II+N,I)
  102       CONTINUE
  103    CONTINUE
         DO 104 J=1,N
            GAM=GAM+M(J,J)*EVEC(J+N,I)
            SCRAP=SCRAP+SCRAP1(J)*EVEC(J+N,I)
  104    CONTINUE
         GAM=GAM/SCRAP
         DO 105 J=1,N2
            EVEC(J,I)=EVEC(J,I)*GAM
            VECR(J,I)=REAL(EVEC(J,I))
            VECI(J,I)=AIMAG(EVEC(J,I))
  105    CONTINUE
  106 CONTINUE
C
      DO 110 I=1,6
       LVR(I)=REAL(EVAL(I))
       EVI(I)=AIMAG(EVAL(I))
       DO 109 J=1,6
        VECR(J,I)=REAL(EVEC(J,I))
        VECI(J,I)=AIMAG(EVEC(J,I))
  109  CONTINUE
  110 CONTINUE
      WRITE(6,408)ALT(I7)
      DO 108 II=1,2
  108 CONTINUE
      DO 27 I=1,N2
         AS(I)=0.0
         BS(I)=0.0
         DO 25 J=1,N2
```

```
            SCRAP1(J)=0.0
            SCRAP2(J)=0.0
            DO 24 JJ=1,N2
               SCRAP1(J)=SCRAP1(J)+A(J,JJ)*EVEC(JJ,I)
               SCRAP2(J)=SCRAP2(J)+B(J,JJ)*EVEC(JJ,I)
24          CONTINUE
25       CONTINUE
         DO 26 JJ=1,N2
            AS(I)=AS(I)+EVEC(JJ,I)*SCRAP1(JJ)
            BS(I)=BS(I)+EVEC(JJ,I)*SCRAP2(JJ)
26       CONTINUE
27    CONTINUE
      NN1(1)=1
      DEL=ABS(EVI(1))
      DELI(1)=0.05/DEL
      IF(DELI(1).GT.0.01)DELI(1)=0.01
      DELI(2)=DELI(1)
      DEL2(2)=DELI(1)/2.0
      DEL2(1)=DELI(1)/2.0
      IF(N.LQ.1)GOTO 885
      DO 37 I=2,N2
         IF(ABS(EVI(I)).GE.12.25*ABS(EVI(1)))GOTO 35
         IF(ABS(EVI(I)).GE.3.5*ABS(EVI(1)))GOTO 36
         NN1(I)=1
         DELI(I)=DELI(1)
         DEL2(I)=DELI(I)/2.0
         GOTO 37
35       CONTINUE
         NN1(I)=4
         DELI(I)=DELI(1)/4.0
         DEL2(I)=DELI(I)/2.0
         GOTO 37
36       CONTINUE
         NN1(I)=2
         DELI(I)=DELI(1)/2.0
         DEL2(I)=DELI(I)/2.0
37    CONTINUE
885   CONTINUE
C
C     DETERMINE SYSTEM RESPONSE USING COMPLEX MODAL SUPERPOSITION AND NUMERICAL
C     INTEGRATION(FIRST DERIVATIVE OF NORMAL COORDINATE VARIES LINEARLY OVER
C     SMALL TIME INTERVAL IS ASSUMED) OF GROUND TIME HISTORY. SEE #125,#128.
C
      DO 901 NTH=1,12


      N5=DURA/DELI(1)
```

```
      DO 28 I=1,N2
         Q(I)=0.0
         ZZ(I,1)=0.0
         ZZ(I,2)=0.0
         IF(I.GT.3)GOTO28
         DM(NTH,I)=0.0
   28 CONTINUE
      DO 903 I=1,N3
       GA(I)=GA1(NTH,I)
  903 CONTINUE
      DO 997 III=1,N5
         T=DELI(1)*(III-1)
         DO 31 I=1,N2
         IN1=NN1(I)
         DO 887 IN2=1,IN1
         TT=T+DELI(I)*IN2
         N6=TT/INCR
         N7=N6+1
         IF((N6.GE.N3).OR.(N6.EQ.0)) GOTO 111
         GATT=(GA(N6)+(TT-N6*INCR)*(GA(N7)-GA(N6))/INCR)*386.06
         GOTO 112
  111    IF(N6.GE.N3) GATT=GA(N3)*386.06
         IF(N6.EQ.0) GATT=GA(1)*386.06*TT/INCR
  112    CONTINUE
         DO 29 II=1,N
            Q(II+N)=-M(II,II)*GATT
            QS(II)=0.0
   29    CONTINUE
            QS(I)=0.0
            DO 30 JJ=N1,N2
               QS(I)=QS(I)+EVEC(JJ,I)*Q(JJ)
   30       CONTINUE
            Z(I,1)=QS(I)-(ZZ(I,2)+DEL2(I)*ZZ(I,1))*BS(I)
            Z(I,1)=Z(I,1)/(AS(I)+BS(I)*DEL2(I))
            Z(I,2)=ZZ(I,2)+DEL2(I)*(Z(I,1)+ZZ(I,1))
            ZZ(I,1)=Z(I,1)
            ZZ(I,2)=Z(I,2)
  887    CONTINUE
   31    CONTINUE
         DO 33 I=1,N
            ACCEL(I)=0.0
            V(I)=0.0
            D(I)=0.0
            DO 32 J=1,N2
               TEST=REAL(Z(J,2)*EVEC(I+N,J))
               D(I)=D(I)+REAL(Z(J,2)*EVEC(I+N,J))
               V(I)=V(I)+REAL(Z(J,2)*EVEC(I,J))
               ACCEL(I)=ACCEL(I)+REAL(Z(J,1)*EVEC(I,J))
```

```
   32         CONTINUE
              IF(ABS(D(I)).GT.ABS(DH(NTH,I)))DH(NTH,I)=D(I)
   33      CONTINUE
  997  CONTINUE
  901  CONTINUE
       WRITE(6,490)(NAME(I),I=1,12)
       WRITE(6,491)8H COMPLEX,(DH(I,3),I=1,12)
       WRITE(6,491)8HSTANDARD,(NMAX(I,3),I=1,12)
       WRITE(6,491)8H ROSENBL,(RMAX(I,3),I=1,12)
       WRITE(6,491)8HUNCOUPLD,(UMAX(I,3),I=1,12)
       CALL ERROR(DH,NMAX,RMAX,UMAX,ERR)
       DO 902 I=1,3
        WRITE(6,491)8H........,(ERR(J,I),J=1,12)
  902  CONTINUE
       CALL AVRGE(ERR,AVRGERR,SDERR)
       WRITE(6,492)(AVRGERR(I),SDERR(I),I=1,3)
  492  FORMAT('-',5X,'AVERAGE ERROR',
      1        'STANDARD',2F10.3,/,' ',
      2        ' ROSENBL',2F10.3,/,' ',
      3        'UNCOUPLD',2F10.3)
  490  FORMAT('0',8X,12A10)
  491  FORMAT(' ',A8,12F10.3)
  998  CONTINUE
       WRITE(6,401)
C      CALL PLOT(199.995,10.555,60)
C      CALL RITE(2.5,6.0,0.15,MSP,MTS,FSP,FTS,DRP,ALS(I6))
       XLEN=2.75
       YLEN=XLEN
       X=4.25
       Y=1.0
       Y1=Y+3.25
       Y2=Y+6.50
       Q1=X+1.0
       YDMAX1=50.0
       IF((MTS+MSP)/2.0.LT.0.009)YDMAX1=250.0
C      CALL PLOTLIN(Q1,Y2,MAXRESP,25,YDMAX1)
       Q1=Q1+X
C      CALL PLOT(Q1+X,0.0,-3)
  999  CONTINUE
C      CALL PLOT(X,0.0,999)
  399  FORMAT(10F8.0)
  400  FORMAT(I5,5F8.0)
  401  FORMAT('1')
  402  FORMAT('1','MASS RATIOS=',2F10.4)
  403  FORMAT(' ','FREQ RATIOS=',2F10.4)
  404  FORMAT(' ','PRIMARY DAMPING RATIO= ',F8.3,/,
      1       ' ','ALPHA SECONDARY        = ',F8.3)
  405  FORMAT('0',11X,' DAMPED FREQ(RAD/S) ',20X,'ZETA',/,
```

```
     1        *  *,*  MODE*,8X,*COMPLEX*,4X,*NORMAL*,8X,
     2        *COMPLEX     IGNORE      STRAIN     DIRECT OMEGXZETA*,/)
406  FORMAT(*  *,I5,5X,2F10.3,5X,5F10.5)
407  FORMAT(*  *,5X,2F12.5,5X,2H**,F10.3,F10.2,3H **,F10.4,T84,
     1        *ERROR=*,F8.2)
408  FORMAT(*-*,*ALPHA TERTIARY        =*,F8.3)
409  FORMAT(*0*,3(8F12.5,/,*  *))
     STOP
     END
     SUBROUTINE ORDER(I1,A)
     INTEGER I1(3)
     REAL A(6),A1(3)
     DO 1 I=1,3
      A1(I)=ABS(A(2*I-1))
   1 CONTINUE
     DO 3 I=1,2
      I1(I)=1
      DO 2 II=1,3
       IF(II.EQ.I)GOTO2
       IF(A1(I).GE.A1(II))I1(I)=I1(I)+1
   2  CONTINUE
   3 CONTINUE
     I1(3)=6-I1(1)-I1(2)
     RETURN
     END
     SUBROUTINE RITE(XOFF,YOFF,S,A,B,C,D,E,F)
     REAL XOFF,YOFF,S,X(6),A,B,C,D,E,F,XP,S1
     INTEGER J(6)
     X(1)=A
     X(2)=B
     X(3)=C
     X(4)=D
     X(5)=E
     X(6)=F
     J(1)=4HMSP=
     J(2)=4HMTS=


     J(3)=4HFSP=
     J(4)=4HFTS=
     J(5)=4HORP=
     J(6)=4HALS=
     S1=1.3*S
     XP=XOFF+4.1*S
     DO 99 I=1,6
        CALL LETTER(4,S,0.0,XOFF,YOFF-(I-1)*S1,J(I))
        ENCODE(6,406,ICM)(X(I))
```

```
      CALL LETTER(6,S,0.0,XP,YCFF-(I-1)*S1,ICH)
   99 CONTINUE
  406 FORMAT(F6.4)
      RETURN
      END
      SUBROUTINE NEWMOD(M,C,K,F,PHI,DR,DM,MMAX1)
      INTEGER N,N3,QQ,QQQ,NN1(10),IND(10)
      REAL M(3,3),C(3,3),K(3,3),F(3),PHI(3,3),DR(3),B(3,3),
     1     MMAX1(12,3),M1(3,3),PF(3),MMASS(3),DR1(3),KSAVE(3,3)
      REAL D(3),V(3),A(3),DM(12,3),GAM(3),AMPMAX(3,3),
     1     AMP(3,3),AMPP(3,3),DELI(3),DEL2(3),DEL3(3),MMAX(3)
      REAL DURA,INCR,GA(1500),GA1(12,1500)
      COMMON /QUAKE/ DURA,INCR,GA1,N3
      N=3
      DO 119 I=1,N
         DO 118 J=1,N
            KSAVE(I,J)=K(I,J)
  118    CONTINUE
  119 CONTINUE
C
CCC   DETERMINATION OF THE DYNAMIC CHARACTERISTICS OF THE EQUIPMENT AND STRUCTURE
CCCC
C           F(I)=STRUCTURE FREQUENCIES
C
      DO 4 I=1,N
         M1(I,I)=1.0/M(I,I)
         DO 3 J=1,N
            K(I,J)=K(I,J)*M1(I,I)
    3    CONTINUE
    4 CONTINUE
C
      CALL EIGENP(N,3,K,48.0,F,A,PHI,B,IND)
C
      NN=N-1
      DO 114 I=1,NN
         JJ=I+1
         DO 113 J=JJ,N
            IF(F(I).LT.F(J))GOTO 113
            SAVE=F(I)
            F(I)=F(J)
            F(J)=SAVE
            DO 112 II=1,N
               SAVE=PHI(II,I)
               PHI(II,I)=PHI(II,J)
               PHI(II,J)=SAVE
  112       CONTINUE
  113    CONTINUE
  114 CONTINUE
```

```
      DO 5 I=1,N
         F(I)=SQRT(F(I))
    5 CONTINUE
C
C  DETERMINE DAMPING COEFFICIENTS AND MODAL MASSES
C
      DO 12 I=1,N
         MMASS(I)=0.0
         DO 11 J=1,N
            MMASS(I)=MMASS(I)+M(J,J)*PHI(J,I)*PHI(J,I)
   11    CONTINUE
   12 CONTINUE
C
C  DETERMINE MODAL PARTICIPATION FACTORS
C
      DO 14 I=1,N
         TERM1=0.0
         DO 13 J=1,N
            TERM1=TERM1+M(J,J)*PHI(J,I)
   13    CONTINUE
         PF(I)=TERM1/MMASS(I)
   14 CONTINUE
      DO 664 I=1,N
         DO 663 J=1,N
            PHI(J,I)=PHI(J,I)*PF(I)
  663    CONTINUE
  664 CONTINUE
      CALL DRATIO(3,N,M,C,KSAVE,F,PHI,DR)
      DO 665 I=1,3
         F(I)=F(I)*SQRT(1.0-DR(I)*DR(I))
  665 CONTINUE
      NN1(1)=1
      DELI(1)=0.05/F(1)
      IF(DELI(1).GT.0.01)DELI(1)=0.01
      IF(N.EQ.1)GOTO 885
      DO 37 I=2,N
         IF(F(I).GE.(12.25*F(1)))GOTO 35
         IF(F(I).GE.(3.5*F(1)))GOTO 36
         NN1(I)=1
         DELI(I)=DELI(1)
         GOTO 37
   35    CONTINUE
         NN1(I)=4
         DELI(I)=DELI(1)/4.0
         GOTO 37
   36    CONTINUE
         NN1(I)=2
         DELI(I)=DELI(1)/2.0
```

```
   37 CONTINUE
  885 CONTINUE
      DO 886 I=1,N
         GAM(I)=F(I)*DELI(I)
         DEL2(I)=386.06*DELI(I)
         DEL3(I)=386.06*DELI(I)*DELI(I)
  886 CONTINUE
      DO 900 NTH=1,12
      DO 3000 IZERO=1,N
         AMPP(IZERO,1)=0.0
         AMPP(IZERO,2)=0.0
         AMPP(IZERO,3)=0.0
         AMPMAX(IZERO,1)=0.0
         AMPMAX(IZERO,2)=0.0
         AMPMAX(IZERO,3)=0.0
         OM(NTH,IZERO)=0.0
 3000 CONTINUE
C
CCC
C   DETERMINE THE SYSTEM RESPONSE BY MODAL SUPERPOSITION AND INTEGRATING
C   NUMERICALLY BASED ON THE ASSUMPTION THAT THE ACCELERATION OF THE SYSTEM
C   VARIES LINEARLY OVER A SHORT PERIOD OF TIME WHILE THE VELOCITY AND
C   DISPLACEMENT VARY AS A QUADRATIC AND A CUBIC RESPECTIVELY.
C
      DO 903 I=1,N3
        GA(I)=GA1(NTH,I)
  903 CONTINUE
      NN=DURA/DELI(1)


      T=0.0
      DO 999 III=1,NN
         DO 888 II=1,N
         QQQ=NN1(II)
         DO 887 QQ=1,QQQ
         TT=T+QQ*DELI(II)
         N1=TT/INCR
         N2=N1+1
         IF((N1.GE.N3).OR.(N1.EQ.0))GOTO 668
         GATT=GA(N1)+(TT-N1*INCR)*(GA(N2)-GA(N1))/INCR
         GOTO 669
  668    IF(N1.GE.N3) GATT=GA(N3)
         IF(N1.EQ.0) GATT=GA(1)*TT/INCR
  669    CONTINUE
            AMP(II,1)=GAM(II)**2.0*AMPP(II,3)+(2.0*DR(II)*GAM(II)
     1           +GAM(II)**2.0)*AMPP(II,2)
            AMP(II,1)=AMP(II,1)+(DR(II)*GAM(II)+GAM(II)*GAM(II)/3.0)
```

```
     1          *AMPP(II,1)+GATT
                AMP(II,1)=-AMP(II,1)/(1.+DR(II)*GAM(II)+GAM(II)**2./6.)
                AMP(II,2)=AMPP(II,2)+(AMP(II,1)+AMPP(II,1))/2.0
                AMP(II,3)=AMPP(II,3)+AMPP(II,2)+AMPP(II,1)/3.0
     1                    +AMP(II,1)/6.0
                IF(ABS(AMPMAX(II,1)).LT.ABS(AMP(II,1)))
     1             AMPMAX(II,1)=AMP(II,1)
                IF(ABS(AMPMAX(II,2)).LT.ABS(AMP(II,2)))
     1             AMPMAX(II,2)=AMP(II,2)
                IF(ABS(AMPMAX(II,3)).LT.ABS(AMP(II,3)))
     1             AMPMAX(II,3)=AMP(II,3)
                AMPP(II,1)=AMP(II,1)
                AMPP(II,2)=AMP(II,2)
                AMPP(II,3)=AMP(II,3)
  887        CONTINUE
  888        CONTINUE
             DO 16 I=1,N
                A(I)=0.0
                V(I)=0.0
                D(I)=0.0
                DO 15 J=1,N
                   A(I)=A(I)+AMP(J,1)*PHI(I,J)
                   V(I)=V(I)+AMP(J,2)*PHI(I,J)*DEL2(J)
                   D(I)=D(I)+AMP(J,3)*PHI(I,J)*DEL3(J)
   15           CONTINUE
C
CC   STORE MAXIMUM VALUES OF RESPONSE
C
                IF(D(I)*D(I).GT.DM(NTH,I)*DM(NTH,I))DM(NTH,I)=D(I)
   16        CONTINUE
             T=T+DELT(1)
  999 CONTINUE
      DO 889 I=1,3
       AMPMAX(I,2)=AMPMAX(I,2)*DEL2(I)
       AMPMAX(I,3)=AMPMAX(I,3)*DEL3(I)
  889 CONTINUE
      CALL ROSEN(3,PHI,AMPMAX,DR,F,PMAX)
      DO 901 I=1,3
       MMAX1(NTH,I)=MMAX(I)
  901 CONTINUE
  900 CONTINUE
      DO 38 I=1,N
       DO 38 J=1,N
        K(I,J)=KSAVE(I,J)
   38 CONTINUE
      RETURN
      END
```

```
      SUBROUTINE DRATIO(NOR,N,M,C,K,F,P,DR)
      REAL M(3,3),C(3,3),K(3,3),F(3),P(3,3),DR(3),KU(3),
     1     CU(3),HU(3),FU(3),ZU(3)
C
      DO 2 I=1,3
         IF(I.EQ.3)GOTO1
         KU(I)=K(I,I)+K(I,I+1)
         CU(I)=C(I,I)+C(I,I+1)
         GOTO2
    1    CONTINUE
         KU(I)=K(I,I)
         CU(I)=C(I,I)
    2 CONTINUE
      DO 3 I=1,3
         HU(I)=SQRT(KU(I)/M(I,I))
         FU(I)=HU(I)/6.28319
         ZU(I)=CU(I)/2.0/M(I,I)/HU(I)
    3 CONTINUE
C
CC  CHOOSE SIMPLIFIED METHOD
C
      IF(NOR.EQ.2)GOTO200
      IF(NOR.EQ.3)GOTO300
  100 CONTINUE
C
CC  DIRECT ASSIGNMENT OF UNCOUPLED DAMPING RATIOS
C
      DO 102 I=1,3
         II=1
         DO 101 J=2,3
            DIFF1=ABS(F(I)-HU(II))
            DIFF2=ABS(F(I)-HU(J))
            IF(DIFF2.GE.DIFF1)GOTO101
            II=J
  101    CONTINUE
         DR(I)=ZU(II)
         HU(II)=-9999.9999
  102 CONTINUE
      GOTO999
  200 CONTINUE
C
CC  STRAIN ENERGY PROPORTIONING OF UNCOUPLED DAMPING RATIOS
C
      DO 201 I=1,3
         DR(I)=ZU(1)*KU(1)*P(1,I)**2+ZU(2)*KU(2)*(P(2,I)-P(1,I))**2
     1        +ZU(3)*KU(3)*(P(3,I)-P(2,I))**2
         DR(I)=DR(I)/(KU(1)*P(1,I)**2+KU(2)*(P(2,I)-P(1,I))**2
     1        +KU(3)*(P(3,I)-P(2,I))**2)
```

```
  201 CONTINUE
      GOTO999
  300 CONTINUE
CC
CC   CALCULATE COUPLED DAMPING RATIOS IGNORING OFF-DIAGONAL TERMS
C
      DO301 I=1,3
        DR(I)=CU(1)*P(1,I)**2+CU(2)*(P(2,I)-P(1,I))**2
     1       +CU(3)*(P(3,I)-P(2,I))**2
        DR(I)=DR(I)/2.0/F(I)
        DR(I)=DR(I)/(M(1,1)*P(1,I)**2+M(2,2)*P(2,I)**2+M(3,3)*P(3,I)**2)
  301 CONTINUE
CC
C
  999 CONTINUE
      RETURN
      END
      SUBROUTINE PLOTLIN(XOFF,YOFF,DATA,IT,YDMAX1)
      COMMON /XYDLIM/ XDMIN,XDMAX,YDMIN,YDMAX
      REAL LIMIT,DATA(2,30,3),DLINE(30),ALPHA(30)


      INTEGER LABEL(5),TITLE(30)
      COMMON IALPHA,ALPHA,XLEN,YLEN,TITLE
C
      DMAX=0.0
      DMIN=0.0
      DO 33 I99=1,3
      DO 2 I=1,2
         DO 1 J=1,IALPHA
            IF(DATA(I,J,I99).GT.DMAX)DMAX=DATA(I,J,I99)
            IF(DATA(I,J,I99).LT.DMIN)DMIN=DATA(I,J,I99)
    1    CONTINUE
    2 CONTINUE
   33 CONTINUE
C
      XDMIN=0.0
      XDMAX=ALPHA(IALPHA)
      IF(YDMAX1.LE.0.0)GOTO34
      DMIN=0.0
      DMAX=YDMAX1
   34 CONTINUE
      ERR=0.20
      DO 37 I99=1,3
       DO 36 I=1,2
        DO 35 J=1,IALPHA
```

```
          IF(DATA(I,J,I99).GT.DMAX)DATA(I,J,I99)=DMAX
   35    CONTINUE
   36   CONTINUE
   37  CONTINUE
       YDMIN=DMIN
       YDMAX=DMAX
       YSCALE=(YDMAX-YDMIN)/YLEN
       XSCALE=(XDMAX-XDMIN)/XLEN
       XORG=XDMIN-XOFF*XSCALE
       DO 99 I99=1,3
       YORG=YDMIN-(YOFF-(I99-1)*3.25)*YSCALE
       XMIN=XORG
       YMIN=YORG
       XMAX=XDMAX+1.
       YMAX=YDMAX+1.
C
C      CALL PLTIN(XSCALE,YSCALE,XORG,YORG,XMIN,XMAX,YMIN,YMAX)
       DO 5 I=1,2
        DO 4 JJ=1,3
         IF((I.EQ.2).AND.(JJ.NE.2))GOTO4
         LIMIT=1.0-(JJ-2)*ERR
         DO 3 J=1,IALPHA
          DLINE(J)=DATA(I,J,I99)*LIMIT
    3    CONTINUE
         CALL ODASHHD(ALPHA,DLINE,IALPHA,1.0,1.0,1,FLOAT(I-1),0.030,IE)
    4   CONTINUE
    5  CONTINUE
C
       CALL FRAME
       CALL XLAB
       CALL YLAB(TITLE(IT+I99-1))
   99  CONTINUE
       RETURN
       END
       SUBROUTINE PLOTT(XD,YD,N)
       CALL UNITTO(XD,YD,XP,YP)
       CALL PLOT(XP,YP,N)
       RETURN
       END
       SUBROUTINE FRAME
       COMMON/XYDLIM/ XDMIN,XDMAX,YDMIN,YDMAX
C
CC  PLOT FRAMEWORK
C
       CALL PLOTT(XDMIN,YDMIN,3)
       CALL PLOTT(XDMAX,YDMIN,2)
       CALL PLOTT(XDMAX,YDMAX,2)
```

```
      CALL PLOTT(XDMIN,YDMAX,2)
      CALL PLOTT(XDMIN,YDMIN,2)
      END
      SUBROUTINE XLAB
      COMMON /XYDLIM/ XDMIN,XDMAX,YDMIN,YDMAX
      COMMON IALPHA,ALPHA,XLEN,YLEN
      INTEGER LABEL(5)
      REAL ALPHA(9)
      XD=XDMIN
      YD=YDMIN
      LABEL(1)=10HALPHA T
      LABEL(2)=10H(DRT/DRP)
      CALL UNITTO(XD,YD,XP,YP)
      YPP=YP-.15
      XPP=XP-0.025
      I=0
      ENCODE(1,20,ICH)(I)
   20 FORMAT(I1)
      CALL LETTER(1,0.05,0.0,XPP,YPP,ICH)
      XD=XDMAX
      CALL UNITTO(XD,YD,XP,YP)
      ENCODE(5,30,ICH)(XDMAX)
   30 FORMAT(F5.2)
      XPP=XP-0.125
      CALL LETTER(5,0.05,0.0,XPP,YPP,ICH)
      XPP=XP-2.25
      CALL LETTER(20,0.10,0.0,XPP,YPP,LABEL)
      ITIC=XDMAX*2.0
      ITIC=ITIC-1
      IF(ITIC.LE.0)GOTO50
      DO 40 I=1,ITIC
         XD=FLOAT(I)/2.0
         YD=YDMIN
         CALL UNITTO(XD,YD,XP,YP)
         CALL PLOT(XP,YP,3)
         CALL PLOT(XP,YP+.1,2)
   40 CONTINUE
   50 CONTINUE
      XD=1.0
      CALL PLOTT(XD,YDMIN,3)
      CALL PLOTT(XD,YDMAX,2)
      YD=0.0
      CALL PLOTT(XDMIN,YD,3)
      CALL PLOTT(XDMAX,YD,2)
      RETURN
      END
      SUBROUTINE YLAB(TITLE)
      INTEGER TITLE
```

```
      COMMON /XYDLIM/ XDMIN,XDMAX,YDMIN,YDMAX
      XD=XDMIN
      YD=YDMIN
      CALL UNITTO(XD,YD,XP,YP)
      XPP=XP-.55
      YPP=YP-.03
      ENCODE(9,20,ICH)(YDMIN)
   20 FORMAT(F9.4)
      CALL LETTER(9,0.05,0.0,XPP,YPP,ICH)
      YD=YDMAX
      CALL UNITTO(XD,YD,XP,YP)
      YPP=YP-.03
      ENCODE(9,20,ICH)(YDMAX)


      CALL LETTER(9,0.05,0.0,XPP,YPP,ICH)
      XPP=XP-.250
      YPP=YP-2.00
      CALL LETTER(10,0.12,90.0,XPP,YPP,TITLE)
      RETURN
      END
      SUBROUTINE UNCOUP(NP,DP,FP,MSP,ALS,FSP,MTS,ALT,FTS,DM)
      REAL NP,FP,DP,MSP,MTS,FSP,FTS,ALS,ALT,DM(12,3),M(3),Z(3),G(3),
     1     A0(3),V0(3),D0(3),A1(3),V1(3),D1(3),GA1(12,1500),INCR,DURA,
     2     GA(1500)
      COMMON /QUAKE/ DURA,INCR,GA1,N3
      PI=4.0*ATAN(1.0)
      M(1)=2.0*PI*FP
      Z(1)=DP
      G(1)=M(1)*0.01
C
CC   NOTE TIME STEP=0.01 SEC.
C
      M(2)=SQRT(FSP*M(1)**2)
      Z(2)=ALS*DP*SQRT(FSP)
      G(2)=M(2)*0.01
      M(3)=SQRT(FTS*M(2)**2)
      Z(3)=ALT*DP*SQRT(FTS*FSP)
      G(3)=M(3)*0.01
      DO 900 NTH=1,12
      DO 903 I=1,N3
      GA(I)=GA1(NTH,I)
  903 CONTINUE
      DO 4 I=1,3
      A0(I)=0.0
      V0(I)=0.0
      D0(I)=0.0
```

```
      DH(NTH,I)=0.0
    4 CONTINUE
      NN=DURA/0.01
      T=0.0
      DO 999 III=1,NN
       TT=T+0.01
       N1=TT/INCR
       N2=N1+1
       IF((N1.GE.N3).OR.(N1.EQ.0))GOTO5
       U=GA(N1)+(TT-N1*INCR)*(GA(N2)-GA(N1))/INCR
       GOTO6
    5  CONTINUE
       IF(N1.GT.N3)U=0.0
       IF(N1.EQ.N3)U=GA(N3)
       IF(N1.EQ.0)U=GA(1)*TT/INCR
    6  CONTINUE
       DO 7 I=1,3
        CALL INTEGR(A0(I),V0(I),D0(I),U,G(I),H(I),Z(I),
     1                    A1(I),V1(I),D1(I))
       IF(ABS(DH(NTH,I)).LT.ABS(D1(I)))DH(NTH,I)=ABS(D1(I))
        U=A1(I)
    7  CONTINUE
       DO 8 I=1,3
        A0(I)=A1(I)
        V0(I)=V1(I)
        D0(I)=D1(I)
    8  CONTINUE
       T=TT
  999 CONTINUE
      DO 9 I=1,3
       DH(NTH,I)=DH(NTH,I)*0.01*0.01*386.06
    9 CONTINUE
  900 CONTINUE
      RETURN
      END
      SUBROUTINE INTEGR(A0,V0,D0,U,G,H,Z,A1,V1,D1)
      A1=-(G*G*D0+(2.*Z*G+G*G)*V0+(Z*G+G*G/3.)*A0+U)
      A1=A1/(1.+Z*G+G*G/6.)
      V1=V0+(A1+A0)/2.
      D1=D0+V0+A0/3.+A1/6.
      RETURN
      END
      SUBROUTINE ROSEN(N,PHI,AMP,DR,F,HMAX)
      REAL A(3,3),AMP(3,3),PHI(3,3),DR(3),F(3),DR1(3),HMAX(3)
      DO 1 I=1,N
       DR1(I)=DR(I)+2.0/F(I)/12.5
    1 CONTINUE
```

```
      DO 5 I=1,N
         A(I,1)=0.0
         A(I,2)=0.0
         A(I,3)=0.0
         DO 4 J=1,N
            DO 3 K=1,N
               C=1+(((F(K)-F(J))/(DR1(J)*F(J)+DR1(K)*F(K)))**2
               C=1./C
               DO 2 L=1,3
                  SAVE=C*ABS(AMP(J,L))*PHI(I,J)*ABS(AMP(K,L))*PHI(I,K)
                  A(I,L)=A(I,L)+SAVE
    2          CONTINUE
    3       CONTINUE
    4    CONTINUE
         A(I,1)=SQRT(ABS(A(I,1)))
         A(I,2)=SQRT(ABS(A(I,2)))
         A(I,3)=SQRT(ABS(A(I,3)))
         HMAX(I)=A(I,3)
    5 CONTINUE
      RETURN
      END
      SUBROUTINE ERROR(Z,A1,A2,A3,ERR)
      REAL Z(12,3),A1(12,3),A2(12,3),A3(12,3),A(12,3),ERR(12,3)
      DO 1 I=1,12
       A(I,1)=A1(I,3)
       A(I,2)=A2(I,3)
       A(I,3)=A3(I,3)
    1 CONTINUE
      DO 3 I=1,3
       DO 2 J=1,12
        ERR(J,I)=100.0*(ABS(A(J,I)/Z(J,3))-1.0)
    2  CONTINUE
    3 CONTINUE
      RETURN
      END
      SUBROUTINE AVRGE(ERR,AVRGERR,SDERR)
      REAL ERR(12,3),AVRGERR(3),SDERR(3)
      DO 1 I=1,3
       SUM=0.0
       SUM1=0.0
       DO 2 J=1,12
        SUM=SUM+ERR(J,I)
        SUM1=SUM1+ERR(J,I)*ERR(J,I)
    2  CONTINUE
       AVRGERR(I)=SUM/12.0
       SDERR(I)=SQRT(ABS((SUM1-SUM*SUM/12.0)/11.0))
    1 CONTINUE
      RETURN
      END
```

APPENDIX. IV

EXPLICIT SOLUTION FOR THE TWO DEGREE OF FREEDOM COMPLEX EIGEN PROBLEM

This appendix presents an explicit solution for the complex eigenvalues and vectors of a two degree of freedom damped system. This is based on the solution for the roots of a quartic equation and is described in most Mathematics Handbooks(a).

The characteristic equation for the system can be represented as

$$\lambda^4 + a\lambda^3 + b\lambda^2 + c\lambda + d = 0$$

where:

$$a = 2\zeta_p\omega_p + 2\zeta_s\omega_s(1+\mu)$$

$$b = 4\zeta_p\zeta_s\omega_p\omega_s + \omega_p^2 + \omega_s^2(1+\mu)$$

$$c = 2\omega_p\omega_s(\zeta_p\omega_s+\zeta_s\omega_p)$$

$$d = \omega_p^2\omega_s^2.$$

Let Y represent any root of the resolvent equation

$$y^3 + py^2 + qy + r = 0$$

where:

$$p = -b$$

$$q = ac - 4d$$

$$r = -(a^2d - 4bd + c^2).$$

A root of this cubic equation can be solved for as follows.

Let

$$a_1 = (3q - p^2)/3$$

$$b_1 = (2p^3 - 9pq + 27r)$$

$$Q = (b_1^2/4) + (a_1^3/27)$$

The root is given by:

$$Y = A + B - p/3$$

(a) Berger, W. H., Handbook of Mathematical Sciences, Fifth Edition, CRC Press, Inc., West Palm Beach, Florida, 1975, pp 43.

where : $A = (-b_1/2 + Q)^{1/3}$

$B = (-b_1/2 - Q)^{1/3}$

The roots of the characteristic equation can now be obtained. First, let

$R = (a^2/4 - b + y)^{1/2}$

The roots are given by

$\lambda_i = -a/4 + R/2 \pm D/2;\ -a/4 - R/2 \pm E/2$

where D and E are quantities dependent on R.

If R=0 then

$D = (F + G)^{1/2}$

$E = (F - G)^{1/2}$

where: $F = 3a^2/4 - 2b$

$G = 2(y^2 - 4d)^{1/2}$

if R≠0 then

$D = (F' + G')^{1/2}$

$E = (F' - G')^{1/2}$

where: $F' = 3a^2/4 - R^2 - 2b$

$G' = (4ab - 8c - a^3)/(4R)$

With the solution for the eigenvalues, the corresponding eigenvectors may be determined. The eigenvector $\{\phi\}$ is of length 2N=4. The third and fourth elements represent displacement mode shape elements for the primary and secondary levels. Elements one and two represent velocity and are equal to the value of the displacement elements multiplied by the eigenvalue λ.

$\{\phi\} = \langle \lambda,\ \lambda S_s,\ 1,\ S_s \rangle^T$

where:

$$S_s = 1 + e/f$$

$$e = \lambda^2 + 2\omega_p\zeta_p\lambda + \omega_p^2$$

$$f = (2\omega_s\zeta_s\lambda + \omega_s^2)$$

APPENDIX V

EXPERIMENTAL EVALUATION OF A THREE LEVEL SYSTEM

APPENDIX V

EXPERIMENTAL EVALUATION OF A THREE LEVEL SYSTEM

A.1 Test Setup

With one of the most dominant features of three level systems being nonproportional damping and since there are no exact closed form solutions for the vibrational characteristics of systems exhibiting nonproportional damping, it was decided that an attempt should be made to experimentally verify the accuracy of the complex modal analysis computer program.

The system to be tested was designed to be a three degree of freedom system with each higher level having a significantly lower mass than the previous. This led to the first problem. Since the highest level of the system became very small, the effect of any attached instrumentation would have a significant effect on the dynamic characteristics of the system. With this in mind, it was decided that only accelerometers would be used as instrumentation. These would only affect the system mass and could be easily accounted for in the total mass of the system.

The system characteristics were set by the uncoupled characteristics of the subsystem. The specific values are

supplied in Table A.1. Connections were developed such that each subsystem would be attached to the fixed base or lower level in the same manner. Pictures of the different aspects of the test setup are given in Figures A.7 to A.12. The subsystem masses were kept constant for the tests while the damping and stiffness were varied. As a result, the mass ratios were constant and the frequency ratios and damping ratios varied.

The different subsystem parameters are supplied in Table A.1. M refers to the mass, F refers to the frequency in Hertz and ζ refers to the damping ratio. The p,s and t refer to the uncoupled primary, secondary and tertiary subsystems.

A.2 System Testing

The dynamic characteristics of the uncoupled subsystems were determined based on their free vibration response (ie. frequency and damping ratio). Once these characteristics were adjusted to the required values, the subsystems were connected together and this coupled system was evaluated.

Each level of the coupled system first had its characteristics set by treating it as a single degree of freedom system. Each level was connected directly to a steel base plate and its vibrational characteristics were determined.

This uncoupled system was given an initial displacement and released. The free vibration was measured by an accelerometer and plotted. Each plot was similar to Figure A.1. From one of these plots the period of the system was measured as the time between successive positive peaks. The frequency was then calculated as the inverse of the period. The damping ratio was also calculated(Ref. 7, pp 48), assuming $\zeta \leq 0.10$, as

$$\zeta = [\ln(X_{m+n}/X_m)]/2\pi n \qquad (A.01)$$

where X_n and X_{m+n} were the amplitudes of the n'th and n+m'th peaks.

The final characteristic of the system was its mass. This was calculated by dividing its weight by the acceleration due to gravity. The weight was determined by adding the weight of half of the attached legs to the weight of the plate and any attached masses.

These characteristics were adjusted by varying the damper, number of legs or total weight until the desired result was achieved. The characteristics were recalculated, by computer, after each adjustment.

Once all three levels had been properly adjusted, they were stacked up into a three level system. The coupled system was then ready to be tested in order to determine its dynamic response. A diagram of the coupled system is given in Figure A.2.

The evaluation of the coupled system involved the

determination of a response curve for the system based on a sinusoidal base motion input to the system. The system was shaken by the shake table over a series of fixed forcing frequencies with a constant peak acceleration sine wave.

As was mentioned in the previous section, The response at the top level of the system was measured using accelerometers since LVDT's were found to affect both the system damping and frequency. The use of accelerometers, however, introduced another problem. The accelerometer measured an absolute acceleration which would be integrated out to an absolute displacement. The comparison of experimental with analytical was to be based on the predicted maximum relative displacement of the top with respect to the base. This would require subtracting the table displacement from the absolute displacement.

Fortunately the tests involved a sinusoidal base motion and a sinusoidal system response. With the phase angle between the total response and the base motion known, the maximum acceleration relative to the base could be calculated as

$$R_{max} = (M^2 - 2MB\cos\phi + B^2)^{1/2} \qquad (A.02)$$

where M = amplitude of total response

B = amplitude of table motion

ϕ = phase angle between the table and total motions.

Once the amplitude of the relative acceleration was

known and since the response was sinusoidal then the maximum relative displacement could be calculated as the maximum relative acceleration divided by the square of the circular frequency of the response.

These results were then plotted up in a response curve. The curve was plotted as maximum third level relative acceleration versus forcing frequency.

A.3 Analytical Calculations

Once the experimental response curve for a particular system had been developed from the testing, a theoretical response curve was required.

In order to calculate the expected system response in the computer program, it was assumed that the uncoupled subsystems were single degree of freedom systems and that the coupled system could be compiled from the uncoupled subsystems as a three degree of freedom lumped mass model.

The calculations required mass, damping and stiffness matrices. These were developed from the vibrational characteristics of the uncoupled system. The simplest matrix was the mass matrix. It was simply a diagonal matrix with the uncoupled masses as the diagonal elements.

$$[M] = \begin{bmatrix} M_p & 0 & 0 \\ 0 & M_s & 0 \\ 0 & 0 & M_t \end{bmatrix} \tag{A.03}$$

where the p, s and t represent the primary, secondary and tertiary systems.

The uncoupled stiffnesses were calculated as

$$K_i = 4\pi^2 F_i^2 M_i \tag{A.04}$$

where F_i equals the uncoupled frequency(Hz). These were then combined into a stiffness matrix as

$$[K] = \begin{bmatrix} K_p+K_s & -K_s & 0 \\ -K_s & K_s+K_t & -K_t \\ 0 & -K_t & K_t \end{bmatrix} \tag{A.05}$$

The final matrix, damping, was based on the uncoupled damping coefficients.

$$C_i = 4\pi M_i F_i \zeta_i \tag{A.06}$$

where ζ_i is the uncoupled damping ratio. These were combined as

$$[C] = \begin{bmatrix} C_p+C_s & -C_s & 0 \\ -C_s & C_s+C_t & -C_t \\ 0 & -C_t & C_t \end{bmatrix} \tag{A.07}$$

The matrices were then used as the input to a modified complex modal analysis program. The basic difference between this and the general program was that it accepted a series of frequecies and then, for each forcing

frequency, generated the required constant peak acceleration sinusoidal base excitation itself.

The program calculated the maximum steady state response for each specified forcing frequency and then plotted the results. The curve was of the same type as that from the experimental work with maximum tertiary relative acceleration plotted against forcing frequency.

A.4 Comparison of Experimental and Analytical Results

The experimental and analytical results were compared by plotting the results on the same graphs. Four of these response curves are shown in Figures A.3 to A.6.

It should be noted that the response is measured along the vertical axis in inches. The solid curve corresponds to the analytical results and the dashed to the experimental. The system parameters are given in Table A.1.

Upon comparing the superimposed response curves for both the experimental and analytical cases, it was concluded that the simplified mathematical model involving complex modal analysis gave a good estimation of the actual system maximum response.

However, when a standard modal analysis program was run for the same type of three level systems, the program yielded a maximum error of only about 4% for system number 5. For most of the systems the error was on the order of about 1%. This demonstrated that the experimental system

that had been set up exhibited nonproportional damping to a very limited extent.

The experimental system could not be set up to reflect mass ratios of the order of a hundred to one or smaller. This severely limited the ability of the experiment to produce nonproportional damping. In order for the system to exhibit nonproportional damping in an experimental setting, the system would have to be of a large scale type, a hundred or more times larger at the primary level.

Although there appeared to be little difference between the nonproportional and proportional analysis, the results of the experimental work indicated that the complex modal analysis program was working properly.

As a result, this provided a verification (along with comparisons between the complex modal analysis and direct integration of the coupled equations of motion) that the computer program was actually calculating the correct response and that numerical investigations could be carried out.

TABLE A.1 Experimental System Parameters

F_p= 3.09 Hz

M_p= 2.95 slugs

M_s/M_p=.158

M_t/M_s=.037

System No	ζ_p	ζ_s	ζ_t	$(F_s/F_p)^2$	$(F_t/F_s)^2$
3	4.0	8.1	0.3	0.97	0.97
4	4.0	8.0	0.2	1.01	1.06
5	4.0	8.0	0.2	1.00	1.00
6	4.0	8.0	0.2	1.00	1.10
7	4.0	8.0	0.2	1.10	1.00
8	4.0	4.0	0.2	1.10	1.10
9	4.0	4.0	0.2	1.10	1.10
10	4.0	4.0	0.2	1.10	1.00
11	4.0	4.0	0.2	1.00	1.00
12	4.0	2.0	0.2	1.00	1.10
13	4.0	2.0	0.2	1.00	1.10
14	4.0	2.0	0.2	1.00	1.00
15	4.0	2.0	0.2	1.10	1.00
16	4.0	2.0	0.2	1.10	1.10
17	4.0	2.0	10.	1.10	1.10
18	4.0	2.0	10.	1.10	1.00
19	4.0	2.0	10.	1.17	1.00
20	4.0	2.0	10.	1.17	1.10
21	4.0	2.0	10.	1.00	1.10
22	4.0	2.0	10.	1.00	1.00
23	4.0	2.0	7.	1.00	1.10
24	4.0	2.0	7.	1.00	1.00
25	4.0	2.0	7.	1.10	1.00
26	4.0	2.0	7.	1.10	1.10

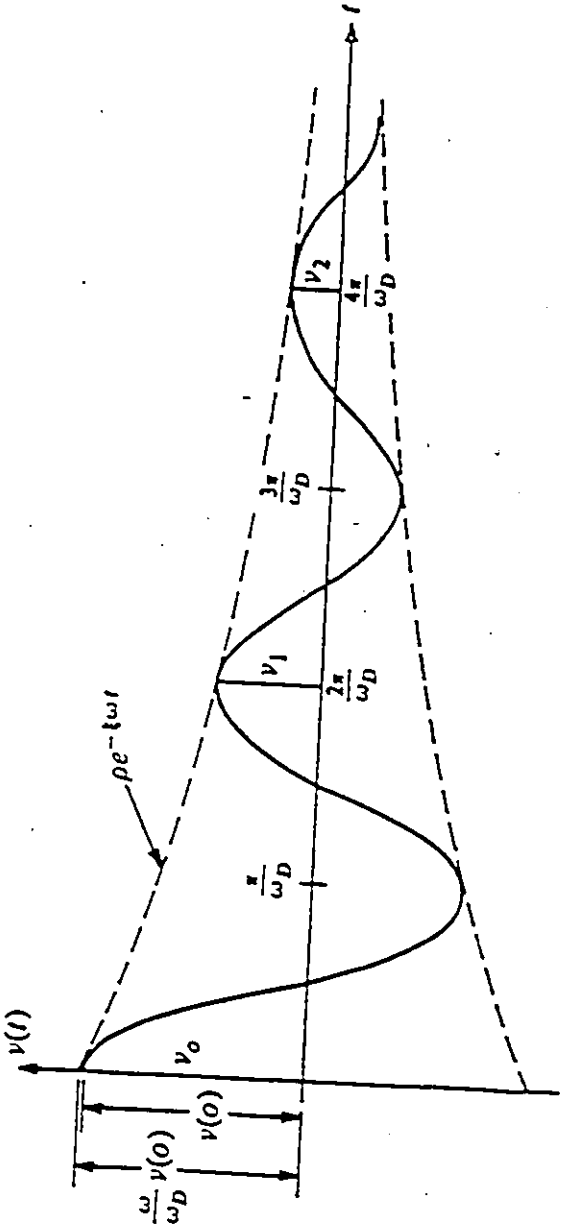

Figure A.1 Free Vibration Response of Underdamped System (Ref. 14, pp 47)

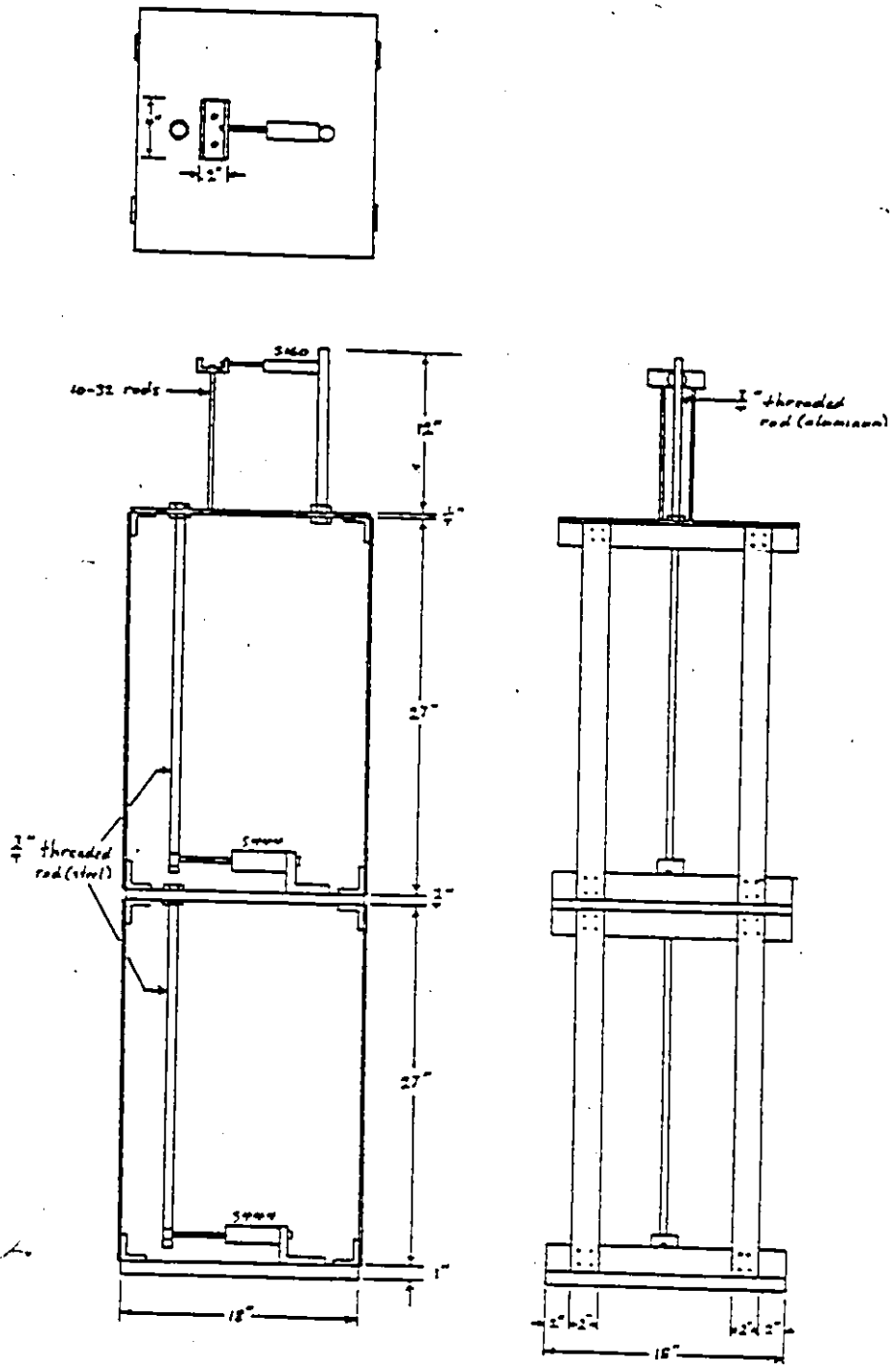

Figure A.2(a) TEST SPECIMEN

NOTES

1. All plates 18" x18"
   - base plate - 1" thick steel
   - primary plate - 1" thick aluminum
   - secondary plate - 1/4" thick aluminum

2. Legs - material - steel
   - sizes - 1"x1/16"
   - 1"x1/8"
   - 1"x3/16"
   - 2"x1/16"
   - 2"x1/8"

3. Leg/Plate connections
   - 2"x1.5"x.25" aluminum angle
   - 10-32 steel bolt fasteners

4. Dampers
   - Series 444 dashpots
   - Series 160 dashpots

   Airpot Corp.
   27 Lois Street
   Norwalk, CT. 06851

Figure A.2(b) TEST SPECIMEN

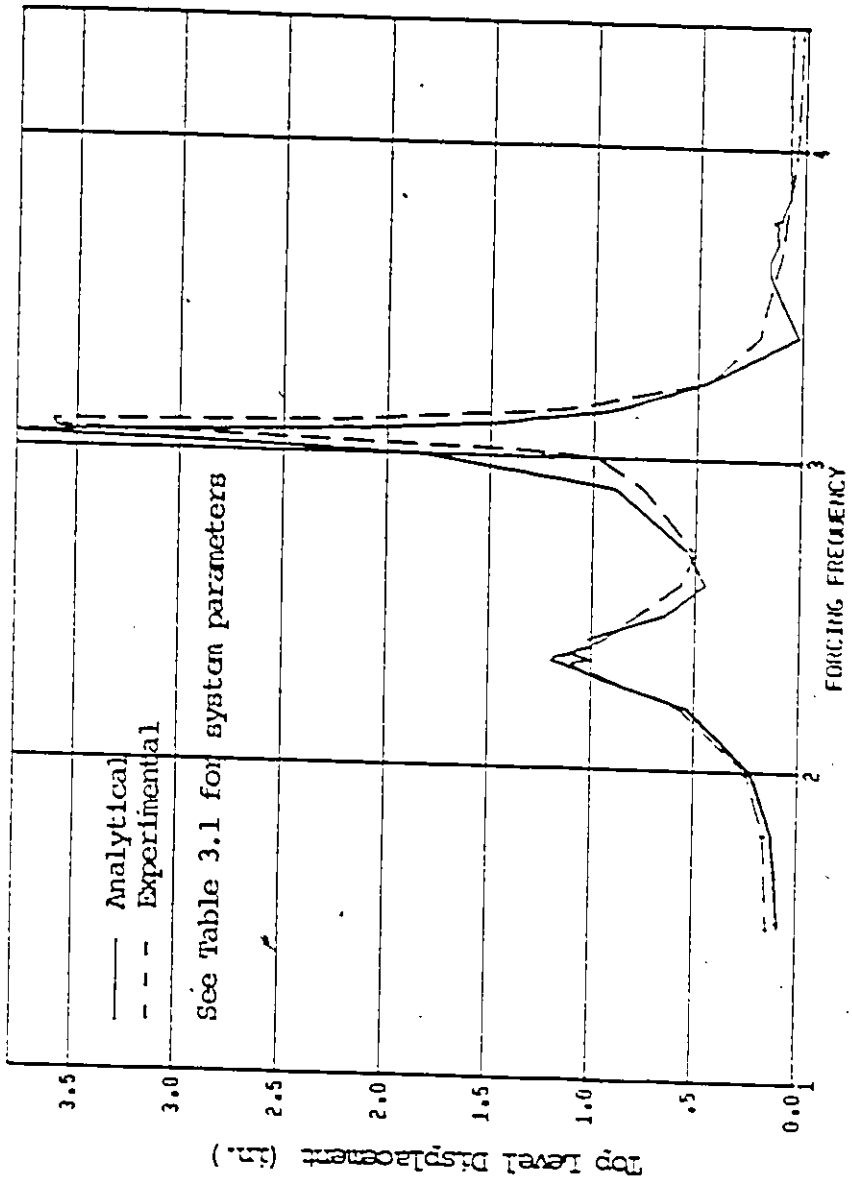

Figure A.3 System 5 Response Curves

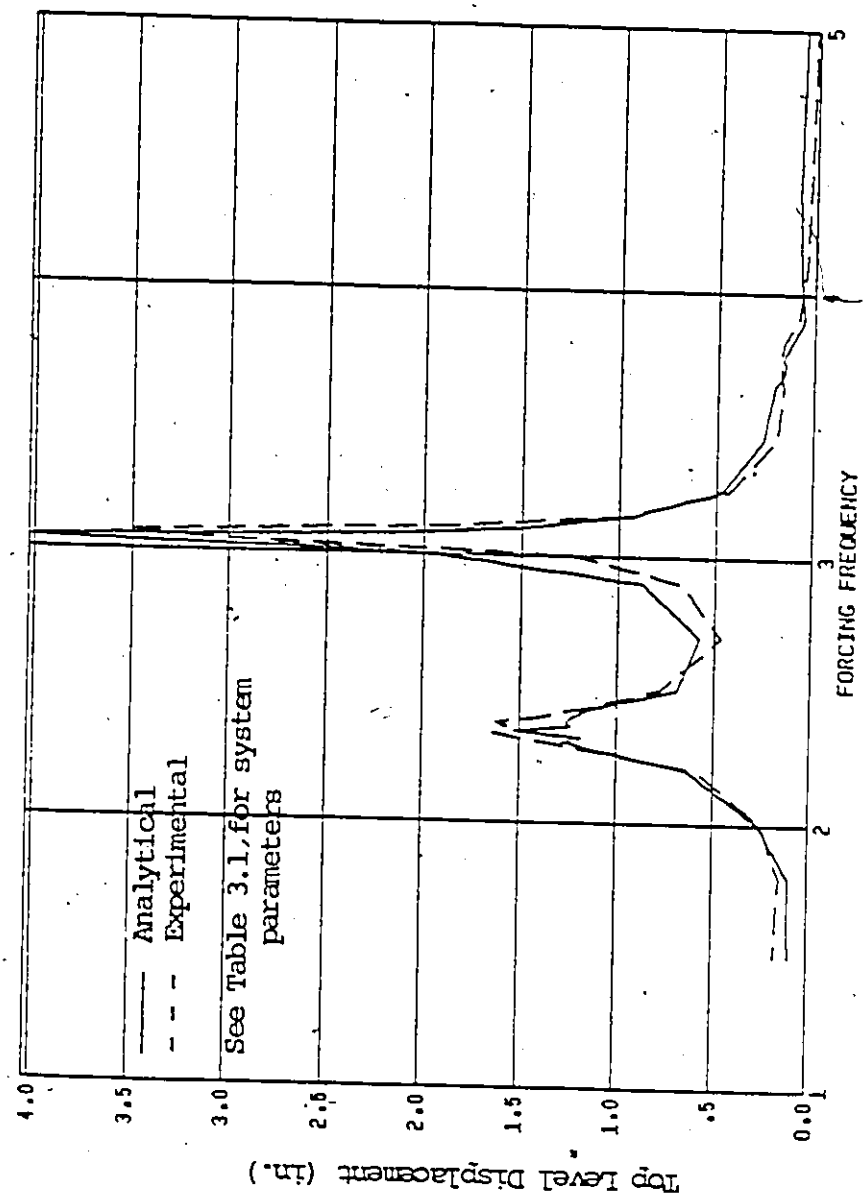

Figure A.4 System 11 Response Curves

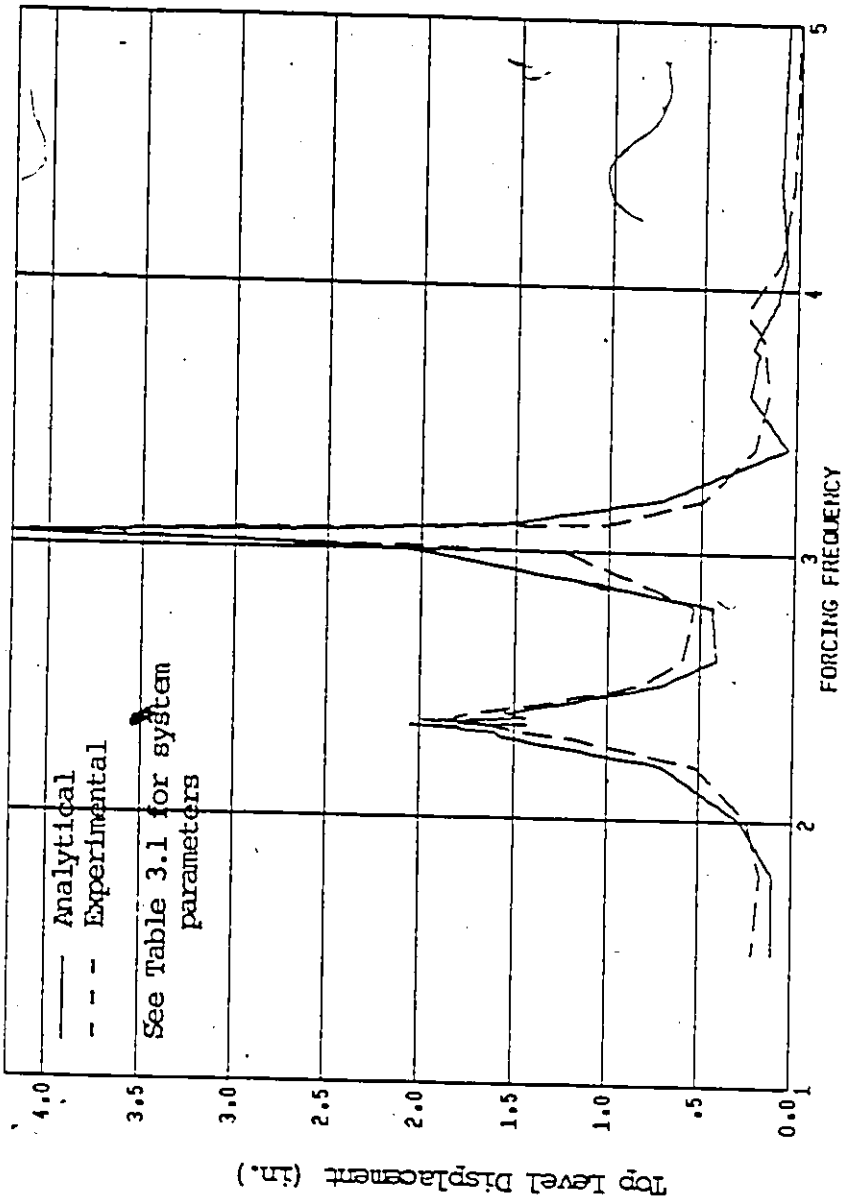

Figure A.5 System 14 Response Curves

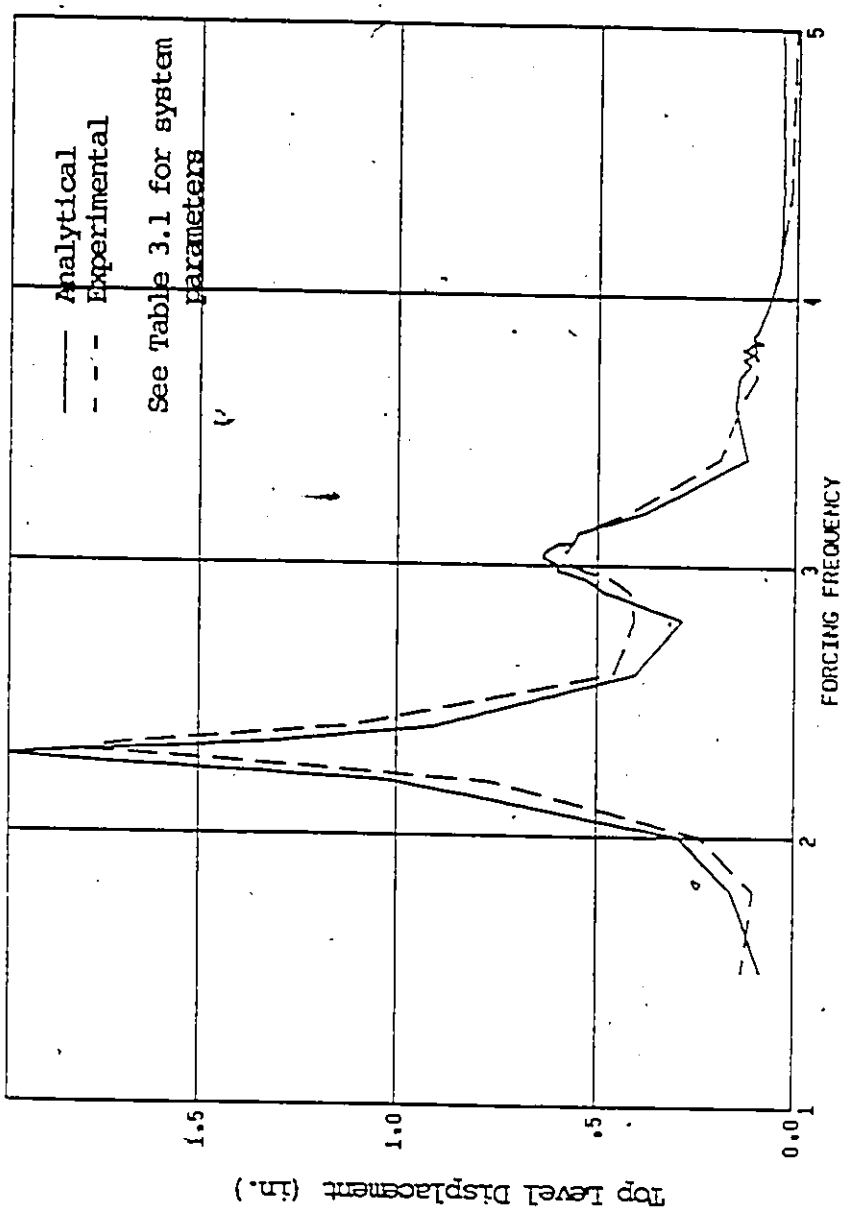

Figure A.6 System 24 Response Curves

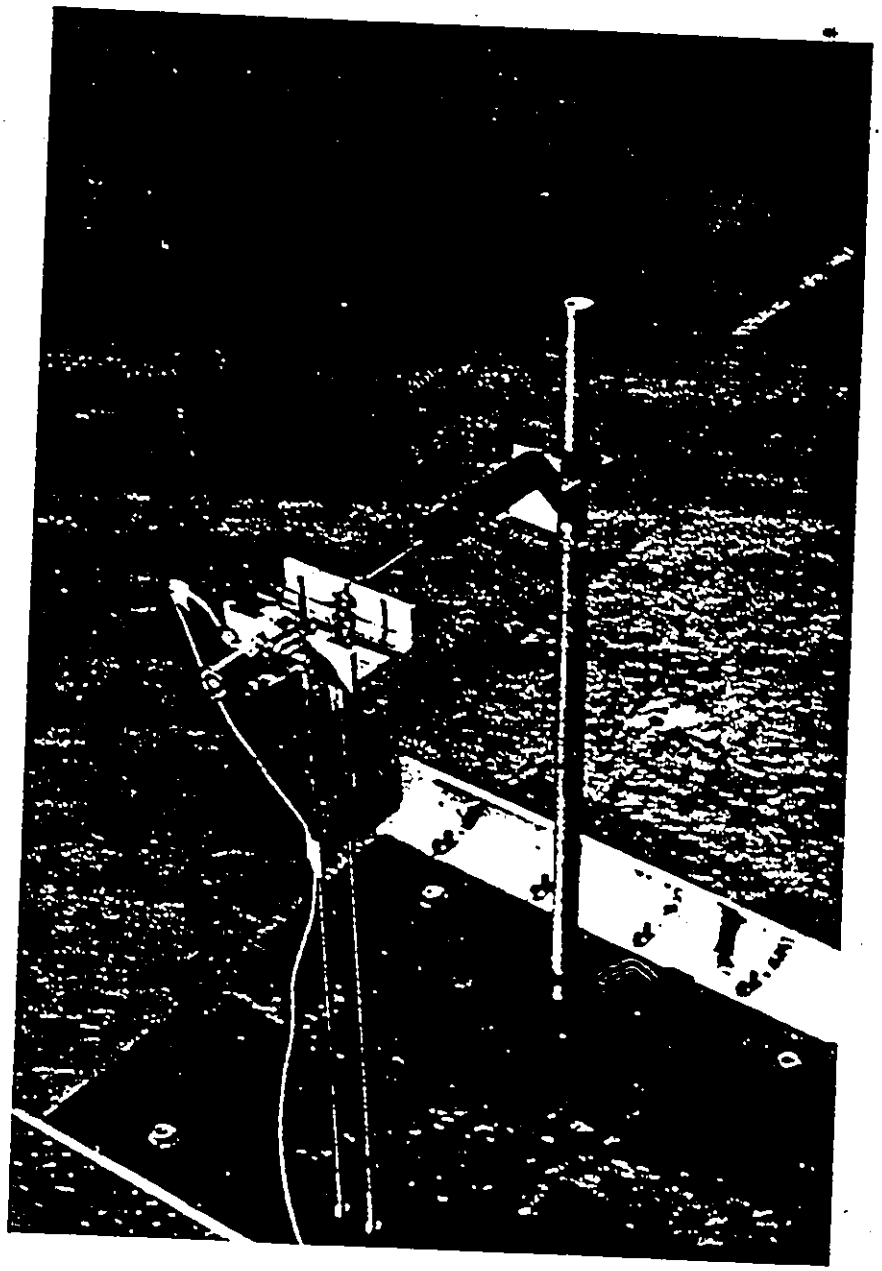

Tertiary Level Subsystem
with Accelerometer and Damper Attached
Figure A.7

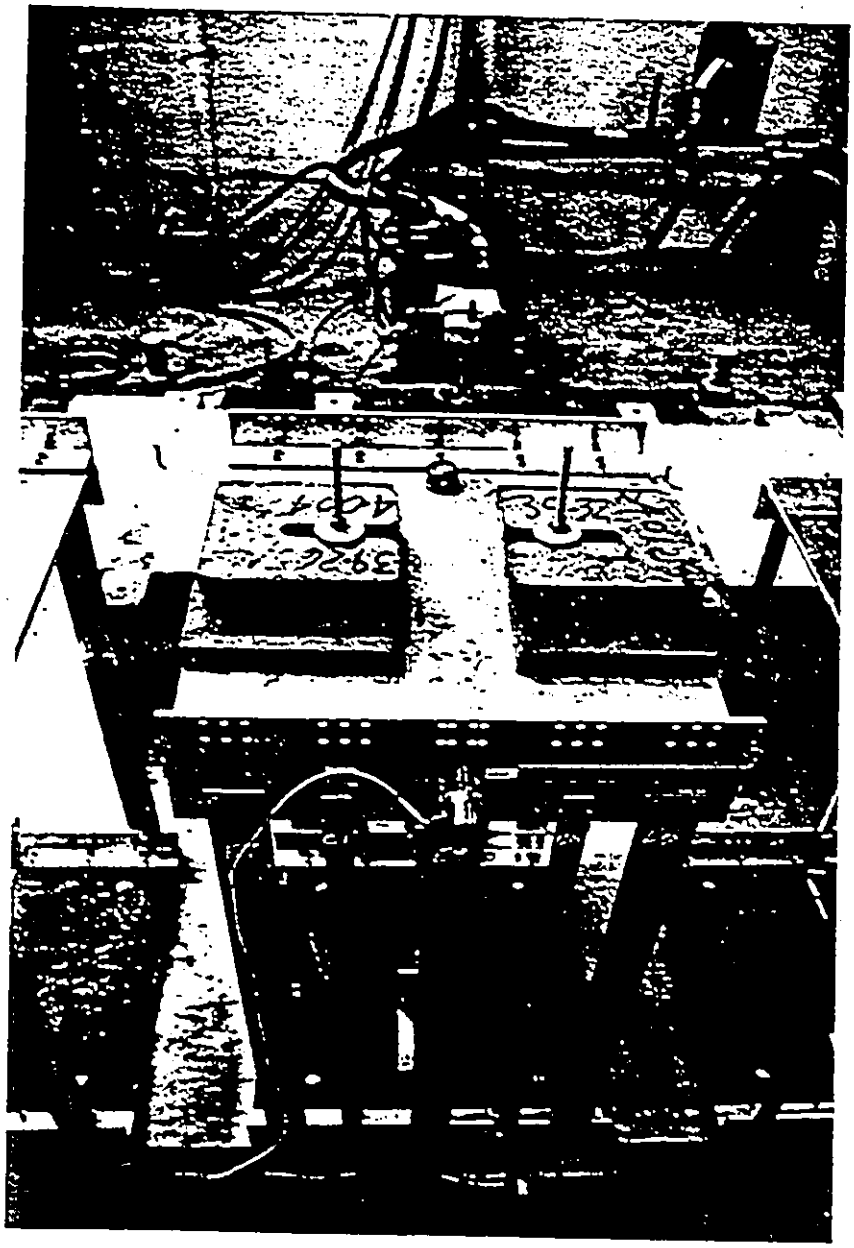

Primary Level Subsystem
Figure A.8

Primary and Two Secondary Level Subsystems
Figure A.9

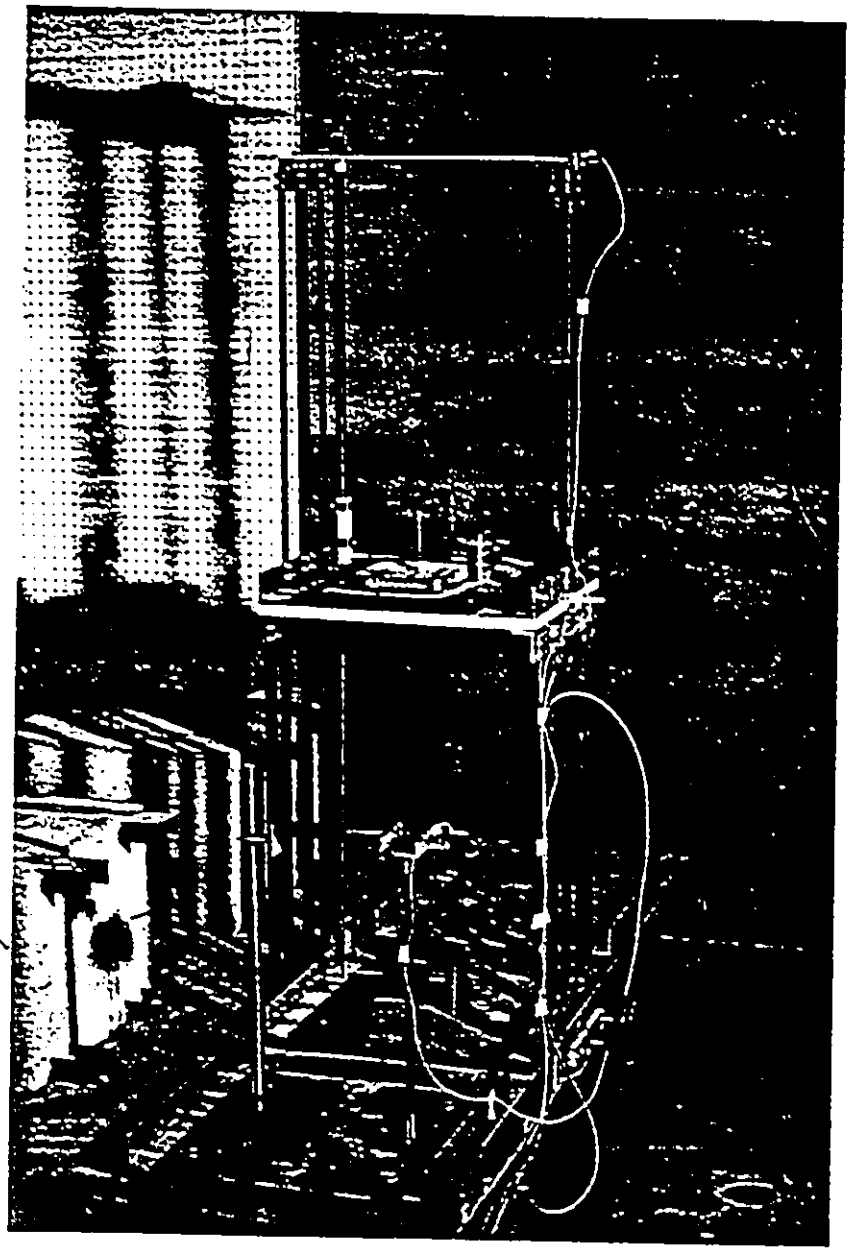

Foreground: Tertiary Subsystem
Background: Coupled Secondary/Tertiary System

Figure A.10

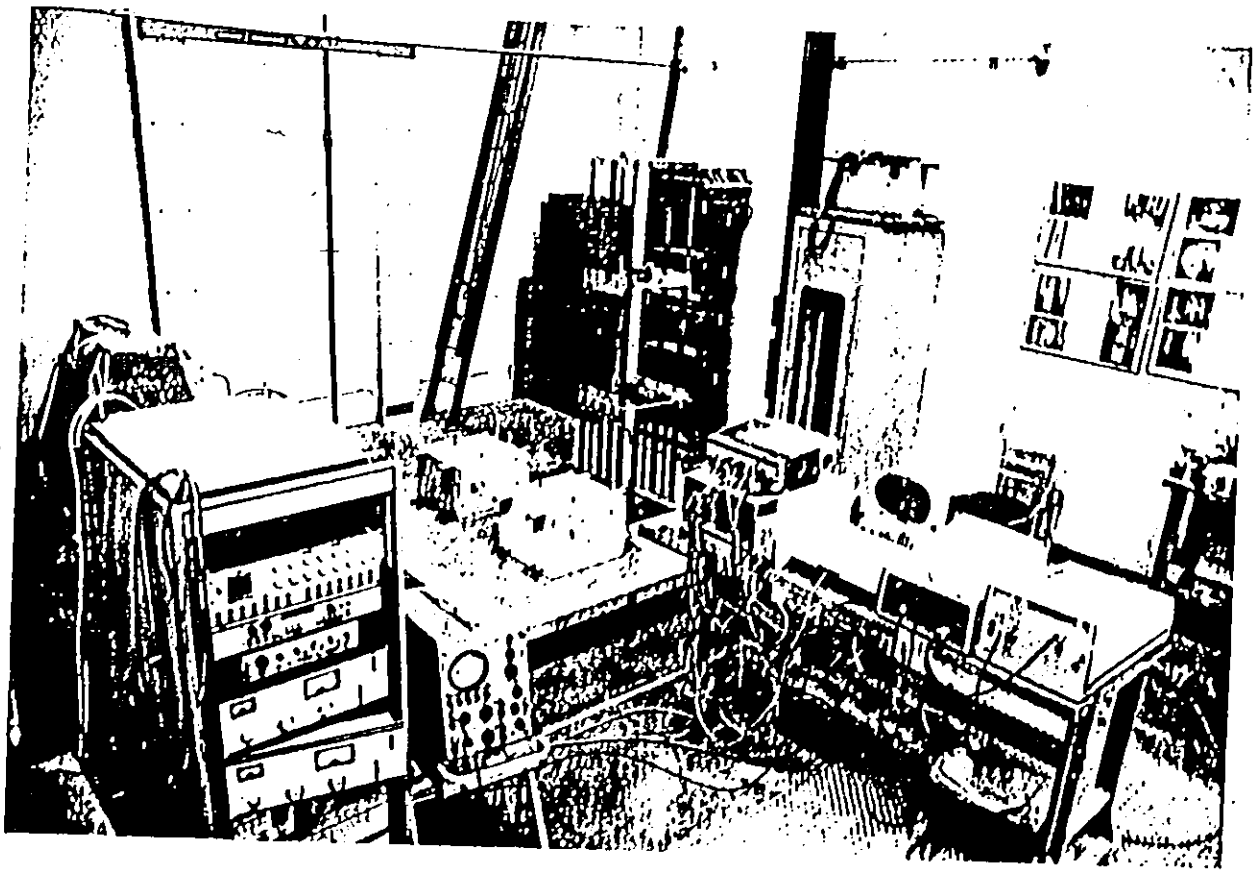

Figure A.11
Foreground: Shake Table Control System (left)
Data Acquisition System (right)
Background: Shake Table with Attached Test System

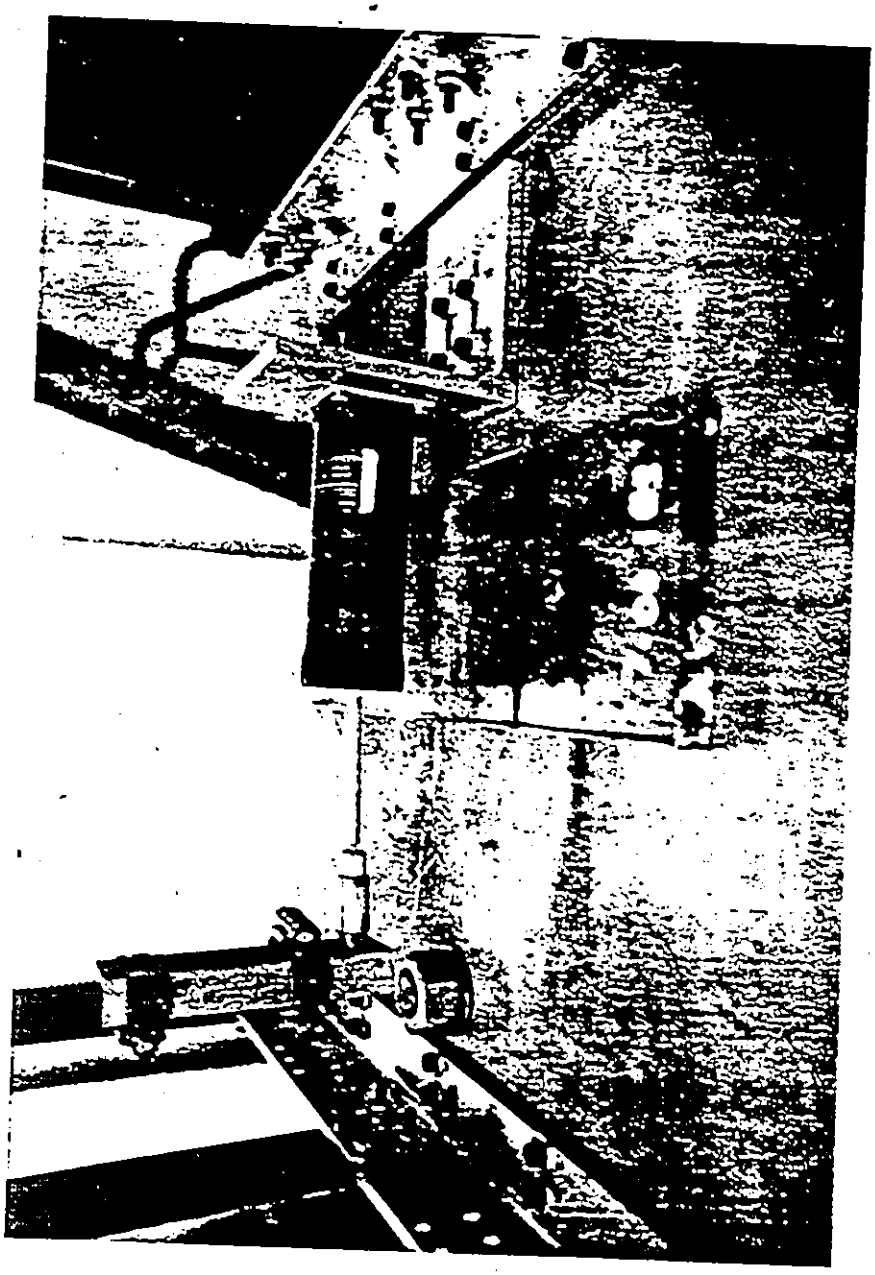

Figure A.12
Primary Damper Attachment